

Aspects of Quantum Entanglement and Indistinguishability

by

Soumya Das

Cryptology and Security Research Unit (CSRU)
Indian Statistical Institute (ISI), Kolkata
203 B.T. Road, Kolkata-700108.

Supervised by

Goutam Paul

Cryptology and Security Research Unit
R. C. Bose Centre for Cryptology and Security
Indian Statistical Institute, Kolkata
203 B.T. Road, Kolkata - 700108, India



A dissertation submitted to Indian Statistical Institute
for the partial fulfillment of the requirements for the degree of
Doctor of Philosophy in Computer Science

August, 2022

*I dedicate this thesis to
My Parents*

Acknowledgements

First and foremost I am extremely grateful to my supervisor **Dr. Goutam Paul** for his invaluable advice, continuous support, and patience from the first day when I have decided to start preparation for the entrance of my Ph. D. His immense knowledge and plentiful experience have encouraged me throughout my academic research and in my daily life.

Most importantly, none of this could have happened without my family. I am deeply grateful to my parents **Subrata Das** and **Swapna Das** and my wife **Sampurna Das** for providing me with unfailing support and continuous encouragement throughout my years of study and through the process of researching and writing this thesis. I would also like to thank my sister, my other family members and all the relatives, friends and well wishers for their continuous support throughout my life. Without their tremendous understanding and encouragement in the past few years, it would be impossible for me to complete my study.

I would like to thank my collaborators **Dr. Anindya Banerji** and **Dr. Ritabrata Sengupta** for their support and tutelage in my research papers. I would like to thank my junior collaborator **Adarsh Chandrashekar** for his work.

Getting through my dissertation required more than academic support, and I have many, many people to thank for listening to and, at times, having to tolerate me over the past three years. I would like to thank **Dr. Manas Mukherjee** and **Dr. Alexander Ling** for hosting my internship in Centre for Quantum Technologies, Singapore. I would like to extend my sincere thanks to **Dr. Ravindra Pratap Singh** of Physical Research Laboratory for a visit to his lab of quantum optics.

I would like to thank all the faculty members, specially **Prof. Bimal Kumar Roy** and **Prof. Subhamoy Maitra**, and all the other staffs of our institute who have helped me for all the academic as well as non-academic issues.

I express my gratitude and appreciation to thank my colleagues **Mostafizur Rahman**, **Probal Banerjee**, **Avishek Majumder**, **Samir Kundu**, **Laltu Sardar**, **Diptendu Chatterjee**, **Pritam Chattopadhyay**, **Amit Jana**, **Snehalika Lall**,

Nayana Das, Bikash Santra and others for their support, company and healthy discussions.

Finally, I want to thank my Master's guide **Dr. Tamaghna Acharya** and my colleagues **Dr. Surajit Basak, Dr. Aritra Roy, Dr. Amartya Banerjee** and **Dr. Avijit Dutta** and others who help be during the entrance exam and interview of this institute. Also I would like to thanks my school tuition teacher **Dr. Indraniv Ray** for his constant support throughout this journey.

Abstract

Entanglement of distinguishable and indistinguishable particles under different scenarios and related properties and results constitute the core component of this thesis. We propose a new error-modeling for Hardy's test and also perform experimental verification of it in superconducting qubits. Further, we point out the difficulties associated with the practical implementation of quantum protocols based on Hardy's test and propose possible remedies. We also propose two performance measures for any two qubits of any quantum computer based on superconducting qubits.

Next, we prove that if quantum particles (either distinguishable or indistinguishable) can simultaneously produce and perform hyper-hybrid entangled state and unit fidelity quantum teleportation respectively then using that cloning of any arbitrary quantum state is possible. This theorem results two no-go theorems: (1) hyper-hybrid entangled state is not possible for distinguishable particles and (2) unit fidelity quantum teleportation is not possible for indistinguishable particles. These theorems establish that there exists some quantum correlation or application unique to indistinguishable particles only and yet some unique to distinguishable particles only, giving a separation between the two domains. We also establish that the hyper-hybrid entangled state is possible using two indistinguishable fermions and we generalize it for bosons and fermions.

We establish a generalized degree of freedom trace-out rule that covers single or multiple degree of freedom scenarios for both distinguishable and indistinguishable systems. Using this, we propose generalized expressions for teleportation fidelity and singlet fraction and derive their relations, applicable for both distinguishable and indistinguishable particles with single or multiple degrees of freedom. We also derive an upper bound for the generalized singlet fraction for distinguishable and indistinguishable particles. We further show how our relation helps to characterize different types of composite states in terms of their distinguishability, separability, presence of maximally entangled structure and the number of degrees of freedom. Finally, we

demonstrate an optical circuit to generate entanglement for distinguishable particles each having two degrees of freedom and characterize it using our relation.

Further, using generalized degree of freedom trace-out rule, we show that, for two indistinguishable particles each having more than one degree of freedom, the monogamy of entanglement can be violated maximally using the measures that are monogamous for distinguishable particles. This results the following theorem that "In qubit systems, indistinguishability is a necessary criterion for maximum violation of monogamy of entanglement by the same measures that are monogamous for distinguishable particles".

For three indistinguishable particles each having multiple degree of freedom, we show that monogamy of entanglement is obeyed using squared concurrence as an entanglement measure. We also establish that the monogamy inequality becomes equality for all pure indistinguishable states, but the inequality remains for mixed indistinguishable states. This can be used as a one-sided test of distinguishability for particles in pure states

We show that the cost of adding an ancilla particle can be bypassed by using an additional degrees of freedom and creating multi-degree of freedom entanglement. Next, we show that entangled indistinguishable particles may alter certain important parameters in cryptographic protocols, in particular, we demonstrate how indistinguishability can change Hardy's probability Finally we propose a novel entanglement swapping protocol without Bell state measurement using only two indistinguishable particles that will be very useful in quantum networks specially in quantum repeaters.

List of publications/preprints

- As a part of this thesis

1. **A New Error-Modeling of Hardy's Paradox for Superconducting Qubits and Its Experimental Verification**

Soumya Das and *Goutam Paul*

ACM Transactions on Quantum Computing, Volume 1, Issue 1, December 2020, Article No. 4, pp 1-24, Published : 2nd October 2020

DOI: [10.1145/3396239](https://doi.org/10.1145/3396239)

Also available at [arXiv:[1712.04925](https://arxiv.org/abs/1712.04925)].

2. **Hyper-hybrid entanglement, indistinguishability, and two-particle entanglement swapping**

Soumya Das, *Goutam Paul*, and *Anindya Banerji*

Physical Review A 102, 052401, Published 2 November 2020

DOI: [10.1103/PhysRevA.102.052401](https://doi.org/10.1103/PhysRevA.102.052401)

Presented at [Quantum Physics and Logic \(QPL\) 2021](#)

Also available at [arXiv:[2101.10089](https://arxiv.org/abs/2101.10089)].

3. **Maximum violation of monogamy of entanglement for indistinguishable particles by measures that are monogamous for distinguishable particles** [arXiv:[2102.00780](https://arxiv.org/abs/2102.00780)]

Goutam Paul, *Soumya Das*, and *Anindya Banerji*

Physical Review A 104, L010402 (as a **Letter**) - Published 20 July 2021

DOI: [10.1103/PhysRevA.104.L010402](https://doi.org/10.1103/PhysRevA.104.L010402)

Also available at [arXiv:2102.00780].

4. **Monogamy of Entanglement for Indistinguishable Particles**

Soumya Das, Goutam Paul, and Ritabrata Sengupta

Status: Communicated on 7th April, 2022 to Physical Review A with manuscript id: LJ17132AR.

5. **Generalized Relation between Teleportation Fidelity and Singlet Fraction for (In)-distinguishable Particles**

Soumya Das, Goutam Paul, and Anindya Banerji

Status: Communicated on 29th September, 2021 to Physical Review A with manuscript id: LJ17778AR.

- Not included in this thesis

1. **Experimental Characterization of Noise using variants of Unitarity Randomized Benchmarking**

Adarsh Chandrashekar, Soumya Das, and Goutam Paul

Status: Communicated on 8th October, 2021 to Physical Review A with manuscript id: AK12142.

Contents

1	Introduction	24
1.1	Quantum physics	24
1.2	Quantum information	26
1.2.1	Quantum entanglement	28
1.2.2	Quantum indistinguishability	32
1.3	Quantum computation	33
1.3.1	Quantum computing technologies	34
1.3.2	Quantum processors and simulators	37
1.4	Motivation of current work	39
1.5	Thesis organization	42
2	Background	46
2.1	Statistical interpretation of experimental results	46
2.1.1	Standard normal distribution vs. Students t-distribution	46
2.1.2	Hypothesis testing and confidence interval	47
2.2	Quantum non-locality	48
2.2.1	Clauser-Horne-Shimony-Holt (CHSH) inequality	49
2.2.2	Hardy's test of non-locality	49
2.2.3	Equivalence between CHSH inequality and Hardy's equations	51
2.2.4	Revisiting known experimental results on Hardy's test and their statistics	51
2.3	Quantum entanglement	53
2.3.1	Definition of entanglement	53

2.3.2	Types of entanglement	54
2.3.3	Representation and degrees of freedom trace-out rule for two distinguishable particles each having n DoFs	56
2.4	Measures of entanglement	57
2.4.1	Concurrence	58
2.4.2	Negativity	58
2.4.3	Other measures of entanglement	59
2.5	Monogamy of entanglement	59
2.5.1	Coffman, Kundu, and Wootters (CKW) monogamy inequality	60
2.5.2	Equivalence of the monogamy of entanglement and the no-cloning theorem for distinguishable particles	61
2.6	Indistinguishability	62
2.6.1	How to distinguish two identical particles?	63
2.7	Entanglement of indistinguishable particles	64
2.7.1	Lo Franco <i>et al.</i> 's approach to represent indistinguishable particles	65
2.7.2	Hyper-hybrid entanglement using indistinguishable particles .	67
2.8	Quantum teleportation	68
2.8.1	Teleportation using distinguishable particles	68
2.8.2	Relation between teleportation fidelity and singlet fraction . .	70
2.9	Entanglement swapping	71
2.9.1	Entanglement swapping using distinguishable particles	72
2.10	Some quantum cryptographic protocols	73
2.10.1	Quantum private query protocol	73
2.10.2	Local Clauser-Horne-Shimony-Holt (CHSH) test	75
2.10.3	Quantum pseudo-telepathy test	76
3	Hardy's non-locality in superconducting qubits	77
3.1	Practical verification of Hardy's test	78
3.1.1	Connection to the CHSH inequality	78
3.2	Our proposed error modeling in superconducting qubits	79

3.2.1	Error distributions in optical circuits vs superconducting qubits	79
3.2.2	Our proposed model for verifying whether Hardy's probability greater than zero in superconducting qubits	80
3.2.3	Bounds in errors in optical circuits vs superconducting qubits	81
3.3	Circuits for Hardy's test using superconducting qubits	82
3.3.1	How to calculate the difference between two Student's t-distributed variables?	88
3.4	Our experimental results and discussion	90
3.4.1	Experiments for Hardy's non-locality using two specific qubits for Alice and Bob	92
3.4.2	Other possible combinations of multi-qubit gate	97
3.4.3	Application of the shift of the peaks in quantum protocols using Hardy's test	99
3.4.4	Verifying whether reducing the number of gates reduces the error in the circuit	100
3.4.5	Study of change of errors with respect to time in superconducting qubits	101
3.4.6	Benchmarking of superconducting quantum devices using Hardy's paradox	102
4	Quantum teleportation and hyper-hybrid entangled state	104
4.1	Hyper-hybrid entangled state for two indistinguishable fermions . . .	105
4.1.1	Generalized Hyper-Hybrid entangled state	107
4.2	Does the scheme of Li <i>et al.</i> [1] work for distinguishable particles? . .	108
4.3	Signaling using unit fidelity quantum teleportation and hyper-hybrid entangled state	109
4.3.1	Description of the protocol	110
4.3.2	Computation of the signaling probability	113
4.3.3	Experimental realization using optical circuits	114

4.4	First no-go theorem: no hyper-hybrid entangled state for distinguishable particles	117
4.5	Second no-go theorem: no unit fidelity quantum teleportation for indistinguishable particles	118
4.6	Physical significance of the two no-go theorems	119
5	Degree of freedom trace-out rule for indistinguishable particles	121
5.1	Representation of the general state of indistinguishable particles . . .	121
5.1.1	Two indistinguishable particles each having two DoFs	122
5.1.2	Two indistinguishable particles each having n DoFs	123
5.1.3	p indistinguishable particles each having n DoFs	124
5.2	DoF trace-out for indistinguishable particles	125
5.2.1	Two indistinguishable particles each having two DoFs	126
5.2.2	Two indistinguishable particles each having n DoFs	127
5.2.3	p indistinguishable particles each having n DoFs	128
5.3	Physical significance of the proposed DoF trace-out rule	128
6	Generalized relation between teleportation fidelity and singlet fraction	130
6.1	Generalized teleportation fidelity	130
6.2	Generalized singlet fraction	132
6.3	Relation between the generalized teleportation fidelity and the generalized singlet fraction	134
6.4	Illustration of the proposed generalized relation to some special states for distinguishable and indistinguishable particles	136
6.5	Generalized singlet fraction for our proposed state	138
6.6	Derivation of the upper bound of generalized singlet fraction	139
6.7	Physical significance of the proposed generalized relation	141
7	Violation of monogamy of entanglement for two indistinguishable particles	143

7.1	Violation of no-cloning theorem using the maximum violation of monogamy of entanglement	143
7.2	Apparent violation of particle-based monogamy of entanglement	145
7.3	Inter-DoF monogamy of Entanglement	146
7.4	Violation of monogamy of entanglement by indistinguishable particles	148
7.5	Physical significance of the maximum violation of monogamy	153
8	Monogamy of entanglement for three or more indistinguishable particles	155
8.1	Calculation of concurrence between two spatial regions between any DoFs	156
8.2	Monogamy of p indistinguishable particles each having n DoFs	158
8.2.1	Monogamy of three indistinguishable particles in spin DoF where two particles are in $ \uparrow\rangle$ eigenstate and one particles in $ \downarrow\rangle$ eigenstate	160
8.2.2	Monogamy of three indistinguishable particles where two particles are in $ \uparrow\rangle$ and $ \downarrow\rangle$ eigenstate respectively in spin DoF and one particle is in $ +l\rangle$ eigenstate in OAM DoF.	166
8.2.3	Monogamy of indistinguishable particles for mixed states	170
8.3	Physical significance of monogamy of entanglement for indistinguishable particles having multiple DoFs	171
9	Applications of entangled distinguishable and indistinguishable particles	173
9.1	Reducing the resource requirement in cryptographic protocols	173
9.2	Attacks on the security of cryptographic protocols.	176
9.3	Entanglement Swapping using only two indistinguishable particles	179
10	Conclusion	183

List of Figures

1-1	Schematic description of classical and all the quantum correlations. Here coherence \supseteq Discord \supseteq Entanglement \supseteq Steerable \supseteq Bell non-local where $A \supseteq B$ represents A is the superset of B	29
1-2	Schematic description of all the particles based on their identity and distinguishability.	32
1-3	A schematic of major quantum computing technologies with corresponding quantum processors available.	35
2-1	From left to right: (a) hyper-entanglement (solid lines), (b) hybrid-entanglement (dotted lines), and (c) hyper-hybrid entangled state of two qubits with two degrees of freedom.	55
2-2	CKW inequality for distinguishable particles using square of the concurrence as entanglement measure.	60
2-3	Circuit to get violation of the no-cloning theorem from the maximum violation of MoE.	61

2-4	Creation of indistinguishable particles from initially separated identical particles. Here s_1 , s_2 , and s_3 are three distinct spatial locations. (a) Initially, two identical particles with are present in s_1 and s_2 in such a way that their wave-functions do not overlap. We label the particles at s_1 and s_2 as A and B respectively. Thus the particles are identical but are distinguishable via their spatial locations. (b) The particles are brought close to each other so that their wave-functions overlap and they become indistinguishable. Now, they cannot be identified by their spatial locations. If the measurement is done in the overlapped region, i.e., s_3 , then it is not possible to detect which particle is measured. Even if the particles are again moved apart, they can no longer be labeled. The information about which of A and B appears at s_1 or s_2 is lost and they remain indistinguishable until they are measured again.	63
2-5	Circuit to generate hyper-hybrid entangled state as proposed by Li <i>et al.</i> [1]. Here the bi-directional arrow represents the measurement is done either in spin DoF or in Path DoF.	68
2-6	Standard teleportation protocol	69
2-7	Standard Entanglement Swapping protocol	72
3-1	The state $ \psi\rangle$ for Equation (3.13).	85
3-2	Quantum circuit and measurement for $P(+1, +1 A_1, B_1)$ for Equation (3.1).	85
3-3	Quantum circuit and measurement for $P(+1, -1 A_2, B_1)$ for Equation (3.2).	86
3-4	Quantum circuit and measurement for $P(-1, +1 A_1, B_2)$ for Equation (3.3).	86
3-5	Quantum circuit and measurement for $P(+1, +1 A_2, B_2)$ for Equation (3.4).	87
3-6	The variation of θ and ϕ in degrees vs the values of q from Equation (3.15).	87

3-7	The variation of the confidence interval size $\left(2t_{\frac{\alpha}{2}} \frac{S_{\epsilon_5}}{\sqrt{n}}\right)$ with the percentage of confidence $(1 - \alpha)\%$ with varying number of samples is $n \in \{10, 30, 50\}$	91
3-8	The variation of q , ϵ_5 and \hat{q}_{lb} against $\theta = \phi$ for CI=99% and $n = 10$ with Q_3 as control qubit and Q_4 as target qubit.	96
3-9	The variation of q , ϵ_5 and \hat{q}_{lb} against $\theta = \phi$ for CI=99% and $n = 10$ with Q_2 as control qubit and Q_1 as target qubit.	99
3-10	Quantum circuit and measurement for $P(+1, +1 A_1, B_2)$ when number of gates are reduced significantly.	100
4-1	The singlet state $ \psi\rangle_{A_1B_1}$ is shared between DoF 1 of Alice and that of Bob, whereas hyper-hybrid entangled state $ \chi\rangle_{PQ}$ is kept by Bob. . .	110
4-2	Our proposed universal quantum cloning machine to demonstrate the impossibility of hyper-hybrid entangled state using distinguishable particles. Inputs to this cloning machine are the unknown quantum state $ \phi\rangle$ of DoF 1 of the particle B (denoted by $ \phi\rangle_{B_1}$) and the hyper-hybrid entangled state $ \chi\rangle_{PQ}$, as shown in Fig. 4-1. More specifically, $ \phi\rangle_{B_1}$ is the state unknown to Bob generated on Bob's side after Alice does measurement on A_1 in either Z basis or X basis. After that, Bob performs BSM on B_1 and P_1 , resulting in one of the four possible Bell states as output, denoted by k . Based on this output k , suitable unitary operations U_k are applied on both the DoFs of Q , i.e., Q_1 and Q_2 , where $U_k \in \{\mathcal{I}, \sigma_x, \sigma_y, \sigma_z\}$, \mathcal{I} being the identity operation and σ_i 's ($i = x, y, z$) the Pauli matrices. As a result, the unknown state $ \phi\rangle$ of B_1 is copied to both Q_1 and Q_2	112

4-3	Bob's circuit for distinguishing between Z and X bases using two types of DoF sorters, i.e., a spin sorter (SS) and a path sorter (PS), and four detectors. Here the output of Fig. 4-2 is used as an input in this circuit. Here, $ \downarrow\rangle$ and $ \uparrow\rangle$ denote the down- and the up-spin states of the particles, respectively. Further, $ T\rangle$ denotes the transverse mode and $ R\rangle$ denotes the reflected modes of a PS.	114
4-4	Bob's circuit for distinguishing between Z and X bases using three types of DoF sorters, i.e., S_1 , S_2 , and S_3 , and eight detectors. Here the output of Fig. 4-2 is used as an input in this circuit.	116
4-5	The two sets Q_{dis} (consisting of quantum properties and applications of distinguishable particles), Q_{indis} (consisting of quantum properties and applications of indistinguishable particles), and their intersection (UFQT, HHES, and ES stand for unit fidelity quantum teleportation, hyper-hybrid entangled state, and entanglement swapping, respectively).	120
6-1	Teleportation operation using (a) two distinguishable particles and (b) two indistinguishable particles, each having n DoFs.	131
6-2	Optical set up to the generation of entangled state between polarization and OAM DoF for distinguishable particles. NLC: nonlinear crystal, DM: dichroic mirror, BD: beam dump, PBS: polarizing beam splitters, SPP: spiral phase plates, M: mirrors, IF: interference filters, DS: detection setup and C.C.: coincidence counter. The detection setups could be made up of spatial light modulators and single-mode fibers coupled to avalanche photo detectors if measuring in OAM or half-wave plates and PBS if measuring in polarization.	136
6-3	Characterization of the different kinds of states based on their separability, indistinguishability and number of DoFs present using the number of DoFs n , generalized Singlet fraction $F_g^{(n)}$ and generalized teleportation fidelity f_g	138

6-4	The variation of generalized teleportation fidelity f_g and generalized singlet fraction $F_g^{(n)}$ with varying the number of DoFs n where the dimension of each DoF is $d = 2$	142
7-1	Consider three particles A, B, C , and a bipartite entanglement measure \mathbb{E} where $\mathbb{E}_{X Y}$ measures the entanglement between the subsystems X and Y of the composite system XY and \mathbb{E}_{max} denotes its maximum value. Using these notations, we show the particle-based monogamy of entanglement obeying Eq. (7.1).	144
7-2	Consider three particles A, B, C , and a bipartite entanglement measure \mathbb{E} where $\mathbb{E}_{X Y}$ measures the entanglement between the subsystems X . Using these notations, we show that A is maximally entangled with B in DoF 1 (i.e., $\mathbb{E}_{A_1 B_1} = \mathbb{E}_{max}$) and with C in DoF 2 (i.e., $\mathbb{E}_{A_2 C_2} = \mathbb{E}_{max}$). In particle view, apparently monogamy of entanglement is violated; but in DoF view, it is not.	145
7-3	Consider three particles A, B, C , and a bipartite entanglement measure \mathbb{E} where $\mathbb{E}_{X Y}$ measures the entanglement between the subsystems X and Y of the composite system XY and \mathbb{E}_{max} denotes its maximum value. Using this notations, we generalize the Eq. (7.1) from particle view to inter-DoF monogamy of entanglement as proposed in Eq. (7.4) which resolves the previous apparent violation in Fig. 7-2.	146
7-4	Consider three particles A, B, C , and a bipartite entanglement measure \mathbb{E} where $\mathbb{E}_{X Y}$ measures the entanglement between the subsystems X and Y of the composite system XY and \mathbb{E}_{max} denotes its maximum value. Now consider the following two scenarios: (a) Two-particle inter-DoF monogamy of entanglement, where $\mathbb{E}_{A_1 A_2}$ measures entanglement between the two DoFs A_1, A_2 of A and $\mathbb{E}_{A_1 B_1}$ between A_1, B_1 ; and (b) $\mathbb{E}_{A_1 B_j}$ between A_1 of A and B_j of B , $j \in \{1, 2\}$	147

8-1	Overlapping of the wave-function of three indistinguishable particles in the localized regions s^1 , s^2 , and s^3 where two of them have $ \uparrow\rangle$ eigenstate and one having $ \downarrow\rangle$ eigenstate in spin degrees of freedom.	161
9-1	The variation of generalized SF $F_g^{(n)}$ for the quantum pseudo-telepathy test using ancilla as particle and using ancilla as degrees of freedom with varying θ in degrees.	175
9-2	A general protocol with A as the sender and B and C are the receivers. $ \psi\rangle_{BC}$ is the initial state at A that has to be shared between B and C . Here U_B and U_C are the unitary operations performed by B and C on their respective particles. (a) The final state after the unitary operations performed by B and C is $ \phi\rangle_{BC}$. (b) If an indistinguishability module is present on the path from A to B and C , then the final state is $ \phi'\rangle_{BC}$	177
9-3	Effects of indistinguishability on Hardy's probability with $\theta = \phi$ in degrees. (a) The variation of Hardy's probability q and modified Hardy's probability due to indistinguishability q' where $\alpha = \beta = \frac{1}{2}$. (b) The variation of modified Hardy's probability q_α with α where $\alpha = \beta$ and $\theta = \phi = 51.827^\circ$	178
9-4	Entanglement swapping with only two indistinguishable particles without Bell state measurements.	180

List of Tables

2.1	Summary of prior works on Hardy’s test in optical set-up where SD=standard deviation and CI=confidence interval.	52
2.2	Significant experiments performed in IBM five-qubit quantum computer and their error statistics where n = number of times the experiment has been performed, s =number of shots in each time, SD=standard deviation, and CI=confidence interval.	53
3.1	Maximally entangled states (MES) and product states (PS) based on different values of θ and ϕ in between 0 to 90 degrees.	84
3.2	Results of $\bar{\epsilon}_4$, standard deviations (SD) and the values of $t_{\frac{\alpha}{2}} \frac{S_{\epsilon_4}}{\sqrt{n}}$ for different confidence intervals (CIs) with $n = 10$ for some values of θ and ϕ for which MES as well as PS are created for the pair of qubits (Q_3, Q_4)	93
3.3	Results of $\bar{\epsilon}_5$, standard deviations (SD) and the values of $t_{\frac{\alpha}{2}} \frac{S_{\epsilon_5}}{\sqrt{n}}$ for different confidence intervals (CIs) with $n = 10$ for some values of θ and ϕ for which NMES are created for the pair of qubits (Q_3, Q_4) . . .	94
3.4	Comparison of the results of q and \hat{q}_{lb} for some values of θ and ϕ for which NMES is created for different confidence interval (CIs) for the pair of qubits (Q_3, Q_4)	95
3.5	The values of $\bar{\epsilon}_5$ for $n = 10$ for all possible pairs of qubits other than (Q_3, Q_4) when $\theta = \phi \in \{45, 51.827, 55\}$ in degrees.	98

3.6	The values of $\bar{\epsilon}_5$ for $n = 10$ for the pair (Q_3, Q_4) before and after one month when $\theta = \phi = 51.827$ in degrees, SD=standard deviation, and CI=confidence interval.	101
8.1	List of possible combinations to create indistinguishability using three indistinguishable particles localized in three regions s^1, s^2 , and s^3 , each having three DoFs denoted by j, j', j'' . Here the second column denotes whether entanglement is calculated in same DoFs or different DoFs of all particles; the third column denotes whether the eigenstate of the contributing DoFs in entanglement is the same or not or in superposition; the fourth, fifth and sixth columns describe the eigenstates of the three particles in the corresponding DoFs; the seventh column describes the relations between the eigenstates of the for entanglement. The eighth, ninth, and tenth columns describe the DoFs numbers (e.g., j means the j th DoF) in which the measurements are done in the localized regions s^1, s^2 , and s^3 respectively; the rest of the columns represent of the squared concurrences are zero or ≥ 0	159

Notation and list of symbols

Symbol	Meaning
q	Value of Hardy's probability
q_{max}	maximum value of Hardy's probability = $\frac{5\sqrt{5}-11}{2} \approx 0.09017$ for two qubits
q_{lb}	lower bound on Hardy's probability
d	Dimension of the system
\mathbb{E}	Entanglement measure
\mathcal{C}	Concurrence
\mathcal{N}	Negativity
$E_{\mathcal{N}}$	Log-negativity
\mathbb{N}_n	$\{1, 2, \dots, n\}$
η	+1 for bosons and -1 for fermions
f	Teleportation fidelity
f_g	Generalized teleportation fidelity
F	Singlet fraction
$F_g^{(n)}$	Generalized singlet fraction
μ	mean
σ	Standard deviation
\mathbb{S}^P	$\{s^1, s^2, \dots, s^P\}$

Abbreviations

Short form	Full form
BSM	Bell State Measurement
CHSH	Clauser-Horne-Shimony-Holt
CI	Confidence interval
DOF	Degrees of Freedom
HHES	Hyper Hybrid Entangled State
HUP	Heisenberg's uncertainty principle
LOCC	Local Operations and Classical Communications
LHV	Local hidden variable
MOE	Monogamy of Entanglement
MES	Maximally entangled state
NMES	Non maximally entangled state
NMR	Nuclear magnetic resonance
PS	Product state
QPQ	Quantum private query
QBA	Quantum Byzantine agreement
SSR	Super selection rule
UFQT	Unit Fidelity Quantum Teleportation

Chapter 1

Introduction

Max Planck, the father of quantum physics, was advised by his supervisor Philipp von Jolly *not to study theoretical physics as it was probably not a great idea, since there was not much left to do* when he was about to start his journey with physics in 1874. A similar quotation is also found in 1900 when William Thomson, a British mathematician, physicist and engineer, (better known as Lord Kelvin) addressed the British Association for the Advancement of Science that “*There is nothing new to be discovered in physics now. All that remains is more and more precise measurement.*” Coincidentally in that same year, quantum physics was born when Max Planck explained the black body radiation using the quantized formulation of electromagnetic energy.

1.1 Quantum physics

At the beginning of the 20th century, there were a number of experimental observations that cannot be explained by the existing theories, often considered classical physics. This includes black-body radiation [2, 3], photo-electric effect [4], Stern-Gerlach experiment [5], Mach-Zehnder interferometer [6, 7], etc. To solve these shortcomings of physics, a new theory came out with the hands of Max Planck, Albert Einstein, etc., and later formulated by Max Born, Werner Heisenberg, Wolfgang Pauli, Erwin Schrödinger, etc. They have revolutionized the history of physics

by their theories which are later verified by experimental results.

Quantum theory is a mathematical tool to model and understand how physical phenomena are happening and to predict what will happen next. It basically describes the behavior of the atomic and the subatomic particles using the wave function. The evolution of this wave function is governed by the Schrödinger equation [8]. When a measurement is performed, how this wave function collapses is the most important problem in quantum theory and is known as the measurement problem [9]. Different solutions are proposed to solve this problem known as the interpretations of quantum theory [10]. These theories mainly concerned about whether quantum mechanics is deterministic or stochastic, the description about the nature of reality, the process of measurement, etc. Most popular interpretation of quantum mechanics is Copenhagen interpretation [11]. Other interpretations includes many world interpretation [12], QBism [13], consistent histories [14], Bohm theory [15, 16], Transactional interpretation [17, 18, 19], etc. This thesis is based on the Copenhagen interpretation which can be explained by the four *postulates of quantum mechanics* [20].

Postulate 1 describes the basic building block of quantum physics, i.e., the state of an isolated quantum system.

Postulate 2 concerned about the dynamics of closed quantum systems. This is governed by the Schrödinger equation, i.e., by the unitary evolution.

Postulate 3 explains the most interesting phenomenon of quantum mechanics, i.e., measurement, which is a process of extracting information from quantum systems.

Postulate 4 deals with the description of the composite system, i.e., a combination of different quantum systems. The rest of quantum mechanics is just the derivation and applications of these postulates.

Till now, quantum theory can be used to mathematically model all the natural events (that cannot be explained using classical theory as said above) other than gravity. Most of the present-day technologies are successful applications of this quantum theory, for example in the electronics industry, chemical industry, communication industry, and most important in the cryptographic industry.

1.2 Quantum information

Quantum information theory deals with how quantum messages can be sent over quantum communication channels. More specifically how information can be compressed as a quantum message and transmitted reliably from the sender to receiver in the presence of noise. The measure of quantum information is von-Neumann entropy [21], like Shannon entropy [22] in classical communication. Since the aim of quantum communication is to compress the information as much as possible by the sender keeping in mind that it should be decoded at the receiving end. The amount of compression is given by the Schumacher's quantum noiseless coding theorem [23, 24] that states that von-Neumann entropy is the optimal compression factor for quantum information. The basic fact for quantum information transfer is that the communicated quantum messages are not generally orthogonal in nature and thus cannot be decoded properly. The limits to which information can be accessible to the receiver is given by the Holevo bound [25].

The basic unit of quantum information is qubit, a two-state system that can be realized using any physical two-level device. Normally, quantum information are encoded in quantum particles degree of freedom (DoF). For example, spin DoF of an electron where up-spin and down-spin is taken as the two level system. Similarly, polarization of a photon can be used as a qubit with horizontal polarization and vertical polarization are used as two levels. Unlike classical bit, qubit can be present as a superposition of the two levels.

Mathematically, qubits are described by a two-dimensional complex Hilbert space. The two levels are represented as a normalized and mutually orthogonal vectors in that space. The notations are used for this representation was given by Paul Dirac which is known as the Dirac-notation [26]. In this notation, two levels are commonly represented as $|0\rangle$ and $|1\rangle$ which is called *ket* vector. These ket vectors are commonly corresponds to column vectors such as $|0\rangle = \begin{pmatrix} 1 \\ 0 \end{pmatrix}$ and $|1\rangle = \begin{pmatrix} 0 \\ 1 \end{pmatrix}$. Another representation of qubits are as a point in a sphere of unit radius, known as the Bloch sphere. The azimuth and elevation angles are the two parameters of the sphere that define

the quantum state. Bloch sphere representation is very much useful to visualize the qubits in the three-dimensional space.

The state vector representations are useful for a single quantum systems. The sub-system of a a composite quantum systems cannot be represented by the state vector. Thus the density matrix formalisms are introduced by von Neumann and Lev Landau. In the Bloch sphere representation, the pure states are those which are represented at the circumference of the sphere. Mixed states are those who reside inside the sphere.

The journey of quantum mechanics was not like a dream one. Some of the scientists were doubtful about it due to its counter-intuitive nature. One of them was famous Albert Einstein, who in 1935, with Boris Podolsky and Nathan Rosen, using a thought experiment [27] questioned the *completeness* of quantum theory which is known as *Einstein-Podolsky-Rosen (EPR) paradox*. It states that any physical theory should be *complete*, i.e., they should respect two conditions: *locality* and *reality*. Since the quantum theory does not satisfy these conditions, it should no longer be a complete theory. The founders and followers of quantum theory argued and debated with this theory for almost two decades but none came up with a complete answer.

In 1964, John Bell came up with an elegant and experimentally testable solution to the EPR paradox. He showed that in quantum theory there exist some correlations which are not compatible with the two assumptions of the EPR paradox which is known as *Bell's Theorem* [28]. The legacy of Bell's work is that he showed he has designed an experiment to test this theorem in lab by using an inequality. If some correlation violates this inequality, then that correlation would not be compatible with locality and reality. This theorem proves that quantum theory is the ultimate theory, however, if some ultimate theory exists, it would not be the complete theory as defined by EPR paradox.

In 1969, four scientists John Clauser, Michael Horne, Abner Shimony, and Richard Holt came up with the most famous Bell inequality known as *CHSH inequality* [29]. This experiment consists of two people, Alice and Bob who have shared a set of pair of particles where each pair has some specific correlation. Now Alice and Bob

performed some measurements in their pairs and note down the results. Now after a series of calculations, they check whether their result is greater than some specific value or not? if so then it violated the CHSH inequality else not. This experiment has been performed a lot of time since its mathematical discovery and it supports that quantum correlation indeed violated the CHSH inequality.

Rather than using the statistical inequalities, the contradiction between quantum theory and any Local hidden variable theory (LHV) theory can also be demonstrated by a simple and elegant way, which is known as all-versus-nothing (AVN) proof of Bell's nonlocality [30]. In this method, a logical paradox is formed in such a way that while doing experiments, in principle, only a single event can be used to reveal the non-locality. Among several AVN proofs, in [31], the authors have demonstrated non-locality without using inequalities which is known as the Greenberger-Horne-Zeilinger (GHZ) paradox. It has been verified experimentally in [32]. However, this paradox applies to three [31] or more qubits [33], but not for two qubits. In 1992, through a thought experiment, Hardy constructed the test of local realism without using inequalities for two qubits, which is called Hardy's test [34, 35]. It is known as the "Best version of Bell's theorem" as indicated by Mermin [36]. This test provides a direct contradiction between the predictions of quantum theory and any LHV theory for two qubits [34, 35] and also for multi-qubits [37]. The applications of Hardy's paradox includes device-independent randomness [38], device-independent quantum key distribution [39], quantum Byzantine agreement (QBA) [40], etc.

1.2.1 Quantum entanglement

One of the most interesting features of quantum physics is quantum entanglement [41]. This counterintuitive property suggest the presence of global states of a composite system which cannot be represented as a product of the states of separate subsystems. Although quantum entanglement itself does not carry useful information, but using it some of the classically impossible tasks can be performed like dense coding [42], teleportation [43], Entanglement swapping [44], quantum key distribution [45], etc.

One of the non-intuitive features of quantum physics is the presence of certain

types of correlation in the composite systems which are not possible using classical particles. The strongest of quantum correlation is Bell non-locality [33]. One of the important applications of it in device-independent quantum cryptography [46]. The next one is quantum steering [47] which is mainly used for subchannel discrimination [48]. The most popular quantum correlation is quantum entanglement [41] which is used for quantum teleportation [43], entanglement swapping [44], quantum key distribution etc [45]. The properties of mixed states can be better explained by quantum

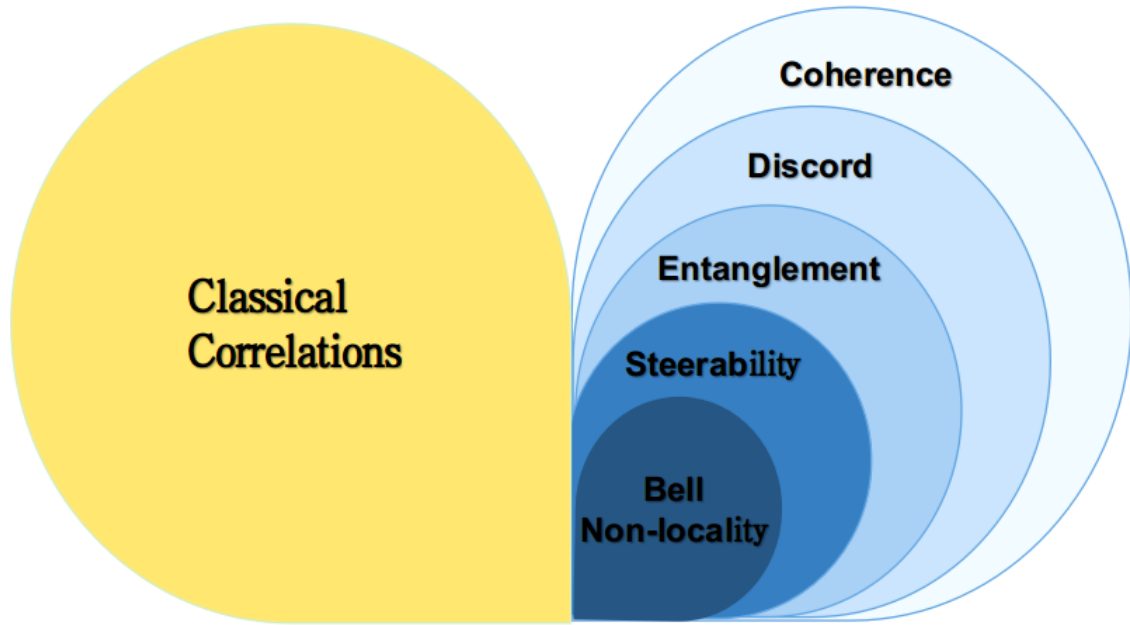


Figure 1-1: Schematic description of classical and all the quantum correlations. Here coherence \supseteq Discord \supseteq Entanglement \supseteq Steerable \supseteq Bell non-local where $A \supseteq B$ represents A is the superset of B .

discord [49] when entanglement fails to capture the necessary information. Although quantum coherence [50] is the weakest of all quantum correlations, still it is useful for quantum thermodynamics, quantum metrology, quantum phase transitions, etc. All these correlations are shown by set-theoretic notions in Fig. 1-1.

There are some unique properties and applications of quantum entanglement which are absent in other correlations. These applications are the main reason why modern industries are also exploring this unique feature.

Quantum teleportation

Quantum teleportation is a process to transfer quantum information from one location to another distant location. In this method, the sender may not know the location of the receiver and does not know about the information being transferred. This process was first proposed in the seminal paper by Bennett *et al.* in 1993 [43] and first experimentally realized in [51] in 1997. The quality of teleportation is measured by teleportation fidelity which measures the overlap between the initial quantum state before teleportation at the sender and the final teleported state at the receiver. Quantum teleportation has applications in entanglement swapping, quantum communication network, etc.

Singlet fraction

Singlet fraction [52] of any quantum state signifies the amount of overlap between a maximally entangled state with it. Singlet fraction is very useful to measure the quantum teleportation fidelity.

Entanglement swapping

Entanglement swapping [44] is the process of transferring quantum entanglement from one place to another distant place. In this method, four particles are required as resource and Bell state measurements (BSM) and local operations and classical communications (LOCC) are required as tools. Better versions with only three distinguishable particles were proposed in two subsequent works, one [53] with BSM and another [54] without BSM. Entanglement swapping is widely applied in quantum repeaters.

Trace-out operation

When two particles are entangled then it is not possible to know the state of the individual particles, rather the information about the global state of the two particles is available. Now the mathematical representation of the partial state of the individual

particles can be known by the trace-out operation [20]. If suppose two particles A and B are entangled, then if trace-out operation is performed over A , then the partial information about the state of the particle B is known. Trace-out operation is very useful to detect, measure and quantify entanglement.

Entanglement measures

For various quantum information processing protocols, it is required to know how much entanglement is contained in a quantum state. The basic properties of an entanglement measure [55, 56] that it should vanish for non-entangled state, should give a positive value for entangled state and should give maximum value for maximally entangled states. There are other properties of entanglement measures like it should be invariant under local unitary transformations, it should not increase under LOCC, etc. Some commonly used entanglement measures are the entanglement of formation [57], log-negativity [58, 59], Tsallis- q entropy [60, 61], Rényi- α entanglement [62, 63], Unified- (q, s) entropy [64, 65], etc.

Monogamy of entanglement

The most interesting feature of quantum entanglement is its restriction upon the shareability among composite systems which is known as *monogamy* [66]. Qualitatively, it states that if two particles share a maximally entangled state, then they cannot share entanglement or even classical correlations with any other particles. Intuitively, it may seem that monogamy feature reduces the usefulness and the possible applications of quantum entanglement in quantum information processing tasks, but surprisingly it has applications on the security of quantum key distribution [67], quantum games [68, 69], quantum state classification [70], interconvertibility between asymptotic quantum cloning and state estimation [71, 72], condensed-matter physics [73, 74], quantum-to-classical transition [75], frustrated spin systems [76], black-hole physics [77], etc.

No Cloning theorem

One of most counter-intuitive feature of quantum physics that it forbids the creation of independent and identical copy of any arbitrary unknown quantum state known as no-cloning theorem [78, 79, 80]. It is derived from the linearity of quantum mechanics. Fundamentally, this theorem preserves the Heisenberg's uncertainty principle (HUP) [81] in quantum physics. If one could make copies of any unknown quantum states, then using those many copies, one can measure position and momentum precisely. That will violate the Heisenberg's uncertainty principle . No cloning theorem has applications in the security of quantum cryptographic protocols [67], quantum error correcting codes [82], etc.

1.2.2 Quantum indistinguishability

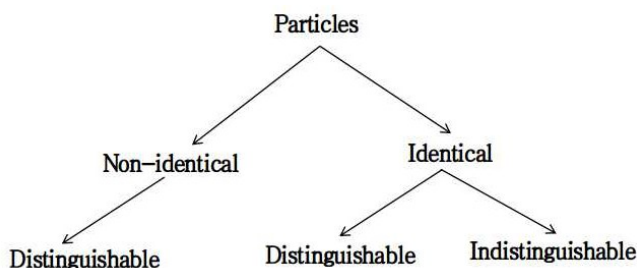


Figure 1-2: Schematic description of all the particles based on their identity and distinguishability.

All particles in the world can be divided into two categories based on their identity: (a) identical particles and (b) non-identical particles. If two particles cannot be distinguished by all of their intrinsic properties like mass, color, shape, charge etc. is known as non-identical particles. All the electrons, positrons, photons, protons, neutrons, up quarks, neutrino, hydrogen atom etc have the same intrinsic properties and they behave the same ways. Classical particles can also be identified if two classical particles have same properties like same shape, color, weight, smell etc. Non-identical particles are always distinguishable in nature but identical particles may become distinguishable by some specific method [83, 84]. This division is shown schematically in Fig. 1-2.

Two identical particles can be made indistinguishable using spatial measurements. When two identical particles are spatially separated and measured by their individual degrees of freedom, then they are distinguishable. However, when two identical particles have all degrees of freedom equal and their wave functions are spatially overlapped (partial or full), then they are indistinguishable. The concept of indistinguishability is related to the measurement process and to the eye of a detector [85, 86]. Some of these aspects are better described in Sec. 2.6.1.

1.3 Quantum computation

Classical computers perform computation using the laws of classical mechanics. However, according to Moore's law [87], the device fabrication technology will saturate to reduce its size in the first two decades of the twenty-first century. Thus as an alternate solution, quantum computation comes into the picture. Quantum computation is the method to perform computation using quantum mechanical phenomena like superpositions, entanglement, etc. The theory of quantum computation suggests that there is a huge advantage of performing a task in quantum computers rather than currently available best classical computers in terms of computing time. It can be shown theoretically that any task that the classical computers take years to complete, quantum computers can do it within a few days.

The abstract notion of computation was developed by the famous mathematician Alan Turing [88]. He proposed the first prototype of modern day computer known as Turing machine. He showed that any algorithmic task can be emulated by the Turing machine. The equivalence between physical concept of computation and the practical implementation in to some physical device was asserted in the famous *Church-Turing thesis*. It states that If any task can be performed in any physical device, then there is an equivalent algorithm that can be performed in a Turing machine. In 1980, famous physicist Richard. P. Feynman proposed that quantum systems can be effectively simulated using a quantum computer, rather than a classical one [89].

1.3.1 Quantum computing technologies

The most important question to make a physical quantum computer is how to make the hardware. There are different kind of technologies are available such as photons, electrons, trapped ions, semiconductors, etc. But there are no consensus among scientists that which technology will be most useful for future quantum computers. However, there are some properties that must be present in any quantum computer.

(i) *Isolated system*: The quantum computers must be isolated from the rest of the universe, otherwise a small amount of noise will interfere the internal operations and may alter the output.

(ii) *Small decoherence time*: An ideal noise-free quantum computer is not practically possible. A negligible amount of noise will destroy the quantum mechanical arrangements over time. The time taken this phenomenon is known as decoherence time. An effective quantum computer should have large decoherence time.

(iii) *Fault-tolerance*: How much error in the quantum computer can be corrected is known as its fault-tolerance capability. The requirement for a fault-tolerant quantum computer was proposed by DiVincenzo, known as DiVincenzo's criteria [90]. All the quantum computers much obey this criteria.

(iv) *Scalability*: The quantum computer much be scalable enough so that when the dimension of the Hilbert space grows, the cost of operation much not be exponentially increasing.

(v) *Universal set of logic*: The quantum computer much operate by a finite set of logical control operations.

Here, we briefly review some of the major quantum computing platforms and corresponding quantum processors based on the above mentioned properties as shown in Fig. 1-3.

Nuclear magnetic resonance (NMR)

The spin of the nuclei of the molecules can be used as a qubit for quantum computing. The spin states can be directly controlled using the radio frequency known as nuclear

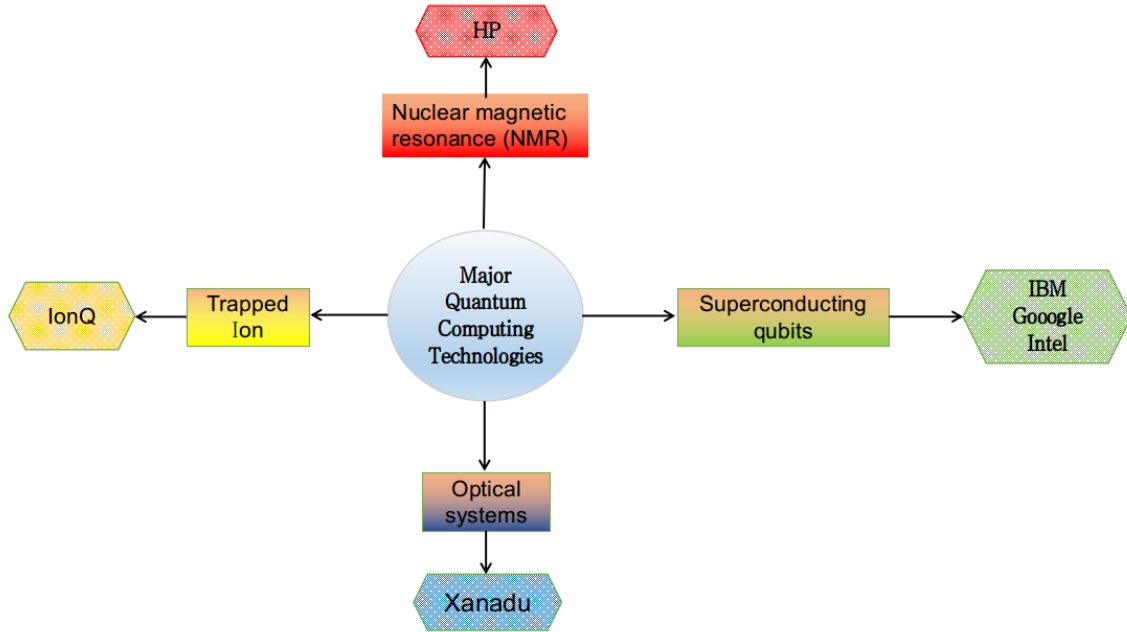


Figure 1-3: A schematic of major quantum computing technologies with corresponding quantum processors available.

magnetic resonance [91, 92, 93] and acts as a single qubit. Two-qubit interactions can be performed by the indirect coupling of the molecular electrons. The measurement of a qubit can be done by observing the current induced in a coil. The major drawback of the NMR technology is the preparation of the pure states. As large number of molecules should be gathered to output a reasonable amount of signal, thus a single qubit is represented by an ensemble of the molecules.

Trapped ion

The spin states of atoms and nuclei can be used as a qubit by trapping them in an electromagnetic cavity known as Ion trapped quantum computers [94, 95]. Once these atoms are trapped, then they are cooled until their spin energy is more than their kinetic energy. Then these atoms are controlled effectively using monochromatic light source. Ion trapped systems have very large decoherence time than other technologies. However controlling large number of atoms and performing joint state operations such as CNOT gates are difficult using ion trap quantum computer.

Superconducting qubits

The benefit of using a superconducting circuit for quantum computing is to control a large number of qubits [96, 97]. Josephson junctions are normally used as a qubit because of its longer coherence time. In a superconductor, a single super-fluid is formed by electron condensate in the Cooper pairs that moves without any resistance. There are two types of superconducting qubits, the charge qubit and the flux qubit that are related to the amplitude and the phase of the circuit respectively. However, superconducting qubits have relatively shorter decoherence time than the other quantum technologies. Also, very low temperature have to be created to use it effectively.

Optical systems

For optical systems [98, 99], photons can be used as a qubit due to negligible amount of decoherence time which is a major advantage compare to other technologies. Different degrees of freedom of photons can be used for encoding the quantum information, such as polarization, orbital angular momentum, path, etc. However, the major drawback for optical quantum computer is efficient control of multi-qubit systems due to non-availability of the required optical non-linearities. Although, with the invention of Knill-Laflamme-Milburn scheme [100], optical quantum computing becomes a possibility with required scalability.

Other technologies

Many other quantum computing technologies have been proposed based on the different technologies. Semiconductor based quantum computer known as quantum dots [101, 102, 103] are one of them where single atom in vacuum is used a qubit after cooling and trapping them. Also, single ballistic electrons [104] in very low temperature can be used as qubit instead of photons. Another example is of using rare-earth ions in crystalline hosts [105] which has long coherence time.

1.3.2 Quantum processors and simulators

Several quantum computing platforms with different archetypes as discussed above are available now, i.e., the way qubits are represented and manipulated. Here, we briefly review some of the major quantum processors available today.

IBM

IBM has given access to its quantum computer that uses superconducting qubits in the cloud and this opens a new door for testing quantum phenomena to the researchers [106]. Till now, there are over 20 devices are made by IBM, from five qubit to 53 qubits, six of which are available online for free for the students and the researchers. Various algorithms and experiments can be performed via cloud access using these simulators.

As there are researchers accessing these real processors, then there can be a long queue to perform experiments. So, IBM came up with quantum simulators that can provide an output like a real quantum computer with used defined noise models for the quantum gates.

The CHSH inequality and the GHZ paradox are already performed in the IBM quantum computer [106]. In [107], the author has implemented some protocols in quantum error correction, quantum arithmetic, quantum graph theory, and fault-tolerant quantum computation in the IBM quantum computer. In [108], the authors have tested the theoretical predictions of entropic uncertainty relation with quantum side information (EUR-QSI) in the IBM quantum computer. Leggett-Garg test [109], compressed quantum computation [110], fault-tolerant state preparation [111], fault-tolerant logical gates [112], quantum cheque [113], quantum permutation algorithm [114], Deutsch-Jozsa-like algorithm [115], Shor's factoring algorithm [116], hybrid quantum linear equation algorithm [117] are also recently performed in the IBM quantum computer.

Google

Google has build a 54 transmon qbit quantum computer named Sycamore based on nonlinear superconducting resonators which was released in 2019 [118]. It is programmable quantum computer capable of performing various quantum algorithms. This is not available for public. Only Google has access for this quantum processor and the are currently research topics are near-term applications such as quantum physics simulation, quantum chemistry and generative machine learning.

Intel

Intel has manufactured a 17 qubits superconducting quantum processor, named Tangle Lake which can incorporate upto 49 qubits [119]. Their research interests are to simulate and analyze natural phenomena, quick answers to phenomenological questions that would take excessive amounts of time on available computers, etc, They are also interests in medicine, astrophysics and weather predictions.

Xanadu

Xanadu is a quantum computer company which provides hardware and softwares for various quantum experiments based on photonic quantum computers [120] which can be accessed via cloud. Their hardware technology uses programmable Gaussian Boson Sampling (GBS) devices. They also provide some open-source quantum software for simulation of quantum algorithms.

Rigetti

Rigetti builds multi-chip quantum processors using superconducting systems which can be accessible via cloud [121]. Their processors incorporates with existing computing infrastructure which aim to solve scaling challenges of fault-tolerant quantum computers. Their mission is to build a 80-qubit quantum computing chip which can be accessible via cloud service.

D-Wave

D-Wave has build a 2000 qubit quantum computer based on quantum annealing technology [122]. It may be noted that although the number of qubits in D-Wave is more than the above quantum computer, that does not mean it is the best among them. D-Wave search solutions to a problem using large number of quits. Thus D-Wave's qubits are can be affected by noise and their quantum states are also more fragile, and their manipulation are less precise.

Other processors and simulators

Other than the above mentioned quantum processors, there are also other quantum computers such as IonQ [123], Microsoft [124], Toshiba [125], Alibaba [126], Amazon web services [127], 1QBit [128], etc.

1.4 Motivation of current work

Now we will briefly describe the open questions associated with the above topics and the motivation of the current works.

There are several tests of non-locality which has been performed in various quantum technologies. For example, Mermin inequalities [30] have been tested experimentally using photons and ion traps [129, 130], subsequently the authors of [131] have tested Mermin polynomial of three, four and five qubits in the IBM quantum computer based on superconducting qubits. Hardy's experiment is the only method to test non-locality for two qubits without using inequalities. Several experiments have been performed to demonstrate Hardy's paradox using polarization, energy-time and orbital angular momentum of photons, entangled qubits, classical light, and two-level quantum states [132, 133, 134, 135, 136, 137, 138, 139, 140, 141], but none in superconducting qubits. However, none of the experimental verifications of Hardy's non-locality have used superconducting qubits. *This motivates us to test Hardy's paradox for two qubits in a quantum computer using superconducting qubits.* This is the motivation behind Chapter 3.

In the last century, physicists were puzzled about whether “the characteristic trait of Quantum Mechanics” [142], i.e., entanglement [27], is real and, if so, whether it can show some nontrivial advantages over classical information processing tasks. The answers to both are positive. In the current century, entanglement of indistinguishable particles and its similarity with as well as difference from that of distinguishable ones have been extensively studied [143, 144, 145, 146, 147, 148, 149, 150, 151, 152, 153, 154, 155, 156, 157, 158, 159, 160, 161, 162, 163]. However, the entanglement between distinguishable and indistinguishable particles raises several non-trivial open questions:

(i) *Hyper-hybrid entangled state (HHES) was created by two indistinguishable bosons [1].*

Is it also possible for two indistinguishable fermions?

(ii) *Is the scheme for HHES, as proposed by Li et al. [1], applicable for two distinguishable particles?*

(iii) *If the scheme for HHES, as proposed by Li et al. [1], is not possible applicable for two distinguishable particles, the can distinguishable particles exhibit HHES through some other scheme?*

(iv) *Is there exist some quantum correlations and applications which unique in the case of distinguishable particles and indistinguishable particles?*

These open problems are the motivations behind Chapter 4.

Partial trace-out operation [41, 20] is a typical method of finding the reduced density matrix of a subsystem which can be either one whole particle or a single DoF for distinguishable systems. However, for indistinguishable systems, applying the above method results in a contradiction in identifying entanglement [149, 164]. Experimental works on such systems [165, 166, 167, 168, 169, 170, 171] existed earlier, but a common mathematical framework for a consistent theoretical interpretation was first attempted in [161, 163], by providing a method of partial trace-out for a whole indistinguishable particle. One may be tempted to think that the same rule can trace out a single DoF also. However, this is not so straightforward. When particles become indistinguishable, performing the partial trace-out of a particular DoF is challenging, because a DoF cannot be associated with a specific particle.

This motivates to search for a DoF trace-out rule which can be applicable to both distinguishable and indistinguishable particles when each particle have multiple DoFs. This is the basic motivation for Chapter 5.

Thus quantum teleportation fidelity [172] plays an important role in quantum information both for distinguishable and indistinguishable particles. One way to measure the teleportation fidelity is by using the singlet fraction [52] of the quantum channel used for teleportation. Singlet fraction for any state is defined as the maximum overlap of that state with the maximally entangled state. The relation between teleportation fidelity and singlet fraction was proposed by Horodecki *et al.* [52]. This relation is only applicable for distinguishable particle with a single degrees of freedom (DoF). However, for indistinguishable particles with multiple DoF, this relation no longer holds. This motivated us to find a new relation between teleportation fidelity and singlet fraction applicable both for distinguishable and indistinguishable particles where each particle have multiple DoFs. This is the basic motivation behind Chapter 6

One important feature of quantum entanglement of distinguishable particles [41] is its restriction upon the shareability among composite systems (consisting of particles or degrees of freedom (DoFs)), known as *monogamy of entanglement* (MoE). Monogamy of entanglement is widely regarded as one of the basic principles of quantum physics [173]. Qualitatively, it is always expected to hold, as a maximal violation will have consequences for the no-cloning theorem. However, it was an open problem that monogamy of entanglement can be violated maximally using indistinguishable particles and using the DoFs of the indistinguishable particles? The problem of monogamy of entanglement using DoFs of indistinguishable particles for two-qubits and more than two qubits are discussed in Chapter 7 and Chapter 8 respectively.

The main motivation of Chapter 9 is to find some new applications of indistinguishable particles. Security and efficiency are two major criteria of a cryptographic protocols. If two cryptographic systems with different resource requirements provide the same level of security, the one with less resources becomes the natural choice. The motivation behind the first application is to find how to reduce resources in the cryp-

tographic protocols without compromising the security. There are several types of attacks such as intercept and resend attack, man-in-the-middle attack, Trojan-horse attack, etc. The motivation of our second application is to find a new attack for quantum cryptographic protocols. The standard Entanglement swapping (ES) [44] required four distinguishable particles as a resource along with Bell state measurement (BSM) [174] and local operations and classical communications (LOCC) [175] as tools. Better versions with only three distinguishable particles were proposed in two subsequent works, one [53] with BSM and another [54] without BSM. Recently, Castellini *et al.* [176] have shown that ES for the indistinguishable case is also possible with four particles (with BSM for bosons and without BSM for fermions). The motivation of our final application is reduce the number of particles further in entanglement swapping protocol using distinguishable or indistinguishable particles?

1.5 Thesis organization

This thesis is organized as follow:

- In Chapter 2, we present the necessary background studies, mathematical formulation, and applications needed to understand our proposed works in rest of the thesis.
- In Chapter 3, We experimentally verify Hardy’s paradox for two qubits on a quantum computer based on superconducting circuits. We argue that for practical verification of Hardy’s test, the error-modeling used for optical circuits cannot be used for superconducting qubits in 3.2. We propose a new error-modeling and a new method to estimate the lower bound on Hardy’s probability for superconducting qubits. We also point out that the earlier tests performed in optical circuits and in the IBM quantum computer have not analyzed the test results in a statistically correct and coherent way in 3.4. We analyze our data using Student’s t-distribution [177] which is the statistically correct way to represent the test results. Our statistical analysis leads to the conclusion that

any two-qubit non-maximally entangled state (NMES) gives a nonzero value of Hardy's probability, whereas any two-qubit maximally entangled state (MES) as well as any product state (PS) yields a zero value of Hardy's probability. We identify the difficulties associated with the practical implementation of quantum protocols based on Hardy's paradox and discuss how to overcome them in 3.4.3. We propose two performance measures for any two qubits of any quantum computer based on superconducting qubits. Finally, we discuss benchmarking of superconducting quantum devices using Hardy's paradox in 3.4.6.

- In Chapter 4, some of the open questions related to distinguishable and indistinguishable particles and their properties and applications. Using systematic calculations we establish that hyper-hybrid entangled state is possible using two indistinguishable fermions in Chapter 4.1 and also presented a generalized version for hyper-hybrid entangled state applicable for bosons and fermions in Chapter 4.1.1. Next, we show that the scheme of Li *et al.* [1] for producing hyper-hybrid entanglement using two indistinguishable particles does not work for distinguishable particles in Chapter 4.2. After that, in Chapter 4.3, we prove that *If quantum particles (either distinguishable or indistinguishable) can simultaneously produce and perform hyper hybrid entangled state and unit fidelity quantum teleportation respectively then using that cloning of any arbitrary quantum state is possible..* Next, in Chapter 4.4, we establish the first *no-go* result: HHES is not possible for distinguishable particles; otherwise, exploiting it, signaling can be achieved. In Chapter 4.5, we prove our second *no-go* result that unit fidelity quantum teleportation is not possible for indistinguishable particles. Using the above two no-go theorem, we establish a separation result using quantum properties and applications between distinguishable and indistinguishable particles in Chapter 4.6.
- In Chapter 5, we have proposed a new degrees of freedom trace-out rule applicable for both distinguishable and indistinguishable particles, each having multiple degrees of freedom. First we represent two indistinguishable particles

each having two DoFs in 5.1.1 and n DoFs in 5.1.2. Then we generalize it for p indistinguishable particles, each having n DoFs in 5.1.3. Next, We establish a generalized DoF trace-out rule for two indistinguishable particles each having two DoFs in 5.2.1 and n DoFs in 5.2.2. This rule is generalized for p indistinguishable particles, each having n DoFs in 5.2.3. Finally we present the physical significance of our DoF trace-out rule in 5.3.

- In Chapter 6, we establish a generalized relation between teleportation fidelity [172] and singlet fraction [52] for both distinguishable and indistinguishable particles with where each particle has multiple DoFs. First we have defined the generalized teleportation fidelity in 6.1 and generalized singlet fraction in 6.2. After generalizing the relation between above two in 6.3, we prove an upper bound for generalized singlet fraction for distinguishable and indistinguishable particles in 6.6. Finally, we state the physical significance of our new generalized relation in 6.7.
- In Chapter 7, using this generalized DoF trace-out, we show that monogamy of entanglement can be violated maximally by indistinguishable particles in qubit systems for measures (such as squared concurrence, log-negativity, etc.) that are monogamous for distinguishable particles. First, we describe the condition for violation of no-cloning theorem using the maximum violation of monogamy of entanglement in 7.1. Then we give an example of an apparent violation of particle-based monogamy of entanglement in 7.2. To remove this ambiguity, we generalized the monogamy relation from particle view to degree of freedom view in 7.3. Then we prove the following theorem that *In qubit systems, indistinguishability is a necessary criterion for maximum violation of monogamy of entanglement by the same measures that are monogamous for distinguishable particles* in 7.4. Finally, we discuss the physical significance of the maximum violation of monogamy in 7.5.
- In Chapter 8, we have shown that monogamy of entanglement using three indistinguishable particles is obeyed using squared concurrence as an entanglement

measure. First, we show how to calculate the concurrence between two spatial regions between any DoFs in 8.1. Then we present the proof of monogamy inequality for three or more indistinguishable particles becomes equality for pure states in 8.2 and for mixed states it remains an inequality in 8.2.3. At last, we discuss the physical significance of our results in 8.3.

- In Chapter 9, we present some applications of indistinguishable particles. First, we show We show that for device independent test such as quantum pseudo-telepathy game [178, 179], the cost of adding an ancilla particle can be bypassed by using an additional degrees of freedom and creating multi-DoF entanglement in quantum private query protocol where the success probability remains the same but the generalized singlet fraction changes in 9.1. Next we show how indistinguishability can change Hardy's probability which can be used as an attack in quantum cryptographic protocols in 9.2. Finally, in Section 9.3, we have proposed an Entanglement Swapping protocol using only two indistinguishable particles without using Bell state measurement.
- In Chapter 10, we summarize each of the contributing chapters, discuss the open problems related to those chapter, and our future plans.

Chapter 2

Background

In this section, all the technical backgrounds to understand the rest of the thesis is presented.

2.1 Statistical interpretation of experimental results

Here, we discuss how any experimental analysis should be performed using some basics of statistics.

2.1.1 Standard normal distribution vs. Students t-distribution

It is known from the central limit theorem [177] that if $\{X_1, X_2, \dots, X_n\}$ are independent and identically distributed random samples drawn from any population with mean μ and variance σ^2 and if n is large, then the sample mean

$$\bar{X} = \frac{1}{n} \sum_i^n X_i \tag{2.1}$$

follows a normal distribution with mean μ and variance σ^2/n , i.e., $\bar{X} \sim N(\mu, \sigma^2/n)$.

It follows that the variable

$$Z = \frac{\bar{X} - \mu}{\sqrt{\sigma^2/n}},$$

follows the standard normal distribution, i.e., $Z \sim N(0, 1)$. If the population variance σ^2 is unknown, it is replaced by its closest approximation, i.e., the sample variance S^2 . Then the quantity follows a Students t-distribution [177] described as

$$T = \frac{\bar{X} - \mu}{\sqrt{S^2/n}}, \quad \text{where } S^2 = \frac{1}{n-1} \sum_{i=1}^n (X_i - \bar{X})^2.$$

Moreover, while normal approximation works only for very large n (ideally infinite), the Students t-distribution holds for small n as well. This distribution is a function of the degrees of freedom, which is one less than the number of times the experiment is repeated. As the number of degrees of freedom tends to infinite, the Student's t-distribution converges to the normal distribution.

2.1.2 Hypothesis testing and confidence interval

We know that it is impossible to conduct any experiment without any error. So, when the conclusion is drawn from an experimental result, it is not appropriate to claim that the results are 100% correct. Statistically speaking, we can only test a hypothesis and conclude the test based on our experimental results with some percentage of confidence in our conclusion. In hypothesis testing [177], we turn a question of interest into a hypothesis about the value of a parameter or a set of parameters. In our case, suppose we want to test whether a given state is NMES or not. Then, according to the notion of hypothesis testing, we can have the following formulation from Equation (3.9).

Test the null hypothesis

$$\mathcal{H}_0 : q = 0 \quad (\text{The unknown state is not an NMES})$$

against the alternative hypothesis

$$\mathcal{H}_1 : q > 0 \quad (\text{The unknown state is an NMES}).$$

So it is evident that our test will be a one-sided test³ as q is a non-negative quantity. The significance level α is equal to the false-positive error or Type I error which is defined by the probability $\Pr(\text{reject } \mathcal{H}_0 \mid \mathcal{H}_0 \text{ is correct})$ where $0 \leq \alpha \leq 1$. The level of confidence is defined by $(1 - \alpha)$ or $100(1 - \alpha)\%$. Let us assume that an experiment is repeated n number of times, where μ , \bar{X} , σ , and S are the population mean, sample mean, population standard deviation and sample standard deviation respectively. Again, let $100(1 - \alpha)\%$ confidence interval (CI) of \bar{X} be the interval $[X_{lb}, X_{ub}]$. This means that we have $100(1 - \alpha)\%$ confidence that μ will lie in between X_{lb} and X_{ub} .

For the standard normal distribution, the expression for $100(1 - \alpha)\%$ confidence interval for the mean in the above situation is $(\bar{X} \pm z_{\frac{\alpha}{2}} \frac{\sigma}{\sqrt{n}})$, where $z_{\frac{\alpha}{2}}$ is the value of the standard normal variable Z such that

$$\Pr(-z_{\frac{\alpha}{2}} < Z < z_{\frac{\alpha}{2}}) = (1 - \alpha).$$

For this case, $X_{lb} = (\bar{X} - z_{\frac{\alpha}{2}} \frac{\sigma}{\sqrt{n}})$ and $X_{ub} = (\bar{X} + z_{\frac{\alpha}{2}} \frac{\sigma}{\sqrt{n}})$. Here, $z_{\frac{\alpha}{2}}$ depends only on the value of α . For the Student's t-distribution, the expression for $100(1 - \alpha)\%$ confidence interval is given by $\bar{X} \pm t_{\frac{\alpha}{2}} \frac{S}{\sqrt{n}}$ where $t_{\frac{\alpha}{2}}$ is given by the following expression

$$\Pr(-t_{\frac{\alpha}{2}} < T < t_{\frac{\alpha}{2}}) = (1 - \alpha).$$

For this case, $X_{lb} = (\bar{X} - t_{\frac{\alpha}{2}} \frac{S}{\sqrt{n}})$ and $X_{ub} = (\bar{X} + t_{\frac{\alpha}{2}} \frac{S}{\sqrt{n}})$. Here, $t_{\frac{\alpha}{2}}$ depends on the value of α and the degrees of freedom $\nu = (n - 1)$, where n is the number of samples used for the experiment. As $\nu \rightarrow \infty$, we have $t_{\frac{\alpha}{2}} \rightarrow z_{\frac{\alpha}{2}}$.

2.2 Quantum non-locality

Quantum non-locality as shown in Fig. 1-1 is the strongest form of quantum correlations. The existence of this type of correlations was first proved by the violations

³Two-sided test typically applies to $\mathcal{H}_0 : X = p$ vs $\mathcal{H}_1 : X \neq p$ and one-sided test $\mathcal{H}_0 : X = p$ vs $\mathcal{H}_1 : X > p$ or $\mathcal{H}_1 : X < p$ where X is the chosen parameter under test and p is a specific value.

of Clauser-Horne-Shimony-Holt (CHSH) inequality. Later, non-locality was proved without using inequality. For, two-qubits, Hardy's test is used to verify non-locality.

2.2.1 Clauser-Horne-Shimony-Holt (CHSH) inequality

The verifications of Bell's theorem can be experimentally performed using CHSH inequality. Let us assume, two parties, Alice and Bob are sharing a physical system which they can measure and see the outcome. They us denote the the measurements of Alice are A_1 and A_2 . Similarly, the measurements of Bob are denoted by B_1 and B_2 . The measurements outputs are denoted by $+1$ or -1 . Now let us calculate the quantity

$$\text{CHSH} = A_1B_1 + A_1B_2 + A_2B_1 - A_2B_2. \quad (2.2)$$

Clearly, from the basic algebra, it can be shown that the maximum and the minimum value of Eq. (2.2) is $+2$ and -2 respectively. Let, $E(\bullet)$ denote the expectation value of a quantity then we can write

$$E(\text{CHSH}) = E(A_1B_1) + E(A_1B_2) + E(A_2B_1) - E(A_2B_2) \leq 2 \quad (2.3)$$

This is known as the CHSH inequality. It can be shown that for some quantum systems this inequality can be violated which supports the existence of non-locality.

2.2.2 Hardy's test of non-locality

Hardy's test of non-locality for two qubits involves two non-communicating distant parties, Alice and Bob. A physical system consisting of two subsystems is shared between them. Alice and Bob can freely measure and observe the measurement results of their own subsystems. Alice can perform the measurement on her own subsystem by choosing freely one of the two $\{+1, -1\}$ -valued random variables A_1 and A_2 . Similarly, Bob can also choose freely one of the two $\{+1, -1\}$ -valued random variables B_1 and B_2 for measuring the subsystem in his possession.

Hardy's test of non-locality starts with the following set of joint probability equa-

tions.

$$P(+1, +1|A_1, B_1) = 0, \quad (2.4)$$

$$P(+1, -1|A_2, B_1) = 0, \quad (2.5)$$

$$P(-1, +1|A_1, B_2) = 0, \quad (2.6)$$

$$P(+1, +1|A_2, B_2) = q, \quad \text{where} \quad \begin{cases} q = 0 & \text{for LHV theory,} \\ q > 0 & \text{for non-locality.} \end{cases} \quad (2.7)$$

Here $P(x, y|A_i, B_j)$ denotes the joint probability of obtaining outcomes $x, y \in \{+1, -1\}$ given that A_i and B_j were the experimental choices made where $i, j \in \{1, 2\}$. If an experiment is designed in such a way that Equations (2.4), (2.5), and (2.6) are satisfied, then for any LHV theory, the right-hand side of Equation (2.7) becomes zero. But if this value is found to be greater than zero for some values of q , then non-locality is established. The set of Equations (2.4)-(2.7) are called *Hardy's equations* and q is called *Hardy's probability*.

It can be easily shown that a greater than zero value of Equation (2.7) implies non-locality under the assumptions of Equations (2.4)-(2.6). Let us assume that, when A_2 and B_2 are measured simultaneously, an event with $A_2 = B_2 = +1$ is detected. It can be seen from Equation (2.5) that the measurement of B_1 must yield the output $+1$, as $A_2 = 1$ can never occur with $B_1 = -1$, the only option left is $B_1 = +1$. Following the same logic, from Equation (2.6), it can be concluded that $A_1 = +1$ must occur, as the value of $B_2 = 1$ can never be detected with $A_1 = -1$. Also, because of the locality assumption, the value of B_1 must be independent of whether Alice measures A_1 or A_2 . Similarly, the value of A_1 must be independent of whether Bob measures B_1 or B_2 . So, it can be concluded from LHV theory that the values of A_1 and B_1 must be $+1$. But this is not possible as shown in Equation (2.4). So, given Equations (2.4)-(2.6) are satisfied, a single occurrence of the event $A_2 = B_2 = +1$ can rule out all possibilities that experiment can be described by an LHV theory.

The maximum value of Hardy's probability q is found to be $q_{max} = \frac{5\sqrt{5}-11}{2} \approx 0.09017$ for two qubits [35, 180]. For the two-qubit system, no MES as well as no PS

obey Hardy’s non-locality, but all NMES exhibit Hardy’s non-locality [181]. This is the specialty of Hardy’s test that only a single event can discard all LHV theories. The motivation of this work is to validate this statement for the quantum computer using superconducting qubits. As every MES of three or higher qubits exhibits Hardy’s non-locality, we restrict our discussion for two qubits only.

2.2.3 Equivalence between CHSH inequality and Hardy’s equations

Using simple set-theoretic arguments, one can show that Hardy’s equations are a special case of the famous CHSH inequality [182]. The CHSH version of Hardy’s Equations [183] is described as

$$P(+1, +1|A_2, B_2) - P(+1, +1|A_1, B_1) - P(+1, -1|A_2, B_1) - P(-1, +1|A_1, B_2) \leq 0. \tag{2.8}$$

A violation of Equation (4.5) means a violation of local realism, which supports non-locality. Putting the ideal values of the probabilities from Equations (2.4)-(2.7) into Equation (4.5), we get $q \leq 0$. So, $q = 0$ supports LHV theory and $q > 0$ supports non-locality.

2.2.4 Revisiting known experimental results on Hardy’s test and their statistics

In this section, first we revisit important experimental works on Hardy’s test in optical set-up. Next, we look into significant experiments performed in IBM quantum computer.

Prior works on Hardy’s test in optical set-up

In this section, we will survey the major experiments performed for Hardy’s test using optical circuits so far. Their set-up and the results are summarized in Table 2.1.

Authors	Year	Distribution of data	number of samples mentioned?	Form: mean \pm SD	CI Representation
Irvine <i>et al.</i> [133]	2005	Not specified	Not specified	Yes	No
Lundeen <i>et al.</i> [134]	2009	Poissonian	Not specified	Yes	No
Yokota <i>et al.</i> [135]	2009	Poissonian	Not specified	Yes	No
Fedrizzi <i>et al.</i> [184]	2011	Not specified	Not specified	Yes	No
Vallone <i>et al.</i> [136]	2011	Not specified	Not specified	Yes	No
Chen <i>et al.</i> [137]	2012	Not specified	Not specified	Yes	No
karimi <i>et al.</i> [138]	2014	Poissonian	Not specified	Yes	No
Zhang <i>et al.</i> [139]	2016	Not specified	Not specified	Yes	No
Fan <i>et al.</i> [140]	2017	Poissonian	Not specified	Yes	No
Chen <i>et al.</i> [141]	2017	Not specified	Not specified	Yes	No
Luo <i>et al.</i> [185]	2018	Poissonian	Not specified	Yes	No
Yang <i>et al.</i> [186]	2019	Poissonian	Not specified	Yes	No

Table 2.1: Summary of prior works on Hardy’s test in optical set-up where SD=standard deviation and CI=confidence interval.

In [133, 184, 136, 137, 139, 141], the authors have represented their coincidence count in mean \pm standard deviation form but they did not specify the distribution of the sample data and the number of samples taken. They also did not represent the confidence on their data.

In [134, 135, 138, 140, 185, 186], the authors have mentioned that they have assumed that all the error bars follow the Poissonian statistics for the coincidence count and they have represented their data in mean \pm standard deviation form. But again, they did not mention the distribution of samples and number of samples they have used and confidence on their data.

Significant experiments performed in superconducting qubits

We present a survey of the other experiments done in the IBM quantum computer and their statistical representation of the results which are summarized in Table 2.2. In [107, 108, 131], the authors have represented the error in their experiments by the standard formula $\sqrt{p(1-p)/8192}$, where p is the estimate of the probability of a given measurement outcome in a given experiment. However, some authors [131,

Authors	Year	n	s	Form: mean \pm SD	CI Representation
S. J. Devitt [107]	2016	1	8192	No	No
Alsina <i>et al.</i> [131]	2016	1	8192	Yes	No
Berta <i>et al.</i> [108]	2016	1	8192	No	No
Huffman <i>et al.</i> [109]	2017	10	8192	Yes	No
Hebenstreit <i>et al.</i> [110]	2017	1	8192	No	No
Behara <i>et al.</i> [113]	2017	1	1024, 4096, 8192	No	No
Yalçinkaya <i>et al.</i> [114]	2017	5	8192	Yes	No
W. Hu [187]	2018	1	8192	No	No
Gangopadhyay <i>et al.</i> [115]	2018	10	8192	Yes	No
Lee <i>et al.</i> [117]	2019	1	1024	No	No

Table 2.2: Significant experiments performed in IBM five-qubit quantum computer and their error statistics where n = number of times the experiment has been performed, s =number of shots in each time, SD=standard deviation, and CI=confidence interval.

[109, 114, 115] have represented their data in the form of mean \pm standard deviation but none of them have represented their data in confidence interval form.

2.3 Quantum entanglement

Here, we discuss the definition of entanglement of distinguishable and indistinguishable particles as proposed in [188, 189, 190] and followed in the rest of the thesis.

2.3.1 Definition of entanglement

Let us consider a many-body system which is represented by the Hilbert space \mathcal{H} . The algebra of all bounded operators, which includes all the observables, is represented by $\mathcal{Z}(\mathcal{H})$. In this algebraic framework, the standard notions of states and the tensor product partitioning of \mathcal{H} are changed into the observables and local structures of $\mathcal{Z}(\mathcal{H})$. Now before defining entanglement, we define *algebraic bipartition* and *local operators*.

Algebraic bipartition

An algebraic bipartition of operator algebra $\mathcal{Z}(\mathcal{H})$ is any pair $(\mathcal{A}, \mathcal{B})$ of commuting subalgebras of $\mathcal{Z}(\mathcal{H})$ such that $\mathcal{A}, \mathcal{B} \in \mathcal{Z}(\mathcal{H})$. If any element of \mathcal{A} commutes with any element of \mathcal{B} , then $[\mathcal{A}, \mathcal{B}] = 0$.

Local operators

For any algebraic bipartition $(\mathcal{A}, \mathcal{B})$, an operator is called a local operator if it can be represented as the product AB , where $A \in \mathcal{A}$ and $B \in \mathcal{B}$.

Entangled states

For any algebraic bipartition $(\mathcal{A}, \mathcal{B})$, a state ρ on the algebra $\mathcal{Z}(\mathcal{H})$ is called separable if the expectation of any local operator AB can be decomposed into a linear convex combination of products of local expectations, as follows

$$\begin{aligned} \text{Tr}(\rho AB) &= \sum_k \lambda_k \text{Tr}(\rho_k^{(1)} A) \text{Tr}(\rho_k^{(2)} B), \\ \lambda_k &\geq 0, \quad \sum_k \lambda_k = 1, \end{aligned} \tag{2.9}$$

where $\rho_k^{(1)}$ and $\rho_k^{(2)}$ are given states on $\mathcal{Z}(\mathcal{H})$; otherwise the state ρ is said to be entangled with respect to the algebraic bipartition $(\mathcal{A}, \mathcal{B})$. Note that, this algebraic bipartition can also be spatial modes like distinct laboratories each controlled by Alice and Bob. If any state cannot be written in the above form, then it would certainly violate the CHSH inequality. Therefore, we use the violation of the CHSH inequality as an indicator of entanglement.

2.3.2 Types of entanglement

Quantum entanglement is encoded in the particle's degrees of freedom (DOFs) like spin, polarization, path, angular momentum, etc. Based on the arrangement entanglement in the DOFs of particles, we have the following types of entanglement structures

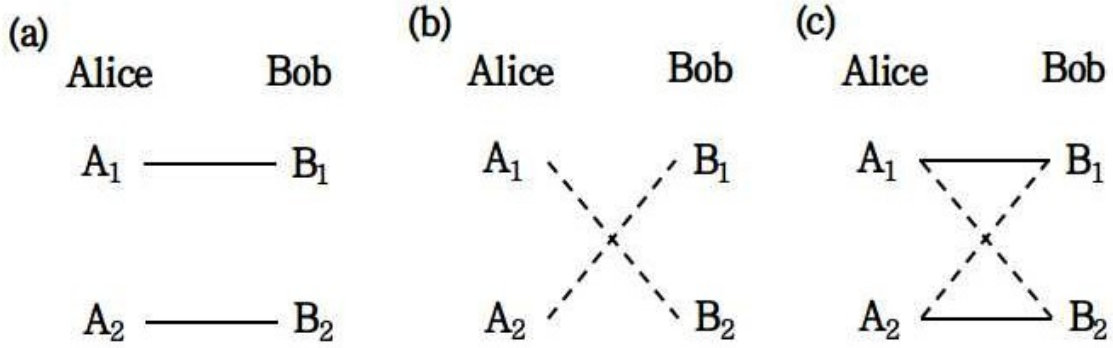


Figure 2-1: From left to right: (a) hyper-entanglement (solid lines), (b) hybrid-entanglement (dotted lines), and (c) hyper-hybrid entangled state of two qubits with two degrees of freedom.

Hyper entanglement

Suppose two particles A and B , each having two DoFs, are with the possession of Alice and Bob. Hyper-entanglement [191] means the simultaneous presence of entanglement in similar kind of multiple DOFs as shown in Fig. 2-1 (a) where A_1 is entangled with B_1 , and A_2 is entangled with B_2 . It is useful for some tasks like complete Bell state analysis [192], entanglement concentration [193], purification [194], etc. [195].

Hybrid entanglement

If the entanglement is present between different DoFs, then it is known as hybrid entanglement [196, 197]. In the Fig. 2-1 (b), A_1 is entangled with B_2 and similarly A_2 is entangled with B_1 . Hybrid entanglement is useful in quantum repeaters [198], quantum erasers [199], quantum cryptography [200], etc. [201, 202, 203].

Hyper-hybrid entanglement

Hyper-Hybrid entanglement means the the simultaneous presence of these two above types of entanglements. In the Fig. 2-1 (c), every DoF of one particle is entangled with all other DoFs of the other particle. Hyper-hybrid entanglement is useful for Complete Bell-state analysis [1]. Although hyper-entanglement and hybrid entanglement were separately known for more than two decades, interestingly, the simultaneous presence

of these two has been proposed very recently by Li *et al.* [1] in 2018 using spin and momentum DoF. The above three types of entanglements are shown schematically in Fig. 2-1.

2.3.3 Representation and degrees of freedom trace-out rule for two distinguishable particles each having n DoFs

Trace-out operation is very useful tool to represent the reduced density matrix of any density matrix. In this section, we will represent the general state, density matrix and the degree of freedom (DoF) trace-out rule for two distinguishable particles.

Let two distinguishable particles A and B each having n DoFs. The i -th and the j -th DoF of A and B are represented by a_i and b_j respectively where $i, j \in \mathbb{N}_n := \{1, 2, \dots, n\}$. Suppose each DoF is d -dimensional whose eigenvalues are denoted by $\mathbb{D}_k := \{D_{k_1}, D_{k_2}, \dots, D_{k_d}\}$ where $k \in \mathbb{N}_n$. The general state of A and B is denoted by

$$|\Psi^{(2,n)}\rangle_{AB} = \sum_{a_1, a_2, \dots, a_n, b_1, b_2, \dots, b_n} \kappa_{b_1 b_2 \dots b_n}^{a_1 a_2 \dots a_n} |a_1 a_2 \dots a_n\rangle \otimes |b_1 b_2 \dots b_n\rangle, \quad (2.10)$$

where $a_i \in \mathbb{D}_i$, $b_j \in \mathbb{D}_j$, and $i, j \in \mathbb{N}_n$.

The general density matrix can be represented as

$$\rho_{AB}^{(2,n)} = \sum_{\substack{a_1, a_2, \dots, a_n, \\ u_1, u_2, \dots, u_n \\ b_1, b_2, \dots, b_n, \\ v_1, v_2, \dots, v_n}} \kappa_{b_1 b_2 \dots b_n}^{a_1 a_2 \dots a_n} \kappa_{v_1 v_2 \dots v_n}^{u_1 u_2 \dots u_n} |a_1 a_2 \dots a_n\rangle |b_1 b_2 \dots b_n\rangle \otimes \langle u_1 u_2 \dots u_n | \langle v_1 v_2 \dots v_n |, \quad (2.11)$$

where $a_i, u_i \in \mathbb{D}_i$, $b_j, v_j \in \mathbb{D}_j$, and $i, j \in \mathbb{N}_n$.

If $\rho_{AB}^{(2,n)} = |\Psi^{(2,n)}\rangle_{AB} \langle \Psi^{(2,n)}|_{AB}$ then Eq. (2.11) is represented as

$$\rho_{AB}^{(2,n)} = \sum_{\substack{a_1, a_2, \dots, a_n, \\ u_1, u_2, \dots, u_n \\ b_1, b_2, \dots, b_n, \\ v_1, v_2, \dots, v_n}} \kappa_{b_1 b_2 \dots b_n}^{a_1 a_2 \dots a_n} \kappa_{v_1 v_2 \dots v_n}^{u_1 u_2 \dots u_n*} |a_1 a_2 \dots a_n\rangle |b_1 b_2 \dots b_n\rangle \otimes \langle u_1 u_2 \dots u_n | \langle v_1 v_2 \dots v_n |, \quad (2.12)$$

where $*$ denotes complex conjugate.

If we want to trace-out the i -th DoF of particle A , then from Eq. (2.11), the

reduced density matrix can be written as

$$\rho_{a_{\bar{i}}} \equiv \text{Tr}_{a_i} \left(\rho_{AB}^{(2,n)} \right) := \sum_{\substack{a_i, a_{\bar{i}}, u_i u_{\bar{i}}, \\ b_1, b_2, \dots, b_n, \\ v_1, v_2, \dots, v_n}} \kappa_{b_1 b_2 \dots b_n v_1 v_2 \dots v_n}^{a_{\bar{i}} u_{\bar{i}}} |a_{\bar{i}}\rangle |b_1 b_2 \dots b_n\rangle \langle u_{\bar{i}}| \langle v_1 v_2 \dots v_n| \{ \langle a_i | c_i \rangle \}, \quad (2.13)$$

where $a_{\bar{i}} = a_1 a_2 \dots a_{i-1} a_{i+1} \dots a_n$ and similar meaning for $u_{\bar{i}}$. One can show that when the DoF trace-out rule in Eq. (2.13) is applied to the same particle for n times, it becomes equivalent to our familiar particle trace-out rule [20, Eq. 2.178].

2.4 Measures of entanglement

There are various methods to measure quantum entanglement [55]. Let us denote an entanglement measure by \mathbb{E} and a density matrix by ρ , then the following properties which any entanglement measure should follow.

1. The value of ρ is zero if ρ is a separable state.
2. The entanglement measure should be invariant under local local unitary transformations, i.e., for any unitary operator U_1 and U_2

$$\mathbb{E}(\rho) = \mathbb{E}(U_1 \otimes U_2 \rho U_1^\dagger \otimes U_2^\dagger). \quad (2.14)$$

3. Entanglement cannot be increased by local operations and classical communications.
4. The convexity property should be obeyed by the entanglement measure, i.e., for any two density matrix ρ_1 and ρ_2

$$\mathbb{E}(\epsilon \rho_1 + (1 - \epsilon) \rho_2) \leq \epsilon \mathbb{E}(\rho_1) + (1 - \epsilon) \mathbb{E}(\rho_2) \quad (2.15)$$

for all $\epsilon \in [0, 1]$.

5. They should follow the additivity property, i.e., for n copies of ρ then

$$\mathbb{E}(\rho^{\otimes n}) = n\mathbb{E}. \quad (2.16)$$

Now, we will briefly review some of the entanglement measures used in this thesis.

2.4.1 Concurrence

For any density matrix ρ , the concurrence \mathcal{C} [204] of ρ can be calculated as

$$\mathcal{C}(\rho) = \max(0, \sqrt{\lambda_4} - \sqrt{\lambda_3} - \sqrt{\lambda_2} - \sqrt{\lambda_1}) \quad (2.17)$$

where λ_i are the eigenvalues of the matrix

$$\mathbb{R} = \rho (\sigma_y \otimes \sigma_y \rho^* \sigma_y \otimes \sigma_y) \quad (2.18)$$

in the decreasing order, $*$ denotes complex conjugation and σ_y is Pauli matrix. This concurrence measure is very useful for pure and mixed states in two dimensions. Moreover, concurrence is not additive.

2.4.2 Negativity

The Negativity \mathcal{N} [58, 59] of any density matrix ρ is defined as

$$\mathcal{N}(\rho) = \frac{\|\rho^{\text{T}_B}\|_1 - 1}{2} \quad (2.19)$$

where $\|\dots\|_1$ denotes the trace-norm, i.e., the sum of all the singular values of the partially transposed reduced density matrix. It can be proved that the negativity is convex in nature. Also it is easy to compute. However, like concurrence, it is also not additive. To achieve additivity, let us define logarithmic negativity as

$$\mathbb{E}_{\mathcal{N}}(\rho) = \log_2 \|\rho^{\text{T}_B}\|_1. \quad (2.20)$$

However, log-negativity is not convex [205].

2.4.3 Other measures of entanglement

Some other commonly used entanglement measures are entanglement of formation [57], Tsallis-q entropy [60, 61], Rényi- α entanglement [62, 63], Unified-(q, s) entropy [64, 65], etc. [55, 56], one-way distillable entanglement [206], squashed entanglement [207, 208], etc. Most of the measures works in two-qubit systems but not applicable in higher dimensions, specially on the mixed states. A universal measure of entanglement which obeys all the features is the ‘‘Holy Grail’’ of quantum entanglement theory.

2.5 Monogamy of entanglement

Monogamy of entanglement (MoE) is an unique feature of quantum correlations which is absent in classical correlations. A bipartite entanglement measure \mathbb{E} that obeys the relation

$$\mathbb{E}_{A|B}(\rho_{AB}) + \mathbb{E}_{A|C}(\rho_{AC}) \leq \mathbb{E}_{A|BC}(\rho_{ABC}), \quad (2.21)$$

for all ρ_{ABC} where $\rho_{AB} = \text{Tr}_C(\rho_{ABC})$, $\rho_{AC} = \text{Tr}_B(\rho_{ABC})$, $\mathbb{E}_{X|Y}$ measures the entanglement between the systems X and Y of the composite system XY , and the vertical bar represents bipartite splitting, is called *monogamous*. Such inequality was first shown for squared concurrence (\mathcal{C}) [204, 209] by Coffman, Kundu and Wootters (CKW) for three parties [66] and later generalized for n parties [210].

Equation (2.21) states that, the sum of the pairwise entanglement between A and the other particles, i.e., B and C cannot exceed the entanglement between A and the remaining particles are taken together as a whole system. From Eq. (2.21), it follows that if $\mathbb{E}_{A|B}(\rho_{AB}) = \mathbb{E}^{max}$, then necessarily $\mathbb{E}_{A|B}(\rho_{AB}) = \mathbb{E}_{A|BC}(\rho_{ABC})$ for any ρ_{ABC} and $\mathbb{E}_{A|C}(\rho_{AC}) = 0$ which leads to the qualitative description of monogamy as stated earlier.

Not all entanglement measures follow Eq. (2.21). Those who follow for all ρ_{ABC} is

known to be monogamous in nature. Some commonly used monogamous entanglement measures for qubit systems are the entanglement of formation [57], log-negativity [58, 59], Tsallis-q entropy [60, 61], Rényi- α entanglement [62, 63], Unified-(q, s) entropy [64, 65], etc. [55, 56]. For higher dimensional systems, squared concurrence is known to violate [211] Eq. (2.21), and only a few entanglement measures are monogamous like one-way distillable entanglement [206] and squashed entanglement [207, 208].

2.5.1 Coffman, Kundu, and Wootters (CKW) monogamy inequality

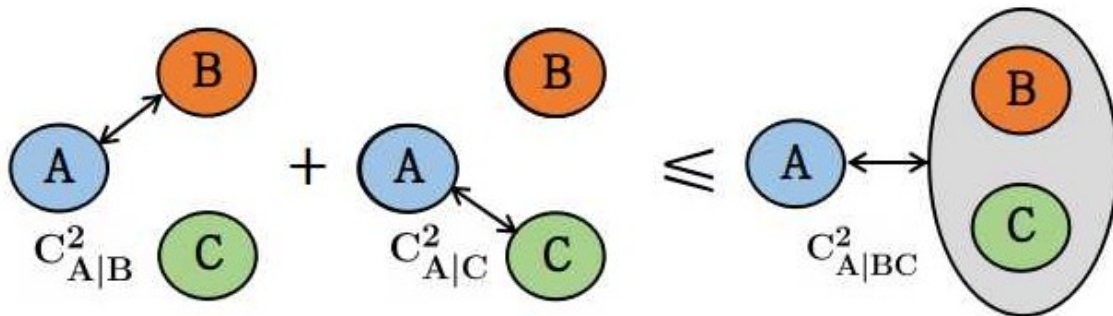


Figure 2-2: CKW inequality for distinguishable particles using square of the concurrence as entanglement measure.

Monogamy of entanglement was first introduced by Coffman, Kundu, and Wootters (CKW) [66] in terms of an inequality which is famously known as CKW inequality for arbitrary states of three qubits using squared concurrence [204, 209] as entanglement measure [55]. Let A , B , and C are three particles whose joint density matrix is ρ_{ABC} . The concurrence between any two particles, let A and B , whose reduced density matrix is $\rho_{AB} = \text{Tr}_C(\rho_{ABC})$, can be calculated as

$$\mathcal{C}_{A|B}(\rho_{AB}) = \max\{\lambda_1 - \lambda_2 - \lambda_3 - \lambda_4, 0\}, \quad (2.22)$$

where λ_i 's ($i \in \{1, 2, 3, 4\}$) are the square root of the eigenvalues of the non-hermitian matrix $\mathbb{R} = \rho_{AB}\tilde{\rho}_{AB}$ in decreasing order, $\tilde{\rho}_{AB} = (\sigma_y \otimes \sigma_y \rho_{AB}^* \sigma_y \otimes \sigma_y)$, σ_y is Pauli

matrix, the asterisk denotes complex conjugation and the vertical represents bipartite splitting. Similarly, $\mathcal{C}_{A|C}(\rho_{AC})$ can be calculated. Now the CKW inequality can be written as

$$\mathcal{C}_{AB}^2(\rho_{AB}) + \mathcal{C}_{AC}^2(\rho_{AC}) \leq \mathcal{C}_{A|BC}^2(\rho_{ABC}). \quad (2.23)$$

This inequality states that sum of the square of the pairwise concurrence between A and the other particles, i.e., B and C cannot exceed the square of the concurrence between A and the remaining particles taken together as a whole system. Equation (2.23) was originally proved for arbitrary states of three qubits. Later it was generalized for multi-qubit systems in [210]. All bipartite qubit systems obey Eq. (2.23).

2.5.2 Equivalence of the monogamy of entanglement and the no-cloning theorem for distinguishable particles

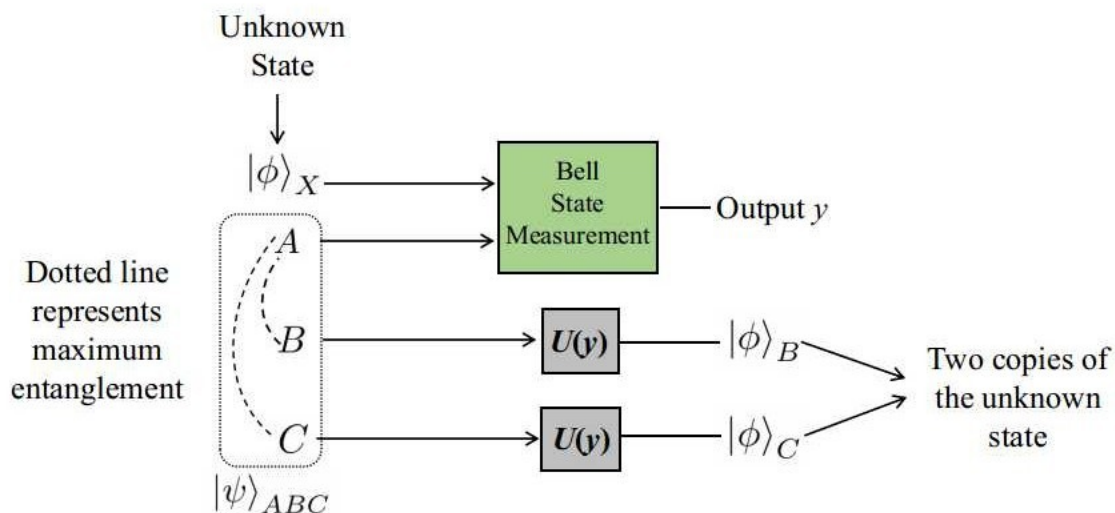


Figure 2-3: Circuit to get violation of the no-cloning theorem from the maximum violation of MoE.

To show that no-cloning implies monogamy of entanglement (MoE), let us prove its contrapositive. When MoE is violated maximally, one can achieve quantum cloning [79, 80] of any unknown quantum state using standard teleportation protocol [43, 212] as follows. Assume a particle A is maximally entangled with the

particles B and C and their joint state is denoted by $|\psi\rangle_{ABC}$ and the particle X is in unknown quantum state $|\phi\rangle_C$. To achieve cloning of the state $|\phi\rangle$, one has to perform Bell state measurements (BSM) [174] jointly on the particles A and X . Based on the measurement result denoted by y , suitable unitary operations U_y have to be performed on the particles B and C so that the state $|\phi\rangle$ appears on each of them, where $U_y \in \{\mathcal{I}, \sigma_x, \sigma_y, \sigma_z\}$, \mathcal{I} being the identity operation and σ_i 's ($i = x, y, z$) the Pauli matrices. Thus we can have two copies of the unknown state $|\phi\rangle$ as $|\phi\rangle_B$ and $|\phi\rangle_C$.

Next, to show that MoE implies no-cloning, again we prove its contrapositive. Let two particles A and B share a maximally entangled state $|\psi\rangle_{AB}$. If possible, suppose one of them, say, B is cloned and we get a copy B_1 of B , then in the tripartite state $|\psi\rangle_{ABB_1}$, A is maximally entangled with both B and B_1 simultaneously, thus violating the MoE maximally.

2.6 Indistinguishability

In the last century, physicists were puzzled about whether "the characteristic trait of Quantum Mechanics" [142], i.e., entanglement [27], is real and, if so, whether it can show some nontrivial advantages over classical information processing tasks. The answers to both are positive, thanks to several experimentally verified quantum protocols like teleportation [43], dense coding [42], quantum cryptography, [45] etc. [41].

In the current century, entanglement of indistinguishable particles and its similarity with as well as difference from that of distinguishable ones have been extensively studied [143, 144, 145, 146, 147, 148, 149, 150, 151, 152, 153, 154, 155, 156, 157, 158, 159, 160, 161, 162, 163]. Here, indistinguishable particles means independently prepared identical particles like bosons or fermions [83, 84], where each particle cannot be addressed individually, i.e., a label cannot be assigned to each. Experiments on quantum dots [168, 170], Bose-Einstein condensates [213, 214], ultracold atomic gases [215], etc., support the existence of entanglement of indistinguishable particles.

2.6.1 How to distinguish two identical particles?

The interesting question comes that if two particles are identical, then can we distinguish them? Let us start with two classical identical particles. Although it is not possible to differentiate them by any of their properties, it is always possible to assign them two different labels, like A and B , and using that it is possible, at least in principle, to always keep track their trajectories. In this way, we can in principle, always distinguish two classical identical particles.

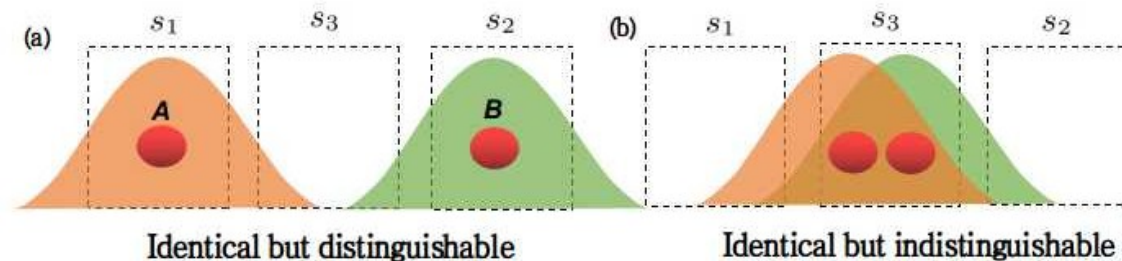


Figure 2-4: Creation of indistinguishable particles from initially separated identical particles. Here s_1 , s_2 , and s_3 are three distinct spatial locations. (a) Initially, two identical particles with are present in s_1 and s_2 in such a way that their wave-functions do not overlap. We label the particles at s_1 and s_2 as A and B respectively. Thus the particles are identical but are distinguishable via their spatial locations. (b) The particles are brought close to each other so that their wave-functions overlap and they become indistinguishable. Now, they cannot be identified by their spatial locations. If the measurement is done in the overlapped region, i.e., s_3 , then it is not possible to detect which particle is measured. Even if the particles are again moved apart, they can no longer be labeled. The information about which of A and B appears at s_1 or s_2 is lost and they remain indistinguishable until they are measured again.

But, unfortunately this method is not possible due to Heisenberg's uncertainty principle [81] which states that it is not possible to uniquely determine the position and momentum exactly at the same time. Thus to distinguish two identical quantum particle, we need to use their spatial locations. Suppose two identical quantum particles A and B are present in distinct spatial locations s_1 and s_2 in such a way that their wave-functions do not overlap. Thus it is possible to keep tract those two particles by their spatial locations as long as their wave functions do not overlap as shown in Fig. 2-4 (a). Now if they are brought close enough that their wave functions overlap, in spatial region s_3 in Fig. 2-4 (b). If the measurement is done in the overlapped

region, i.e., s_3 , then it is not possible to detect which particle is measured. Even if the particles are again moved apart, they can no longer be labeled. The information about which of A and B appears at s_1 or s_2 is lost and they remain indistinguishable until they are measured again. However, this method does not apply for classical particles as their wave functions are so small that they cannot overlap.

Particle exchange phase is an intrinsic property for states of indistinguishable particles when swapping single-particle states [216, 217]. This is a basic scenario based on no-which way information is preserved. The direct measurement of the particle exchange phase (for photons, also including simulations for the case of fermions and anyons) is demonstrated for the first time in [218, 219, 220]. This method is extended and demonstrated more recently where one can use independent identical particles and make them entangled by making them spatially overlapped in separated sites [161, 163]. This has been demonstrated experimentally in [221, 222, 223]. In [221], the authors have designed an experiment where they tuned the remote spatial indistinguishability of two independent photons. This is done by individually controlling their spatial distribution in two distant regions. This results polarization entanglement from uncorrelated photons. In [222], the authors investigate the entanglement between two indistinguishable bosons that is created by spatial overlap. In [223], the authors show that it is possible to activate and distribute of entanglement between two photons in their polarization DoFs that does not require a pair of entangled photons and the Bell-state measurements.

2.7 Entanglement of indistinguishable particles

Experiments on quantum dots [168, 170], Bose-Einstein condensates [213, 214], ultracold atomic gases [215], etc., support the existence of entanglement of indistinguishable particles. The notion of entanglement for distinguishable particles is well studied in the literature [41], where the standard bipartite entanglement is measured by Schmidt coefficients [20], von Neumann entropy [57], concurrence [66], log negativity [59], etc. [55]. Indistinguishability, on the other hand, is represented and ana-

lyzed via particle-based first quantization approach [143, 144, 145, 146, 147, 148, 149] or mode-based second-quantization approach [150, 151, 152, 153]. Entanglement in such a scenario requires measures [155, 156, 157, 158, 159, 160, 161] different from those of distinguishable particles, but there is no consensus on this in the scientific community [162, Sec. III], particularly on the issues of physicality [146, 151], accessibility [214, 155], and usefulness [158, 159] of such entanglement. Very recently, the resource theory of indistinguishable particles [161, 163] has been proposed aiming to settle this debate.

2.7.1 Lo Franco *et al.*'s approach to represent indistinguishable particles

If the state vector of two indistinguishable particles are labeled by ϕ and ψ , then the two-particle state is represented by a single entity $|\phi, \psi\rangle$. The two-particle probability amplitudes is represented by

$$\langle\varphi, \zeta|\phi, \psi\rangle := \langle\varphi|\phi\rangle \langle\zeta|\psi\rangle + \eta \langle\varphi|\psi\rangle \langle\zeta|\phi\rangle, \quad (2.24)$$

where φ, ζ are one-particle states of another global two-particle state vector and $\eta = 1$ for bosons and $\eta = -1$ for fermions. The right hand side of Eq. (2.24) is symmetric if one-particle state position is swapped with another, i.e., $|\phi, \psi\rangle = \eta |\psi, \phi\rangle$. From Eq. (2.24), the probability of finding two particles in the same state $|\varphi\rangle$ is $\langle\varphi, \varphi|\phi, \psi\rangle = (1 + \eta) \langle\varphi|\phi\rangle \langle\varphi|\psi\rangle$ which is zero for fermions due to Pauli exclusion principle [224] and maximum for bosons. As Eq. (2.24) follows symmetry and linearity property, the symmetric inner product of states with spaces of different dimensionality is defined as

$$\langle\psi_k| \cdot |\varphi_1, \varphi_2\rangle \equiv \langle\psi_k | \varphi_1, \varphi_2\rangle = \langle\psi_k|\varphi_1\rangle |\varphi_2\rangle + \eta \langle\psi_k|\varphi_2\rangle |\varphi_1\rangle, \quad (2.25)$$

where $|\tilde{\Phi}\rangle = |\varphi_1, \varphi_2\rangle$ is the un-normalized state of two indistinguishable particles and $|\psi_k\rangle$ is a single-particle state. Equation (2.25) can be interpreted as a projective

measurement where the two-particle un-normalized state $|\tilde{\Phi}\rangle$ is projected into a single particle state $|\psi_k\rangle$. Thus, the resulting normalized pure-state of a single particle after the projective measurement can be written as

$$|\phi_k\rangle = \frac{\langle\psi_k|\tilde{\Phi}\rangle}{\sqrt{\langle\Pi_k^{(1)}\rangle_{\Phi}}}, \quad (2.26)$$

where $|\Phi\rangle := \frac{1}{\sqrt{\mathbb{N}}}|\tilde{\Phi}\rangle$ with $\mathbb{N} = 1 + \eta |\langle\varphi_1|\varphi_2\rangle|^2$ and $\Pi_k^{(1)} = |\psi_k\rangle\langle\psi_k|$ is the one-particle projection operator. The one-particle identity operator can be defined as $\mathbb{I}^{(1)} := \sum_k \Pi_k^{(1)}$. So, using the linearity property of projection operators, one can write similar to Eq. (2.25):

$$|\psi_k\rangle\langle\psi_k| \cdot |\varphi_1, \varphi_2\rangle = \langle\psi_k|\varphi_1\rangle |\psi_k, \varphi_2\rangle + \eta \langle\psi_k|\varphi_2\rangle |\varphi_1, \psi_k\rangle. \quad (2.27)$$

Note that

$$\mathbb{I}^{(1)} |\Phi\rangle = 2 |\Phi\rangle, \quad (2.28)$$

where the probability of resulting the state $|\psi_k\rangle$ is $p_k = \langle\Pi_k^{(1)}\rangle_{\Phi}/2$. The partial trace in this method is can be written as

$$\begin{aligned} \rho^{(1)} &= \frac{1}{2} \text{Tr}^{(1)} |\Phi\rangle\langle\Phi| \\ &= \frac{1}{2} \sum_k \langle\psi_k|\Phi\rangle\langle\Phi|\psi_k\rangle \\ &= \sum_k p_k |\phi_k\rangle\langle\phi_k|, \end{aligned} \quad (2.29)$$

where the factor 1/2 comes from Eq. (2.28).

Another useful concept that of *localized partial trace* [161], which means that local measurements are being performed on a region of space M where the particle has a non-zero probability of being found. So, performing the localized partial trace on a region M , we get

$$\rho_M^{(1)} = \frac{1}{\mathbb{N}_M} \text{Tr}_M^{(1)} |\Phi\rangle\langle\Phi|, \quad (2.30)$$

where \mathbb{N}_M is a normalization constant such that $\text{Tr}^{(1)} \rho_M^{(1)} = 1$. The entanglement

entropy can be calculated as

$$E_M(|\Phi\rangle) := S(\rho_M^{(1)}) = -\sum_i \lambda_i \ln \lambda_i, \quad (2.31)$$

where $S(\rho) = -\text{Tr}(\rho \ln \rho)$ is the von Neumann entropy and λ_i are the eigenvalues of $\rho_M^{(1)}$. We will call the state as entangled state if we get a non-zero value of Eq. (2.31).

2.7.2 Hyper-hybrid entanglement using indistinguishable particles

The circuit of Yurke *et al.* [216, 217] to generate quantum entanglement between the same DoFs of two indistinguishable particles (bosons and fermions) is extended by Li *et al.* [1] to generate inter-DoF entanglement between two indistinguishable bosons. Details of their generation scheme are as follows.

For bosons, the second quantization formulation deals with bosonic operators $b_{i,\mathbf{p}}$ with $|i, \mathbf{p}\rangle = b_{i,\mathbf{p}}^\dagger |0\rangle$, where $|0\rangle$ is the vacuum and $|i, \mathbf{p}\rangle$ describes a particle with spin $|i\rangle$ and momentum \mathbf{p} . These operators satisfy the canonical commutation relations:

$$[b_{i,\mathbf{p}_i}, b_{j,\mathbf{p}_j}] = 0, \quad [b_{i,\mathbf{p}_i}, b_{j,\mathbf{p}_j}^\dagger] = \delta(\mathbf{p}_i - \mathbf{p}_j) \delta_{ij}. \quad (2.32)$$

Analysis of the circuit of Li *et al.* [1] for bosons involves an array of hybrid beam splitters (HBS) [1, Fig. 3], phase shifts, four orthogonal external modes L , D , R and U and two orthogonal internal modes \uparrow and \downarrow as shown in Fig. 2-5. Here, particles exiting through the modes L and D are received by Alice (A) who can control the phases φ_L and φ_D , whereas particles exiting through the modes R and U are received by Bob (B) who can control the phases φ_R and φ_U .

In this circuit, two particles, each with spin $|\downarrow\rangle$, enter the set up in the mode R and L for Alice and Bob respectively. The initial state of the two particles is $|\Psi_0\rangle = b_{\downarrow,R}^\dagger b_{\downarrow,L}^\dagger |0\rangle$. Now, the particles are sent to HBS such that one output port of HBS is sent to other party (R or L) and the other port remains locally accessible (D or U). Next, each party applies state-dependent (or spin-dependent) phase shifts.

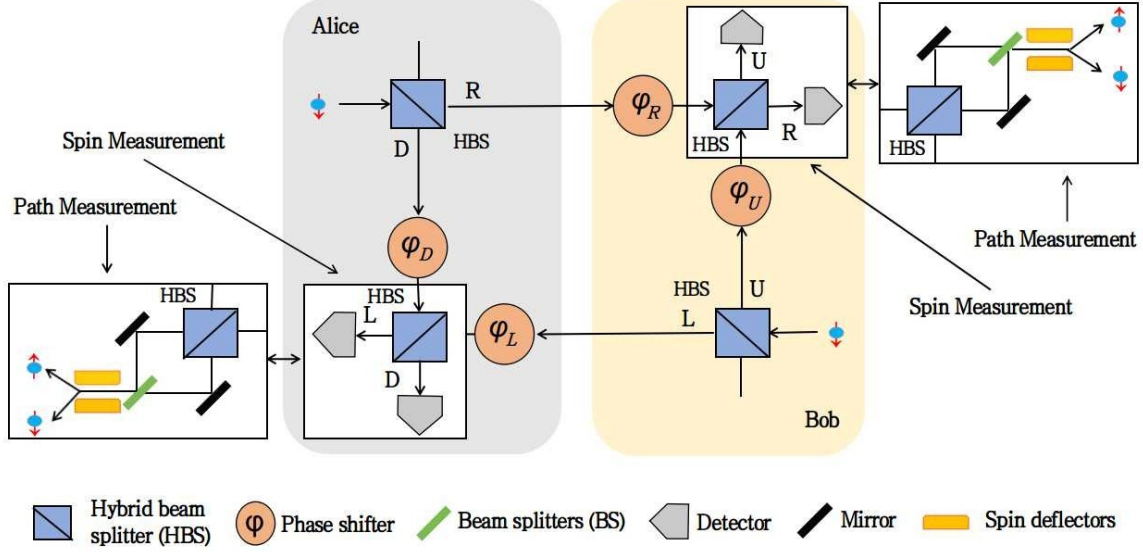


Figure 2-5: Circuit to generate hyper-hybrid entangled state as proposed by Li *et al.* [1]. Here the bi-directional arrow represents the measurement is done either in spin DoF or in Path DoF.

Lastly, the output of local mode and that received from the other party is mixed with HBS and then the measurement is performed in either external or internal modes. The final state can be written as

$$\begin{aligned}
 |\Psi\rangle = & \frac{1}{4} \left[e^{i\varphi_R} (b_{\downarrow,R}^\dagger + ib_{\uparrow,U}^\dagger) + ie^{i\varphi_D} (b_{\uparrow,D}^\dagger + ib_{\downarrow,L}^\dagger) \right] \\
 & \otimes \left[e^{i\varphi_L} (b_{\downarrow,L}^\dagger + ib_{\uparrow,D}^\dagger) + ie^{i\varphi_U} (b_{\uparrow,U}^\dagger + ib_{\downarrow,R}^\dagger) \right] |0\rangle.
 \end{aligned} \tag{2.33}$$

2.8 Quantum teleportation

The verbal description of quantum teleportation is presented in Section 1.2.1. In this section, we present the details mathematics of the teleportation process.

2.8.1 Teleportation using distinguishable particles

One of the major breakthrough application of quantum theory is teleportation of unknown quantum state of a particle [43, 212]. The brief description of quantum teleportation protocol is as follows:

1. Alice possess a particle X with an unknown quantum state $|\phi\rangle_X$ which as to

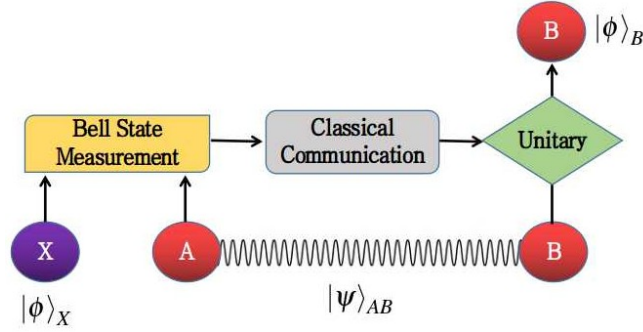


Figure 2-6: Standard teleportation protocol

be teleported to Bob who is at distant from Alice. Also Alice and Bob shares a maximally entangled state $|\psi\rangle_{AB}$ where particle A is with Alice and particle B is with Bob.

2. Alice performs Bell state measurements (BSM) [43] jointly in her particles A and X and sends the measurement result to Bob via classical communication channels.
3. Based on the measurement result of Alice, Bob performs some unitary operation on his particle B . Now the unknown state is teleported from the particle X to B .

One may argue that we get a cloned version of the state $|\phi\rangle$ but after BSM, the original particle is destroyed so that we can have only one copy of the state $|\phi\rangle_B$ at Bob's side. This process is shown schematically in Fig. 2-6.

Fidelity calculation

The fidelity of quantum teleportation (f) [225] is the overlap between the initial quantum state before teleportation denoted by the density matrix ρ_{in} and the density matrix obtain after teleportation denoted by ρ_{out} which is defined as

$$f := \text{Tr} \sqrt{\sqrt{\rho_{in}} \rho_{out} \sqrt{\rho_{in}}}. \quad (2.34)$$

If the shared entanglement between Alice and Bob is maximally entangled then we get unit fidelity quantum teleportation (UFQT) and if the entanglement is non-maximal then we get the fidelity in between 0 and $\frac{2}{3}$. If there is no entanglement between Alice and Bob, i.e., for separable states, the fidelity is $\frac{2}{3}$.

2.8.2 Relation between teleportation fidelity and singlet fraction

Let us assume Alice will teleport an unknown state to Bob. They share a singlet state of two spin- s particles denoted by

$$P_+ = |\psi_+\rangle \langle \psi_+|, \quad |\psi_+\rangle = \frac{1}{\sqrt{d}} \sum_{i=0}^d |i\rangle |i\rangle, \quad d = s2 + 1. \quad (2.35)$$

Teleportation fidelity [172] measures the closeness between the initial state ρ^{in} that we want to teleport and the final state ρ^{out} obtained after the teleportation protocol. It is given by

$$f := \text{Tr} \sqrt{\sqrt{\rho^{in}} \rho^{out} \sqrt{\rho^{in}}}. \quad (2.36)$$

On the other hand, singlet fraction [52] of a state ρ measures the maximum overlap of ρ with maximally entangled states. It is given by

$$F := \max_{\psi} \langle \psi | \rho | \psi \rangle, \quad (2.37)$$

where $|\psi\rangle$ varies over all maximally entangled states.

Now we will derive the relation between teleportation fidelity and singlet fraction for the one-parameter family of states as given in [52] which is given by

$$\rho_p = pP_+ + (1-p) \frac{I \otimes I}{d^2}, \quad 0 \leq p \leq 1 \quad (2.38)$$

This is called noisy singlets which is the most natural generalizations of the $2X2$ Werner states. Now we will calculate teleportation fidelity and singlet fraction for the state given in Eq. (2.38).

For standard teleportation protocol [43], the fidelity is 1 for singlet state. For a completely random noise represented by the second term of the right hand side of Eq. (2.38), i.e., $\frac{I \otimes I}{d^2}$ as the average final state after teleportation will be $\frac{I}{d}$ at the receiver the final state after teleportation will not depend on the initial state before teleportation. Thus the fidelity will be $\frac{1}{d}$. Thus for the state in Eq. (2.38), the teleportation fidelity is given by

$$f = p + (1 - p)\frac{1}{d}, \quad \frac{1}{d} \leq p \leq 1. \quad (2.39)$$

The singlet fraction for the state in Eq. (2.38) can be calculated using Eq. (2.37). Clearly, for singlet state, the value of F is 1 and for the completely random noise, the value of F is $\frac{1}{d^2}$. Thus the value of F for the state in Eq. (2.38) is given by

$$F = p + (1 - p)\frac{1}{d^2}, \quad \frac{1}{d^2} \leq p \leq 1. \quad (2.40)$$

Thus for Eq. (2.39) and (2.40), we get

$$f = \frac{Fd + 1}{d + 1}. \quad (2.41)$$

We can now formate that the state ρ_p in Eq (2.38) is separable *if and only if*

$$0 \leq p \leq \frac{1}{(d + 1)}, \quad \text{or} \quad \frac{1}{d^2} \leq p \leq \frac{1}{d}, \quad \text{or} \quad \frac{1}{d} \leq f \leq \frac{2}{(d + 1)}. \quad (2.42)$$

2.9 Entanglement swapping

A brief overview of entanglement swapping process is described in Section 1.2.1. In this section, we present the details mathematical background of the entanglement swapping process.

2.9.1 Entanglement swapping using distinguishable particles

Entanglement swapping is the process of creating entanglement between two particles who have never interacted before. The entanglement swapping protocol is as follows:

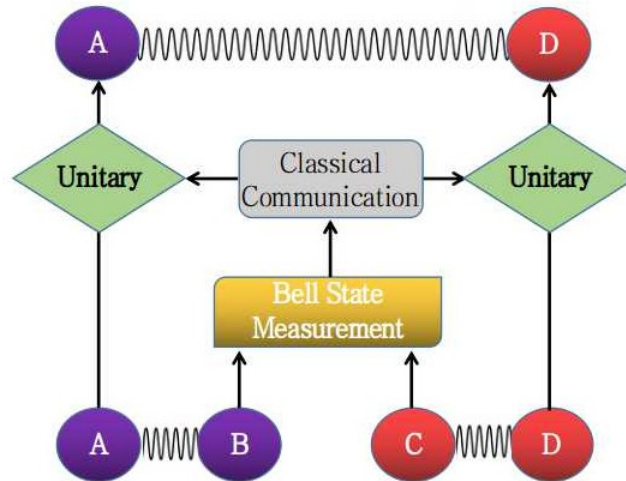


Figure 2-7: Standard Entanglement Swapping protocol

1. Suppose two pair of particles A and B is maximally entangled and similarly another pair of particles C and D is also maximally entangled. Now the particles A and D is never interacted before. Our aim is to create entanglement between the particles A and D .
2. Particles B and C are brought to a lab and BSM is performed jointly in the particles B and C and the measurement result is send to the labs having particles A and D via classical communication channels.
3. Now based on the measurement result, suitable unitary operation is performed to the particles A and D . After that, the particles A and D becomes entangled.

This process is shown schematically in Fig. 2-7. This is very useful for quantum repeaters.

2.10 Some quantum cryptographic protocols

In this section, we discuss three cryptographic protocols, namely, Quantum private query [226, 227], Local Clauser-Horne-Shimony-Holt (CHSH) protocol [228], and Quantum pseudo-telepathy protocol [178, 179].

2.10.1 Quantum private query protocol

Quantum private query (QPQ) is a cryptographic protocol which deals with the communication between a database owner and its clients. Registered client can query about required entry in the database and the server returns appropriate answer to that query. The security in this protocol depends upon two things:

1. The server should not reveal any extra information to the clients other than their queries.
2. The server should not gain any extra information about the queries of the clients.

Conventionally, it is assumed Bob as the database owner or the server and Alice as the client. Like other cryptographic protocols, the communication will start with the key establishment part. But there is a major difference with normal quantum key distribution protocols where the whole key is shared between Alice and Bob. Here, the key is distributed between Alice and Bob such that

1. Bob, the database owner knows the whole key.
2. Alice, the client knows only a part of the key or the value of some specific positions of the key.
3. The database owner has no information about the positions of the key known to the clients.

As a result, unlike normal quantum key distribution protocols, there is no need for any external advisories. Here, Alice and Bob both may work like adversary to each other. The motivation of Alice will be to gain more information about the database

whereas Bob will try to know the position of the bits of the key known to Alice and hence gain information about her queries.

Here, we will discuss the QPQ protocol as proposed in [226, 227] which is based on B92 quantum key distribution [229] scheme. There are two phases

1. *Key generation:* in this phase, a secure key is established between Bob and Alice. This can be done in two ways:

(a) The source shares entangled pair of particles to Bob and Alice in the specific form

$$|\psi\rangle_{BA} = \frac{1}{\sqrt{2}} (|0\rangle_B |\phi_0\rangle_A + |1\rangle_B |\phi_1\rangle_A) \quad (2.43)$$

where

$$\begin{aligned} |\phi_0\rangle_A &= \cos\left(\frac{\theta}{2}\right) |0\rangle + \sin\left(\frac{\theta}{2}\right) |1\rangle \\ |\phi_1\rangle_A &= \cos\left(\frac{\theta}{2}\right) |0\rangle - \sin\left(\frac{\theta}{2}\right) |1\rangle \end{aligned}$$

and $0 < \theta < \frac{\pi}{2}$.

(b) Now, after sharing Bob measures his qubits in $\{|0\rangle_B, |1\rangle_B\}$ basis and Alice measures her qubits in either $\{|\phi_0\rangle_A, |\phi_0^\perp\rangle_A\}$ basis or $\{|\phi_1\rangle_A, |\phi_1^\perp\rangle_A\}$ basis.

By simple calculations, it can be concluded if Alice's measurement output is $|\phi_0^\perp\rangle$ or $|\phi_1^\perp\rangle$, then Bob's measurement output must be 1 or 0 respectively. After classical post-processing, by this way, a key can be established between Alice and Bob such a way that Alice can get only one or more bits of information of the whole key whereas Bob has the knowledge of the whole key but Bob has no information about the bit or bits of the key is known to Alice.

2. *Private query:* After the key is established let K , then let us assume Alice knows the j th bit of key and she make a query about the i th element of the database. Then she calculated an inter $s = (j - i)$. Alice sends s to Bob. He then shifts the key K by s amount and generates a new key, say \bar{K} . Using this new key \bar{K} ,

Bob encrypts his database using a one-time pad. Bob then transmits the whole database to Alice. Alice can easily get the j th bit by decrypting the database.

Device independent tests

The security of the above protocol lies in the fact that the source share the specific state to the Bob as given in Eq. (2.43) for a specific value of θ . It can be shown that if the state is not exactly the same, i.e., for some value $\theta + \epsilon$ where $\epsilon \neq 0$, the Alice can always generate more information [227]. To mitigate this problem, Bob has to has to remove the trust on the source and her should test the correctness of the state given to him at his end. There are several tests to check the correctness of the given state. The test is chooses which gives the maximum success probability.

2.10.2 Local Clauser-Horne-Shimony-Holt (CHSH) test

Bob has to perform this local CHSH test on some of the randomly chosen n pairs. The main steps are

1. Bob choose two random bit strings $x_i, y_i \in \{0, 1\}$ where $i \in \{1, 2, \dots, n\}$.
2. If $x_i = 0$, the Bob measures the first particle in $\{|0\rangle, |1\rangle\}$ basis, else in $\{|+\rangle, |-\rangle\}$ basis.
3. Similarly, if $y_i = 0$, the the Bob measures the first particle in $\{|\psi_1\rangle, |\psi_1^\perp\rangle\}$ basis, else in $\{|\psi_2\rangle, |\psi_2^\perp\rangle\}$ basis where

$$\begin{aligned} |\psi_1\rangle &= \cos\left(\frac{\psi_1}{2}\right) |0\rangle + \sin\left(\frac{\psi_1}{2}\right) |1\rangle, \\ |\psi_2\rangle &= \cos\left(\frac{\psi_2}{2}\right) |0\rangle + \sin\left(\frac{\psi_2}{2}\right) |1\rangle. \end{aligned} \tag{2.44}$$

4. The measurement result is stored in another bit stings $a_i, b_i \in \{0, 1\}$ such that if the measurement result of fist particle is $|0\rangle$ or $|+\rangle$, then $a_i = 0$, else $a_i = 1$.
5. Similarly, if the measurement result of second particle is $|\psi_1\rangle$ or $|\psi_2\rangle$, then $a_i = 0$, else $a_i = 1$.

6. The test is called successful if $a_i \otimes b_i = x_i \wedge y_i$.

The success probability of this test is

$$P_s = \frac{1}{8} (\sin\theta (\sin\psi_1 + \sin\psi_2) + \cos\psi_1 - \cos\psi_2) + \frac{1}{2} \quad (2.45)$$

which is dependent on the values of θ , ψ_1 , and ψ_2 . The maximum value of P_s is 0.85.

2.10.3 Quantum pseudo-telepathy test

Using Quantum pseudo-telepathy test [178, 179] the success probability can reach upto unity. The steps of this tests are given below

1. With the help of an ancilla qubit X , the state in Eq. (2.43) can be transformed into the following state

$$|\psi\rangle_{BAX} = \frac{1}{\sqrt{2}} \left(\cos\frac{\theta}{2} |000\rangle_{BAX} + \sin\frac{\theta}{2} |010\rangle_{BAX} + \cos\frac{\theta}{2} |111\rangle_{BAX} - \sin\frac{\theta}{2} |100\rangle_{BAX} \right). \quad (2.46)$$

2. Now Bob will randomly select a three bit numbers such that there is an even number of 1's in the string. Now based of the input, he performs some specific measurements in the state in Eq. 2.46. Based on the outputs, he has to produce output that contains an even number of 1's if and only if the number of 1's in the input is divisible by 4.

Now using some specific measurements as given in [179] it can be shown that the success probability is

$$P_s = \frac{1}{4} (3 + \cos\theta). \quad (2.47)$$

This value goes to 1 asymptotically.

Chapter 3

Hardy's non-locality in superconducting qubits

In this chapter, we will introduce a new error-modeling for superconducting qubits and its experimental verification in IBM quantum experience. Here, we argue that for practical verification of Hardy's test, the error-modeling used for optical circuits cannot be used for superconducting qubits. So, we propose a new error-modeling and a new method to estimate the lower bound on Hardy's probability for superconducting qubits. We also point out that the earlier tests performed in optical circuits and in the IBM quantum computer have not analyzed the test results in a statistically correct and coherent way. We analyze our data using Student's t-distribution [177] which is the statistically correct way to represent the test results. We experimentally verify Hardy's paradox for two qubits on a quantum computer based on superconducting circuits. Our statistical analysis leads to the conclusion that any two-qubit non-maximally entangled state (NMES) gives a nonzero value of Hardy's probability, whereas any two-qubit maximally entangled state (MES) as well as any product state (PS) yields a zero value of Hardy's probability. We identify the difficulties associated with the practical implementation of quantum protocols based on Hardy's paradox and discuss how to overcome them. We propose two performance measures for any two qubits of any quantum computer based on superconducting qubits.

This chapter is based on the work in [230].

3.1 Practical verification of Hardy's test

In the section 2.2.2 of Chapter 2, we have discussed the standard Hardy's paradox. In this section, we will discuss how Hardy's paradox can be verified practically.

For any experimental set-up, it is quite obvious that the joint probabilities described in Equations (2.4)-(2.7) in the section 2.2.2 of Chapter 2 of may not be zero due to errors caused by any external environment or internal device or both. So, Equations (2.4)-(2.7) can be written with some error parameter ϵ [231]. Here we present the error-model in a slightly different manner so that the result of the practical experiment on an unknown state can be interpreted in a statistically correct and coherent way.

$$P(+1, +1|A_1, B_1) = \epsilon_1, \quad (3.1)$$

$$P(+1, -1|A_2, B_1) = \epsilon_2, \quad (3.2)$$

$$P(-1, +1|A_1, B_2) = \epsilon_3, \quad (3.3)$$

$$P(+1, +1|A_2, B_2) = \epsilon_5 = \epsilon_4 + q, \quad \text{where} \quad \begin{cases} q = 0 & \text{for LHV theory,} \\ q > 0 & \text{for non-locality,} \end{cases} \quad (3.4)$$

and $0 \leq \epsilon_i \leq 1, \forall i \in \{1, 2, 3, 5\}$. The bounds of ϵ_4 become $0 \leq (\epsilon_4 + q) \leq 1$ or $-q \leq \epsilon_4 \leq (1 - q)$. For every MES and every PS of two qubits, the right-hand side of Equation (3.4) is $\epsilon_5 = \epsilon_4$, i.e., $q = 0$, which supports LHV theory. But for every NMES, it is $\epsilon_5 = \epsilon_4 + q$ where $q > 0$, which supports non-locality. Thus, by inspecting the values of q in an experiment, it may be possible to infer whether the underlying state is MES/PS or NMES.

3.1.1 Connection to the CHSH inequality

Using simple set-theoretic arguments, one can show that Hardy's equations are a special case of the famous CHSH inequality [182]. The CHSH version of Hardy's

Equations [183] is described as

$$P(+1, +1|A_2, B_2) - P(+1, +1|A_1, B_1) - P(+1, -1|A_2, B_1) - P(-1, +1|A_1, B_2) \leq 0. \quad (3.5)$$

A violation of Equation (3.5) means a violation of local realism, which supports non-locality. Putting the ideal values of the probabilities from Equations (2.4)-(2.7) into Equation (3.5), we get $q \leq 0$. So, $q = 0$ supports LHV theory and $q > 0$ supports non-locality. But when the practical values of the probabilities from Equations (3.1)-(3.4) are put into Equation (3.5), we get

$$\epsilon_5 - \epsilon_1 - \epsilon_2 - \epsilon_3 \leq 0, \quad \text{or} \quad \epsilon_5 \leq \epsilon_1 + \epsilon_2 + \epsilon_3. \quad (3.6)$$

i.e.,

$$\epsilon_5 \leq \epsilon_1 + \epsilon_2 + \epsilon_3. \quad (3.7)$$

3.2 Our proposed error modeling in superconducting qubits

In this section, we have first elaborated the difference between the error distribution in optical and superconducting qubits. Then we have proposed a new error modeling for superconducting qubits. Finally, we have discussed bounds in errors in optical circuits vs superconducting qubits.

3.2.1 Error distributions in optical circuits vs superconducting qubits

If we perform Hardy's experiment in optical set-up [132, 133, 134, 135, 136, 137, 138, 139, 140, 141, 185, 186], errors can occur in many different ways, such as: (i) the preparation of the ideal quantum state, (ii) in the construction of the measurement operators A_i and B_j where $i, j \in \{1, 2\}$ (as defined in Section 2.2.2 in Chapter 2),

(iii) due to the detection problems of the particles (this includes particle loss), etc. Introducing an error in Equation (2.4) due to the above-mentioned reasons has a direct impact on Equation (2.7), i.e., the logic of Hardy's argument ceases to work. Similarly, when Equation (2.5) and Equation (2.6) are non-zero, they make a contribution to the right-hand side of Equation (2.7). So, in an optical set-up, if Equation (3.7) is violated, it leads to the violation of local realism. No estimation of q is required. The work [133] does exactly this check of Equation (3.7) in its optical circuits.

But in the case of superconducting qubits, there are three types of errors, namely gate error, readout error, and multi-qubit gate error [106]. Unlike in optical circuits, these errors are common to all superconducting qubits circuit and not specific to the circuits to test Hardy's paradox. So, having an error in Equation (2.4) does not have any impact on the right-hand side of Equation (2.7) and Hardy's argument still works with this error. Similar reason applies when Equation (2.5) and Equation (2.6) are not zero. So, in this case, to test the violation of local realism, we will estimate the value of q in Equation (3.4) by a new method which will be described in the next section.

3.2.2 Our proposed model for verifying whether Hardy's probability greater than zero in superconducting qubits

We recall from Equation (3.4) that $\epsilon_5 = \epsilon_4 + q$. While doing the experiment, we can observe only the values of ϵ_5 . To estimate the value of q , we need to get the values of ϵ_4 . Now, the values of ϵ_4 can be observed from the experiment directly for every MES as well as PS of two qubits as $q = 0$, but it cannot be observed directly for NMES as $q > 0$.

However, because of the nature of errors in superconducting qubits as explained in Section 3.2.1, the values of ϵ_4 in both the cases (for $q = 0$ & $q > 0$) will follow the same distribution. So, its maximum value, say Σ_4 , can be estimated from a large number of known MES and PS (with $q = 0$), and then this estimate can be used in

Equation (3.4) to infer about q for any unknown state as follows:

$$\epsilon_5 \leq \Sigma_4 + q, \quad \text{or} \quad q \geq \epsilon_5 - \Sigma_4. \quad (3.8)$$

or

$$q \geq \epsilon_5 - \Sigma_4. \quad (3.9)$$

From Equation (3.9), we can define the lower bound on q as

$$q_{lb} = \epsilon_5 - \Sigma_4. \quad (3.10)$$

If $q_{lb} > 0$, then Equation (3.9) implies that Hardy's probability $q > 0$.

3.2.3 Bounds in errors in optical circuits vs superconducting qubits

For Hardy's test in optical circuits, if $\epsilon_1 = \epsilon_2 = \epsilon_3 = \epsilon$, then from Equation (3.7), we can get the bounds in errors, i.e., $0 \leq \epsilon < \frac{1}{3}$ [180]. But if $\epsilon_1 \neq \epsilon_2 \neq \epsilon_3$, then these bounds are not valid because there may be a case where any of $\epsilon_1, \epsilon_2, \epsilon_3$ can be close to one and the rest close to zero. Then theoretically the bounds in errors are between zero and one.

For Hardy's test in superconducting qubits, as explained in Section 3.2.1, all the error parameters $\epsilon_1, \epsilon_2, \epsilon_3, \epsilon_4, \epsilon_5$ follow the same distribution. So, the bounds in $\epsilon_1, \epsilon_2, \epsilon_3, \epsilon_4, \epsilon_5$ will also be the same, i.e., in between zero and one. But to verify Hardy's circuit, the maximum value of ϵ_4 , i.e., Σ_4 needs to be bounded. From Equation (3.9), the theoretical bound of Σ_4 is $(1 - q_{max}) = (1 - 0.09017) \approx 0.90983$. So, this bound is also valid for $\epsilon_1, \epsilon_2, \epsilon_3$. In the case of optical circuits, when $\epsilon_1 \neq \epsilon_2 \neq \epsilon_3$, the bounds are trivial, but for the case of superconducting qubits, the error bounds are defined independently, i.e., whether all of them takes the same value or not. It may be noted that if we get a value of any of $\epsilon_1, \epsilon_2, \epsilon_3$ greater than 0.90983, then that circuit cannot be used for Hardy's test using superconducting qubits. But in optical circuits, in theory, if we get one of the values of $\epsilon_1, \epsilon_2, \epsilon_3$ greater than 0.90983 and the

rest zero, we still can perform Hardy’s test.

The basic motivation for performing Hardy’s test in superconducting qubits is to show the violation of local realism in superconducting qubits. Though Hardy’s paradox is already tested in optical circuits [132, 133, 134, 135, 184, 136, 137, 138, 139, 140, 141, 185, 186], none of them have been able to estimate the lower bound on Hardy’s probability, i.e., q_{lb} from their experiments. The advantage of performing Hardy’s test in superconducting qubits is that we can estimate the lower bound on of Hardy’s probability q_{lb} as discussed in Section 3.2.2.

3.3 Circuits for Hardy’s test using superconducting qubits

We perform a series of experiments to check Hardy’s non-locality for two qubits in the IBM quantum computer [106]. For simplicity, we use the *ibmqx4*¹ chip which is five-qubit, as we only need two qubits for our experiment. This experiment can also be done using other chips consisting of any other number of qubits (more than or equal to two). It uses a particular physical type of qubit called a superconducting transmon qubit made from superconducting materials niobium and aluminum, patterned on a silicon substrate. During all the experiments, the fridge temperature is maintained at 0.021 K. Any experiment in the IBM quantum computer can be performed for 1 shot, 1024 shots, 4096 shots or 8192 shots in every run.

In the current IBM *ibmqx4* chip topology [106], for using multi-qubit gates like *CNOT*, there is a restriction, i.e., not all pairs of qubits can be used for circuit implementation. The list of possible combinations are given in details in the IBM website [106] and it is also discussed in Section 3.4.2 in details. It should be noted that all the qubits are subject to different types of errors as given in the IBM website [106]. Initially, we implement our circuit by choosing any possible pair of qubits and then

¹IBM has several chips and a subset of those becomes available for experiments from time to time. Currently, the *ibmqx4* chip is under maintenance, while the available chips are *ibmqx2*, *ibmq_vigo*, *ibmq_ourense* and *ibmq_16_melbourne*.

validate the results for the rest of the possible combinations of qubits.

In [183], a circuit consisting of two coupled electronic Mach-Zehnder (MZ) interferometers has been proposed for Hardy's test which is similar to the Hardy's original thought experiment [34]. We implement this circuit in the IBM quantum computer. As described in [183], there are three important parameters of this experiment: beam splitters $U_B(\theta) = \begin{pmatrix} \cos\theta & -\sin\theta \\ \sin\theta & \cos\theta \end{pmatrix}$, phase shifter $U_P(\phi) = \begin{pmatrix} 1 & 0 \\ 0 & e^{i\phi} \end{pmatrix}$, and the coupling $U_C(\phi) = \begin{pmatrix} 1 & & & \\ & 1 & & \\ & & 1 & \\ & & & e^{i2\phi} \end{pmatrix}$ which can be expressed as

$$\begin{aligned} U_B(\theta) &= U_3(2\theta, 0, 0), \\ U_P(\phi) &= U_1(\lambda), \\ U_C(\phi) &= M_3 \cdot CNOT \cdot M_2 \cdot CNOT \cdot M_1, \end{aligned} \tag{3.11}$$

where

$$\begin{aligned} U_1(\lambda) &= \begin{pmatrix} 1 & 0 \\ 0 & e^{\lambda i} \end{pmatrix}, \\ U_3(\theta, \lambda, \phi) &= \begin{pmatrix} \cos\frac{\theta}{2} & -e^{-\lambda i} \sin\frac{\theta}{2} \\ e^{-\lambda i} \sin\frac{\phi}{2} & e^{i(\phi+\lambda)} \cos\frac{\theta}{2} \end{pmatrix}, \\ M_1 &= Id \otimes U_1(-\lambda), \\ M_2 &= U_1(\lambda) \otimes U_1(-\lambda), \\ M_3 &= Id \otimes U_1(2\lambda). \end{aligned} \tag{3.12}$$

CNOT is a controlled-NOT gate and *Id* is the identity gate. Here $U_1(\lambda)$, $U_3(\theta, \lambda, \phi)$, *CNOT*, and *Id* are available as standard gates provided by the IBM quantum computer [106]. We decompose the coupling $U_C(\phi)$ by the standard IBM gates is shown in Equation (3.11). But it can also be decomposed in different ways such that the total number of gates are reduced further and that is left as future work.

θ	ϕ	state	$ \psi\rangle$
0	any value	PS	$\frac{1}{\sqrt{2}}(0\rangle + 1\rangle) \otimes 0\rangle$
any value	0	PS	$\frac{1}{\sqrt{2}}(0\rangle + 1\rangle) \otimes (\cos\theta 0\rangle + \sin\theta 1\rangle)$
90	any value	PS	$\frac{1}{\sqrt{2}}(0\rangle + e^{i2\phi} 1\rangle) \otimes 1\rangle$
45	90	MES	$\frac{1}{2}(00\rangle + 01\rangle + 10\rangle - 11\rangle)$

Table 3.1: Maximally entangled states (MES) and product states (PS) based on different values of θ and ϕ in between 0 to 90 degrees.

For Hardy's test, the state $|\psi\rangle$ for Alice and Bob is considered in [183] as

$$|\psi\rangle = V_0(V_1 \otimes V_2)|00\rangle = \frac{\cos\theta}{\sqrt{2}}(|00\rangle + |10\rangle) + \frac{\sin\theta}{\sqrt{2}}(|01\rangle + e^{i2\phi}|11\rangle), \quad (3.13)$$

where $V_0 = U_C(\phi)$, $V_1 = U_B\left(\frac{\pi}{4}\right)$, and $V_2 = U_B(\theta)$. The state $|\psi\rangle$ is expressed by the IBM gates is shown in Figure 3-1 where Q_A and Q_B are the qubits for Alice and Bob respectively. The values of θ and ϕ in between 0 to 90 degrees for which $|\psi\rangle$ is found to be MES as well as PS are given in Table 3.1. The measurements for Alice and Bob are described as follows.

$$\begin{aligned} A_1 &= U_B\left(\frac{\pi}{4}\right) = U_3\left(\frac{\pi}{2}, 0, 0\right), \\ B_1 &= U_B(0) = U_3(0, 0, 0), \\ A_2 &= U_P(2\phi) U_B\left(\frac{\pi}{4}\right) U_P(-2\phi) = U_1(2\lambda) U_3\left(\frac{\pi}{2}, 0, 0\right) U_1(-2\lambda), \\ B_2 &= U_P(\phi) U_B(\chi) U_P(-\phi) = U_1(\lambda) U_3(2\chi, 0, 0) U_1(-\lambda), \end{aligned} \quad (3.14)$$

where $\cot\chi = \tan\theta\cos\phi$. The measurements are done in σ_z basis. The experimental circuits of Equations (2.4), (2.5), (2.6), and (2.7) for the state $|\psi\rangle$ using the above measurements in the IBM quantum computer are given in Figures 3-2, 3-3, 3-4, and 3-5 respectively. The theoretical value of $P(+1, +1|A_2, B_2)$ is given by $|\langle\psi|A_2 \otimes B_2|\psi\rangle|^2$,

which using Equation (3.13) and Equation (3.14) becomes

$$q = \left| \frac{1}{2} \cos\theta \cos\chi (1 - e^{-2i\phi}) \right|^2. \quad (3.15)$$

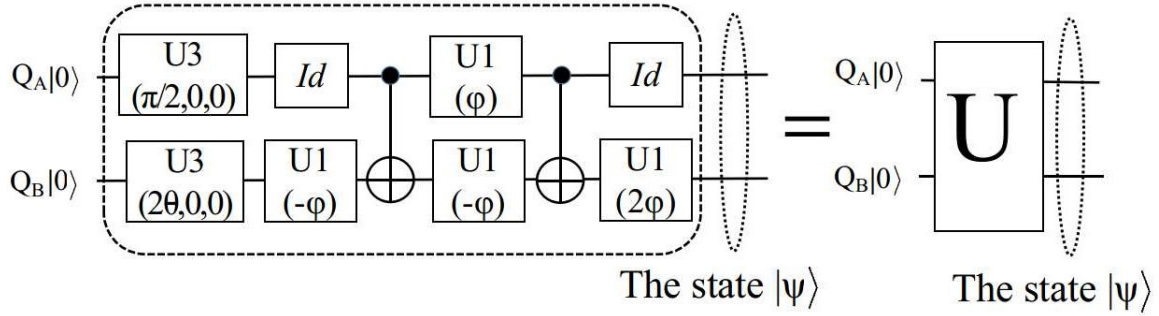


Figure 3-1: The state $|\psi\rangle$ for Equation (3.13).

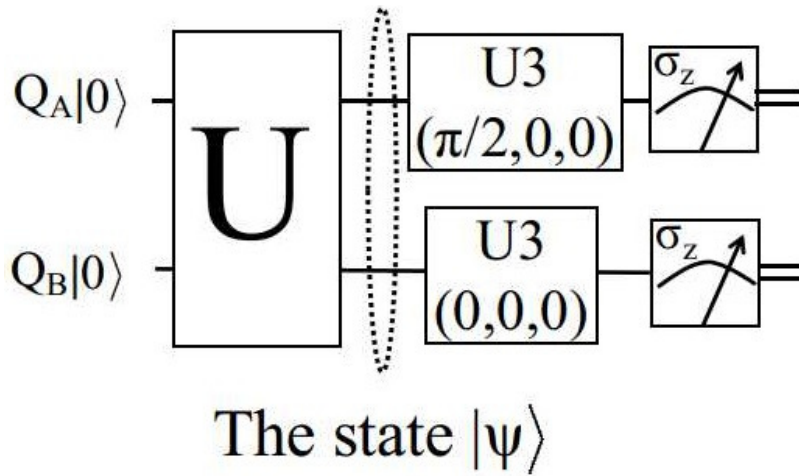


Figure 3-2: Quantum circuit and measurement for $P(+1, +1|A_1, B_1)$ for Equation (3.1).

The maximum value of q , i.e., q_{max} is found from Equation (3.15) when

$$\cos(2\theta) = \cos(2\phi) = 2 - \sqrt{5}. \quad (3.16)$$

If the variation of θ and ϕ are carried out in between 0 to 90 degrees, then q_{max} occurs at $\theta = \phi = 51.827$ degrees approximately. But in general similar analysis can be done for any values of θ and ϕ . In Figure 3-6, we plot² the values of q from Equation (3.15)

²We use MATLAB[®] to get these values.

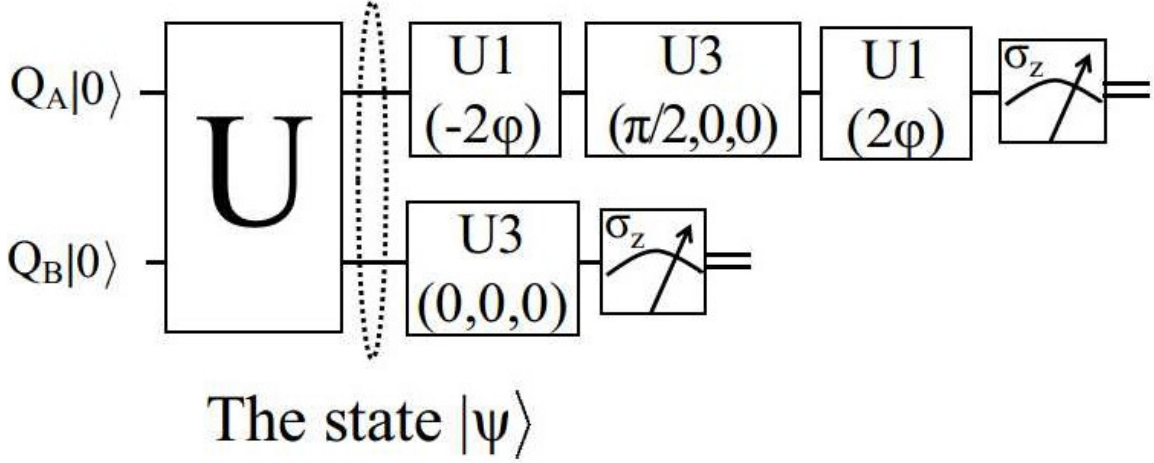


Figure 3-3: Quantum circuit and measurement for $P(+1, -1|A_2, B_1)$ for Equation (3.2).

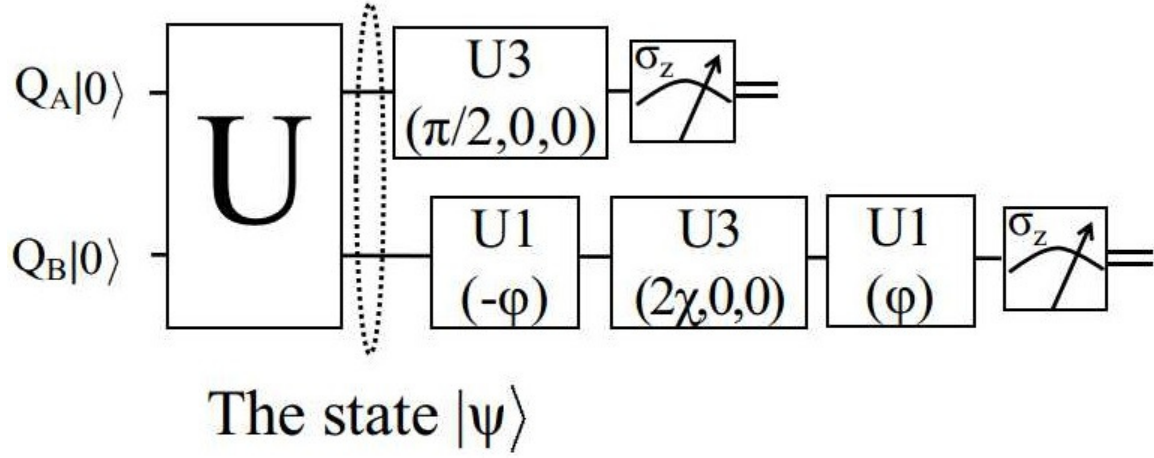


Figure 3-4: Quantum circuit and measurement for $P(-1, +1|A_1, B_2)$ for Equation (3.3).

by varying θ and ϕ from 0 to 360 degrees. In this figure, we can see that q_{max} is achieved for $\theta = \phi = 51.827$ degrees and also for other values of θ and ϕ such that Equation (3.16) is satisfied.

For $\phi = 90$ and $\theta \neq \{0, 45, 90\}$ degrees, from Equation (3.13), we get $|\psi\rangle$ as NMES. This means, if we perform Hardy's test, a non-zero value of q in Equation (2.7) has to be found. But when $\phi = 90$ degree, we get $\chi = 90$ degree which means the right-hand side of Equation (3.15) is zero. So, in this experimental set-up, Hardy's test fails for all NMES for the values of $\phi = 90$ and $\theta \neq \{0, 45, 90\}$ degrees.

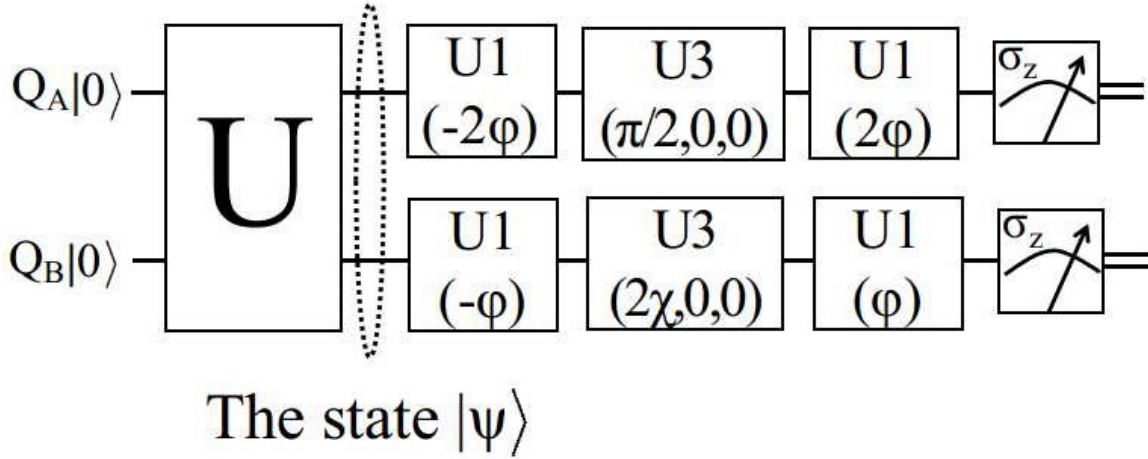


Figure 3-5: Quantum circuit and measurement for $P(+1, +1|A_2, B_2)$ for Equation (3.4).

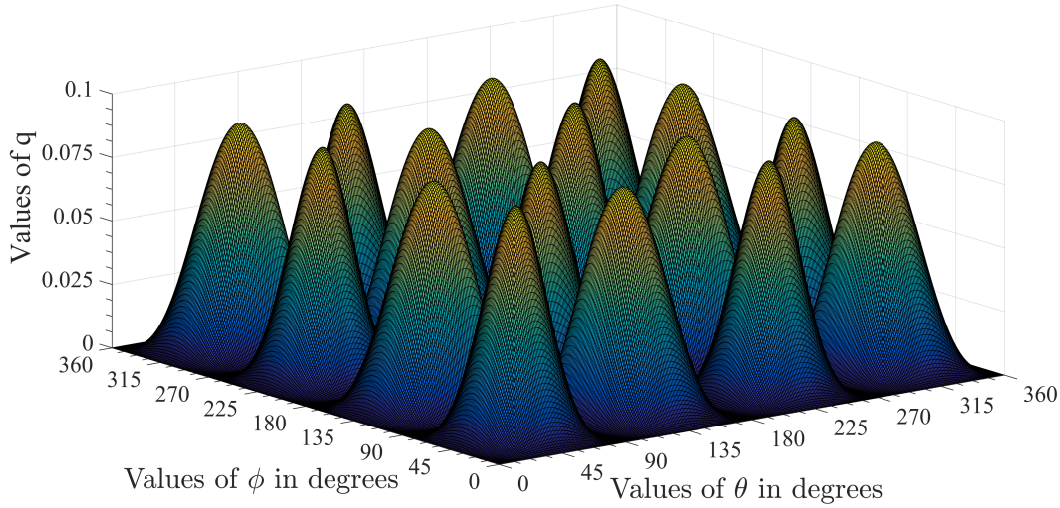


Figure 3-6: The variation of θ and ϕ in degrees vs the values of q from Equation (3.15).

Boundary values of χ

In Section 3.3, χ is defined as $\cot\chi = \tan\theta\cos\phi$. When $\theta = 90$ degree and $\phi = 90$ degree, we get $\tan\theta = \infty$ and $\cos\phi = 0$, which leads to $\cot\chi = \infty \cdot 0$. This is an indeterminate form.

When $\theta \rightarrow 90+$ and $\phi \rightarrow 90+$, the value of χ is positive. When $\theta \rightarrow 90+$ and $\phi \rightarrow 90-$, the value of χ is negative. When $\theta \rightarrow 90-$ and $\phi \rightarrow 90+$, the value of χ is negative. When $\theta \rightarrow 90-$ and $\phi \rightarrow 90-$, the value of χ is positive.

So, the limit does not exist. More formally,

$$\begin{aligned}
& \lim_{(\theta, \phi) \rightarrow (\frac{\pi}{2}, \frac{\pi}{2})} \tan \theta \cos \phi \\
&= \lim_{(x, y) \rightarrow (0, 0)} \tan \left(x + \frac{\pi}{2} \right) \cos \left(y + \frac{\pi}{2} \right) \\
&= \lim_{(x, y) \rightarrow (0, 0)} \cot x \sin y,
\end{aligned} \tag{3.17}$$

where $x = \left(\theta - \frac{\pi}{2} \right)$ and $y = \left(\phi - \frac{\pi}{2} \right)$. Now changing the co-ordinate system from rectangular to polar co-ordinate system and substituting $x = r \cos \varphi$ and $y = r \sin \varphi$, we can write the above expression as

$$\begin{aligned}
& \lim_{r \rightarrow 0} \cot (r \cos \varphi) \sin (r \sin \varphi) \\
&= \lim_{r \rightarrow 0} \frac{\cos (r \cos \varphi)}{\sin (r \cos \varphi)} \sin (r \sin \varphi) \\
&= \lim_{r \rightarrow 0} \frac{\left(1 - (r \cos \varphi)^2 + \dots \right)}{\left(r \cos \varphi - \frac{(r \cos \varphi)^3}{3!} + \dots \right)} \left(r \sin \varphi - \frac{(r \sin \varphi)^3}{3!} + \dots \right) \\
&= \lim_{r \rightarrow 0} \frac{\left(1 - (r \cos \varphi)^2 + \dots \right)}{r \left(\cos \varphi - \frac{r^2 (\cos \varphi)^3}{3!} + \dots \right)} r \left(\sin \varphi - \frac{r^2 (\sin \varphi)^3}{3!} + \dots \right) \\
&= \frac{\sin \varphi}{\cos \varphi} = \tan \varphi.
\end{aligned} \tag{3.18}$$

So, χ doesn't have any definite value, but it depends on φ .

3.3.1 How to calculate the difference between two Student's t-distributed variables?

In the section 2.1 of Chapter 2, we have discussed how to perform analysis of any experimental results. Using that we will now calculate q_{lb} .

To calculate q_{lb} from Equation (3.10), we need to calculate the statistics for the difference of two random variables X and Y corresponding to the experimental values of ϵ_5 and Σ_4 respectively. Here both X and Y are assumed to follow standard normal distributions. Also, for n number of samples, let the sample means of X and Y be \bar{X} and \bar{Y} respectively and the sample standard deviations be S_X and S_Y respectively.

Then for some value of α , let $(\bar{X} \pm t_X)$ where $t_X = t_{\frac{\alpha}{2}} \frac{S_X}{\sqrt{n}}$ represents the $(1 - \alpha)\%$ confidence interval around the mean of X . Similarly, let $(\bar{Y} \pm t_Y)$ where $t_Y = t_{\frac{\alpha}{2}} \frac{S_Y}{\sqrt{n}}$ represents the same for the random variable Y . Now if we want to calculate the value of another Student's t-distributed random variable W such that $W = X - Y$, then the sample mean \bar{W} of W is given by $\bar{W} = (\bar{X} - \bar{Y})$ and the sample standard deviation is given by $S_W = \sqrt{S_X^2 + S_Y^2}$. Then the $(1 - \alpha)\%$ confidence interval around mean of W is $(\bar{W} \pm t_W)$ where $t_W = t_{\frac{\alpha}{2}} \frac{S_W}{\sqrt{n}}$. Now the value of W_{lb} will be

$$W_{lb} = (\bar{W} - t_W) = \left(\bar{X} - \bar{Y} - t_{\frac{\alpha}{2}} \frac{\sqrt{S_X^2 + S_Y^2}}{\sqrt{n}} \right). \quad (3.19)$$

We can use Equation (3.19) to estimate \hat{q}_{lb} of q_{lb} as defined in Equation (3.10) as

$$\hat{q}_{lb} = (\bar{\epsilon}_5 - \bar{\Sigma}_4 - \Delta) \quad \text{where} \quad \Delta = t_{\frac{\alpha}{2}} \frac{\sqrt{S_{\epsilon_5}^2 + S_{\Sigma_4}^2}}{\sqrt{n}}. \quad (3.20)$$

Here $\bar{\epsilon}_5$ and S_{ϵ_5} are the sample mean and sample standard deviation of ϵ_5 respectively over n number of samples. Similarly, $\bar{\Sigma}_4$ and S_{Σ_4} are the corresponding quantities for Σ_4 . When the value of α increases, the confidence in data $(1 - \alpha)$ decreases. So, the value of t_W increases because the value of $t_{\frac{\alpha}{2}}$ is computed from the minimum side of the distribution and as per Equation (3.19), the value of W_{lb} decreases. Thus, in Equation (3.20), as α increases, Δ increases, and so \hat{q}_{lb} decreases. Note that, all the statistical analysis is done for certain fixed data [177].

Given an unknown state, to find whether that state is NMES or not, create an experimental set-up where Equations (2.4)-(2.6) are satisfied theoretically and Equations (3.1)-(3.3) are validated experimentally. Then we use a two-phase procedure as presented in Algorithm 1.

In this way, we can identify whether an unknown state is NMES or not with some confidence. If it is NMES, then we can estimate a lower bound on Hardy's probability of that NMES. The two-phase process is similar to the scenario of classical error-control coding [232] wherein off-line phase channel noise is estimated using known messages and subsequently that estimation is used in the on-line phase to correct the

OFF-LINE PHASE (Estimation of $\bar{\Sigma}_4$ from unknown MES & PS):

- 1 Do the experiment for Equation (3.4) for k numbers of known MES as well as PS to get the values of $\bar{\epsilon}_4$.
- 2 Then from that data, calculate the values of $\bar{\Sigma}_4 = \max\{\bar{\epsilon}_4\}$ and S_{Σ_4} .

ON-LINE PHASE (Estimation of \hat{q}_{lb} from the unknown state):

- 3 Do the experiment for Equation (3.4) to calculate $\bar{\epsilon}_5$ and S_{ϵ_5} for the unknown state.
- 4 Calculate the value of Δ from Equation (3.20).
- 5 Plug-in the values of $\bar{\epsilon}_5$, $\bar{\Sigma}_4$ and Δ in Equation (3.20) to get an estimate \hat{q}_{lb} of the lower bound q_{lb} on q .
- 6 **if** $\hat{q}_{lb} > 0$ (i.e., if $\bar{\epsilon}_5 > \bar{\Sigma}_4 + \Delta$) **then**
 - | the unknown state is NMES and the value of Hardy's probability q of that unknown state is greater than or equals to the value of \hat{q}_{lb} , i.e., $q \geq \hat{q}_{lb}$**end**
- else**
 - | no decision can be made about the unknown state.**end**

Algorithm 1: Estimation for the lower bound q_{lb} on q , i.e., \hat{q}_{lb} for superconducting qubits.

transmission error of unknown messages.

3.4 Our experimental results and discussion

The confidence interval around the mean for Student's t-distribution depends upon two quantities.

1. The degrees of freedom for Student's t-distribution which is one less than the number of samples taken for the experiment.
2. The percentage of confidence we need on our data.

Based on these two quantities, we get the confidence interval around the mean for any data.

In the IBM five-qubit quantum computer, any experiment can be performed for 1 shot or one of 1024, 4096 and 8192 (which is the maximum available) shots. It means that these many number of times the experiment is performed internally and

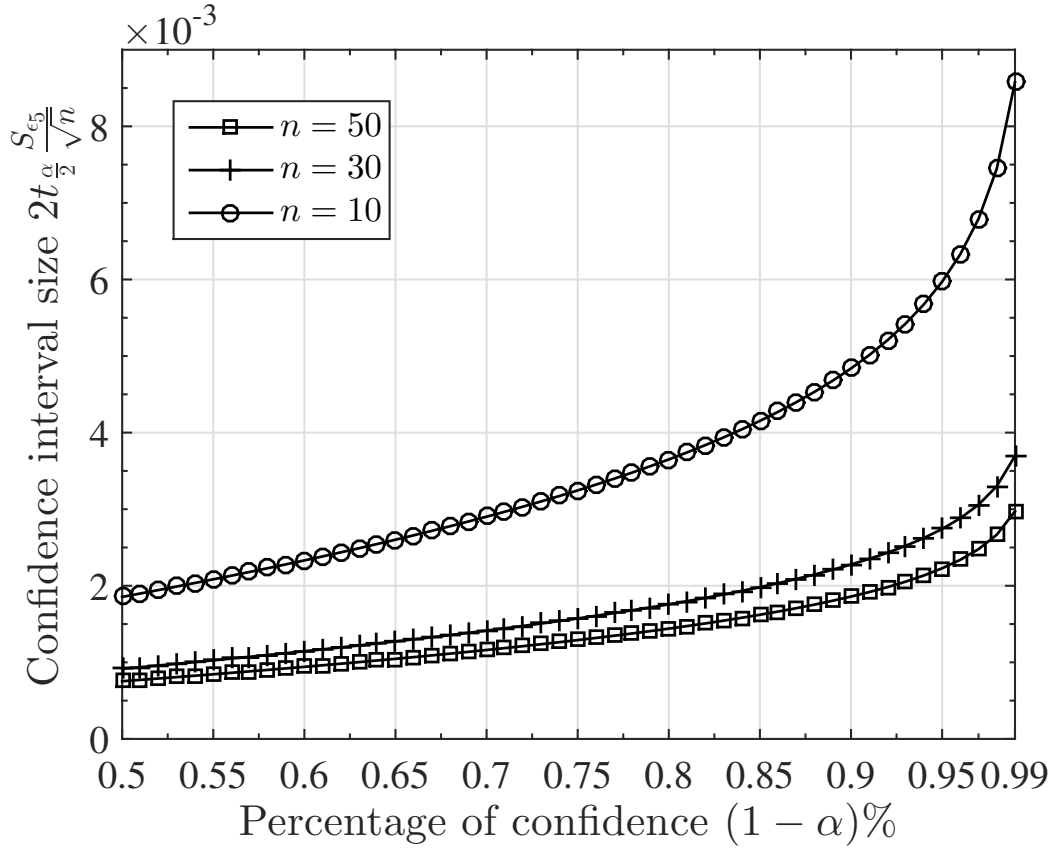


Figure 3-7: The variation of the confidence interval size $\left(2t_{\frac{\alpha}{2}} \frac{S_{\epsilon_5}}{\sqrt{n}}\right)$ with the percentage of confidence $(1 - \alpha)\%$ with varying number of samples is $n \in \{10, 30, 50\}$.

the average of that is reported as output. But if we repeat any experiment with 8192 shots for a few times, we may see a significant deviation among each of the average values. Further, if we perform any experiment for 8192 shots, then the IBM quantum experience does not provide us with all the samples of those shots, rather it only provides the mean value. So if we perform any experiment only once with 8192 shots and make a conclusion based on the result, then that is not a statistically correct way. Instead, if someone does the experiment n number of times with 8192 shots/time and then estimates the mean and the standard deviation assuming Student's t-distribution with required confidence interval, then that would be statistically more accurate. We will show the variation of the same result by varying n and the percentage of confidence interval for Hardy's experiment.

In Figure 3-7, we show the variation of the confidence interval size $2t_{\frac{\alpha}{2}} \frac{S_{\epsilon_5}}{\sqrt{n}}$ with the

percentage of confidence $(1 - \alpha) \%$ with varying number of samples $n \in \{10, 30, 50\}$. Each of the samples is the mean of Hardy’s experiment run for 8192 shots. It can be seen that the confidence interval size increases with a decreasing number of samples. Also, for a fixed number of samples, the interval size increases with an increasing percentage of confidence in data. From this result, it can be concluded that if an experiment in the IBM quantum computer is done only on one sample for 8192 shots, then that would not be a statistically correct way of representation since each of the samples can deviate from the mean significantly. As we have limited access to the IBM quantum computer, we take $n = 10$ and the experiments are run for MES, PS, and NMES for some values of θ and ϕ in between 0 to 90 degrees as shown in Table 3.2 and Table 3.3.

We perform experiments with different combinations of qubits for Alice and Bob and discuss the results below.

3.4.1 Experiments for Hardy’s non-locality using two specific qubits for Alice and Bob

In this section, we check Hardy’s non-locality by taking a specific combination of qubits from all available combinations in the IBM quantum computer. Later we will discuss rest of the possible combinations.

Experimental validation of the circuit for Hardy’s test

We perform the experiments for Equations (3.1), (3.2), and (3.3) (Figures 3-2, 3-3 and 3-4 respectively) for the values of θ and ϕ in degrees. The values of $\bar{\epsilon}_1$, $\bar{\epsilon}_2$ and $\bar{\epsilon}_3$ in each of the experiments are found to be less than 0.1, implying that Equations (3.1), (3.2) and (3.3) are satisfied. These results indicate that this experimental set-up is now valid for Hardy’s test. As discussed in Section 3.1, for practical verification of Hardy’s test using superconducting qubits, only one experiment for Equation (3.4) (Figure 3-5) has to be performed to establish non-locality, that is why the details of the results for $\bar{\epsilon}_1$, $\bar{\epsilon}_2$ and $\bar{\epsilon}_3$ are not presented. The experimental results

State	θ, ϕ	$\bar{\epsilon}_4$ ($q = 0$)	SD (S_{ϵ_4})	$t_{\frac{\alpha}{2}} \frac{S_{\epsilon_4}}{\sqrt{n}}$ for different CIs			
				99%	95%	90%	80%
MES	45, 90	0.0807	0.0037	0.003802	0.002647	0.002145	0.001618
PS	0, 0	0.0193	0.0014	0.001439	0.001001	0.000812	0.000612
PS	90, 0	0.0209	0.0015	0.001542	0.001073	0.00087	0.000656
PS	45, 0	0.0217	0.0019	0.001953	0.001359	0.001101	0.000831
PS	90, 45	0.0282	0.0013	0.001336	0.00093	0.000754	0.000569

Table 3.2: Results of $\bar{\epsilon}_4$, standard deviations (SD) and the values of $t_{\frac{\alpha}{2}} \frac{S_{\epsilon_4}}{\sqrt{n}}$ for different confidence intervals (CIs) with $n = 10$ for some values of θ and ϕ for which MES as well as PS are created for the pair of qubits (Q_3, Q_4) .

of Equation (3.4) are presented in Table 3.2 and Table 3.3 for some selected values of θ and ϕ .

Test of non-locality when $q = q_{max}$

From Table 3.2, for the MES, i.e., $\theta = 45$ and $\phi = 90$ degrees, we get $\bar{\epsilon}_4 = 0.0807$, $S_{\epsilon_4} = 0.0037$, and the values of $t_{\frac{\alpha}{2}} \frac{S_{\epsilon_4}}{\sqrt{n}}$ for different confidence intervals. We take four possible confidence intervals: 99%, 95%, 90%, and 80%. Similarly, for the PS, we get $\bar{\epsilon}_4$ to be less than 0.03 (there are only one MES possible but ideally an infinite number of PS possible as shown in Table 3.1. But due to limited access to the IBM quantum computer, we take $k = 50$ number of PS as indicated in Algorithm 1. As for all the PS, we get $\bar{\epsilon}_4$ to be less than 0.03, we present some of the values of the PS in Table 3.2). As stated earlier, when $\theta = \phi = 51.827$ degrees, we get $q = q_{max}$ for NMES. So, to test the non-locality when $q = q_{max}$, we have to check whether $\hat{q}_{lb} > 0$ as given in Equation (3.20). From Table 3.2, we get $\bar{\Sigma}_4 = 0.0807$ and $S_{\Sigma_4} = 0.0037$ which is value we get from the off-line phase as stated in Algorithm 1. This value is constant for the pair of qubits (Q_3, Q_4) and will be different for other pairs. Now we will calculate the value of \hat{q}_{lb} .

From the experiment, we get $\bar{\epsilon}_5 = 0.1281$ with $S_{\epsilon_5} = 0.0039$ and the values of confidence intervals are given for $(1 - \alpha) \in \{0.99, 0.95, 0.90, 0.80\}$. To calculate \hat{q}_{lb}

State	θ, ϕ	$\bar{\epsilon}_5$ ($q > 0$)	SD (S_{ϵ_5})	$t_{\frac{\alpha}{2}} \frac{S_{\epsilon_5}}{\sqrt{n}}$ for different CIs			
				99%	95%	90%	80%
NMES	51.827, 51.827	0.1281	0.0039	0.004008	0.00279	0.002261	0.001706
NMES	55, 55	0.1273	0.0045	0.004625	0.003219	0.002609	0.001968
NMES	45, 45	0.1041	0.0044	0.004522	0.003148	0.002551	0.001924
NMES	30, 60	0.0832	0.0052	0.005344	0.00372	0.003014	0.002274
NMES	60, 30	0.0553	0.0028	0.002878	0.00200	0.001623	0.001225
NMES	10, 80	0.067	0.0038	0.00391	0.00272	0.0022	0.00166
NMES	80, 10	0.0241	0.0016	0.001644	0.001145	0.000927	0.0007

Table 3.3: Results of $\bar{\epsilon}_5$, standard deviations (SD) and the values of $t_{\frac{\alpha}{2}} \frac{S_{\epsilon_5}}{\sqrt{n}}$ for different confidence intervals (CIs) with $n = 10$ for some values of θ and ϕ for which NMES are created for the pair of qubits (Q_3, Q_4).

with different confidence intervals, we will use Equation (3.20). From Table 3.4, when $\theta = \phi = 51.827$ degrees, we get $\hat{q}_{lb} > 0$ for different confidence intervals. The error in estimating the value of \hat{q}_{lb} is approximately 52%. If we increase the number of samples in the experiment, i.e., the value of n , then \hat{q}_{lb} will also increase as seen in Figure 3-7. But despite the errors in the experiment, when $q = q_{max}$, we get the lower bound on Hardy's probability greater than zero with 99% confidence on the data.

Test of non-locality when $q < q_{max}$

From Table 3.4, when $\theta = \phi = 55$ degrees ($q = 0.0886$), by a similar analysis, we get \hat{q}_{lb} to be around 0.042, for different confidence intervals, i.e., $\hat{q}_{lb} > 0$. The error in estimating the value of \hat{q}_{lb} , in this case, is around 52.5%. Similarly, when $\theta = \phi = 45$ ($q = 0.0833$), the value of \hat{q}_{lb} is around 0.02. But the error in this case in estimating \hat{q}_{lb} is around 76%. Clearly these results support a non-zero value of Hardy's probability.

But when $\theta = 30$ and $\phi = 60$ ($q = 0.0433$), we estimate $\hat{q}_{lb} < 0$. Similar result is obtained when $\theta = 60$ and $\phi = 30$ ($q = 0.0433$). So, from these results we cannot conclude that the state is really an NMES or not when $q = 0.0433$.

When the value of q is decreased further, when $q = 0.00088$, the values of \hat{q}_{lb} again become less than zero. So, from these results, we cannot conclude about the state as discussed above.

State	θ, ϕ	q	\hat{q}_{lb} for different CIs			
			99%	95%	90%	80%
NMES	51.827, 51.827	0.09017	0.041876	0.043554	0.044283	0.045049
NMES	55, 55	0.0886	0.040613	0.042432	0.043222	0.044052
NMES	45, 45	0.0833	0.017492	0.019287	0.020067	0.020886
NMES	30, 60	0.0433	-0.004058	-0.002066	-0.001199	-0.000290
NMES	60, 30	0.0433	-0.030168	-0.028718	-0.02809	-0.027429
NMES	10, 80	0.00088	-0.019154	-0.017495	-0.016773	-0.016018
NMES	80, 10	0.00088	-0.060742	-0.059484	-0.058937	-0.058363

Table 3.4: Comparison of the results of q and \hat{q}_{lb} for some values of θ and ϕ for which NMES is created for different confidence interval (CIs) for the pair of qubits (Q_3, Q_4)

Summary of the above two experiments

We know that in Hardy's test, we should get Hardy's probability $q > 0$ for all NMES. But, from the above experimental data, we get for some NMES, the estimated lower bound on Hardy's probability $\hat{q}_{lb} \leq 0$. The mismatch between theoretical value and the estimated value from the experiments can be explained with respect to Equation (3.9) as follows:

- for those NMES when q is larger than $\bar{\Sigma}_4$, the distinction between $\bar{\epsilon}_5$ and $\bar{\Sigma}_4$ is clear and $\hat{q}_{lb} > 0$.
- But for those NMES when q is less than $\bar{\Sigma}_4$, it is hard to distinguish between $\bar{\epsilon}_5$ and $\bar{\Sigma}_4$, and we have $\hat{q}_{lb} \leq 0$.

we can observe that for those NMES when q is larger than $\bar{\Sigma}_4$, the distinction between $\bar{\epsilon}_5$ for those NMES and $\bar{\Sigma}_4$ for all MES as well as PS is clear, i.e., $\hat{q}_{lb} > 0$. But for those NMES when the value of q is less than $\bar{\Sigma}_4$ for all MES as well as PS, it is hard to distinguish between $\bar{\epsilon}_5$ for those NMES and $\bar{\Sigma}_4$ for all MES as well as PS, i.e., $\hat{q}_{lb} \leq 0$.

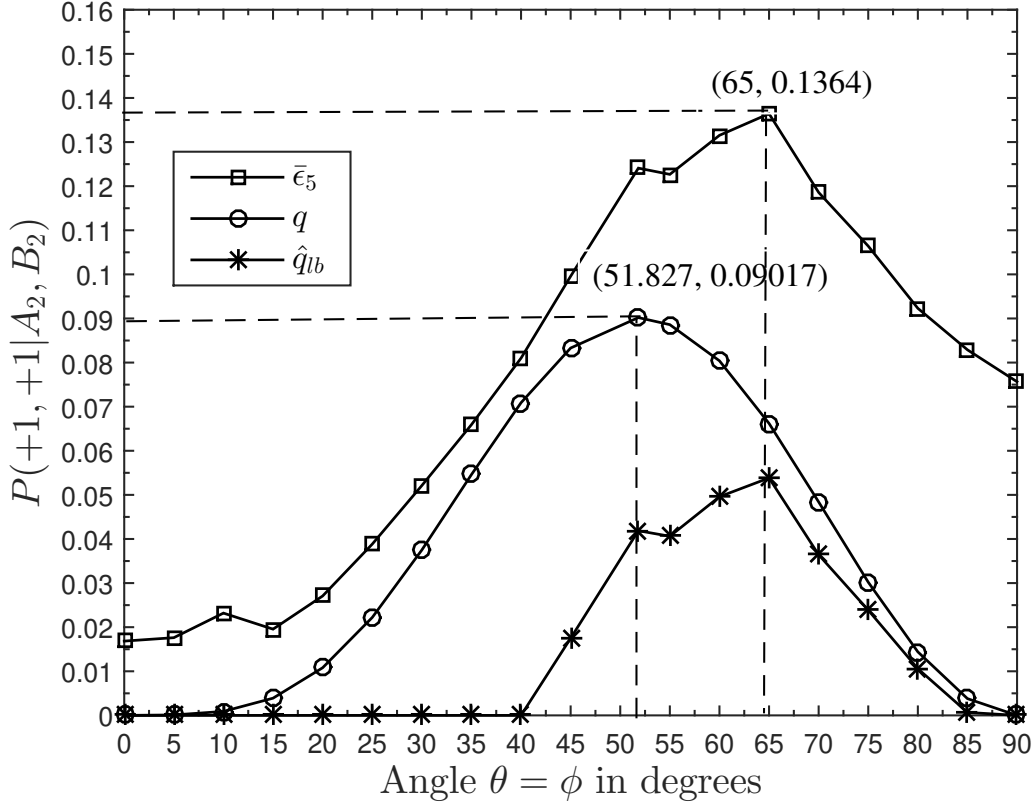


Figure 3-8: The variation of q , ϵ_5 and \hat{q}_{lb} against $\theta = \phi$ for CI=99% and $n = 10$ with Q_3 as control qubit and Q_4 as target qubit.

Consistency check

The above summary indicates that as q decreases, so does $\bar{\epsilon}_5$. Thus it is a natural question to ask, whether at $q = q_{max}$, we get $\bar{\epsilon}_5 = \bar{\epsilon}_5^{max}$ or not, where

$$\bar{\epsilon}_5^{max} = \max_{0 \leq \theta = \phi \leq 90} \{\bar{\epsilon}_{5\theta=\phi}\}. \quad (3.21)$$

We conduct another set of experiments to investigate this. If we take $\theta = \phi$ and vary it from 0 to 90 degrees, a bell-shaped curve is obtained with a peak at $\theta = \phi = 51.827$ degrees for q as shown in Figure 3-8 (a). For limited control of the IBM quantum computer, we plot $\bar{\epsilon}_5$, q and \hat{q}_{lb} with $(1 - \alpha) = 0.99$ for $\theta = \phi$ varying from 0 to 90 degrees with an increment of 5 degrees, i.e., $\theta = \phi = 5i$, where $i \in \{0, 1, \dots, 18\}$ (when $i = 18$ we get $\theta = \phi = 90$, then the value of χ is undefined as shown in the

Section 3.3. So we take $\theta = \phi = 89.99$ for this case).

From Figure 3-8 (a), we observe $\bar{\epsilon}_5^{max}$, as defined in Equation (3.21), is shifted right where $\theta = \phi = 65$ degrees, instead of $\theta = \phi = 51.827$ degrees. To get a more accurate result of $\bar{\epsilon}_5^{max}$, we repeat this experiment for $75 \geq \theta = \phi \geq 55$ degrees with an increment of one degree. The result shows that $\bar{\epsilon}_5^{max}$ occurs where $\theta = \phi = 62$ degrees (not shown in Figure 3-8 (a)). This procedure can be repeated again if the more precise occurrence of $\bar{\epsilon}_5^{max}$ is needed. We also observe that $\hat{q}_{lb} > 0$ when $85 \geq \theta = \phi \geq 40$ degrees and zero elsewhere, whereas $q > 0$ for $90 > \theta = \phi > 0$ degrees. This mismatch happens because of the reasons stated in Section 3.4.1. From these results it can be concluded that although in the IBM quantum computer, we get a non-zero value of the lower bound on Hardy's probability for NMES, but the errors occurred in the computer need to be more stable.

Summary

In summary, for the parameters θ and ϕ that lead to $q = 0$, our experimental outcome gives us $\bar{\epsilon}_4$ for MES and PS. For the parameters (θ and ϕ) that lead to $q > 0$, our experimental outcome gives us $\bar{\epsilon}_5$ for NMES. From Equation (3.20), the value of $\bar{\epsilon}_5$ for NMES is greater than $(\bar{\Sigma}_4 + \Delta)$ implying $\hat{q}_{lb} > 0$. But when the value of $\bar{\epsilon}_5$ is in the same range or less than $\bar{\epsilon}_4^{max}$, then it implies $\hat{q}_{lb} \leq 0$.

3.4.2 Other possible combinations of multi-qubit gate

In this section, we check Hardy's non-locality for the rest of the available combinations of qubits in the IBM quantum computer.

Check for non-locality

There are currently six combinations of multi-qubit gate implementation available in *ibmqx4* [106]. For the multi-qubit *CNOT* gate that we use, the possible control qubit and target qubit pairs other than (Q_3, Q_4) , are summarized in Table 3.5. We measure $\bar{\epsilon}_5$ for $\theta = \phi \in \{45, 51.827, 55\}$ degrees with all combinations of pairs of qubits. It

Control qubit	Target qubit	values of $\bar{\epsilon}_5$ for $n = 10$ for $\theta = \phi$		
		45	51.827	55
Q_2	Q_0	0.101022	0.111367	0.116217
Q_3	Q_2	0.094067	0.112275	0.114400
Q_1	Q_0	0.099931	0.119311	0.119497
Q_2	Q_1	0.138400	0.136175	0.134289
Q_2	Q_4	0.138505	0.150186	0.157253

Table 3.5: The values of $\bar{\epsilon}_5$ for $n = 10$ for all possible pairs of qubits other than (Q_3, Q_4) when $\theta = \phi \in \{45, 51.827, 55\}$ in degrees.

can be seen, when $\theta = \phi = 51.827$ degrees, the value of $\bar{\epsilon}_5$ is minimum for the pair (Q_2, Q_0) and maximum for the pair (Q_2, Q_4) . All the experiments described earlier have been performed using all combinations of these pair of qubits as described in Table 3.5 and similar conclusions of the non-locality are obtained as we get for the pair (Q_3, Q_4) .

Consistency check and shift of the peaks

We want to see, for other possible two-qubit pairs, whether $\bar{\epsilon}_5^{max}$ (as defined in Equation (3.21)) occurs when $q = q_{max}$ or not. We also want to see, in case there is any shift, whether it is in the same direction as shown in Figure 3-8 for the pair (Q_3, Q_4) or not.

From Table 3.5, it can be seen for the pair (Q_2, Q_1) , when $\theta = \phi = 51.827$ degrees, the value of $\bar{\epsilon}_5$ is less than the value when $\theta = \phi = 45$ degrees and greater than the value when $\theta = \phi = 55$ degrees, i.e., $\bar{\epsilon}_{5\theta=\phi=45} > \bar{\epsilon}_{5\theta=\phi=51.827} > \bar{\epsilon}_{5\theta=\phi=55}$. To verify this result, we perform a similar experiment for the pair (Q_2, Q_1) as we did for the pair (Q_3, Q_4) (as shown in Figure 3-8). Results are shown in Figure 3-9 which indicates that there is a shift of the value of $\bar{\epsilon}_5^{max}$ to the left for the pair (Q_2, Q_1) and it occurs when $\theta = \phi = 40$ degrees. For the rest of the pairs, we find that $\bar{\epsilon}_5^{max}$ is shifted to the right, i.e., $\bar{\epsilon}_{5\theta=\phi=55} > \bar{\epsilon}_{5\theta=\phi=51.827} > \bar{\epsilon}_{5\theta=\phi=45}$ as shown in Table 3.5. So, we can conclude that $\bar{\epsilon}_5^{max}$ did not occur at $q = q_{max}$, rather it is shifted to the right or to the left due to the errors.

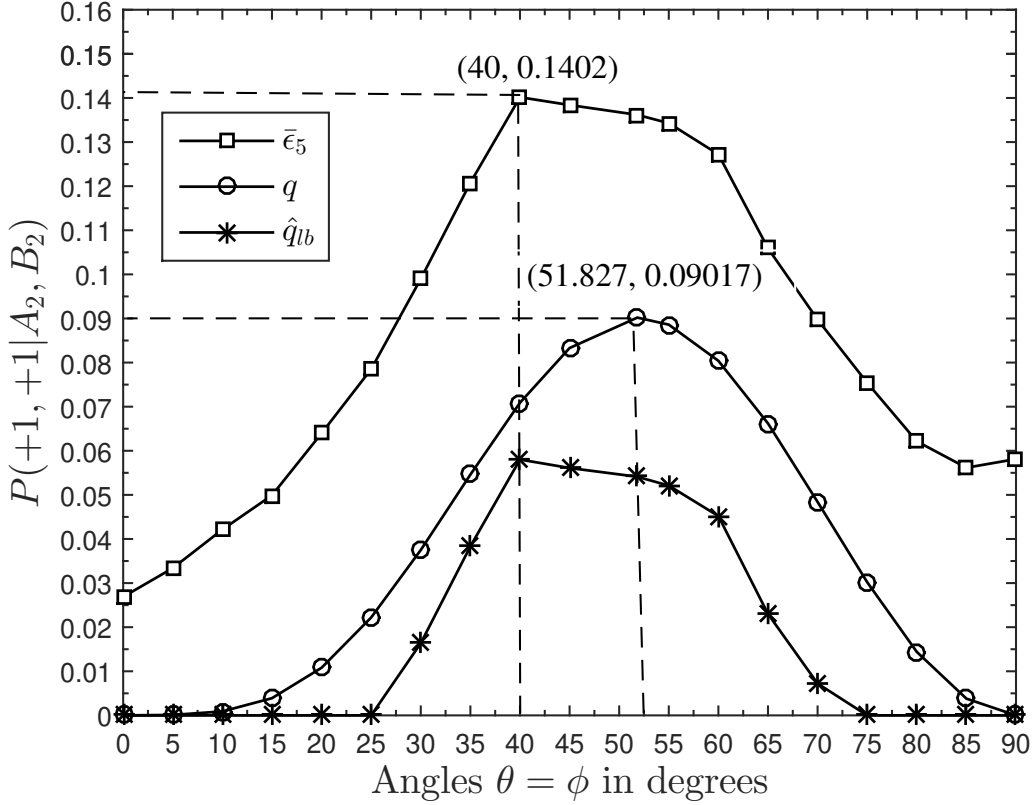


Figure 3-9: The variation of q , ϵ_5 and \hat{q}_{lb} against $\theta = \phi$ for CI=99% and $n = 10$ with Q_2 as control qubit and Q_1 as target qubit.

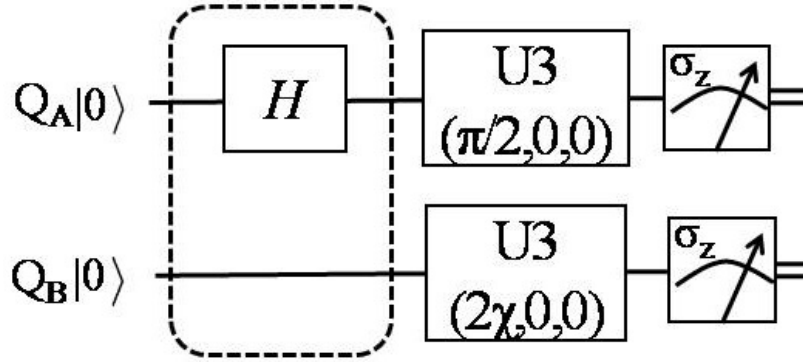
3.4.3 Application of the shift of the peaks in quantum protocols using Hardy's test

For some of the protocols like quantum Byzantine agreement [40], it is necessary to check whether Hardy's state (the state for which Equations (2.4)-(2.7) are satisfied) is actually prepared or not. Suppose, theoretically $q = q_{max}$ is achieved for a specific value ρ of the relevant parameter (of which q is a function, like θ and ϕ in our experiment). Because of the peak shifts as described in Section 3.4.1 and 3.4.2, in practical experiments, q_{max} should not be estimated corresponding to the exact value of ρ , but in an interval around ρ .

During the experiment, let the value of q_{max} with the addition of errors be Q_{max} (like $\bar{\epsilon}_5^{max}$ in our experiment). Now if the errors in the experiment are not stable, it

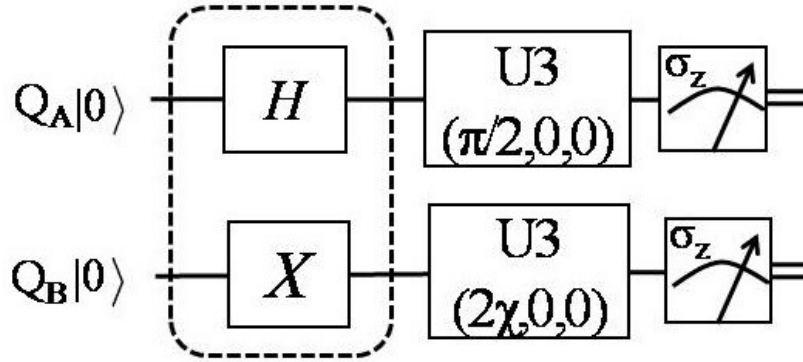
is expected that Q_{max} will lie in an interval around ρ , i.e., $\{\rho - \delta, \rho + \delta\}$ for some $\delta > 0$. For example, in our experimental set-up, δ is found to be 12 degrees when $\rho = (51.827, 51.827)$ in degrees of the parameter (θ, ϕ) .

3.4.4 Verifying whether reducing the number of gates reduces the error in the circuit



$$|\psi\rangle = \frac{1}{\sqrt{2}}(|0\rangle + |1\rangle) \otimes |0\rangle$$

(a) Quantum circuit for the PS $|\psi\rangle = \frac{1}{\sqrt{2}}(|0\rangle + |1\rangle) \otimes |0\rangle$ when $\theta = \phi = 0$ degrees.



$$|\psi\rangle = \frac{1}{\sqrt{2}}(|0\rangle + |1\rangle) \otimes |1\rangle$$

(b) Quantum circuit for the PS $|\psi\rangle = \frac{1}{\sqrt{2}}(|0\rangle + |1\rangle) \otimes |1\rangle$ when $\theta = 90$ and $\phi = 0$ degrees.

Figure 3-10: Quantum circuit and measurement for $P(+1, +1|A_1, B_2)$ when number of gates are reduced significantly.

To verify whether reducing the number of gates in the circuit reduces the error or not, we perform another series of experiments for (Q_3, Q_4) pair of qubits. For

$\theta = \phi = 0$, we get a PS, i.e., $|\psi\rangle = \frac{1}{\sqrt{2}}(|0\rangle + |1\rangle) \otimes |0\rangle$. This state can be created easily by using a Hadamard gate H in Alice's qubit and U_1 and U_3 used in Figure 3-5, becomes the identity (Id) gate. So, the number of gates is reduced significantly. For the modified circuit as shown in Figure 3-10 (a), the value of $\bar{\epsilon}_4 = 0.0084$ for $n = 10$ is less than the previous value (as shown in Table 3.2), i.e., 0.0193

Also, for $\theta = 90, \phi = 0$, we get a PS $|\psi\rangle = \frac{1}{\sqrt{2}}(|0\rangle + |1\rangle) \otimes |1\rangle$. For this state, a Hadamard gate on Alice's qubit and a bit flip gate X on Bob's qubit is required as shown in Figure 3-10 (b). Experimental results show that $\bar{\epsilon}_4 = 0.0079$ for $n = 10$ is again less than the previous value (as shown in Table 3.2), i.e., 0.0209.

These experiments are repeated for the rest of the pairs of qubits and similar results are obtained. We can conclude that reducing the number of gates reduces the error in the circuit of the IBM quantum computer.

3.4.5 Study of change of errors with respect to time in superconducting qubits

Time line	$\bar{\epsilon}_5$	SD (S_{ϵ_5})	$t_{\frac{\alpha}{2}} \frac{S_{\epsilon_5}}{\sqrt{n}}$ for different CIs			
			99%	95%	90%	80%
Before	0.16254	0.0078	0.154524	0.15696	0.158018	0.159129
After	0.1281	0.0039	0.124092	0.12531	0.125839	0.126394

Table 3.6: The values of $\bar{\epsilon}_5$ for $n = 10$ for the pair (Q_3, Q_4) before and after one month when $\theta = \phi = 51.827$ in degrees, SD=standard deviation, and CI=confidence interval.

During the experiments, the IBM quantum computer has undergone maintenance for nearly one month when some of the experiments were done. To present all the results in the same time-line, we repeat all the previous experiments. When we compare the data of one month earlier experiments, we find a significant change of values, similar to what was reported in [131]. For the pair (Q_3, Q_4) when $\theta = \phi = 51.827$ degrees, one month earlier, we got the value of $\bar{\epsilon}_5 = 0.16254$, $S_{\epsilon_5} = 0.0078$ and the values of $t_{\frac{\alpha}{2}} \frac{S_{\epsilon_5}}{\sqrt{n}}$ for different values of confidence intervals are given in Table 3.6. From this, we can see that the value of $\bar{\epsilon}_5$ one month earlier is greater than the values

of what we get one month later. A similar trend is noticed for the rest of the data.

3.4.6 Benchmarking of superconducting quantum devices using Hardy's paradox

Benchmarking is the process by which the performance of any computing device is evaluated. In the current era of Noisy Intermediate-Scale Quantum (NISQ) [233], choosing a universal metric for benchmarking is extremely difficult, because computing can be performed using various quantum technologies such as superconducting qubits [234, 235], ion trap [236], optical lattices [237], quantum dots [238], nuclear magnetic resonance (NMR) [93], etc. Also, how the noise affects the devices and their characterization are not well-understood.

Researchers have proposed different metrics for benchmarking, for instance, fidelity [239], unitarity [240], quantum volume [241], quantum chemistry [242], etc., each having their own drawbacks [243]. In [131], the authors have also demonstrated non-locality in the case of Mermin polynomials for three, four and five qubits. They have concluded that the fidelity of the quantum computer decreases when the number of qubits is increased from three. However, they do not mention anything for two qubits. From the experimental test of Hardy's paradox, we propose two metrics for benchmarking of two qubits of any superconducting quantum device as discussed below.

First, from Section 3.4.1 and 3.4.1, it can be seen that, for those states where $q > \bar{\Sigma}_4$, we get $\hat{q}_{lb} > 0$ which supports a non-zero value of Hardy's probability. When $\bar{\epsilon}_4^{max} < q < q_{max}$, the previous conclusion is still valid. But for those states where $q < \bar{\Sigma}_4$, no conclusion can be drawn about the value of Hardy's probability as $\hat{q}_{lb} \leq 0$. So, the minimum value of q from which we get $\hat{q}_{lb} > 0$ (as illustrated in Table 3.4), can be the performance measure of a quantum computer. Lesser the value of q which supports $\hat{q}_{lb} > 0$, the better the performance of the quantum computer. This parameter measures how well the device realizes NMES states.

Second, although we get q_{max} at $\theta = \phi = 51.827$ degrees, during the experiment,

due to unstable errors, the value of $\bar{\epsilon}_5^{max}$ may be shifted to any nearby value, as shown in Section 3.4.1 and 3.4.2. In our case, it shifted to the left for the pair (Q_2, Q_1) and to the right for the rest of the pairs of qubits. For our experiment when $\theta = \phi$, the amount of shift is 12 degrees. So, the amount of shift can be considered as a performance measure of a quantum computer. The smaller the shift, the better is the performance. This parameter measures the precision of the quantum device.

Chapter 4

Quantum teleportation and hyper-hybrid entangled state

In this Section, we show that some properties and applications of distinguishable and indistinguishable entanglement. First, we show that hyper-hybrid entanglement can exist for two indistinguishable fermions. Then I have generalized it for both bosons and fermions. Next, we prove that *quantum particles (either distinguishable or indistinguishable) can simultaneously produce and perform hyper hybrid entangled state and unit fidelity quantum teleportation respectively then using that cloning of any arbitrary quantum state is possible.* As the no-cloning theorem cannot be violated using in quantum theory, the logical conclusion from this statement can be written in the form of two no-go theorems; (i) *no-hyper hybrid entangled state for distinguishable particles* and (ii) *no-unit fidelity quantum teleportation for indistinguishable particles.* Finally we show the overall picture of the properties and applications of distinguishable and indistinguishable particles.

This chapter is based on the work in [244].

4.1 Hyper-hybrid entangled state for two indistinguishable fermions

Yurke and Stolar [216, 217] had proposed an optical circuit to generate quantum entanglement between the same DoFs of two identical particles (bosons and fermions) from initially separated independent sources. Some recent experiments realizing entanglement between the same DoFs of identical particles whose degree of spatial indistinguishability can be arbitrarily harnessed [221, 245, 223, 220]. The experiments are realized not only with photons but also simulating fermions. Recently, the above method has been extended by Li *et al.* [1] to generate hyper-hybrid entangled state between two independent bosons among their internal (e.g., spin) DoFs, external (e.g., momentum) DoFs, and across. We show that their circuit can also be used for independent fermions obeying the Pauli exclusion principle [224], albeit with different detection probabilities.

For fermions, the second quantization formulation deals with fermionic creation operators $f_{i,\mathbf{p}}$ with $|i, \mathbf{p}\rangle = f_{i,\mathbf{p}}^\dagger |0\rangle$, where $|0\rangle$ is the vacuum and $|i, \mathbf{p}\rangle$ describes a particle with spin $|i\rangle$ and momentum \mathbf{p} . These operators satisfy the canonical anticommutation relations:

$$\{f_{i,\mathbf{p}_i}, f_{j,\mathbf{p}_j}\} = 0, \quad \{f_{i,\mathbf{p}_i}, f_{j,\mathbf{p}_j}^\dagger\} = \delta(\mathbf{p}_i - \mathbf{p}_j) \delta_{ij}. \quad (4.1)$$

Analysis of the circuit of Li *et al.* [1, Fig. 2] as shown in Fig. 2-5 for fermions involves an array of hybrid beam splitters (HBSs) [1, Fig. 3]; phase shifter; four orthogonal external modes L , D , R , and U ; and two orthogonal internal modes \uparrow and \downarrow . Here, particles exiting through the modes L and D are received by Alice (A), who can control the phases ϕ_L and ϕ_D , whereas particles exiting through the modes R and U are received by Bob (B), who can control the phases ϕ_R and ϕ_U .

In this circuit [1, Fig. 2] as shown in Fig. 2-5, two particles, each with spin $|\downarrow\rangle$, enter the setup in the mode R and L for Alice and Bob, respectively. The initial state of the two particles is $|\Psi_0\rangle = f_{\downarrow,R}^\dagger f_{\downarrow,L}^\dagger |0\rangle$. Now, the particles are sent to the HBS such

that one output port of the HBS is sent to the other party (R or L) and the other port remains locally accessible (D or U). Next, each party applies path-dependent phase shifts. Lastly, the output of the local mode and that received from the other party are mixed with the HBS and then the measurement is performed in either external or internal modes. The final state can be written as

$$\begin{aligned}
|\Psi\rangle &= \frac{1}{4} \left[e^{i\phi_R} (f_{\downarrow,R}^\dagger + i f_{\uparrow,U}^\dagger) + i e^{i\phi_D} (f_{\uparrow,D}^\dagger + i f_{\downarrow,L}^\dagger) \right] \\
&\otimes \left[e^{i\phi_L} (f_{\downarrow,L}^\dagger + i f_{\uparrow,D}^\dagger) + i e^{i\phi_U} (f_{\uparrow,U}^\dagger + i f_{\downarrow,R}^\dagger) \right] |0\rangle.
\end{aligned} \tag{4.2}$$

Alice and Bob can perform coincidence measurements both in external DoFs or both in internal DoFs or with one party in the internal DoF and the other in the external DoF. Now from Eq. (4.2), the detection probabilities when each party gets exactly one particle where both Alice and Bob measure in external DoFs are given by

	$B : R$	$B : U$	
$A : D$	$\frac{1}{4} \cos^2 \phi$	$\frac{1}{4} \sin^2 \phi$,
$A : L$	$\frac{1}{4} \sin^2 \phi$	$\frac{1}{4} \cos^2 \phi$	

(4.3)

where $\phi = (\phi_D - \phi_L - \phi_R + \phi_U) / 2$.

Now we assign dichotomic variables $+1$ and -1 for the detection events $\{L, U\}$ and $\{D, R\}$, respectively. Let Pr_{mn} denote the probabilities of the coincidence events for Alice and Bob obtaining $m = \pm 1$ and $n = \pm 1$, respectively. The normalized expectation value is then given by

$$\begin{aligned}
E(\phi_A, \phi_B) &= \frac{Pr_{++} - Pr_{-+} - Pr_{+-} + Pr_{--}}{Pr_{++} + Pr_{-+} + Pr_{+-} + Pr_{--}} \\
&= \cos(\phi_A - \phi_B),
\end{aligned} \tag{4.4}$$

where $\phi_A = (\phi_D - \phi_L)$ and $\phi_B = (\phi_U - \phi_R)$. Now the CHSH [29] inequality can be written as

$$|E(\phi_A^0, \phi_B^0) + E(\phi_A^1, \phi_B^0) + E(\phi_A^0, \phi_B^1) - E(\phi_A^1, \phi_B^1)| \leq 2, \tag{4.5}$$

where the superscripts 0 and 1 stand for two detector settings for each particles. Now for $\phi_A^0 = 0$, $\phi_A^1 = \pi$, $\phi_B^0 = \frac{\pi}{4}$, and $\phi_B^1 = -\frac{\pi}{4}$, Eq. (4.5) can be violated maximally by obtaining Tsirelson's bound $2\sqrt{2}$ [246].

Now if Alice and Bob both measure in internal DoFs, then the detection probabilities can be written as

$$\begin{array}{c|cc}
 & B : \downarrow & B : \uparrow \\
 \hline
 A : \downarrow & \frac{1}{4}\sin^2\phi & \frac{1}{4}\cos^2\phi \\
 A : \uparrow & \frac{1}{4}\cos^2\phi & \frac{1}{4}\sin^2\phi
 \end{array} \quad (4.6)$$

If Alice measures in the internal DoF and Bob measures in the external DoF, then the detection probabilities can be written as

$$\begin{array}{c|cc}
 & B : R & B : U \\
 \hline
 A : \downarrow & \frac{1}{4}\sin^2\phi & \frac{1}{4}\cos^2\phi \\
 A : \uparrow & \frac{1}{4}\cos^2\phi & \frac{1}{4}\sin^2\phi
 \end{array} \quad (4.7)$$

If Alice measures in the external DoF and Bob measures in the internal DoF, then the detection probabilities can be written as

$$\begin{array}{c|cc}
 & B : \downarrow & B : \uparrow \\
 \hline
 A : D & \frac{1}{4}\cos^2\phi & \frac{1}{4}\sin^2\phi \\
 A : L & \frac{1}{4}\sin^2\phi & \frac{1}{4}\cos^2\phi
 \end{array} \quad (4.8)$$

Now by applying similar analysis for Eqs. (4.6), (4.7), and (4.8) as performed for Eqs. (4.4) and (4.5), one can show maximal violation of Bell's inequality.

4.1.1 Generalized Hyper-Hybrid entangled state

Interestingly, following the approach by Yurke and Stolar [216], we can generalize the detection probabilities of hyper-hybrid entangled state for indistinguishable bosons

and fermions into a single formulation as shown below. Let

$$\begin{aligned} \phi_1 &= \phi_D - \phi_L, \\ \phi_2 &= \begin{cases} -(\phi_R - \phi_U) & \text{for bosons} \\ -(\phi_R - \phi_U) + \frac{\pi}{2} & \text{for fermions.} \end{cases} \end{aligned} \quad (4.9)$$

The generalized detection probabilities of Eqs. (4.3), (4.6), (4.7), and (4.8) are, respectively, given by

	$B : R$	$B : U$	
$A : D$	$\frac{1}{4}\cos^2(\phi_1 - \phi_2)$	$\frac{1}{4}\sin^2(\phi_1 - \phi_2)$,
$A : L$	$\frac{1}{4}\sin^2(\phi_1 - \phi_2)$	$\frac{1}{4}\cos^2(\phi_1 - \phi_2)$	

(4.10)

	$B : \downarrow$	$B : \uparrow$	
$A : \downarrow$	$\frac{1}{4}\sin^2(\phi_1 - \phi_2)$	$\frac{1}{4}\cos^2(\phi_1 - \phi_2)$,
$A : \uparrow$	$\frac{1}{4}\cos^2(\phi_1 - \phi_2)$	$\frac{1}{4}\sin^2(\phi_1 - \phi_2)$	

(4.11)

	$B : R$	$B : U$	
$A : \downarrow$	$\frac{1}{4}\sin^2(\phi_1 - \phi_2)$	$\frac{1}{4}\cos^2(\phi_1 - \phi_2)$,
$A : \uparrow$	$\frac{1}{4}\cos^2(\phi_1 - \phi_2)$	$\frac{1}{4}\sin^2(\phi_1 - \phi_2)$	

(4.12)

	$B : \downarrow$	$B : \uparrow$	
$A : D$	$\frac{1}{4}\cos^2(\phi_1 - \phi_2)$	$\frac{1}{4}\sin^2(\phi_1 - \phi_2)$.
$A : L$	$\frac{1}{4}\sin^2(\phi_1 - \phi_2)$	$\frac{1}{4}\cos^2(\phi_1 - \phi_2)$	

(4.13)

Computations, following Eqs. (4.4) and (4.5), lead to the maximum violation of Bell's inequality.

4.2 Does the scheme of Li *et al.* [1] work for distinguishable particles?

We are interested to see whether the circuit of Li *et al.* [1, Fig. 2] as shown in Fig. 2-5 gives the same results for two distinguishable particles. Let us calculate the term in

the first row and first column of Eq. (4.3) for fermions. It says that the probability of Alice detecting a particle in detector D and Bob detecting a particle in detector R is given by

$$\left| \frac{1}{4} \left[e^{i(\phi_R + \phi_L)} + e^{i(\phi_D + \phi_U)} \right] \right|^2 = \frac{1}{4} \cos^2 \phi. \quad (4.14)$$

If the particles are made distinguishable, this probability is calculated as

$$\left| \frac{1}{4} e^{i(\phi_R + \phi_L)} \right|^2 + \left| \frac{1}{4} e^{i(\phi_D + \phi_U)} \right|^2 = \frac{1}{8}. \quad (4.15)$$

As for other terms of Eq. (4.3), each term of Eqs (4.6), (4.7), and (4.8) reduces to $\frac{1}{8}$. From that, one can easily show that the right hand side of Eq. (4.4) becomes zero. Thus the Bell violation is not possible by the CHSH test. Similar calculations for the bosons lead to the same conclusion. So, the circuit of [1] would not work for distinguishable particles.

4.3 Signaling using unit fidelity quantum teleportation and hyper-hybrid entangled state

In this section we will prove out main theorem and also derive two corollaries from that theorem.

Theorem 1. *If quantum particles (either distinguishable or indistinguishable) can simultaneously produce and perform hyper hybrid entangled state and unit fidelity quantum teleportation respectively then using that cloning of any arbitrary quantum state is possible.*

It is well-known that unit fidelity quantum teleportation [225] for distinguishable particles is possible using BSM and LOCC. Here, we show that if hyper-hybrid entangled state for distinguishable particles could exist, then one could construct a universal quantum cloning machine (UQCM) [79, 80] using unit fidelity quantum teleportation and hyper-hybrid entangled state, and further, use that UQCM to achieve signaling. Throughout this thesis, by signaling we mean faster-than-light or superluminal

communication across spacelike separated regions.

Proof. Now we give a details proof of the Theorem 1.

4.3.1 Description of the protocol

Our signaling protocol works in three phases, as follows.

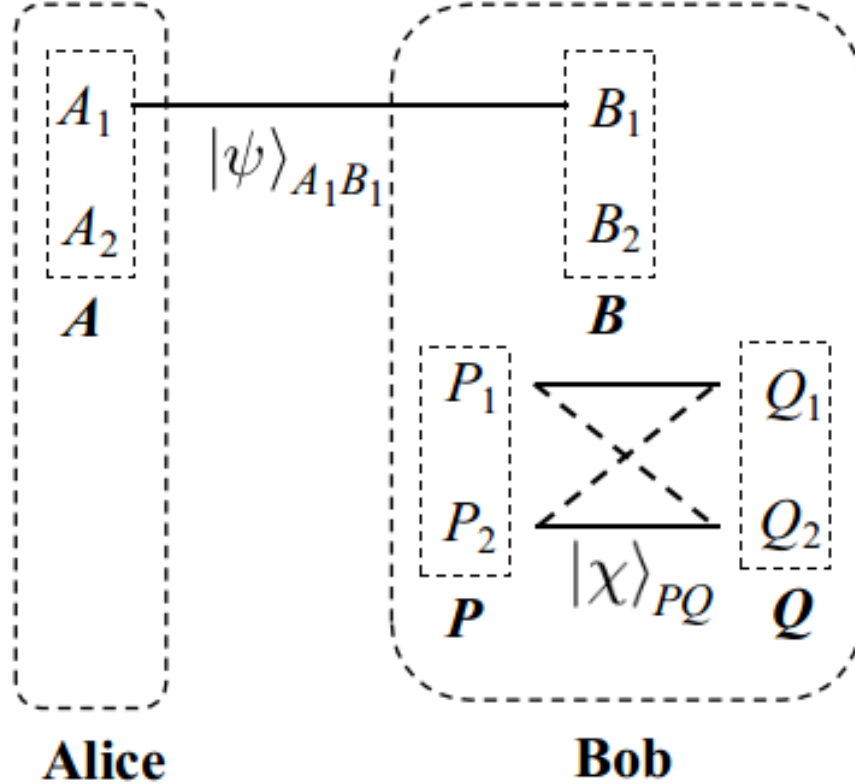


Figure 4-1: The singlet state $|\psi\rangle_{A_1B_1}$ is shared between DoF 1 of Alice and that of Bob, whereas hyper-hybrid entangled state $|\chi\rangle_{PQ}$ is kept by Bob.

First phase: initial set-up.

Suppose there are four particles A , B , P , and Q each having two DoFs 1 and 2. The particle A is with Alice and the remaining three are with Bob, who is spacelike separated from Alice. The pair $\{A, B\}$ is in the singlet state in DoF 1 denoted by $|\psi\rangle_{A_1B_1}$ and the pair $\{P, Q\}$ is in hyper-hybrid entangled state using both the DoFs 1 and 2 denoted by $|\chi\rangle_{PQ}$. To access the DoF i of particle X , we use the notation X_i ,

where $X \in \{A, B, P, Q\}$ and $i \in \{1, 2\}$. The situation is depicted in Fig. 4-1. Note that $|\psi\rangle_{A_1B_1}$ can be expressed in any orthogonal basis. We have taken only Z basis or computational basis $\{|0\rangle, |1\rangle\}$ and X basis or Hadamard basis $\{|+\rangle, |-\rangle\}$ such that

$$\begin{aligned} |\psi\rangle_{A_1B_1} &= \frac{1}{\sqrt{2}} \left(|01\rangle_{A_1B_1} - |10\rangle_{A_1B_1} \right) \\ &= \frac{1}{\sqrt{2}} \left(|+-\rangle_{A_1B_1} - |-+\rangle_{A_1B_1} \right). \end{aligned} \quad (4.16)$$

Alice wants to transfer binary information instantaneously to Bob. Before going apart, Alice and Bob agree on the following convention.

1. If Alice wants to send zero to Bob, then she would measure in Z basis on the DoF 1 of her particle so that the state of the DoF 1 of the particle at Bob's side would be either $|0\rangle$ or $|1\rangle$.
2. If Alice wants to send 1 to Bob, then she would measure in X basis on the DoF 1 of her particle so that the state of the DoF 1 of the particle at Bob's side would be either $|+\rangle$ or $|-\rangle$.

Second phase: cloning of any unknown state.

There are two steps of our proposed UQCM as follows.

1. Alice does measurement on DoF 1 of her particle A , i.e., A_1 in either Z basis or X basis. After this measurement, the state on DoF 1 of particle B , i.e., B_1 on Bob's side, is in an unknown state $|\phi\rangle \in \{|0\rangle, |1\rangle, |+\rangle, |-\rangle\}$ and it is denoted by $|\phi\rangle_{B_1}$.
2. After Alice's measurement, Bob performs BSM on DoF 1 of particles B and P , i.e., on B_1 and P_1 . This results in an output k as one of the four possible Bell states (as seen in standard teleportation protocol [43]). Based on this output k , suitable unitary operations U_k are applied on both the DoFs of Q , i.e., Q_1 and Q_2 , where $U_k \in \{\mathcal{I}, \sigma_x, \sigma_y, \sigma_z\}$, \mathcal{I} being the identity operation and σ_i 's ($i = x, y, z$) the Pauli matrices. As the first DoF of particle P , P_1 is maximally entangled

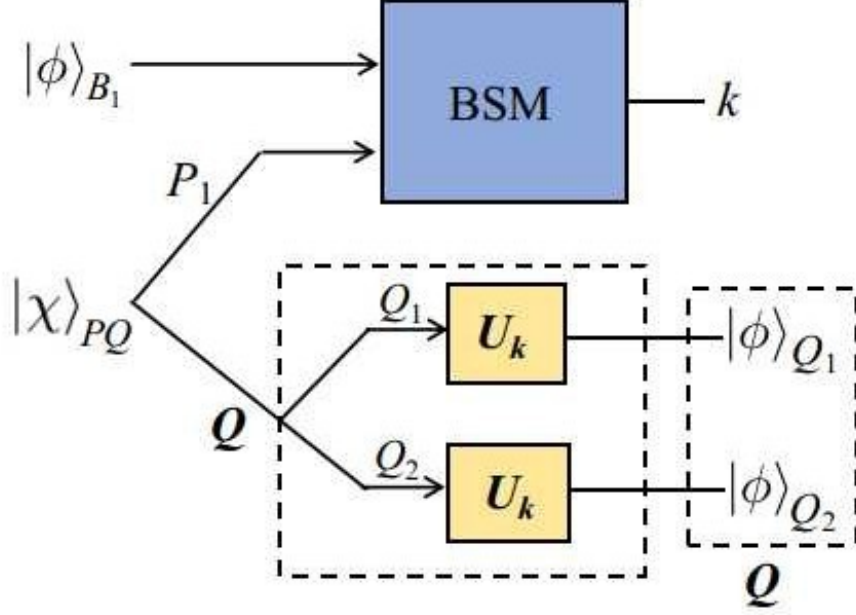


Figure 4-2: Our proposed universal quantum cloning machine to demonstrate the impossibility of hyper-hybrid entangled state using distinguishable particles. Inputs to this cloning machine are the unknown quantum state $|\phi\rangle$ of DoF 1 of the particle B (denoted by $|\phi\rangle_{B_1}$) and the hyper-hybrid entangled state $|\chi\rangle_{PQ}$, as shown in Fig. 4-1. More specifically, $|\phi\rangle_{B_1}$ is the state unknown to Bob generated on Bob's side after Alice does measurement on A_1 in either Z basis or X basis. After that, Bob performs BSM on B_1 and P_1 , resulting in one of the four possible Bell states as output, denoted by k . Based on this output k , suitable unitary operations U_k are applied on both the DoFs of Q , i.e., Q_1 and Q_2 , where $U_k \in \{\mathcal{I}, \sigma_x, \sigma_y, \sigma_z\}$, \mathcal{I} being the identity operation and σ_i 's ($i=x, y, z$) the Pauli matrices. As a result, the unknown state $|\phi\rangle$ of B_1 is copied to both Q_1 and Q_2 .

with both the DoFs of Q , i.e., Q_1 and Q_2 ; thus, using BSM on DoFs B_1 and P_1 and suitable unitary operations on DoFs Q_1 and Q_2 , the unknown state $|\phi\rangle$ on DoF B_1 is copied to both the DoFs Q_1 and Q_2 . This part of the circuit, shown in Fig. 4-2, acts as a UQCM.

Third phase: decoding Alice's measurement basis.

Now from the two copies of the unknown state $|\phi\rangle$ on the two DoFs of Q , i.e., $|\phi\rangle_{Q_1}$ and $|\phi\rangle_{Q_2}$, Bob tries to discriminate the measurement bases of Alice, so that he can decode the information sent to him. For that, Bob measures both the DoFs of Q in Z

basis, resulting in either 0 or 1 in each of the DoFs. Now there are two possibilities.

1. If Alice has measured in Z basis, then Bob's possible measurement results on the two DoFs of Q are $\{00, 11\}$.
2. On the other hand, if Alice has measured in X basis, then Bob's possible measurement results on the two DoFs of Q are $\{00, 01, 10, 11\}$.

Suppose, Bob adopts the following strategy. Whenever his measurement results are all zero or all one (i.e., 00 or 11), then he concludes that Alice has sent a zero, and whenever he measures otherwise (i.e., 01 or 10) then he concludes that Alice has sent a 1.

4.3.2 Computation of the signaling probability

Let the random variables X_A and X_B denote the bit sent by Alice and the bit decoded by Bob, respectively. Hence, under the above strategy, Bob's success probability of decoding, which is also the probability of signaling, is given by

$$\begin{aligned}
 P_{sig} &= \Pr(X_A=0 \wedge X_B=0) + \Pr(X_A=1 \wedge X_B=1) \\
 &= \Pr(X_A=0) \cdot \Pr(X_B=0 | X_A=0) \\
 &\quad + \Pr(X_A=1) \cdot \Pr(X_B=1 | X_A=1) \\
 &= \frac{1}{2} \cdot 1 + \frac{1}{2} \cdot \frac{2}{4} = 0.75.
 \end{aligned} \tag{4.17}$$

To increase P_{sig} further, Bob can use hyper-hybrid entangled state involving N DoFs of P and Q , with $N \geq 3$. Then he can make N copies of the unknown state $|\phi\rangle$ into the DoFs of Q . Analogous, to the strategy above for the case $N=2$, here also if all the measurement results of Bob in the N DoFs of Q in Z basis are the same, i.e., all-zero case or the all-one case, then Bob concludes that Alice has sent a zero; otherwise, he concludes that Alice has sent a 1. Thus, the above expression of P_{sig} changes to

$$\frac{1}{2} \cdot 1 + \frac{1}{2} \cdot \frac{2^N - 2}{2^N}.$$

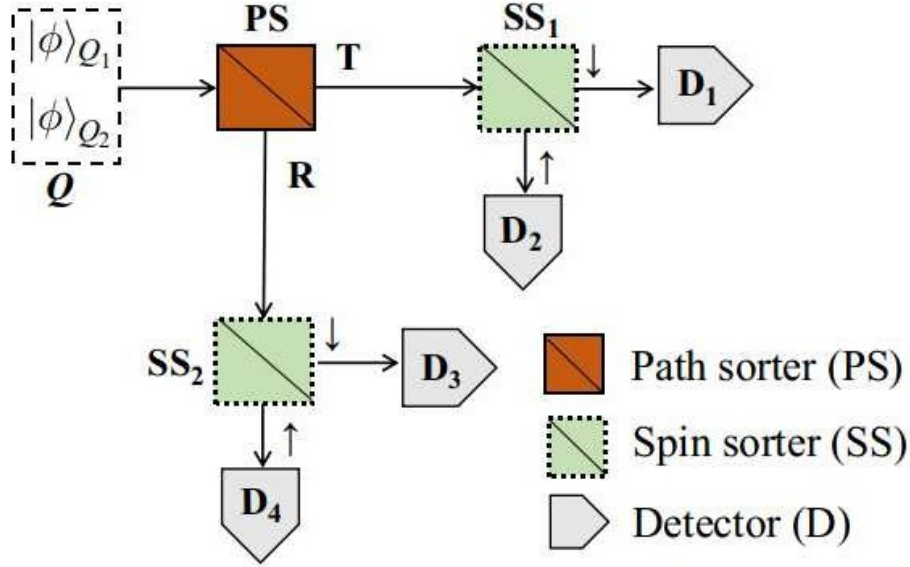


Figure 4-3: Bob's circuit for distinguishing between Z and X bases using two types of DoF sorters, i.e., a spin sorter (SS) and a path sorter (PS), and four detectors. Here the output of Fig. 4-2 is used as an input in this circuit. Here, $|\downarrow\rangle$ and $|\uparrow\rangle$ denote the down- and the up-spin states of the particles, respectively. Further, $|T\rangle$ denotes the transverse mode and $|R\rangle$ denotes the reflected modes of a PS.

In other words,

$$P_{sig} = 1 - \frac{1}{2^N}. \quad (4.18)$$

By making N larger and larger, P_{sig} can be made arbitrarily close to 1. \square

4.3.3 Experimental realization using optical circuits

For the experimental realization of the above protocol, we propose a circuit with DoF sorters, such as a spin sorter (SS), path sorter (PS), etc. (A spin sorter can be realized in an optical system using a polarizing beam splitter for sorting between the horizontal $|H\rangle$ and the vertical $|V\rangle$ polarizations of a photon. For an alternative implementation in atomic systems using Raman process, one can see [1, Fig. 3].)

Suppose DoFs 1 and 2 are spin and path, respectively, with the two output states $\{|\downarrow\rangle, |\uparrow\rangle\}$ and $\{|T\rangle, |R\rangle\}$. Here, $|\downarrow\rangle$ and $|\uparrow\rangle$ denote the down and the up spin states of the particles and $|T\rangle$ and $|R\rangle$ denote the transverse and the reflected modes of a

PS, respectively. Without loss of generality, we take

$$\begin{aligned}
|0\rangle &= |\downarrow\rangle = |T\rangle, \quad |1\rangle = |\uparrow\rangle = |R\rangle, \\
|+\rangle &= \frac{1}{\sqrt{2}} (|\downarrow\rangle + |\uparrow\rangle) = \frac{1}{\sqrt{2}} (|T\rangle + |R\rangle), \\
|-\rangle &= \frac{1}{\sqrt{2}} (|\downarrow\rangle - |\uparrow\rangle) = \frac{1}{\sqrt{2}} (|T\rangle - |R\rangle).
\end{aligned} \tag{4.19}$$

The circuit, shown in Fig. 4-3, takes as input particle Q with DoFs 1 and 2, each having the cloned state $|\phi\rangle$ from the output of the circuit in Fig. 4-2. Bob places a path sorter PS followed by two spin sorters SS_1 and SS_2 on two output modes of PS . Let D_1 (D_3) and D_2 (D_4) be the detectors at the two output ports of SS_1 (SS_2).

If Alice measures in Z basis, Bob detects the particles in $\{D_1, D_4\}$ with unit probability. On the other hand, if she measures in X basis, the particles would be detected in each of the detector sets $\{D_1, D_4\}$ and $\{D_2, D_3\}$ with a probability of 0.5. When Bob detects the particles in either D_2 or D_3 , he instantaneously knows that the measurement basis of Alice is X . In this case, the signaling probability is 0.75, which can be obtained by putting $N = 2$ in Eq. (4.18).

For better signaling probability, one can use three DoFs 1, 2, and 3, instead of two, in the joint state $|\chi\rangle_{PQ}$. The scheme for three DoFs is shown in Fig. 4-4, where S_i represents the sorter for DoF i , for $i \in \{1, 2, 3\}$. Now, if Alice measures in Z basis, Bob detects the particles in $\{D_1, D_8\}$ with probability 1. But if she measures in X basis, the particles would be detected in $\{D_1, D_8\}$ with probability $\frac{2}{2^3}$ and in $\{D_2, \dots, D_7\}$ with probability $\frac{2^3-2}{2^3} = 0.75$. In this case, the signaling probability is 0.875, which can be obtained by putting $N = 3$ in Eq. (4.18).

We can generalize the above schematic as follows. Suppose, each of P and Q has N DoFs (each degree having two eigenstates), numbered 1 to N , in hyper-hybrid entangled state $|\chi\rangle_{PQ}$. We also need to use N corresponding types of DoF sorters. Now, if Alice measures in Z basis, Bob detects the particles in $\{D_1, D_{2^N}\}$ with probability 1. But if she measures in X basis, the particles are detected in $\{D_1, D_{2^N}\}$ with probability $\frac{2}{2^N}$ and in detectors $\{D_2, \dots, D_{2^N-1}\}$ with probability $\frac{2^N-2}{2^N}$. For N DoFs, the signaling probability is given in Eq. (4.18).

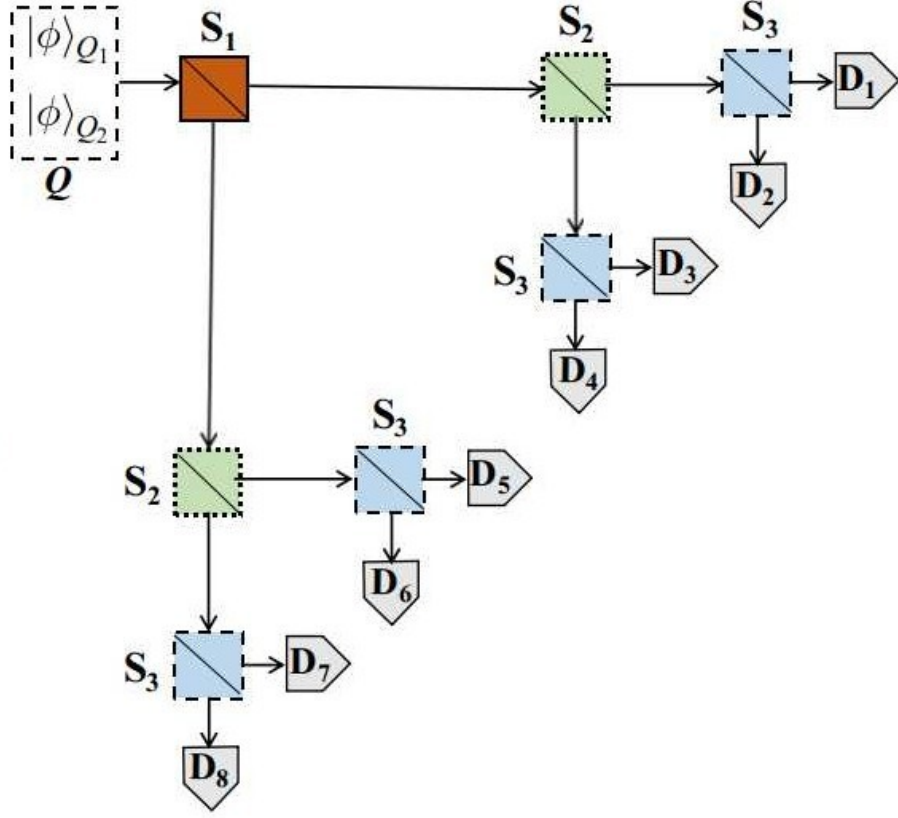


Figure 4-4: Bob's circuit for distinguishing between Z and X bases using three types of DoF sorters, i.e., S_1 , S_2 , and S_3 , and eight detectors. Here the output of Fig. 4-2 is used as an input in this circuit.

Increasing signaling probability without increasing the number of DoFs

From Eq. (4.18), it is clear that the signaling is possible only when N is infinitely large. The existence of such a huge number of accessible DoFs may be questionable. Interestingly, we devise an alternative schematic that can drive the asymptotic success probability to 1 with only two DoFs but using many copies of the singlet state shared between Alice and Bob and the same number of copies of hyper-hybrid entangled state at Bob's disposal.

Suppose, Alice and Bob share M copies of the singlet state $\{|\psi^{(1)}\rangle_{A_1B_1}, |\psi^{(2)}\rangle_{A_1B_1}, \dots, |\psi^{(M)}\rangle_{A_1B_1}\}$ and Bob also has an equal number of copies of hyper-hybrid entangled states $\{|\chi^{(1)}\rangle_{PQ}, |\chi^{(2)}\rangle_{PQ}, \dots, |\chi^{(M)}\rangle_{PQ}\}$ (a single copy of the singlet state and hyper-hybrid entangled state is shown in Fig. 4-1). Now the

cloning can be performed in the following two steps.

1. Alice performs measurement in her preferred basis on each DoF 1 of her M particles so that on the DoF 1 of each of the M particles on Bob's side, a copy of the unknown state $|\phi\rangle$ is obtained.
2. After that, Bob performs BSM on each of the M pairs of $\{B_1, P_1\}$ and suitable unitary operations so that the unknown state $|\phi\rangle$ is copied to each of the M pairs of $\{Q_1, Q_2\}$.

Now Bob passes each of the M copies of Q as shown in Fig. 4-3 and adopts the following strategy. If Bob receives each of the M particles in D_1 or D_4 , then he concludes that Alice has measured in Z basis. On the other hand, if Bob observes any one of the M particles in D_2 or D_3 , then he concludes that Alice has measured in X basis. Under this strategy, Bob encounters a decoding error whenever Alice has measured in X basis, but he receives all the M particles in D_1 or D_4 . In this case, the probability that a single particle is detected in the detector set $\{D_1, D_4\}$ is $\frac{1}{2}$ and hence the probability that all the M particles are detected in the above set is $\frac{1}{2^M}$. Hence, the corresponding success probability of signaling is given by

$$P_{sig} = 1 - \frac{1}{2^M}, \quad (4.20)$$

which also asymptotically goes to 1.

Thus we have the following logical version of Theorem 1

$$\text{HHES} \wedge \text{UFQT} \Rightarrow \text{Signaling}. \quad (4.21)$$

4.4 First no-go theorem: no hyper-hybrid entangled state for distinguishable particles

Proof. Unit fidelity quantum teleportation can be performed by distinguishable particles [43]. Thus if hyper-hybrid entangled state is also possible for distinguishable

particles, it would lead to signaling as shown in Section 4.3. Thus a logical conclusion is that in a world where special relativity holds barring signaling, hyper-hybrid entangled state is not possible using distinguishable particles. Thus we can write this no-go theorem logically as

$$\text{No-signaling} \Rightarrow \text{no-HHES} \wedge \text{UFQT}. \quad (4.22)$$

□

4.5 Second no-go theorem: no unit fidelity quantum teleportation for indistinguishable particles

Proof. Earlier, we have shown that signaling for distinguishable particles can be achieved using unit fidelity quantum teleportation and hyper-hybrid entangled state as black-boxes. unit fidelity quantum teleportation for distinguishable particles is already known [43], and so we have concluded that hyper-hybrid entangled state for distinguishable particles must be an impossibility.

Using massive identical particles, Marzolino and Buchleitner [247] have shown that unit fidelity quantum teleportation is not possible using a finite and fixed number of indistinguishable particles, due to the particle number conservation superselection rule (SSR) [248, 249]. Interestingly, several independent works [249, 250, 251] have already established that this superselection rule can be bypassed. So, an obvious question is: whether it is possible to perform unit fidelity quantum teleportation for indistinguishable particles bypassing the superselection rule. This question is also answered in the negative in [247].

Very recently, for indistinguishable particles, Lo Franco and Compagno [163] have achieved a quantum teleportation fidelity of 5/6, overcoming the classical teleportation fidelity bound 2/3 [252]. But they have not proved whether this value is optimal

or whether unit fidelity can be achieved or not.

Systematic calculations show that our earlier scheme of quantum cloning and signaling (Figs. 4-1 and Fig. 4-2) would still work, even if one replaces the unit fidelity quantum teleportation and hyper-hybrid entangled state tools for distinguishable particles with those of the indistinguishable ones (assuming that such tools exist). As signaling is not possible in quantum theory, we have concluded that hyper-hybrid entangled state for distinguishable particles is not possible. But, for indistinguishable particles, the creation of hyper-hybrid entangled state is possible [1]. Thus, a logical conclusion is that, to prevent signaling, unit fidelity quantum teleportation must not be possible for indistinguishable particles. So, this no-go theorem can be represented logically as

$$\text{No-signaling} \Rightarrow \text{HHES} \wedge \text{no-UFQT}. \quad (4.23)$$

□

4.6 Physical significance of the two no-go theorems

From the above two no-go results, we can establish a separation result between distinguishable and indistinguishable particles. Let Q_{dis} and Q_{indis} be the two sets consisting of quantum properties and applications of distinguishable and indistinguishable particles, respectively, as shown in Fig. 4-5.

Several earlier works have attempted extending many results on one of these two sets to the other. For example, quantum teleportation was originally proposed for distinguishable particles [43, 212]. But recent works [163, 247] have extended it for indistinguishable particles. Similarly, duality of entanglement as proposed in [253] was thought to be a unique property of indistinguishable particles. But later its existence for distinguishable particle was shown in [254]. Another unique property of quantum correlation is quantum coherence, which was proposed for distinguishable particles in [255] and later for indistinguishable particles in [256]. Einstein-Podolsky-

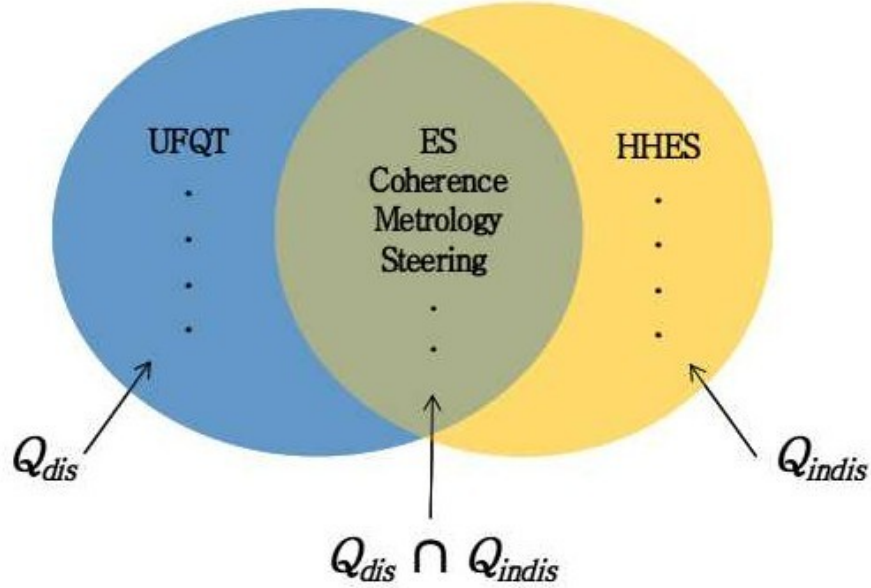


Figure 4-5: The two sets Q_{dis} (consisting of quantum properties and applications of distinguishable particles), Q_{indis} (consisting of quantum properties and applications of indistinguishable particles), and their intersection (UFQT, HHES, and ES stand for unit fidelity quantum teleportation, hyper-hybrid entangled state, and entanglement swapping, respectively).

Rosen steering [142] was extended from distinguishable particles to a special class of indistinguishable particles called Bose-Einstein condensates [257]. Entanglement swapping, originally proposed for distinguishable particles in [44, 53, 54], was also shown for indistinguishable particles in [176].

To the best of our knowledge, there is no known quantum correlation or application that is unique for distinguishable particles only and does not hold for indistinguishable particles, and vice versa. In Section 4.4 of this paper, we have shown that hyper-hybrid entangled state is unique to the set Q_{indis} , and in Section 4.5 we have established that unit fidelity quantum teleportation is unique to the set Q_{dis} . Thus, we demonstrate a clear separation between these two sets.

Chapter 5

Degree of freedom trace-out rule for indistinguishable particles

The representation and the trace-out rule of the state of two indistinguishable particles each having single DoF is discussed in Chapter 2.7.1. In this Chapter, we first discuss the representation of the general state of indistinguishable particles each having multiple DoFs using the notions of [161, 163]. Next, we discuss our proposed DoF trace-out operation of indistinguishable particles when each particle have multiple DoFs. Finally we discuss the physical significance of the proposed DoF trace-out rule.

This chapter is based on the work in [258, 259].

5.1 Representation of the general state of indistinguishable particles

Lo Franco *et al.* [161, 163] have defined the partial trace-out rule for indistinguishable particles where each particle has a spatial label and a single DoF. But as the notions of [161, 163] for indistinguishable particles is not readily applicable for particles having multiple DoFs, we have extended their notions to overcome this problem.

5.1.1 Two indistinguishable particles each having two DoFs

Assume two indistinguishable particles each having two DoFs are associated with two spatial labels α^1 and α^2 . Here a_j^i ranges over $\mathbb{D}_j := \{D_{j_1}, D_{j_2}, \dots, D_{j_{k_j}}\}$, represents the eigenvalue of the j -th DoF of the particle in the α^i -th localized region where $i, j \in \mathbb{N}_2 = \{1, 2\}$ and $k_j \geq 2$, since each DoF must have at least two distinct eigenvalues. The general state of such a system is written as

$$|\Psi^{(2,2)}\rangle := \sum_{\alpha^1, \alpha^2, a_1^1, a_2^1, a_1^2, a_2^2} \eta^u \kappa_{a_1^1, a_2^1, a_1^2, a_2^2}^{\alpha^1, \alpha^2} |\alpha^1 a_1^1 a_2^1, \alpha^2 a_1^2 a_2^2\rangle, \quad (5.1)$$

where α^1, α^2 ranges over $\mathbb{S}^P := \{s^1, s^2, \dots, s^P\}$ which refers to distinct spatial modes with $P \geq 2$. Here u represents the summation of parity of the cyclic permutations of all the n DoFs. Thus u can be represented as $u = u_1 + u_2 + \dots + u_n = \sum_i u_j$ where u_j is the parity of j -th DoF. The value of η is $+1$ for bosons and -1 for fermions. If we have the following condition that

$$\left(\alpha^i = \alpha^{i'}\right) \wedge \left(a_j^i = a_j^{i'}\right) \quad (5.2)$$

for any $i \neq i'$ where $\alpha^i, \alpha^{i'} \in \mathbb{S}^P$ and $j \in \mathbb{N}_2$, then we get $\eta = 0$ for fermions due to Pauli exclusion principle [224].

The value of k_j may vary with j . For example, consider two DoFs: polarization and optical orbital angular momentum (OAM), associated with a system of indistinguishable photons. Generally, the polarization belongs to a two-dimensional Hilbert space, whereas the orbital angular momentum lies in an infinite-dimensional Hilbert space governed by the azimuthal index l . In practical implementations, this mismatch in Hilbert space dimensions between the two DoFs is taken care of by mapping the larger dimensional space to the lower dimensional one [260, 261]. For orbital angular momentum, the infinite-dimensional Hilbert space is generally mapped into a two-dimensional one with the eigenvalues $\{2l, 2l + 1\}$ or $\{+l, -l\}$. Also, the Hilbert space is sometimes restricted to smaller dimensions by proper state engineering in which case only certain chosen values of l are allowed.

Following the above notations, the general density matrix of two indistinguishable particles each having two DoFs is expressed as

$$\rho^{(2,2)} := \sum_{\alpha^i, \beta^i, a_j^i, b_j^i} \eta^{(u+\bar{u})} \kappa_{a_1^1 a_2^1, a_1^2 a_2^2, b_1^1 b_2^1, b_1^2 b_2^2}^{\alpha^1, \alpha^2, \beta^1, \beta^2} |\alpha^1 a_1^1 a_2^1, \alpha^2 a_1^2 a_2^2\rangle \langle \beta^1 b_1^1 b_2^1, \beta^2 b_1^2 b_2^2|, \quad (5.3)$$

where α^i, β^i ranges over \mathbb{S}^P , a_j^i, b_j^i ranges over \mathbb{D}_j , and $i, j \in \mathbb{N}_2$. Here u is as defined in Eq. (5.1) and \bar{u} comes due to density matrix. If we have the following condition that

$$\{(\alpha^i = \alpha^{i'}) \wedge (a_j^i = a_j^{i'})\} \vee \{(\beta^i = \beta^{i'}) \wedge (b_j^i = b_j^{i'})\} \quad (5.4)$$

for any $i \neq i'$ where $i, i' \in \mathbb{N}_2$ and $j \in \mathbb{N}_2$, then we get $\eta = 0$ for fermions due to Pauli exclusion principle [224].

The general density matrix of the state in Eq. (5.1) is represented as

$$\rho^{(2,2)} := \sum_{\alpha^i, \beta^i, a_j^i, b_j^i} \eta^{(u+\bar{u})} \kappa_{a_1^1 a_2^1, a_1^2 a_2^2}^{\alpha^1, \alpha^2} \kappa_{b_1^1 b_2^1, b_1^2 b_2^2}^{\beta^1, \beta^2*} |\alpha^1 a_1^1 a_2^1, \alpha^2 a_1^2 a_2^2\rangle \langle \beta^1 b_1^1 b_2^1, \beta^2 b_1^2 b_2^2|, \quad (5.5)$$

where the notations are same as Eq. (5.3).

In the next section, we extend this notions to two indistinguishable particles each having n DoFs.

5.1.2 Two indistinguishable particles each having n DoFs

Lets us consider two indistinguishable particles each having n DoFs. Following the same notations of Eq. (5.1), the general state of Eq. (5.1) of two particles from two DoFs to n DoFs can be represented as

$$|\Psi^{(2,n)}\rangle := \sum_{\alpha^i, a_j^i} \eta^u \kappa_{a_1^1 a_2^1 \dots a_n^1, a_1^2 a_2^2 \dots a_n^2}^{\alpha^1, \alpha^2} |\alpha^1 a_1^1 a_2^1 \dots a_n^1, \alpha^2 a_1^2 a_2^2 \dots a_n^2\rangle, \quad (5.6)$$

where a_j^i ranges over \mathbb{D}_j , $i \in \mathbb{N}_2 = \{1, 2\}$, and $j \in \mathbb{N}_n = \{1, 2, \dots, n\}$.

The general density matrix of two indistinguishable particles each having n DoFs

following Eq. (5.3) can be described as

$$\rho^{(2,n)} := \sum_{\alpha^i, \beta^i, a_j^i, b_j^i} \eta^{(u+\bar{u})} \kappa_{\alpha_1^1 a_1^1 \dots a_n^1, \alpha_1^2 a_2^2 \dots a_n^2, \beta_1^1 b_1^1 \dots b_n^1, \beta_1^2 b_2^2 \dots b_n^2} |\alpha^1 a_1^1 a_2^1 \dots a_n^1, \alpha^2 a_1^2 a_2^2 \dots a_n^2, \beta^1 b_1^1 b_2^1 \dots b_n^1, \beta^2 b_1^2 b_2^2 \dots b_n^2\rangle, \quad (5.7)$$

where where a_j^i, b_j^i , ranges over \mathbb{D}_j , $i \in \mathbb{N}_2 = \{1, 2\}$, and $j \in \mathbb{N}_n = \{1, 2, \dots, n\}$.

In the next section, we describe the most general state of p indistinguishable particles each having n DoFs.

5.1.3 p indistinguishable particles each having n DoFs

In this section, we describe the most general state of p indistinguishable particles each having n DoF. For better understanding, we are describing the notations once again.

The P spatial labels are represented by α^i where α^i ranges over $\mathbb{S}^P := \{s^1, s^2, \dots, s^P\}$. We write the set $\{1, 2, \dots, n\}$ as \mathbb{N}_n . Here a_j^i ranges over $\mathbb{D}_j := \{D_{j_1}, D_{j_2}, \dots, D_{j_{k_j}}\}$, represents the eigenvalue of the j -th DoF of the particle in the α^i -th localized region where $j \in \mathbb{N}_n$. Thus the general state of p indistinguishable particles each having n DoFs is defined as

$$|\Psi^{(p,n)}\rangle := \sum_{\alpha^i, a_j^i} \eta^u \kappa_{\alpha_1^1 a_1^1 \dots a_n^1, \alpha_1^2 a_2^2 \dots a_n^2, \dots, \alpha_1^p a_2^p \dots a_n^p} |\alpha^1 a_1^1 a_2^1 \dots a_n^1, \alpha^2 a_1^2 a_2^2 \dots a_n^2, \dots, \alpha^p a_1^p a_2^p \dots a_n^p\rangle. \quad (5.8)$$

Here u represents the summation of parity of the cyclic permutations of all the n DoFs. Thus u can be represented as $u = u_1 + u_2 + \dots + u_n = \sum_i u_j$ where u_j is the parity of j -th DoF. The value of η is $+1$ for bosons and -1 for fermions. If we have the following condition that if

$$\left(\alpha^i = \alpha^{i'}\right) \wedge \left(a_j^i = a_j^{i'}\right) \quad (5.9)$$

for any $i \neq i'$ where $\alpha^i, \alpha^{i'} \in \mathbb{S}^P$ and $j \in \mathbb{N}_n$, then we get $\eta = 0$ for fermions due to Pauli exclusion principle [224].

Following the above notations, the general density matrix of p indistinguishable

particles each having n DoFs is defined as

$$\rho^{(p,n)} := \sum_{\alpha^i, \beta^i, a_j^i, b_j^i} \eta^{(u+\bar{u})} \kappa_{a(n)}^{\alpha^{(p)}, \beta^{(p)}} |\alpha^1 a_1^1 a_2^1 \dots a_n^1, \alpha^2 a_1^2 a_2^2 \dots a_n^2, \dots, \alpha^p a_1^p a_2^p \dots a_n^p\rangle \langle \beta^1 b_1^1 b_2^1 \dots b_n^1, \beta^2 b_1^2 b_2^2 \dots b_n^2, \dots, \beta^p b_1^p b_2^p \dots b_n^p|, \quad (5.10)$$

where

$$\kappa_{a(n), b(n)}^{\alpha^{(p)}, \beta^{(p)}} = \kappa_{a_1^1 a_2^1 \dots a_n^1, a_1^2 a_2^2 \dots a_n^2, \dots, a_1^p a_2^p \dots a_n^p, b_1^1 b_2^1 \dots b_n^1, b_1^2 b_2^2 \dots b_n^2, \dots, b_1^p b_2^p \dots b_n^p}^{\alpha^1, \alpha^2, \dots, \alpha^p, \beta^1, \beta^2, \dots, \beta^p} \quad (5.11)$$

and α^i, β^i ranges over \mathbb{S}^p , a_j^i, b_j^i ranges over \mathbb{D}_j , $i \in \mathbb{N}_P$ and $j \in \mathbb{N}_n$. Here u is as defined in Eq. (5.8) and \bar{u} comes due to density matrix. If we have the following condition that

$$\{(\alpha^i = \alpha^{i'}) \vee (\beta^i = \beta^{i'})\} \wedge \{(a_j^i = a_j^{i'}) \vee (b_j^i = b_j^{i'})\} \quad (5.12)$$

for any $i \neq i'$ where $i, i' \in \mathbb{N}_P$ and $j \in \mathbb{N}_n$, then we get $\eta = 0$ for fermions due to Pauli exclusion principle [224].

The density matrix of Eq. (5.8) is described as

$$\rho^{(p,n)} := \sum_{\alpha^i, \beta^i, a_j^i, b_j^i} \eta^{(u+\bar{u})} \kappa_{a(n)}^{\alpha^{(p)}} \kappa_{b(n)}^{\beta^{(p)*}} |\alpha^1 a_1^1 a_2^1 \dots a_n^1, \alpha^2 a_1^2 a_2^2 \dots a_n^2, \dots, \alpha^p a_1^p a_2^p \dots a_n^p\rangle \langle \beta^1 b_1^1 b_2^1 \dots b_n^1, \beta^2 b_1^2 b_2^2 \dots b_n^2, \dots, \beta^p b_1^p b_2^p \dots b_n^p|, \quad (5.13)$$

where

$$\begin{aligned} \kappa_{a(n)}^{\alpha^{(p)}} &= \kappa_{a_1^1 a_2^1 \dots a_n^1, a_1^2 a_2^2 \dots a_n^2, \dots, a_1^p a_2^p \dots a_n^p}^{\alpha^1, \alpha^2, \dots, \alpha^p}, \\ \kappa_{b(n)}^{\beta^{(p)}} &= \kappa_{b_1^1 b_2^1 \dots b_n^1, b_1^2 b_2^2 \dots b_n^2, \dots, b_1^p b_2^p \dots b_n^p}^{\beta^1, \beta^2, \dots, \beta^p}, \end{aligned} \quad (5.14)$$

and rest of the notations are the same as Eq. (5.10).

5.2 DoF trace-out for indistinguishable particles

In this section, we propose a DoF trace-out rule for indistinguishable particles where each particle has more than one DoF. In [161, 163], they propose the trace-out rule for indistinguishable particles having single DoF. One may be tempted to think that the same rule can trace-out a single DoF for indistinguishable particles having single DoF, will work for indistinguishable particles having multiple DoFs. However, this is not so straightforward. When particles become indistinguishable with multiple DoFs, performing the partial trace-out of a particular DoF is challenging, because a DoF

cannot be associated with a specific particle. To trace out DoFs of such particles, particularly when the particles are entangled in multiple DoFs, we have proposed a solution. Also, our DoF trace-out rule can treat the cases of both distinguishable and indistinguishable particles under a uniform mathematical framework.

5.2.1 Two indistinguishable particles each having two DoFs

If we want to perform partial trace in only one region, say $s^x \in \mathbb{S}^P$, then the non-normalized density matrix can be written as

$$\tilde{\rho}_M^{(1)} = \text{Tr}_M(\rho^{(2,2)}) = \sum_{m_1, m_2, \dots, m_n} \langle s^x m_1 m_2 \dots m_n | \rho^{(2,2)} | s^x m_1 m_2 \dots m_n \rangle, \quad (5.15)$$

where m_j span \mathbb{D}_j , where $j \in \mathbb{N}_2$.

To perform DoF trace-out of the j -th DoF, $j \in \mathbb{N}_2$, of spatial region $s^x \in \mathbb{S}^P$, we define the reduced density matrix of Eq. (5.3) as

$$\begin{aligned} \rho_{s_j^x} &\equiv \text{Tr}_{s_j^x}(\rho^{(2,2)}) \equiv \sum_{m_j \in \mathbb{D}_j} \langle s^x m_j | \rho^{(2,2)} | s^x m_j \rangle \\ &:= \eta^{(u+\bar{u})} \sum_{m_j} \left\{ \sum_{\substack{\alpha^1, \alpha^2, a_j^1, a_j^2, a_1^1, a_1^2, \\ \beta^1, \beta^2, b_j^1, b_j^2, b_1^1, b_1^2}} \kappa_{a_j^1, a_j^2, a_1^1, a_1^2, b_j^1, b_j^2, b_1^1, b_1^2}^{\alpha^1 \alpha^2, \beta^1, \beta^2} \langle s^x m_j | \alpha^1 a_j^1 \rangle \langle \beta^1 b_j^1 | s^x m_j \rangle | \alpha^1 a_j^1, \alpha^2 a_1^1 a_1^2 \rangle \langle \beta^1 b_j^1, \beta^2 b_1^1 b_1^2 | \right. \\ &\quad + \eta \sum_{\substack{\alpha^1, \alpha^2, a_1^1, a_1^2, a_j^2, a_j^1, \\ \beta^1, \beta^2, b_j^1, b_j^2, b_1^1, b_1^2}} \kappa_{a_1^1, a_1^2, a_j^2, a_j^1, b_j^1, b_j^2, b_1^1, b_1^2}^{\alpha^1 \alpha^2, \beta^1, \beta^2} \langle s^x m_j | \alpha^2 a_j^2 \rangle \langle \beta^1 b_j^1 | s^x m_j \rangle | \alpha^1 a_1^1 a_1^2, \alpha^2 a_j^2 \rangle \langle \beta^1 b_j^1, \beta^2 b_1^1 b_1^2 | \\ &\quad + \eta \sum_{\substack{\alpha^1, \alpha^2, a_j^1, a_j^2, a_1^1, a_1^2, \\ \beta^1, \beta^2, b_1^1, b_1^2, b_j^2, b_j^1}} \kappa_{a_j^1, a_j^2, a_1^1, a_1^2, b_1^1, b_1^2, b_j^2, b_j^1}^{\alpha^1 \alpha^2, \beta^1, \beta^2} \langle s^x m_j | \alpha^1 a_j^1 \rangle \langle \beta^2 b_j^2 | s^x m_j \rangle | \alpha^1 a_j^1, \alpha^2 a_1^1 a_1^2 \rangle \langle \beta^1 b_1^1 b_1^2, \beta^2 b_j^2 | \\ &\quad \left. + \sum_{\substack{\alpha^1, \alpha^2, a_1^1, a_1^2, a_j^2, a_j^1, \\ \beta^1, \beta^2, b_1^1, b_1^2, b_j^2, b_j^1}} \kappa_{a_1^1, a_1^2, a_j^2, a_j^1, b_1^1, b_1^2, b_j^2, b_j^1}^{\alpha^1 \alpha^2, \beta^1, \beta^2} \langle s^x m_j | \alpha^2 a_j^2 \rangle \langle \beta^2 b_j^2 | s^x m_j \rangle | \alpha^1 a_1^1 a_1^2, \alpha^2 a_j^2 \rangle \langle \beta^1 b_1^1 b_1^2, \beta^2 b_j^2 | \right\}, \end{aligned} \quad (5.16)$$

where $\bar{j} := (3-j)$. The parameter η is $+1$ (-1) for bosons (fermions). Similarly, the

trace-out operation of the state in Eq. (5.5) using the above rule.

Equation (5.16) can be generalized for n DoFs and it includes particle trace-out as a special case for $n=1$ as shown in the next section. Similarly, to get the description of the reduced system $\rho_{s_i^x}$ consisting of a single DoF, we have to apply our trace-out rule $(n-1)$ times.

5.2.2 Two indistinguishable particles each having n DoFs

Next we define DoF trace-out rule for indistinguishable particles from the general density matrix of two particles as defined in Eq. (5.7). Suppose we want to trace-out the j -th DoF of location $s^x \in \mathbb{S}^P$. Then the DoF reduced density matrix is

$$\begin{aligned}
\rho_{s_j^x} &\equiv \text{Tr}_{s_j^x} \left(\rho^{(2,n)} \right) \equiv \sum_{m_j \in \mathbb{D}_j} \langle s^x m_j | \rho^{(2,n)} | s^x m_j \rangle \\
&:= \sum_{m_j} \left\{ \sum_{\substack{\alpha^1, \alpha^2, a_j^1, a_j^2, a_1^2, a_2^2, \dots, a_n^2 \\ \beta^1, \beta^2, b_j^1, b_j^2, b_1^2, b_2^2, \dots, b_n^2}} \kappa_p \langle s^x m_j | \alpha^1 a_j^1 \rangle \langle \beta^1 b_j^1 | s^x m_j \rangle | \alpha^1 a_j^1, \alpha^2 a_1^2 a_2^2 \dots a_n^2 \rangle \langle \beta^1 b_j^1, \beta^2 b_1^2 b_2^2 \dots b_n^2 | \right. \\
&\quad + \eta \sum_{\substack{\alpha^1, \alpha^2, a_1^1, a_2^1, \dots, b_n^1 a_j^2, a_j^2 \\ \beta^1, \beta^2, b_j^1, b_j^2, b_1^2, b_2^2, \dots, b_n^2}} \langle s^x m_j | \alpha^2 a_j^2 \rangle \langle \beta^1 b_j^1 | s^x m_j \rangle | \alpha^1 a_1^1 a_2^1 \dots a_n^1 \alpha^2 a_j^2 \rangle \langle \beta^1 b_j^1, \beta^2 b_1^2 b_2^2 \dots b_n^2 | \\
&\quad + \eta \sum_{\substack{\alpha^1, \alpha^2, a_j^1, a_j^2, a_1^2, a_2^2, \dots, a_n^2 \\ \beta^1, \beta^2, b_1^1, b_2^1, \dots, b_n^1 b_j^2, b_j^2}} \langle s^x m_j | \alpha^1 a_j^1 \rangle \langle \beta^2 b_j^2 | s^x m_j \rangle | \alpha^1 a_j^1, \alpha^2 a_1^2 a_2^2 \dots a_n^2 \rangle \langle \beta^1 b_1^1 b_2^1 \dots b_n^1, \beta^2 b_j^2 | \\
&\quad \left. + \sum_{\substack{\alpha^1, \alpha^2, a_1^1, a_2^1, \dots, a_n^1 a_j^2, a_j^2 \\ \beta^1, \beta^2, b_1^1, b_2^1, \dots, b_n^1 b_j^2, b_j^2}} \langle s^x m_j | \alpha^2 a_j^2 \rangle \langle \beta^2 b_j^2 | s^x m_j \rangle | \alpha^1 a_1^1 a_2^1 \dots a_n^1, \alpha^2 a_j^2 \rangle \langle \beta^1 b_1^1 b_2^1 \dots b_n^1, \beta^2 b_j^2 | \right\}, \tag{5.17}
\end{aligned}$$

where

$$\begin{aligned}
\kappa_p &= \kappa_{a_j^1, a_j^2, a_1^2, a_2^2, \dots, a_n^2, b_j^1, b_j^2, b_1^2, b_2^2, \dots, b_n^2}, \\
\kappa_q &= \kappa_{a_1^1, a_2^1, \dots, b_n^1 a_j^2, a_j^2, b_j^1, b_j^2, b_1^2, b_2^2, \dots, b_n^2}, \\
\kappa_r &= \kappa_{a_j^1, a_j^2, a_1^2, a_2^2, \dots, a_n^2, b_1^1, b_2^1, \dots, b_n^1, b_j^2, b_j^2}, \\
\kappa_s &= \kappa_{a_1^1, a_2^1, \dots, a_n^1, a_j^2, a_j^2, b_1^1, b_2^1, \dots, b_n^1, b_j^2, b_j^2}, \tag{5.18}
\end{aligned}$$

It may be noted that for $n=2$, the DoF trace-out rule defined in Eq. (5.17) reduces

to Eq. (5.16). For $n=1$, this becomes equivalent to the particle trace-out rule as defined Eq. (2.29). On the other hand, for $n>1$, if we apply DoF trace-out rule of Eq. (5.16) n times, the effect will not be the same as the particle trace-out in Eq. (2.29). The reason behind this is as follows. For indistinguishable particles, the particle trace-out operation vanishes all the DoFs together for one particle; whereas each DoF trace-out operation leaves an expression with many terms each of which vanishes the corresponding DoF from one particle at a time and retains the same DoF in the remaining particles.

5.2.3 p indistinguishable particles each having n DoFs

Finally, we define DoF trace-out rule for p indistinguishable particles each having n DoFs from the general density matrix Eq. (5.10). Suppose we want to trace-out the j -th DoF of location $s^x \in \mathbb{S}^P$, then the DoF reduced density matrix is

$$\rho_{s_j^x} \equiv \text{Tr}_{s_j^x}(\rho^{(p,n)}) \equiv \sum_{m_j \in \mathbb{D}_j} \langle s^x m_j | \rho^{(p,n)} | s^x m_j \rangle. \quad (5.19)$$

This can be expanded similarly as shown in Eq. (5.17).

5.3 Physical significance of the proposed DoF trace-out rule

Our DoF trace-out rule plays a very critical role with respect to the recently introduced complex systems with inter-DoF entanglements [1, 262, 263]. When such entanglement exists, measuring or non-measuring one of the participating DoFs would influence the measurement results of the other participating DoFs. In an experiment involving such systems, the DoF trace-out can operationally be implemented simply by choosing to measure a particular DoF in a particular spatial location while ignoring the others. However, the statistics so obtained cannot be predicted using the existing trace-out rules in either the first or the second quantization notations.

The physical meaning of the term $\rho_{s^{x_j}}$ in Eq. (5.16) is that it represents the description of the reduced system after measuring the whole system in the j -th DoF in the spatial region s^x . On the other hand, the physical interpretation of the term $\rho_{s^{x_j}}$ is that if someone measures only the i -th DoF in the spatial region s_x , then the measure statistics would be equivalent to the system $\rho_{s^{x_i}}$. It can be noted that our DoF trace-out rule in Eq. (5.16) is order independent. Our framework expressed in Eq. (5.16) can deal with all such systems with inter-DoF correlations in indistinguishable particles, leading to the prediction of perfect measurement statistics.

Further, it generalizes the standard existing trace-out rule and is therefore suitable for such entanglement structures of distinguishable particles as well. More specifically, for distinguishable particles, tracing out a single DoF of a particle is analogous to tracing out a whole particle; for indistinguishable particles, on the other hand, tracing out a single DoF is performed for a specific spatial location where wave-functions of multiple particles might be overlapping. These overlaps are taken care of in the inner-product terms in the expression of Eq. (5.16).

In short, the physical significance of our result is that it extends the standard density matrix approach of quantum information to systems of indistinguishable particles entangled in multiple degrees of freedom.

Chapter 6

Generalized relation between teleportation fidelity and singlet fraction

In this chapter, we generalize the existing relation between teleportation fidelity and singlet fraction for both distinguishable and indistinguishable particles where each particle have multiple DoFs. We also describe the physical significance of the proposed generalized relation. Then we propose an optical scheme to generate inter-DoF entangled state for distinguishable particles where the non-triviality of the above relation is explained.

This chapter is based on the work in [\[264\]](#).

6.1 Generalized teleportation fidelity

For particles having a single DoF, there is only one teleportation channel. But, when multiple DoFs, say n , are available for each particle, then up to n^2 teleportation channels are possible. So the previous definition of teleportation fidelity will not work for distinguishable particles and indistinguishable particles each having multiple DoFs. For any teleportation protocol, the motivation is to maximize the information transfer. So we define the generalized teleportation fidelity in such a way that it captures the

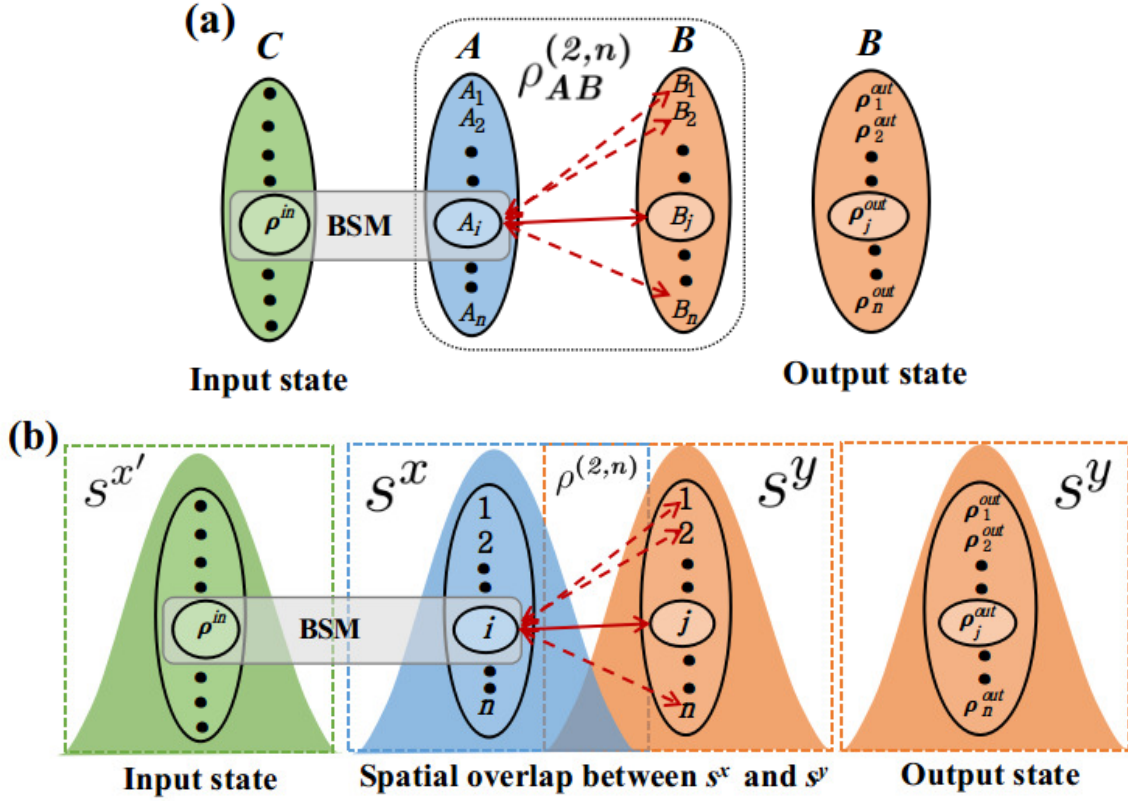


Figure 6-1: Teleportation operation using (a) two distinguishable particles and (b) two indistinguishable particles, each having n DoFs.

maximum fidelity over all possible channels.

Suppose $\rho_{AB}^{(2,n)}$ denotes the joint state of two distinguishable particles A and B , each having n DoFs following Eq. (2.11). Another particle C having n DoFs nearby to A , has an unknown state in any DoF denoted by ρ^{in} which has to be teleported to B . For teleportation operation, Bell state measurement (BSM) is performed with the DoF of C having the unknown state ρ^{in} and the i -th DoF of particle A . After BSM, the unknown state is teleported to all the DoFs of B as shown in Fig. 6-1 (a). We denote the teleported state on the j -th DoF of the particle B by ρ_j^{out} where $j \in \mathbb{N}_n = \{1, 2, \dots, n\}$. The teleportation fidelity between the i -th DoF of A and the j -th DoF of B is given by

$$f_j^i := \text{Tr} \sqrt{\sqrt{\rho^{in}} \rho_j^{out} \sqrt{\rho^{in}}}. \quad (6.1)$$

As the goal of any teleportation protocol is to maximize the fidelity, so we define the

generalized teleportation fidelity for the state $\rho_{AB}^{(2,n)}$ as

$$f_g := \max_{i,j \in \mathbb{N}_n} \{f_j^i\}. \quad (6.2)$$

The teleportation operation using indistinguishable particles [247, 163] is almost the same as that of using distinguishable particles. Consider two indistinguishable particles with density matrix $\rho^{(2,n)}$ as defined in Eq. (5.7), located in the spatial regions s^x and s^y where $s^x, s^y \in \mathbb{S}^P$. The particle C , distinguishable from them, is located in the spatial region $s^{x'} \in \mathbb{S}^P$ nearby to s^x , having an unknown state ρ^{in} in one of its DoF. This unknown state has to be teleported in the spatial region s^y . Now Bell state measurement is performed on the i -th DoF of the spatial region s^x and the DoF of C having the unknown state ρ^{in} . After this operation, ρ^{in} is teleported (probabilistically) to all the DoFs of the spatial region s^y as shown in Fig. 6-1 (b). We denote the teleported state of the j -th DoF of the spatial region s^y by ρ_j^{out} and the teleportation fidelity between the i -th DoF of spatial location s^x and the j -th DoF of the spatial region s^y is denoted by $f_j^i := \text{Tr} \sqrt{\sqrt{\rho^{in}} \rho_j^{out} \sqrt{\rho^{in}}}$. With this notation in the case of indistinguishable particles, the generalized teleportation fidelity for any arbitrary $\rho^{(2,n)}$ is calculated in the same way as Eq. (6.2).

6.2 Generalized singlet fraction

For two distinguishable particles, say A and B , each having n DoFs as in Eq. (2.11), if a_i is maximally entangled with b_j , then all the other pairs of the form $\{a_i, b_k\}$, $k \neq j$, as well as $\{a_l, b_j\}$, $l \neq i$, become separable due to monogamy of entanglement between DoFs [262, 263]. For two indistinguishable particles each having n DoFs as in Eq. (5.7), it is possible to have all $\{a_i, b_j\}$ pairs are maximally entangled as shown in [258]. The current definition of singlet fraction does not capture all such scenarios for distinguishable particles and indistinguishable particles. So the motivation behind our generalized singlet fraction is to capture all the entangled or separable structures between two distinguishable particles or indistinguishable particles. So we take

the summation of all the singlet fraction possible for any particular DoF. Then we maximized that value for all DoFs of the both particles.

For two distinguishable particles A and B with the joint state $\rho_{AB}^{(2,n)}$ as shown in (2.11), we define the generalized singlet fraction as

$$F_g^{(n)} := \max \left\{ \max_i \{F(i)\}, \max_j \{F(j)\} \right\}, \quad (6.3)$$

where

$$\begin{aligned} F(i) &:= \max_{\psi_{a_i b_j}} \sum_{j=1}^n P_{a_i b_j}, \\ F(j) &:= \max_{\psi_{a_i b_j}} \sum_{i=1}^n P_{a_i b_j}, \\ P_{a_i b_j} &:= \langle \psi_{a_i b_j} | \rho_{a_i b_j} | \psi_{a_i b_j} \rangle, \\ \rho_{a_i b_j} &:= \text{Tr}_{a_{\bar{i}} b_{\bar{j}}} (\rho_{AB}^{(2,n)}). \end{aligned} \quad (6.4)$$

Here $a_{\bar{i}} = a_1 a_2 \cdots a_{i-1} a_{i+1} \cdots a_n$ and similar meaning for $b_{\bar{j}}$. In the terms $\max_{\psi_{a_i b_j}} \left\{ \sum_{j=1}^n P_{a_i b_j} \right\}$, the i -th DoF of A is kept fixed and $|\psi_{a_i b_j}\rangle$ spans all possible maximally entangled states between the i -th DoF of A and the j -th DoF of B . Similarly for the other term, the j -th DoF of B is kept fixed.

Next consider two indistinguishable particles with joint state $\rho^{(2,n)}$ as in (5.7), each having n DoFs. The generalized singlet fraction for two spatial regions $s^x, s^y \in \mathbb{S}^P$ as shown in Fig. 6-1 (b) can be calculated similarly using Eq. (6.3) where

$$\begin{aligned} F(i) &= \max_{\psi_{s_i^x s_j^y}} \sum_{j=1}^n P_{s_i^x s_j^y}, \\ F(j) &= \max_{\psi_{s_i^x s_j^y}} \sum_{i=1}^n P_{s_i^x s_j^y}, \\ P_{s_i^x s_j^y} &:= \langle \psi_{s_i^x s_j^y} | \rho_{s_i^x s_j^y} | \psi_{s_i^x s_j^y} \rangle, \\ \rho_{s_i^x s_j^y} &:= \text{Tr}_{s_i^x s_j^y} (\rho^{(2,n)}) \end{aligned} \quad (6.5)$$

Here $|\psi_{s_i^x s_j^y}\rangle$ spans all possible maximally entangled states between the i -th DoF of s^x and the j -th DoF of s^y and $s^x, s^y \in \mathbb{S}^P$, following the DoF trace-out rule in Chapter 5.

6.3 Relation between the generalized teleportation fidelity and the generalized singlet fraction

Consider a two-parameter family of states for two particles each having n DoFs as

$$\rho_p^{(2,n)} := p\mathbb{P}^{(2,n)} + (1-p)\frac{\mathbb{I}^n \otimes \mathbb{I}^n}{d^{2n}}, \quad 0 \leq p \leq 1. \quad (6.6)$$

This equation is applicable for both distinguishable and indistinguishable particles.

For two distinguishable particles A and B , the state $\rho_p^{(2,n)}$ is an arbitrary $\rho_{AB}^{(2,n)}$ as in Eq. (2.11) and $\mathbb{P}^{(2,n)}$ is a special form of $\rho_{AB}^{(2,n)}$ such that for every a_i , there exists at least one b_j with $\mathbb{P}_{a_i b_j} = \text{Tr}_{a_i b_j}(\mathbb{P}^{(2,n)})$ is d -dimensional maximally entangled where $i, j \in \mathbb{N}_n$.

For two indistinguishable particles, $\rho_p^{(2,n)}$ is an arbitrary state $\rho^{(2,n)}$ of Eq. (5.7), and $\mathbb{P}^{(2,n)}$ is a special form of $\rho^{(2,n)}$ such that $\mathbb{P}_{s_i^x s_j^y} = \text{Tr}_{s_i^x s_j^y}(\mathbb{P}^{(2,n)})$ is maximally entangled for all $i, j \in \mathbb{N}_n$. This type of state is possible using indistinguishable particle [258]. But for distinguishable particles, such type of state is not possible as they obey monogamy of entanglement [262].

First, we calculate the generalized teleportation fidelity for the state $\rho_p^{(2,n)}$ of Eq. (6.6) and for that we have to calculate the same separately for both $\mathbb{P}^{(2,n)}$ and completely random noise $\frac{\mathbb{I}^n \otimes \mathbb{I}^n}{d^{2n}}$. We denote f_{max} to be the value of f_g for the state $\mathbb{P}^{(2,n)}$. Note that, the difference between f_g and f_{max} is that the first one is the maximum value of f_j^i for an arbitrary state $\rho_{AB}^{(2,n)}$ or $\rho^{(2,n)}$ but the second one is the maximum value of f_j^i for the special state $\mathbb{P}^{(2,n)}$.

For distinguishable particles, $\max_{(i,j)} \{f_j^i\} = 1$ occurs for the pair (i, j) such that $\mathbb{P}_{a_i b_j}$ is maximally entangled. For indistinguishable particles, $f_{max} < 1$ due to the *no-go* theorem of [244]. The value of f_g for $\frac{\mathbb{I}^n \otimes \mathbb{I}^n}{d^{2n}}$ is the same for both distinguishable particles and indistinguishable particles which is $\frac{1}{d}$ as $\rho^{out} = \frac{\mathbb{I}}{d}$ independent of the initial state ρ^{in} before teleportation. Thus the value of f_g for Eq. (6.6) is Thus we calculate the generalized teleportation fidelity applicable for both distinguishable and

indistinguishable particles for the state in Eq. (6.6) as

$$f_g = p f_{max} + (1-p) \frac{1}{d}, \quad (6.7)$$

where $f_{max} = 1$ for distinguishable particles and $f_{max} < 1$ for indistinguishable particles.

Next, we calculate the generalized singlet fraction for the state $\rho_p^{(2,n)}$ of Eq. (6.6). We denote $F_{max}^{(n)}$ be the value of $F_g^{(n)}$ for the state $\mathbb{P}^{(2,n)}$. We know that distinguishable particles obey monogamy of entanglement. So, let us fix a particular i , then $P_{a_i b_j} = \langle \psi_{a_i b_j} | \mathbb{P}_{a_i b_j}^{(2,n)} | \psi_{a_i b_j} \rangle$ would be 1 for a particular j , say j' , as $\mathbb{P}_{a_i b_{j'}}^{(2,n)}$ is maximally entangled. When $j \neq j'$, we get $P_{a_i b_j} = \frac{1}{d}$ as $\mathbb{P}_{a_i b_j}^{(2,n)}$ is separable, where $i, j, j' \in \mathbb{N}_n$. So, for the rest of the $(n-1)$ DoFs, we get $P_{a_i b_j} = \frac{1}{d}$. Thus the value of $F_{max}^{(n)}$ for distinguishable particles is $\left(1 + \frac{n-1}{d}\right)$.

It is proved in [258] that indistinguishable particles does not obey monogamy. So, if we fix any particular i , then the value of $P_{s_i^x s_j^y}$ can be 1 for all the values of j , as $\mathbb{P}_{s_i^x s_j^y}$ can be maximally entangled for all the values of j . So, for indistinguishable particles the value of $\max_i \{F(i)\}$ is n , and similarly the value of $\max_j \{F(j)\} = n$, leading to $F_{max}^{(n)} = n$. For $\frac{\mathbb{I}^n \otimes \mathbb{I}^n}{d^{2n}}$, we get $P_{a_i b_j} = P_{s_i^x s_j^y} = \frac{1}{d^2}$ for all i and j . So, the value of $F_g^{(n)}$ is $\frac{n}{d^2}$ which is the same for distinguishable particles and indistinguishable particles. Thus, the value of $F_g^{(n)}$ in Eq. (6.6) is

$$F_g^{(n)} = p F_{max}^{(n)} + (1-p) \frac{n}{d^2}. \quad (6.8)$$

Using Eq. (6.7) and Eq. (6.8), we get the relation between the generalized teleportation fidelity and the generalized singlet fraction as

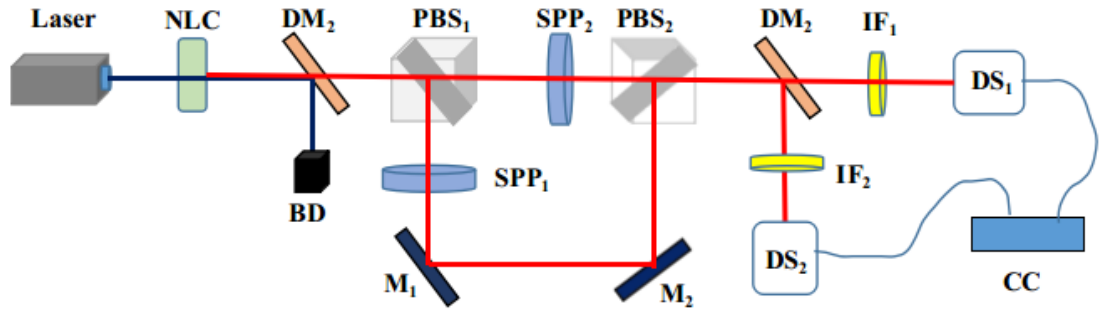
$$f_g = \frac{\left(F_g^{(n)} - \frac{n}{d^2}\right) \left(f_{max} - \frac{1}{d}\right)}{\left(F_{max}^{(n)} - \frac{n}{d^2}\right)} + \frac{1}{d}, \quad (6.9)$$

where $f_g \in \left[\frac{1}{d}, f_{max}\right]$ and $F_g^{(n)} \in \left[\frac{n}{d^2}, F_{max}^{(n)}\right]$. Whether the particles are distinguishable or indistinguishable, the same Eq. (6.9) holds, only the values of f_{max} and $F_{max}^{(n)}$ varies.

For particles having single DoF, i.e., $n=1$, Eq. (6.9), reduces to the standard particle version of Eq. (2.41).

6.4 Illustration of the proposed generalized relation to some special states for distinguishable and indistinguishable particles

If two particles each having a single DoF are maximally entangled, then the value of generalized singlet fraction is one. However, the converse is not necessarily true which we illustrate by proposing an optical circuit using two distinguishable particles each having two DoFs, polarization and orbital angular momentum (OAM).



NLC : nonlinear crystal **DM**: dichroic mirror **BD**: beam dump **PBS**: polarizing beam splitter
SPP: spiral phase plate **M**: mirror **IF**: interference filter **DS**: detection setup **CC**: coincidence counter

Figure 6-2: Optical set up to the generation of entangled state between polarization and OAM DoF for distinguishable particles. NLC: nonlinear crystal, DM: dichroic mirror, BD: beam dump, PBS: polarizing beam splitters, SPP: spiral phase plates, M: mirrors, IF: interference filters, DS: detection setup and C.C.: coincidence counter. The detection setups could be made up of spatial light modulators and single-mode fibers coupled to avalanche photo detectors if measuring in OAM or half-wave plates and PBS if measuring in polarization.

In Fig. 6-2, a nonlinear crystal (β barium borate, periodically poled potassium triphosphate etc.) is pumped by a pulsed laser from which a pump photon is absorbed and two photons are generated governed by the phase-matching conditions:

$$\omega_p = \omega_s + \omega_i, \quad \mathbf{k}_p = \mathbf{k}_s + \mathbf{k}_i \quad (6.10)$$

where $\hbar\omega_j$ is the energy and $\hbar\mathbf{k}_j$ is the momentum of the j -th photon. The indices p , s and i stand for pump, signal and idler respectively. The signal and idler photon pair produced in this method under non-degenerate type II spontaneous parametric down conversion are correlated in polarization. It is represented in the most general form as

$$|\Psi_i\rangle = \cos\theta |H\rangle_{\omega_s} |V\rangle_{\omega_i} + e^{i\phi} \sin\theta |V\rangle_{\omega_s} |H\rangle_{\omega_i}, \quad (6.11)$$

where $|H\rangle$ and $|V\rangle$ denotes horizontal and vertical polarization, θ controls the normalization factor and ϕ is a phase term that arises from birefringence in the nonlinear crystal. Since $\omega_s \neq \omega_i$ (under non-degenerate phase matching) this leads to distinguishability between the signal and idler photons. Let this state be now incident on a broadband polarizing beam splitter (PBS) which allows $|H\rangle$ photons to pass through to the transmitted path, while $|V\rangle$ photons are directed to the reflected path. Each of the paths contains a spiral phase plate (SPP) of equal topological charge l which can take any value from $-\infty$ to $+\infty$ through 0. SPP are optical devices with continuously varying thickness. photons pick up OAM l on passing through them. This results in the output wavefront possessing a helical nature corresponding to the topological charge. The two paths are again combined at another broadband PBS resulting in the state

$$|\Psi_f\rangle = \cos\theta |H, +l\rangle_{\omega_s} |V, -l\rangle_{\omega_i} + e^{i\phi} \sin\theta |V, -l\rangle_{\omega_s} |H, +l\rangle_{\omega_i}. \quad (6.12)$$

The handedness of l is sensitive to reflections and changes by $\exp(i\pi)$ under each reflection. The difference in the handedness of l arises in the above equation due to an unequal number of reflections between the transmitted and reflected arms.

The generalized singlet fraction of the above state is 1 as shown in Section 6.5. Similar conclusion can be drawn for two indistinguishable particles as proposed in [261]. Note that, our proposed state in Eq. (6.13) is different from [261] as we use non-degenerate phase-matching to make use of distinguishable photons. Thus, the singlet fraction alone might not be the best quantifier for the presence of maximal entanglement.

Another special state is hyper-hybrid entangled state [1] with two particles each having two DoFs. The maximum value of $F_g^{(2)}=2$ for this state is achieved as each DoF of one particles is maximally entangled with all the other DoFs of other particle as shown in [258].

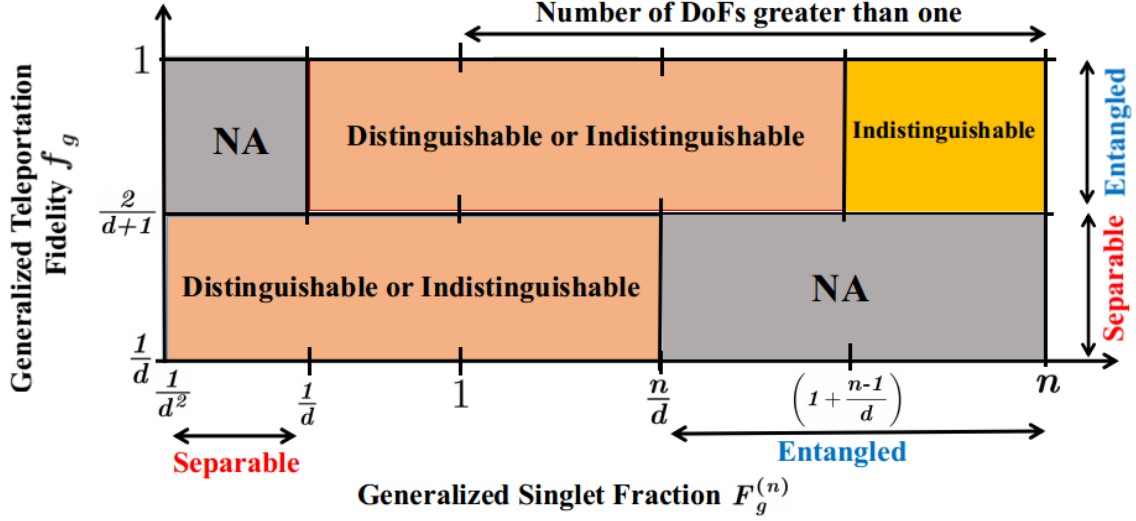


Figure 6-3: Characterization of the different kinds of states based on their separability, indistinguishability and number of DoFs present using the number of DoFs n , generalized Singlet fraction $F_g^{(n)}$ and generalized telepotation fidelity f_g .

6.5 Generalized singlet fraction for our proposed state

Here, we will calculate the value of generalized singlet fraction for the state proposed in Eq. (10) of the main text. The state is written as

$$|\Psi_f\rangle = \cos\theta |H, +l\rangle_{\omega_s} |V, -l\rangle_{\omega_i} + e^{i\phi} \sin\theta |V, -l\rangle_{\omega_s} |H, +l\rangle_{\omega_i}. \quad (6.13)$$

The density matrix of this state is

$$\begin{aligned}
\rho_f = |\Psi_f\rangle\langle\Psi_f| = & \cos^2\theta |H, +l\rangle_{\omega_s} |V, -l\rangle_{\omega_i} \langle H, +l|_{\omega_s} \langle V, -l|_{\omega_i} \\
& + e^{-i\phi} \cos\theta \sin\theta |H, +l\rangle_{\omega_s} |V, -l\rangle_{\omega_i} \langle V, -l|_{\omega_s} \langle H, +l|_{\omega_i} \\
& + e^{i\phi} \cos\theta \sin\theta |V, -l\rangle_{\omega_s} |H, +l\rangle_{\omega_i} \langle H, +l|_{\omega_s} \langle V, -l|_{\omega_i} \\
& + \sin^2\theta |V, -l\rangle_{\omega_s} |H, +l\rangle_{\omega_i} \langle V, -l|_{\omega_s} \langle H, +l|_{\omega_i}.
\end{aligned} \tag{6.14}$$

Now tracing out both the OAM DoFs from the density matrix ρ_f using Eq. (2.13), we get

$$\rho = \cos^2\theta |H\rangle_{\omega_s} \langle H|_{\omega_s} |V\rangle_{\omega_i} \langle V|_{\omega_i} + \sin^2\theta |V\rangle_{\omega_s} \langle V|_{\omega_s} |H\rangle_{\omega_i} \langle H|_{\omega_i}. \tag{6.15}$$

Now the singlet fraction for Eq. (6.15) is

$$\max_{\psi} \langle \psi | \rho | \psi \rangle = \frac{1}{2} (\cos^2\theta + \sin^2\theta) = \frac{1}{2}. \tag{6.16}$$

where $|\psi\rangle$ varies over all maximally entangled states. So, the singlet fraction of the above state is $\frac{1}{2}$. If we calculate singlet fraction of the other entanglement connections by the similar way, it will also be $\frac{1}{2}$. So, the generalized singlet fraction of the state $|\Psi_f\rangle$ using the Eq.(8) of main text is $F_g^{(2)} = 1$.

6.6 Derivation of the upper bound of generalized singlet fraction

It is already shown in Section 6.3 that the maximum value of the generalized singlet fraction for indistinguishable particles having n DoFs is n . Now we will derive for the maximum value of the generalized singlet fraction for distinguishable particles.

Suppose a particle A is entangled with n other distinguishable particles labeled as B_1, B_2, \dots, B_n , each having a single DoF with dimension d . Its joint state is represented as $\rho_{AB_1B_2\dots B_n}^{(1)}$. Now we can calculate the singlet fraction between A and B_j for $i \in \mathbb{N}_n =$

$\{1, 2, \dots, n\}$ as

$$F_{AB_j} = \max_{\psi} \langle \psi | \rho_{AB_j}^{(1)} | \psi \rangle, \quad (6.17)$$

where $\rho_{AB_j}^{(1)} = \text{Tr}_{B_{\bar{j}}}(\rho_{AB_1 B_2 \dots B_n}^{(1)})$ and $B_{\bar{j}} = B_1 B_2 \dots B_{j-1} B_{j+1} \dots B_n$. Here, $|\psi\rangle$ varies over all maximally entangled states.

The monogamy relation with respect to A is given in [265] as

$$\sum_{j=1}^n F_{AB_j} \leq \frac{d-1}{d} + \frac{1}{n+d-1} \left(\sum_{j=1}^n \sqrt{F_{AB_j}} \right)^2. \quad (6.18)$$

This relation is valid if B_1, B_2, \dots, B_n are the n DoFs of the particle B . Then we want to the bound of $F_g^{(n)}$ for the state $\rho_{AB}^{(n)}$ as defined in Eq. (2.11).

We take any n numbers of random variable $x_1, x_2 \dots x_n$ such that any $0 \leq x_j \leq 1$ for $j \in \mathbb{N}_n$. Then we have

$$\begin{aligned} \left(\sum_{j=1}^n \sqrt{x_j} \right)^2 &= (\sqrt{x_1} + \sqrt{x_2} + \dots + \sqrt{x_n})^2 \\ &= \sum_{j=1}^n x_j + 2 \sum_{\substack{i,j=1 \\ i>j}}^n \sqrt{x_i x_j} \\ &\leq n \left(\sum_{j=1}^n x_j \right) \quad [\text{using A.M.} \geq \text{G.M. inequality, i.e., } (x_i + x_j) \geq 2\sqrt{x_i x_j}]. \end{aligned} \quad (6.19)$$

Using Eq. (6.19), we have

$$\left(\sum_{j=1}^n \sqrt{F_{A_i B_j}} \right)^2 \leq n \left(\sum_{j=1}^n F_{A_i B_j} \right) \quad (6.20)$$

for any $i \in \mathbb{N}_n$. Now, substituting Eq. (6.20) in Eq. (6.18), we can write

$$\sum_{j=1}^n F_{A_i B_j} \leq \left(1 + \frac{n-1}{d} \right). \quad (6.21)$$

This bound is valid over all the DoFs of A , i.e.,

$$\max_i \left\{ \sum_{j=1}^n F_{A_i B_j} \right\} \leq \left(1 + \frac{n-1}{d} \right). \quad (6.22)$$

Similarly, we can write

$$\max_j \left\{ \sum_{i=1}^n F_{A_i B_j} \right\} \leq \left(1 + \frac{n-1}{d} \right). \quad (6.23)$$

From Eq. (6.22) and Eq. (6.23), we can write

$$\max \left\{ \max_i \left\{ \sum_{j=1}^n F_{A_i B_j} \right\}, \max_j \left\{ \sum_{i=1}^n F_{A_i B_j} \right\} \right\} \leq \left(1 + \frac{n-1}{d} \right). \quad (6.24)$$

From the main text of Eq. (5), we have the bound as

$$F_g^{(n)} = \max \left\{ \max_i \left\{ \sum_{j=1}^n F_{A_i B_j} \right\}, \max_j \left\{ \sum_{i=1}^n F_{A_i B_j} \right\} \right\} \leq \left(1 + \frac{n-1}{d} \right). \quad (6.25)$$

for $i, j \in \mathbb{N}_n$.

6.7 Physical significance of the proposed generalized relation

We investigate the answers to the following questions about any arbitrary two-particle state ρ .

(i) *The number of DoFs n in each particle?*

Using $F_g^{(n)}$: If $F_g^{(n)} > 1$, then $n > 1$, because $F_g^{(1)} \leq 1$ from Eq. (2.41).

(ii) *The particles are distinguishable or indistinguishable?*

For distinguishable particles the bound for generalized singlet fraction is $(1 + (n - 1)/d)$ that can be proved using the monogamy of singlet fraction [265] as shown in Section 6.6. Thus if $F_g^{(n)} > (1 + (n - 1)/d)$, then the particles are indistinguishable, else no conclusion can be drawn.

If $f_g=1$, then the particles are distinguishable because unit fidelity teleportation is not possible for indistinguishable particles [244], else no conclusion can be drawn.

(iii) *Is any entanglement is present in ρ ?*

If $f_g > 2/(d+1)$ or $F_g^{(n)} > n/d$, then atleast one entanglement structure is present between any pair of DoFs.

(iv) *How many maximally entangled state is present?*

If $F_g^{(n)} = n$, then n number of maximally entangled structure is present for any DoF.

If $f_g=1$, then the particles are distinguishable, so only one maximally entangled structure is present.

All these answers are pictorially represented in Fig. 6-3. For $d=2$, the relation between n , $F_g^{(n)}$, and f_g are plotted in Fig. 6-4 where $1 \leq n \leq 100$ using Eq. (6.9).

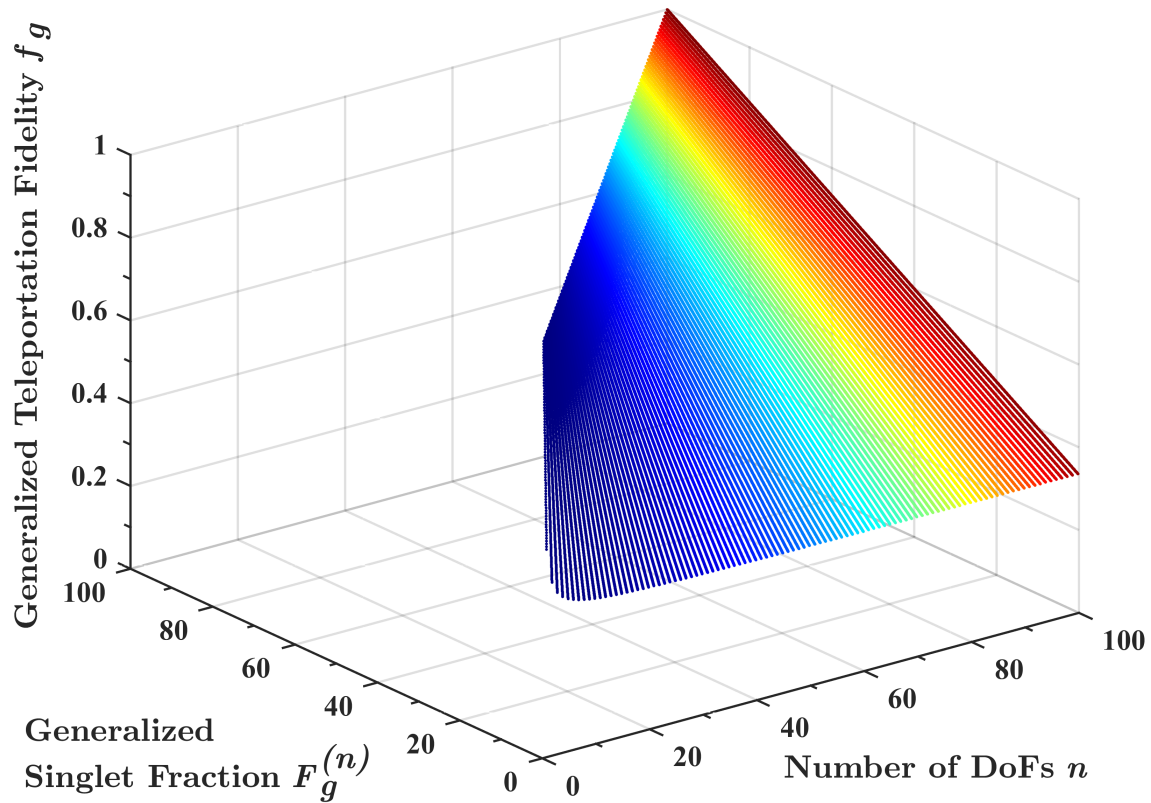


Figure 6-4: The variation of generalized teleportation fidelity f_g and generalized singlet fraction $F_g^{(n)}$ with varying the number of DoFs n where the dimension of each DoF is $d=2$.

Chapter 7

Violation of monogamy of entanglement for two indistinguishable particles

In this Section, we show that Maximum Violation of monogamy of Entanglement for two indistinguishable particles, each particles having two degrees of freedom is possible using measures which are monogamous for distinguishable particles. To show that, we first derives the condition for maximum violation of monogamy of entanglement. Then we re-write the standard inequality of monogamy of entanglement from particle view to DoF view. Finally we have shown the maximum violation of monogamy of entanglement using an optical circuit.

This chapter is based on the work in [\[258\]](#).

7.1 Violation of no-cloning theorem using the maximum violation of monogamy of entanglement

In this section, we briefly overview the monogamy inequality for any general entanglement measure. Then we discuss the condition for the violation of no-cloning theorem using the maximum violation of monogamy of entanglement.

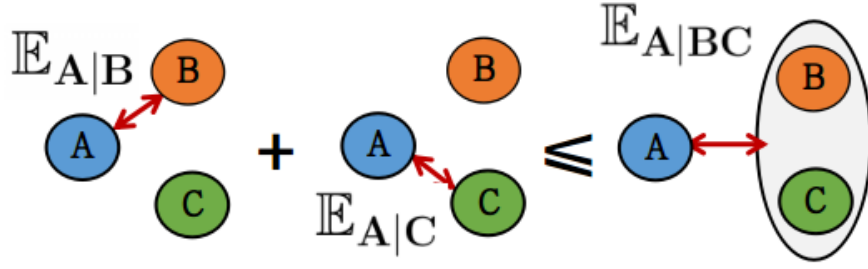


Figure 7-1: Consider three particles A, B, C , and a bipartite entanglement measure \mathbb{E} where $\mathbb{E}_{X|Y}$ measures the entanglement between the subsystems X and Y of the composite system XY and \mathbb{E}_{max} denotes its maximum value. Using these notations, we show the particle-based monogamy of entanglement obeying Eq. (7.1).

A bipartite entanglement measure \mathbb{E} that obeys the relation

$$\mathbb{E}_{A|B}(\rho_{AB}) + \mathbb{E}_{A|C}(\rho_{AC}) \leq \mathbb{E}_{A|BC}(\rho_{ABC}), \quad (7.1)$$

for all ρ_{ABC} where $\rho_{AB} = \text{Tr}_C(\rho_{ABC})$, $\rho_{AC} = \text{Tr}_B(\rho_{ABC})$, $\mathbb{E}_{X|Y}$ measures the entanglement between the systems X and Y of the composite system XY , and the vertical bar represents bipartite splitting, is called *monogamous* as shown in Fig. 7-1. Such inequality was first shown for squared concurrence (\mathcal{C}) [204, 209] by Coffman, Kundu and Wootters (CKW) for three parties [66] and later generalized for n parties [210].

Suppose a bipartite entanglement measure \mathbb{E} attains the maximum value \mathbb{E}_{max} for maximally entangled states. Consider a situation when

$$\begin{aligned} \mathbb{E}_{A|B}(\rho_{AB}) &< \mathbb{E}_{max}, \\ \mathbb{E}_{A|C}(\rho_{AC}) &< \mathbb{E}_{max}, \\ \mathbb{E}_{A|B}(\rho_{AB}) + \mathbb{E}_{A|C}(\rho_{AC}) &> \mathbb{E}_{max}. \end{aligned} \quad (7.2)$$

Obviously, this causes a violation of monogamy of entanglement which we call a *non-maximal violation*. Consider another situation, when

$$\begin{aligned} \mathbb{E}_{A|B}(\rho_{AB}) &= \mathbb{E}_{max}, \\ \mathbb{E}_{A|C}(\rho_{AC}) &= \mathbb{E}_{max}, \end{aligned} \quad (7.3)$$

i.e., when A is maximally entangled with both B and C , we call the corresponding violation as the *maximal violation* of monogamy of entanglement. For qubit systems with distinguishable particles, the first situation above would not lead to a violation of the no-cloning theorem [79, 80], but the second situation would do as shown in 2.5.2.

7.2 Apparent violation of particle-based monogamy of entanglement

When two particles are entangled, they share correlations in well-defined DoFs such as spin, path, orbital angular momentum (OAM), etc. Particle-based monogamy of entanglement however sometimes is misleading and incomplete. For example, suppose A is maximally entangled in polarization DoF with B and in OAM DoF with C [266] as shown in Fig. 7-2.

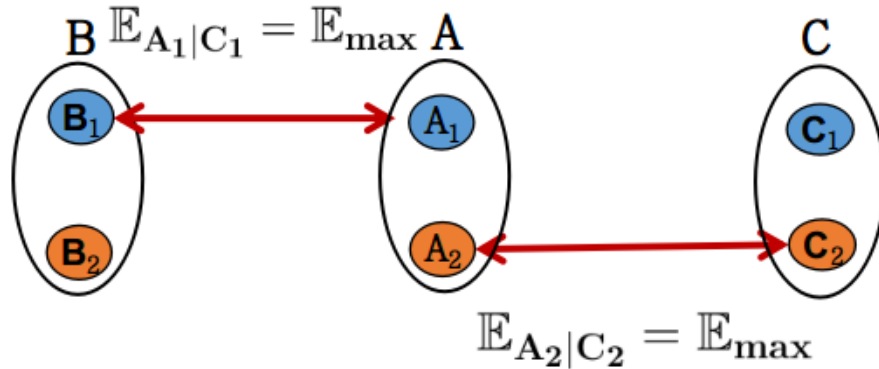


Figure 7-2: Consider three particles A , B , C , and a bipartite entanglement measure \mathbb{E} where $\mathbb{E}_{X|Y}$ measures the entanglement between the subsystems X . Using these notations, we show that A is maximally entangled with B in DoF 1 (i.e., $\mathbb{E}_{A_1|B_1} = \mathbb{E}_{max}$) and with C in DoF 2 (i.e., $\mathbb{E}_{A_2|C_2} = \mathbb{E}_{max}$). In particle view, apparently monogamy of entanglement is violated; but in DoF view, it is not.

This situation apparently violates Eq. (7.1) and satisfies Eq. (7.3). But using this state along with the standard teleportation protocol does not lead to cloning. This contradiction motivates us to re-consider the monogamy with respect to DoFs of each particle.

7.3 Inter-DoF monogamy of Entanglement

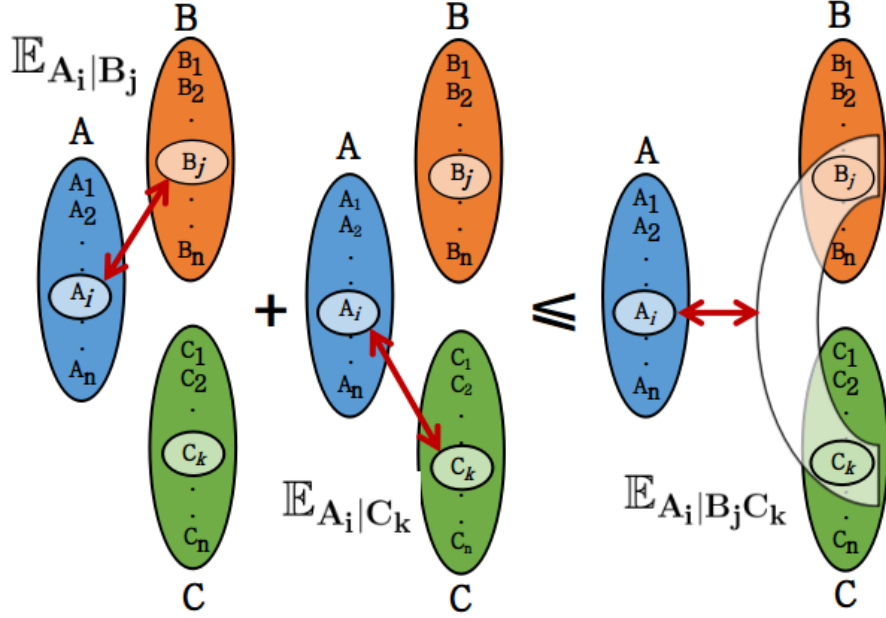


Figure 7-3: Consider three particles A , B , C , and a bipartite entanglement measure \mathbb{E} where $\mathbb{E}_{X|Y}$ measures the entanglement between the subsystems X and Y of the composite system XY and \mathbb{E}_{max} denotes its maximum value. Using this notations, we generalize the Eq. (7.1) from particle view to inter-DoF monogamy of entanglement as proposed in Eq. (7.4) which resolves the previous apparent violation in Fig. 7-2.

The above result holds irrespective of whether A , B and C are single-DoF particles or DoFs of the same/different particles as shown in Fig. 7-1 and 7-2. The entanglement measures which are monogamous for distinguishable particles are also so for systems of indistinguishable particles, where A , B , and C are distinct spatial locations [150, 148, 253] with one particle each. However, interesting scenarios might arise when the involved particles are entangled in multiple DoFs which we investigate here.

Here we reformulate Eq. (7.1) in a more general framework to include multiple DoFs of the same/different particles/entities. Although this is not a contribution, we include it here to establish the background for subsequent analysis.

Consider three entities A , B , and C , each with n DoFs, numbered 1 to n . If the joint state of the i -th, j -th and k -th DoFs of A , B , and C respectively is represented

by $\rho_{A_i B_j C_k}$, then the inter-DoF monogamy of entanglement can be formulated as

$$\mathbb{E}_{A_i|B_j}(\rho_{A_i B_j}) + \mathbb{E}_{A_i|C_k}(\rho_{A_i C_k}) \leq \mathbb{E}_{A_i|B_j C_k}(\rho_{A_i B_j C_k}), \quad (7.4)$$

where $\rho_{A_i B_j} = \text{Tr}_{C_k}(\rho_{A_i B_j C_k})$, $\rho_{A_i C_k} = \text{Tr}_{B_j}(\rho_{A_i B_j C_k})$, and $\mathbb{E}_{X_i|Y_j}$ measures the entanglement between subsystems X_i and Y_j of the composite system $X_i Y_j$ as is shown in Fig. 2-2 (c). It means that if the i -th DoF of A is maximally entangled with the j -th DoF of B , then it cannot share any correlation with the k -th DoF of C .

The inter-DoF monogamy of entanglement of Eq. (7.4) is more general than the particle-based monogamy of entanglement of Eq. (7.1). The former includes the latter when the three DoFs i , j , and k belong to three different particles A , B , and C respectively. However, the inter-DoF monogamy of entanglement can capture many other scenarios that are illustrated in Fig. 7-4 (a) and (b). Two interesting types of

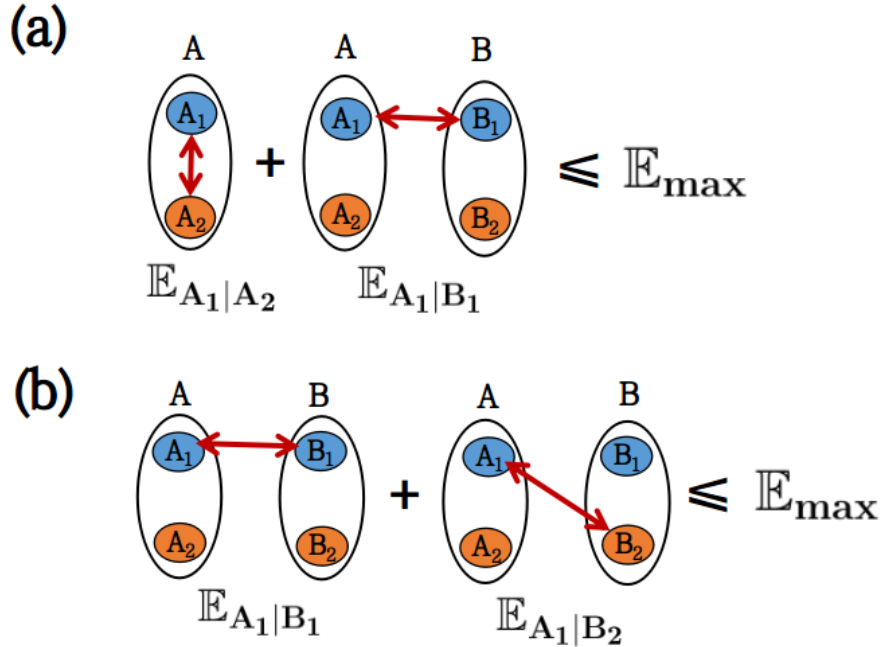


Figure 7-4: Consider three particles A , B , C , and a bipartite entanglement measure \mathbb{E} where $\mathbb{E}_{X|Y}$ measures the entanglement between the subsystems X and Y of the composite system XY and \mathbb{E}_{max} denotes its maximum value. Now consider the following two scenarios: (a) Two-particle inter-DoF monogamy of entanglement, where $\mathbb{E}_{A_1|A_2}$ measures entanglement between the two DoFs A_1 , A_2 of A and $\mathbb{E}_{A_1|B_1}$ between A_1 , B_1 ; and (b) $\mathbb{E}_{A_1|B_j}$ between A_1 of A and B_j of B , $j \in \{1, 2\}$.

monogamy of entanglement involving only two particles can also be explained using the inter-DoF formulation.

(i) *Type I*: Here, monogamy of entanglement is calculated using $\mathbb{E}_{A_i|A_j}$ and $\mathbb{E}_{A_i|B_k}$, as shown in Fig. 7-4 (a). Equation (7.4) can capture this scenario by setting $A=B$. The recent analysis for distinguishable particles in [262, 263] is a specific example of this type.

(ii) *Type II*: Here, monogamy of entanglement is calculated using $\mathbb{E}_{A_i|B_j}$ and $\mathbb{E}_{A_i|B_k}$, as shown in Fig. 7-4 (b). Equation (7.4) can capture this scenario by setting $B=C$.

This formulation also includes the case of single-particle entanglement [146, 260, 267], when all the three DoFs come from a single particle. Equation (7.4) can capture this scenario by setting $A=B=C$. Further, inter-DoF monogamy of entanglement is also valid for indistinguishable particles where the labels A , B , and C denote spatial locations with each mode containing exactly one particle and i , j , and k represents the DoFs at each spatial mode.

7.4 Violation of monogamy of entanglement by indistinguishable particles

The inter-DoF monogamy of entanglement is not absolute and can be violated maximally by indistinguishable particles. For illustration, consider two-particle inter-DoF entanglement [1, Eq. (4)] between spin and path as shown in Eq. (2.33). It can be represented as $|\Psi^{(2,2)}\rangle$ of Eq. (5.1) with the parameters $\alpha^1, \alpha^2 \in \{s^1, s^2\}$, $a_1^1, a_1^2 \in \{L, D, R, U\}$, $a_2^1, a_2^2 \in \{\uparrow, \downarrow\}$. The coefficients

$$\begin{aligned}
\kappa_{s^2 R \downarrow}^{s^1 L \downarrow} &= -\kappa_{s^2 U \uparrow}^{s^1 D \uparrow} = \frac{1}{4}(\kappa_1 + \kappa_2), \\
\kappa_{s^2 R \downarrow}^{s^1 D \uparrow} &= \kappa_{s^2 U \uparrow}^{s^1 L \downarrow} = \frac{i}{4}(\kappa_1 - \kappa_2), \\
\kappa_{s^2 R \downarrow}^{s^2 R \downarrow} &= \kappa_{s^2 U \uparrow}^{s^2 U \uparrow} = \frac{i\kappa_1}{4}, \\
\kappa_{s^1 D \uparrow}^{s^1 D \uparrow} &= \kappa_{s^1 L \downarrow}^{s^1 L \downarrow} = \frac{i\kappa_2}{4},
\end{aligned} \tag{7.5}$$

and the rest are 0, where

$$\begin{aligned}\kappa_1 &= e^{i(\phi_R + \phi_L)}, \\ \kappa_2 &= e^{i(\phi_D + \phi_U)}.\end{aligned}\tag{7.6}$$

Next we show maximal violation of monogamy of entanglement through squared concurrence measure as follows.

First, we calculate concurrence of the state $|\Psi^{(2,2)}\rangle$ as described in Eq. (7.5).

Projecting $\rho^{(2,2)} = |\Psi^{(2,2)}\rangle\langle\Psi^{(2,2)}|$ onto the (operational) subspace spanned by the computational basis

$$\begin{aligned}\Omega_{s^1 s^2} &= \{ |s^1 L \downarrow, s^2 R \downarrow\rangle, |s^1 L \downarrow, s^2 U \downarrow\rangle, |s^1 L \downarrow, s^2 R \uparrow\rangle, |s^1 L \downarrow, s^2 U \uparrow\rangle, |s^1 L \uparrow, s^2 R \downarrow\rangle, \\ & |s^1 L \uparrow, s^2 U \downarrow\rangle, |s^1 L \uparrow, s^2 R \uparrow\rangle, |s^1 L \uparrow, s^2 U \uparrow\rangle, |s^1 D \downarrow, s^2 R \downarrow\rangle, |s^1 D \downarrow, s^2 U \downarrow\rangle, \\ & |s^1 D \downarrow, s^2 R \uparrow\rangle, |s^1 D \downarrow, s^2 U \uparrow\rangle, |s^1 D \uparrow, s^2 R \downarrow\rangle, |s^1 D \uparrow, s^2 U \downarrow\rangle, |s^1 D \uparrow, s^2 R \uparrow\rangle, \\ & |s^1 D \uparrow, s^2 U \uparrow\rangle\},\end{aligned}\tag{7.7}$$

by the projector

$$\Pi_{s^1 s^2} = \sum_{\sigma, \tau = \{\uparrow, \downarrow\}, s = \{L, D\}, v = \{R, U\}} |s^1 \zeta \sigma, s^2 \nu \tau\rangle \langle s^1 \zeta \sigma, s^2 \nu \tau|,\tag{7.8}$$

one gets the distributed resource state where each localized region s^1 and s^2 have exactly one particle as

$$\begin{aligned}|\Psi^{(2,2)}\rangle_{s^1 s^2} &= \frac{\Pi_{s^1 s^2} |\Psi^{(2,2)}\rangle}{\sqrt{\langle\Psi^{(2,2)}|\Pi_{s^1 s^2}|\Psi^{(2,2)}\rangle}} \\ &= \sum_{a_1^1 \in \{L, D\}, a_1^2 \in \{R, U\}, a_2^1, a_2^2 \in \{\uparrow, \downarrow\}} \kappa_{s^2 a_1^2 a_2^2}^{s^1 a_1^1 a_2^1} |s^1 a_1^1 a_2^1, s^2 a_1^2 a_2^2\rangle,\end{aligned}\tag{7.9}$$

where the non-zero coefficients are

$$\begin{aligned}\kappa_{s^2 R \downarrow}^{s^1 L \downarrow} &= -\kappa_{s^2 U \uparrow}^{s^1 D \uparrow} = \frac{1}{2\sqrt{2}} (\kappa_1 + \kappa_2), \\ \kappa_{s^2 R \downarrow}^{s^1 D \uparrow} &= \kappa_{s^2 U \uparrow}^{s^1 L \downarrow} = \frac{i}{2\sqrt{2}} (\kappa_1 - \kappa_2).\end{aligned}\tag{7.10}$$

The density matrix $\rho_{s^1 s^2}^{(2,2)} = |\Psi^{(2,2)}\rangle_{s^1 s^2} \langle \Psi^{(2,2)}|$ can also be calculated as

$$\rho_{s^1 s^2}^{(2,2)} = \frac{\Pi_{s^1 s^2} \rho^{(2,2)} \Pi_{s^1 s^2}}{\text{Tr}(\Pi_{s^1 s^2} \rho^{(2,2)})}, \quad (7.11)$$

where $\rho^{(2,2)} = |\Psi^{(2,2)}\rangle \langle \Psi^{(2,2)}|$.

Now from Eq. (7.11), if we trace-out the path DoFs of location s^1 and s^2 using Eq. (5.16) (the order does not matter), we get the reduced density matrix as

$$\begin{aligned} \rho_{a_2^1 a_2^2}^{s^1 s^2} &= \text{Tr}_{s^1 a_1^1 a_1^2} \left(\rho_{s^1 s^2}^{(2,2)} \right) \\ &= \sum_{a_2^1, a_2^2, b_2^1, b_2^2 \in \{\uparrow, \downarrow\}} \kappa_{s^2 a_2^2}^{s^1 a_2^1} \kappa_{s^2 b_2^2}^{s^1 b_2^1*} |s^1 a_2^1, s^2 a_2^2\rangle \langle s^1 b_2^1, s^2 b_2^2|, \end{aligned} \quad (7.12)$$

where

$$\begin{aligned} \kappa_{s^2 \downarrow}^{s^1 \downarrow} &= -\kappa_{s^2 \uparrow}^{s^1 \uparrow} = \frac{1}{2\sqrt{2}} (\kappa_1 + \kappa_2), \\ \kappa_{s^2 \downarrow}^{s^1 \uparrow} &= \kappa_{s^2 \uparrow}^{s^1 \downarrow} = \frac{i}{2\sqrt{2}} (\kappa_1 - \kappa_2), \end{aligned} \quad (7.13)$$

and rest are zero where complex conjugates are calculated accordingly.

The physical significance of the reduced density matrix $\rho_{a_2^1 a_2^2}^{s^1 s^2}$ can be explained as follows: if we measure only the spin DoFs in the spatial regions s^1 and s^2 , then the measurement statistics would be equivalent to the reduced density matrix $\rho_{a_2^1 a_2^2}^{s^1 s^2}$. This can be obtained by applying our DoF trace-out rule two times by taking the spatial regions first as $s^x = s^1$ and then $s^x = s^2$ (or taking first as $s^x = s^2$ and then $s^x = s^1$, as the order does not matter) in Eq. (5.16) where $m_i \in \{L, D, R, U\}$. On the other hand, when we measure the path DoF in the spatial region s^1 and the spin DoF in the spatial region s^2 , then the measurement statistics would be equivalent to the reduced density matrix $\rho_{a_2^1 a_2^2}^{s^1 s^2}$. This can be obtained by performing our DoF trace-out rule by taking first $s^x = s^1$ where $m_i \in \{L, D, R, U\}$ and then $s^x = s^2$ where $m_i \in \{\uparrow, \downarrow\}$ or vice-versa in Eq. (5.16).

To calculate the maximum violation using squared concurrence, first we calculate the following:

$$\tilde{\rho}_{a_2^1 a_2^2}^{s^1 s^2} = \sigma_y^{s^1} \otimes \sigma_y^{s^2} \rho_{a_2^1 a_2^2}^{s^1 s^2*} \sigma_y^{s^1} \otimes \sigma_y^{s^2}, \quad (7.14)$$

where $\sigma_y^X = |X\rangle\langle X| \otimes \sigma_y$, $X \in \{s^1, s^2\}$, σ_y is Pauli matrix and the asterisk denotes complex conjugation. So, the expression becomes

$$\tilde{\rho}_{a_2^1 a_2^2}^{s^1 s^2} = \sum_{a_2^1, a_2^2, b_2^1, b_2^2 \in \{\uparrow, \downarrow\}} \tilde{\kappa}_{s^2 a_2^2}^{s^1 a_2^1} \tilde{\kappa}_{s^2 b_2^2}^{s^1 b_2^1*} |s^1 a_2^1, s^2 a_2^2\rangle \langle s^1 b_2^1, s^2 b_2^2|, \quad (7.15)$$

where

$$\begin{aligned} \tilde{\kappa}_{s^2 \downarrow}^{s^1 \downarrow} \tilde{\kappa}_{s^2 \downarrow}^{s^1 \downarrow*} &= -\tilde{\kappa}_{s^2 \downarrow}^{s^1 \downarrow} \tilde{\kappa}_{s^2 \uparrow}^{s^1 \uparrow*} = -\tilde{\kappa}_{s^2 \uparrow}^{s^1 \uparrow} \tilde{\kappa}_{s^2 \downarrow}^{s^1 \downarrow*} = \tilde{\kappa}_{s^2 \uparrow}^{s^1 \uparrow} \tilde{\kappa}_{s^2 \uparrow}^{s^1 \uparrow*} = \frac{1}{2} \cos^2 \phi, \\ \tilde{\kappa}_{s^2 \downarrow}^{s^1 \downarrow} \tilde{\kappa}_{s^2 \downarrow}^{s^1 \uparrow*} &= \tilde{\kappa}_{s^2 \downarrow}^{s^1 \downarrow} \tilde{\kappa}_{s^2 \uparrow}^{s^1 \downarrow*} = -\tilde{\kappa}_{s^2 \uparrow}^{s^1 \uparrow} \tilde{\kappa}_{s^2 \downarrow}^{s^1 \uparrow*} = -\tilde{\kappa}_{s^2 \uparrow}^{s^1 \uparrow} \tilde{\kappa}_{s^2 \uparrow}^{s^1 \downarrow*} = \frac{1}{2} \cos \phi \sin \phi, \\ \tilde{\kappa}_{s^2 \downarrow}^{s^1 \uparrow} \tilde{\kappa}_{s^2 \downarrow}^{s^1 \downarrow*} &= \tilde{\kappa}_{s^2 \uparrow}^{s^1 \downarrow} \tilde{\kappa}_{s^2 \downarrow}^{s^1 \downarrow*} = \tilde{\kappa}_{s^2 \downarrow}^{s^1 \uparrow} \tilde{\kappa}_{s^2 \uparrow}^{s^1 \uparrow*} = \tilde{\kappa}_{s^2 \uparrow}^{s^1 \downarrow} \tilde{\kappa}_{s^2 \uparrow}^{s^1 \uparrow*} = \frac{1}{2} \cos \phi \sin \phi, \\ \tilde{\kappa}_{s^2 \downarrow}^{s^1 \uparrow} \tilde{\kappa}_{s^2 \downarrow}^{s^1 \uparrow*} &= \tilde{\kappa}_{s^2 \downarrow}^{s^1 \uparrow} \tilde{\kappa}_{s^2 \uparrow}^{s^1 \downarrow*} = \tilde{\kappa}_{s^2 \uparrow}^{s^1 \downarrow} \tilde{\kappa}_{s^2 \downarrow}^{s^1 \uparrow*} = \tilde{\kappa}_{s^2 \uparrow}^{s^1 \downarrow} \tilde{\kappa}_{s^2 \uparrow}^{s^1 \downarrow*} = \frac{1}{2} \sin^2 \phi, \end{aligned} \quad (7.16)$$

with $\phi = \frac{1}{2} \{\phi_D + \phi_U - \phi_R - \phi_L\}$. Now we calculate concurrence as

$$\mathcal{C}_{a_2^1 a_2^2}^{s^1 s^2} \left(\rho_{a_2^1 a_2^2}^{s^1 s^2} \right) = \max \left\{ 0, \sqrt{\lambda_4} - \sqrt{\lambda_3} - \sqrt{\lambda_2} - \sqrt{\lambda_1} \right\}, \quad (7.17)$$

where λ_i are the eigenvalues, in decreasing order, of the non-Hermitian matrix

$$\mathbb{R} = \rho_{a_2^1 a_2^2}^{s^1 s^2} \tilde{\rho}_{a_2^1 a_2^2}^{s^1 s^2} = \sum_{a_2^1, a_2^2, b_2^1, b_2^2 \in \{\uparrow, \downarrow\}} \bar{\kappa}_{s^2 a_2^2}^{s^1 a_2^1} \bar{\kappa}_{s^2 b_2^2}^{s^1 b_2^1*} |s^1 a_2^1, s^2 a_2^2\rangle \langle s^1 b_2^1, s^2 b_2^2|, \quad (7.18)$$

where

$$\begin{aligned} \bar{\kappa}_{s^2 \downarrow}^{s^1 \downarrow} \bar{\kappa}_{s^2 \downarrow}^{s^1 \downarrow*} &= -\bar{\kappa}_{s^2 \downarrow}^{s^1 \downarrow} \bar{\kappa}_{s^2 \uparrow}^{s^1 \uparrow*} = -\bar{\kappa}_{s^2 \uparrow}^{s^1 \uparrow} \bar{\kappa}_{s^2 \downarrow}^{s^1 \downarrow*} = \bar{\kappa}_{s^2 \uparrow}^{s^1 \uparrow} \bar{\kappa}_{s^2 \uparrow}^{s^1 \uparrow*} = \frac{1}{4} \cos^2 \phi, \\ \bar{\kappa}_{s^2 \downarrow}^{s^1 \downarrow} \bar{\kappa}_{s^2 \downarrow}^{s^1 \uparrow*} &= \bar{\kappa}_{s^2 \downarrow}^{s^1 \downarrow} \bar{\kappa}_{s^2 \uparrow}^{s^1 \downarrow*} = -\bar{\kappa}_{s^2 \uparrow}^{s^1 \uparrow} \bar{\kappa}_{s^2 \downarrow}^{s^1 \uparrow*} = -\bar{\kappa}_{s^2 \uparrow}^{s^1 \uparrow} \bar{\kappa}_{s^2 \uparrow}^{s^1 \downarrow*} = \frac{1}{4} \cos \phi \sin \phi, \\ \bar{\kappa}_{s^2 \downarrow}^{s^1 \uparrow} \bar{\kappa}_{s^2 \downarrow}^{s^1 \downarrow*} &= \bar{\kappa}_{s^2 \uparrow}^{s^1 \downarrow} \bar{\kappa}_{s^2 \downarrow}^{s^1 \downarrow*} = \bar{\kappa}_{s^2 \downarrow}^{s^1 \uparrow} \bar{\kappa}_{s^2 \uparrow}^{s^1 \uparrow*} = \bar{\kappa}_{s^2 \uparrow}^{s^1 \downarrow} \bar{\kappa}_{s^2 \uparrow}^{s^1 \uparrow*} = \frac{1}{4} \cos \phi \sin \phi, \\ \bar{\kappa}_{s^2 \downarrow}^{s^1 \uparrow} \bar{\kappa}_{s^2 \downarrow}^{s^1 \uparrow*} &= \bar{\kappa}_{s^2 \downarrow}^{s^1 \uparrow} \bar{\kappa}_{s^2 \uparrow}^{s^1 \downarrow*} = \bar{\kappa}_{s^2 \uparrow}^{s^1 \downarrow} \bar{\kappa}_{s^2 \downarrow}^{s^1 \uparrow*} = \bar{\kappa}_{s^2 \uparrow}^{s^1 \downarrow} \bar{\kappa}_{s^2 \uparrow}^{s^1 \downarrow*} = \frac{1}{4} \sin^2 \phi. \end{aligned} \quad (7.19)$$

So, the eigenvalues of \mathbb{R} are $\{1, 0, 0, 0\}$. Thus

$$\mathcal{C}_{a_2^1 |s_2^2}^{s^1 |s_2^2} \left(\rho_{a_2^1 |s_2^2}^{s^1 |s_2^2} \right) = 1. \quad (7.20)$$

Similar calculations follows that, $\mathcal{C}_{a_2^1 |s_2^1}^{s^1 |s_2^1} \left(\rho_{a_2^1 |s_2^1}^{s^1 |s_2^1} \right) = 1$.

Likewise, we can also calculate the log-negativity [58, 59] for the density matrix

$\rho_{s_{a_2^1}^1 s_{a_2^2}^2}$ in Eq. (7.12). For that, we need the eigenvalues of the density matrix $\rho_{s_{a_2^1}^1}$ after taking the partial transpose with respect to $s_{a_2^2}^2$. The eigenvalues are found to be $\{-\frac{1}{2}, \frac{1}{2}, \frac{1}{2}, \frac{1}{2}\}$. Thus the value of negativity is $\frac{1}{2}$ and so the log-negativity is given by

$$E_{\mathcal{N}}\left(\rho_{s_{a_2^1}^1 s_{a_2^2}^2}\right) = 1. \quad (7.21)$$

Similar calculations give $E_{\mathcal{N}}\left(\rho_{s_{a_2^1}^1 s_{a_1^2}^2}\right) = 1$.

All other monogamous measures of entanglement for qubit systems such as entanglement of formation [57], log-negativity [58, 59], Tsallis-q entropy [60, 61], Rényi- α entanglement [62, 63], Unified-(q, s) entropy [64, 65], one-way distillable entanglement [206], squashed entanglement [207, 208] etc. [55] are calculable from the reduced density matrix. If one starts with the same reduced density matrix as in Eq. (7.12), one can easily show that all the above measures attain their respective maximum value for both the subsystems $\{s_{a_2^1}^1, s_{a_2^2}^2\}$ and $\{s_{a_2^1}^1, s_{a_1^2}^2\}$ simultaneously, thereby violating the monogamy of entanglement. Thus, for any bipartite monogamous entanglement measure \mathbb{E} , we get

$$\mathbb{E}_{s_{a_2^1}^1 | s_{a_2^2}^2}\left(\rho_{s_{a_2^1}^1 s_{a_2^2}^2}\right) = \mathbb{E}_{s_{a_2^1}^1 | s_{a_1^2}^2}\left(\rho_{s_{a_2^1}^1 s_{a_1^2}^2}\right) = 1. \quad (7.22)$$

Interestingly, this violation is irrespective of any particular entanglement measure like squared concurrence. It can be shown that such a violation happens in indistinguishable particles by any monogamous bipartite entanglement measure for qubit systems. This leads to the following result.

Theorem 2. *In qubit systems, indistinguishability is a necessary criterion for maximum violation of monogamy of entanglement by the same measures that are monogamous for distinguishable particles.*

7.5 Physical significance of the maximum violation of monogamy

Monogamy of entanglement is widely regarded as one of the basic principles of quantum physics [173]. Qualitatively, it is always expected to hold, as a maximal violation will have consequences for the no-cloning theorem. So much so, that a quantitative violation is interpreted as the non-monogamistic nature of the entanglement measure and not of the system of particles itself [268]. Some of those non-monogamous measures can be elevated to be monogamous through convex roof extension [269].

Through Theorem 2, we establish a qualitative violation of monogamy of entanglement which was hitherto unheard of. We show that using quantum indistinguishability, it is possible to maximally violate the monogamy of entanglement for all such entanglement measures which are known to be monogamous for distinguishable systems. To establish this theorem, we first needed to modify the qualitative definition of monogamy of entanglement itself, transiting from the particle-view to the DoF-view and had to introduce the DoF trace-out rule for indistinguishable particles. Thus, this is a non-trivial extension of the well-known monogamy of entanglement.

Further, our framework also takes into account the recently introduced inter-DoF entanglement [1]. Quantum physics dictates the measurement results of a particular DoF when it is correlated with another DoF. Taking a partial trace while keeping the rule of quantum physics intact is extremely non-trivial and requires a rigorous mathematical treatment. Our framework, therefore, captures these nuances of quantum physics better than any other existing framework.

Theorem 2 unveils a non-trivial difference between distinguishable and indistinguishable systems. For distinguishable systems, monogamy of entanglement and no-cloning theorem imply one another as shown in 2.5.2. The significance of our result is that for indistinguishable systems, the no-cloning theorem remains more fundamental than monogamy of entanglement and the former does not necessarily imply the latter. In fact, no-cloning is derived from the linearity of quantum mechanics [78] and hence even indistinguishable particles are also bound to follow it. It appears that

the only way to reconcile the co-existence of monogamy of entanglement violation and no-cloning for indistinguishable particles is to consider that such particles do not yield unit fidelity in quantum teleportation [247, 163, 244]

Moreover, indistinguishability is not a sufficient condition for violation of monogamy of entanglement. There can be scenarios where indistinguishable subsystems may be maximally entangled, respecting monogamy. Only specific entanglement structures (such as the circuit discussed in this work) can lead to a maximum violation of monogamy of entanglement. That is why we call indistinguishability a necessary criterion for maximum violation of monogamy of entanglement.

Theorem 2 raises a few fundamental questions on the properties of entanglement for indistinguishable particles.

(i) There are several applications of monogamy of entanglement for distinguishable particles such as [67, 68, 69, 70, 71, 72, 77]. In particular, for cryptographic applications [67, 68, 69], monogamy of entanglement provides security in the distinguishable scenario. What happens to such applications in the indistinguishable case?

(ii) Can there be a new application of sharability of maximal entanglement among indistinguishable particles that are not possible for distinguishable ones?

(iii) Do indistinguishable particles also exhibit maximum violation of monogamy for general quantum correlations [270] such as discord [271, 272, 273, 274], coherence [275, 276], steering [277, 278, 279], etc.

Chapter 8

Monogamy of entanglement for three or more indistinguishable particles

For distinguishable particles, MoE is known to hold, irrespective of whether the DoFs involved come from two particles [262, 263, 258] or more [66, 210]. For two indistinguishable particles, it has been shown that monogamy does not necessarily hold and can be violated maximally [258] as shown in Chapter 7. So a natural question arises, whether MoE always holds for three or more indistinguishable particles or not?

There are fundamental difference between the physicality of entanglement of distinguishable particles and that of indistinguishable ones. For example, two distinguishable particles with orthogonal eigenstates in one of the DoFs are separable as they can be written in tensor product. However, two indistinguishable particles can become entangled even under the conditions of orthogonal eigenstates, differently from two distinguishable particles which remain in a product state [161, Methods]. So, if three or more particles becomes indistinguishable in the same/different localized regions in their same/different eigenstates of same/different DoFs in an arbitrary manner, whether MoE holds or not is not immediately obvious and needs non-trivial analysis. This is the motivation behind this chapter. Here, we use concurrence as entanglement measure to calculate the monogamy of entanglement.

This chapter is based on the work in [259].

8.1 Calculation of concurrence between two spatial regions between any DoFs

In the general state given in Eq. (5.10), it is possible that each localized region have more than one particle. To calculate the concurrence, we have to ensure that each of the localized regions s^1, s^2, \dots, s^p has only one particle. For that we have to apply a projector as following.

Projecting $\rho^{(p,n)}$ onto the operational subspace spanned by the basis

$$\begin{aligned} & \mathcal{B}^{s^1 s^2 \dots s^p} \\ & = \{ |s^1 D_{1_1}^1 \dots D_{n_1}^1, s^2 D_{1_1}^2 \dots D_{n_1}^2, \dots, s^p D_{1_1}^p \dots D_{n_1}^p \rangle, \\ & \quad |s^1 D_{1_2}^1 \dots D_{n_1}^1, s^2 D_{1_1}^2 \dots D_{n_1}^2, \dots, s^p D_{1_1}^p \dots D_{n_1}^p \rangle, \\ & \quad \vdots \\ & \quad |s^1 D_{1_{k_1}}^1 \dots D_{n_{k_n}}^1, s^2 D_{1_{k_1}}^2, \dots, s^p D_{1_{k_1}}^p D_{2_{k_2}}^p \dots D_{n_{k_n}}^p \rangle \} \end{aligned} \quad (8.1)$$

by the projector

$$\mathcal{P}_{s^1 s^2 \dots s^p} = \sum_{x_j^i \in \mathbb{D}_j, i \in \mathbb{N}_p, j \in \mathbb{N}_n} |s^1 x_1^1 x_2^1 \dots x_n^1, s^2 x_1^2 x_2^2 \dots x_n^2, \dots, s^p x_1^p x_2^p \dots x_n^p \rangle \langle s^1 x_1^1 x_2^1 \dots x_n^1, s^2 x_1^2 x_2^2 \dots x_n^2, \dots, s^p x_1^p x_2^p \dots x_n^p | \quad (8.2)$$

results in

$$\rho_{s^1 s^2 \dots s^p}^{(p,n)} = \frac{\mathcal{P}_{s^1 s^2 \dots s^p} \rho^{(p,n)} \mathcal{P}_{s^1 s^2 \dots s^p}}{\text{Tr}(\mathcal{P}_{s^1 s^2 \dots s^p} \rho^{(p,n)})}. \quad (8.3)$$

To calculate the concurrence between two spatial regions, we have to trace out other $(p-2)$ regions using the method described in [258]. The trace out rule for tracing out say $s^h \in \mathbb{S}^p$ region can be described as

$$\rho_{(\mathbb{S}^p - \{s^h\})}^{(p-1,n)} = \text{Tr}_{s^h}(\rho^{(p,n)}) = \sum_{m_1^h, m_2^h, \dots, m_n^h} \langle s^h m_1^h m_2^h \dots m_n^h | \rho^{(p,n)} | s^h m_1^h m_2^h \dots m_n^h \rangle, \quad (8.4)$$

where m_j^h span \mathbb{D}_j for $j \in \mathbb{N}_n$.

This if we trace out k number of particles from the localized regions $s^{h_1}, s^{h_2}, \dots, s^{h_k}$, then the reduced density matrix is be represented as

$$\begin{aligned} \rho_{(\mathbb{S}^p - \{s^{h_1}, s^{h_2}, \dots, s^{h_k}\})}^{(p-h, n)} &= \text{Tr}_{s^{h_1}, s^{h_2}, \dots, s^{h_k}} \left(\rho^{(p, n)} \right) \\ &= \sum_{s^{h_i} \in \mathbb{S}^p, m_j^{h_i} \in \mathbb{D}_j} \langle s^{h_1} m_1^{h_1} m_2^{h_1} \dots m_n^{h_1}, \dots, s^{h_k} m_1^{h_k} m_2^{h_k} \dots m_n^{h_k} | \rho^{(p, n)} | s^{h_1} m_1^{h_1} m_2^{h_1} \dots m_n^{h_1}, \dots, s^{h_k} m_1^{h_k} m_2^{h_k} \dots m_n^{h_k} \rangle. \end{aligned} \quad (8.5)$$

Suppose we want to calculate the concurrence between the particle in the location s^r and the particle in the location s^t where $s^r, s^t \in \mathbb{S}^p$, we apply the DoF trace-out rule as defined in [258]. Thus the reduced density matrix is

$$\rho_{s^r, s^t}^{(2, n)} = \text{Tr}_{(\mathbb{S} - \{s^r, s^t\})} \left(\rho^{(p, n)} \right). \quad (8.6)$$

To calculate the concurrence between the v -th DoF of the particle in the location s^r and the w -th DoF of the particle in the location s^t where $1 \leq v, w \leq n$, we have to trace-out all the other non-contributing DoFs from these two locations using the DoF trace-out rule as defined in [258]. So, the reduced density matrix of the v -th and w -th DoF of the locations s^r and s^t respectively is given by

$$\rho_{s_v^r, s_w^t}^{(2, 1)} = \text{Tr}_{(s_{\bar{v}}^r, s_{\bar{w}}^t)} \left(\rho_{s^r, s^t}^{(2, n)} \right) = \sum_{m_j^r, m_j^t \in \mathbb{D}_j} \langle \psi_{m_{\bar{v}}}^{s^r}, \psi_{m_{\bar{w}}}^{s^t} | \rho_{s^r, s^t}^{(2, n)} | \psi_{m_{\bar{v}}}^{s^r}, \psi_{m_{\bar{w}}}^{s^t} \rangle, \quad (8.7)$$

where $|\psi_{m_{\bar{v}}}^{s^r}\rangle = |s^r m_1^r m_2^r \dots m_{(v-1)}^r m_{(v+1)}^r \dots m_n^r\rangle$ and

$|\psi_{m_{\bar{w}}}^{s^t}\rangle = |s^t m_1^t m_2^t \dots m_{(w-1)}^t m_{(w+1)}^t \dots m_n^t\rangle$.

To calculate the concurrence of $\rho_{s_v^r, s_w^t}^{(2, 1)}$, i.e., $\mathcal{C}_{s_v^r | s_w^t}$, we have to calculate the following

$$\tilde{\rho}_{s_v^r, s_w^t} = \sigma_y^{s^r} \otimes \sigma_y^{s^t} \rho_{s_v^r, s_w^t}^* \sigma_y^{s^r} \otimes \sigma_y^{s^t}. \quad (8.8)$$

where $\sigma_y^{s^r} = |s^r\rangle \langle s^r| \otimes \sigma_y$, and similarly $\sigma_y^{s^t} = |s^t\rangle \langle s^t| \otimes \sigma_y$, and σ_y is Pauli matrix and the asterisk denotes complex conjugation.

Now we have to calculate the eigenvalues of the non-hermitian matrix

$$\mathcal{R}_{s_v^r, s_w^t} = \rho_{s_v^r, s_w^t} \tilde{\rho}_{s_v^r, s_w^t}. \quad (8.9)$$

Finally the concurrence is calculated as the

$$\mathcal{C}_{s_v^r | s_w^t} = \max \left\{ 0, \sqrt{\lambda_4} - \sqrt{\lambda_3} - \sqrt{\lambda_2} - \sqrt{\lambda_1} \right\}, \quad (8.10)$$

where λ_i 's are the eigenvalues of $\mathcal{R}_{s_v^r, s_w^t}$ in decreasing order.

8.2 Monogamy of p indistinguishable particles each having n DoFs

As the state-space structure of distinguishable and indistinguishable particles are completely different and so the proof for MoE shown for distinguishable particles in [66] is not applicable for indistinguishable particles. So, we calculate the MoE for all the possible ways in which indistinguishability can occur. First, we calculate it for three particles each having three DoFs, for example spin, OAM, and path DoF having eigenstates $\{|\uparrow\rangle, |\downarrow\rangle\}$, $\{|+l\rangle, |-l\rangle\}$, and $\{|R\rangle, |L\rangle\}$ respectively in three localized regions \mathbb{S}^3 . We describe the first five cases where one of the eigenstates of the DoFs contributed for entanglement, and the other non-contributing DoFs can take arbitrary values. Then we consider the other cases where contributing DoFs for entanglement can be in arbitrary superposition of their eigenstates. Finally, we generalize it for p indistinguishable particles each having n DoFs.

Suppose there are p number of indistinguishable particles, each having n DoFs. Recall that, the k -th eigenvalue of the j th DoF of a particle is represented by $\mathcal{D}_{j_k} \in \mathbb{D}_j$ (the set of eigenvalues of the j th DoF). As we are considering squared concurrence measure, so we take only two eigenstates of each DoF. For any eigenvalue λ , we use the notion $|\lambda\rangle$ for the corresponding eigenstate. In Table 8.2, we summarize the list of possible combinations to create indistinguishability using three indistinguishable particles, each having three DoFs denoted by j , j' , and j'' , localized in three regions s^1 , s^2 , and s^3 . Calculations for concurrences are done using the method described in Section 8.1. These cases can be extended for p number of indistinguishable particles as shown below.

DoF	Eigenstate	1st particle	2nd particle	3rd particle	Relations	measures in the DoF					
						s^1	s^2	s^3			
1	Same	$ \mathcal{D}\rangle_{jk}$	$ \mathcal{D}\rangle_{jk}$	$ \mathcal{D}\rangle_{jk}$	Nil	j	j	j	0	0	0
2	Same	$ \mathcal{D}\rangle_{jk}$	$ \mathcal{D}\rangle_{jk}$	$ \mathcal{D}\rangle_{j_{k'}}$	$\mathcal{D}_{jk}, \mathcal{D}_{j_{k'}} \in \mathbb{D}_j, \mathcal{D}\rangle_{j_{k'}} = \mathcal{D}\rangle_{jk}^\perp$	j	j	j	≥ 0	≥ 0	≥ 0
3	Different	$ \mathcal{D}\rangle_{jk}$	$ \mathcal{D}\rangle_{jk}$	$ \mathcal{D}\rangle_{j_l'}$	$j \neq j', \mathcal{D}_{jk} \in \mathbb{D}_j, \mathcal{D}_{j_l'} \in \mathbb{D}_{j'}$	j	j	j'	0	0	0
4	Different	$ \mathcal{D}\rangle_{jk}$	$ \mathcal{D}\rangle_{j_{k'}}$	$ \mathcal{D}\rangle_{j_l'}$	$ \mathcal{D}\rangle_{j_{k'}} = \mathcal{D}\rangle_{jk}^\perp, \mathcal{D}_{j_l'} \in \mathbb{D}_{j'}$	j	j	j'	≥ 0	0	≥ 0
5	Different	$ \mathcal{D}\rangle_{jk}$	$ \mathcal{D}\rangle_{j_h''}$	$ \mathcal{D}\rangle_{j_l'}$	$j \neq j' \neq j'', \mathcal{D}_{j_h''} \in \mathbb{D}_{j''}$	j	j''	j'	0	0	0
6	Same	$ \mathcal{D}\rangle_{jk}$	$ \mathcal{D}\rangle_{jk}$	$\kappa_{jk} \mathcal{D}\rangle_{jk} + \kappa_{j_{k'}} e^{i\phi} \mathcal{D}\rangle_{j_{k'}}$	$\kappa_{jk}^2 + \kappa_{j_{k'}}^2 = 1$	j	j	j	≥ 0	≥ 0	≥ 0
7	Same	$ \mathcal{D}\rangle_{jk}$	$ \mathcal{D}\rangle_{j_{k'}}$	$\kappa_{jk} \mathcal{D}\rangle_{jk} + \kappa_{j_{k'}} e^{i\phi} \mathcal{D}\rangle_{j_{k'}}$	$ \mathcal{D}\rangle_{j_{k'}} = \mathcal{D}\rangle_{jk}^\perp, \kappa_{jk}^2 + \kappa_{j_{k'}}^2 = 1$	j	j	j	≥ 0	≥ 0	≥ 0
8	Same superposition	$\kappa_{jk} \mathcal{D}\rangle_{jk} + \kappa_{j_{k'}} e^{i\phi} \mathcal{D}\rangle_{j_{k'}}$	$\kappa_{jk} \mathcal{D}\rangle_{jk} + \kappa_{j_{k'}} e^{i\phi} \mathcal{D}\rangle_{j_{k'}}$	$\kappa_{jk} \mathcal{D}\rangle_{jk} + \kappa_{j_{k'}} e^{i\phi} \mathcal{D}\rangle_{j_{k'}}$	$\kappa_{jk}^2 + \kappa_{j_{k'}}^2 = 1$	j	j	j	0	0	0
9	Same superposition	$\kappa_{jk} \mathcal{D}\rangle_{jk} + \kappa_{j_{k'}} e^{i\phi_1} \mathcal{D}\rangle_{j_{k'}}$ where $\kappa_{jk}^2 + \kappa_{j_{k'}}^2 = 1$	$\kappa_{j_{k'}} \mathcal{D}\rangle_{j_{k'}} + \kappa_{j_l'} e^{i\phi_2} \mathcal{D}\rangle_{j_l'}$ where $\kappa_{j_{k'}}^2 + \kappa_{j_l'}^2 = 1$	$\kappa_{j_l'} \mathcal{D}\rangle_{j_l'} + \kappa_{j_{k'}} e^{i\phi_3} \mathcal{D}\rangle_{j_{k'}}$ where $\kappa_{j_l'}^2 + \kappa_{j_{k'}}^2 = 1$	$\phi_1 \neq \phi_2 \neq \phi_3$ $\kappa_{jk} \neq \kappa_{j_{k'}} \neq \kappa_{j_l'}^2$ $\kappa_{j_{k'}} \neq \kappa_{j_l'}^2$	j	j	j	≥ 0	≥ 0	≥ 0
10	Different	$ \mathcal{D}\rangle_{jk}$	$ \mathcal{D}\rangle_{jk}$	$\kappa_{j_l'} \mathcal{D}\rangle_{j_l'} + \kappa_{j_{l'}} e^{i\phi} \mathcal{D}\rangle_{j_{l'}}$	$\kappa_{j_l'}^2 + \kappa_{j_{l'}}^2 = 1$	j	j	j'	0	0	0
11	Different	$ \mathcal{D}\rangle_{jk}$	$ \mathcal{D}\rangle_{j_{k'}}$	$\kappa_{j_l'} \mathcal{D}\rangle_{j_l'} + \kappa_{j_{l'}} e^{i\phi} \mathcal{D}\rangle_{j_{l'}}$	$\kappa_{j_l'}^2 + \kappa_{j_{l'}}^2 = 1$	j	j	j'	≥ 0	0	≥ 0
12	Different superposition	$ \mathcal{D}\rangle_{jk}$	$\kappa_{jk} \mathcal{D}\rangle_{jk} + \kappa_{j_{k'}} e^{i\phi} \mathcal{D}\rangle_{j_{k'}}$ where $\kappa_{jk}^2 + \kappa_{j_{k'}}^2 = 1$	$\kappa_{j_l'} \mathcal{D}\rangle_{j_l'} + \kappa_{j_{l'}} e^{i\phi} \mathcal{D}\rangle_{j_{l'}}$ where $\kappa_{j_l'}^2 + \kappa_{j_{l'}}^2 = 1$	$j \neq j'$	j	j	j'	≥ 0	≥ 0	≥ 0
13	Different superposition	$\kappa_{jk} \mathcal{D}\rangle_{jk} + \kappa_{j_{k'}} e^{i\phi} \mathcal{D}\rangle_{j_{k'}}$ where $\kappa_{jk}^2 + \kappa_{j_{k'}}^2 = 1$	$\kappa_{j_h''} \mathcal{D}\rangle_{j_h''} + \kappa_{j_{h'}} e^{i\phi''} \mathcal{D}\rangle_{j_{h'}}$ where $\kappa_{j_h''}^2 + \kappa_{j_{h'}}^2 = 1$	$\kappa_{j_l'} \mathcal{D}\rangle_{j_l'} + \kappa_{j_{l'}} e^{i\phi'} \mathcal{D}\rangle_{j_{l'}}$ where $\kappa_{j_l'}^2 + \kappa_{j_{l'}}^2 = 1$	$j \neq j' \neq j''$ $\mathcal{D}_{j_{k'}}, \mathcal{D}_{j_{h''}} \in \mathbb{D}_j, \mathcal{D}_{j_{h'}} \in \mathbb{D}_{j''}$ $\mathcal{D}_{j_{l'}} \in \mathbb{D}_{j'}$	j	j''	j'	0	0	0

Table 8.1: List of possible combinations to create indistinguishability using three indistinguishable particles localized in three regions s^1 , s^2 , and s^3 , each having three DoFs denoted by j, j', j'' . Here the second column denotes whether entanglement is calculated in same DoFs or different DoFs of all particles; the third column denotes whether the eigenstate of the contributing DoFs in entanglement is the same or not or in superposition; the fourth, fifth and sixth columns describe the eigenstates of the three particles in the corresponding DoFs; the seventh column describes the relations between the eigenstates of the for entanglement. The eighth, ninth, and tenth columns describe the DoFs numbers (e.g., j means the j th DoF) in which the measurements are done in the localized regions s^1 , s^2 , and s^3 respectively; the rest of the columns represent of the squared concurrences are zero or ≥ 0 .

Case 1: Entanglement is calculated in the same DoF of all particles. Each particle is in the eigenstate $|\mathcal{D}\rangle_{j_k}$ of the j th DoF. Then after calculation, we get $\mathcal{C}_{s^1|s^2}^2=0$, $\mathcal{C}_{s^1|s^3}^2=0$, and $\mathcal{C}_{s^1|s^2s^3}^2=0$. Similar result holds for p indistinguishable particles having the eigenstate $|\mathcal{D}\rangle_{j_k}$ of the j th DoF.

Case 2: Entanglement is calculated in the same DoF for all particles. For three indistinguishable particles, if two of them are in the eigenstate $|\mathcal{D}\rangle_{j_k}$ and one is in the eigenstate $|\mathcal{D}\rangle_{j_{k'}}$ where $|\mathcal{D}\rangle_{j_{k'}}=|\mathcal{D}\rangle_{j_k}^\perp$, then $\mathcal{C}_{s^1|s^2}^2 \geq 0$, $\mathcal{C}_{s^1|s^3}^2 \geq 0$, and $\mathcal{C}_{s^1|s^2s^3}^2 \geq 0$ as shown in Section 8.2.1. Similar result holds for p indistinguishable particles in \mathbb{S}^p locations with each particle having n DoFs where $(q+r)$ number of particles are in the eigenstate $|\mathcal{D}\rangle_{j_k}$ and rest of $(p-q-r)$ number of particles are in the eigenstate $|\mathcal{D}\rangle_{j_{k'}}$.

8.2.1 Monogamy of three indistinguishable particles in spin DoF where two particles are in $|\uparrow\rangle$ eigenstate and one particles in $|\downarrow\rangle$ eigenstate

In this section, we calculate the monogamy of entanglement using three indistinguishable particles each having two DoFs, are localized in three spatial regions s^1 , s^2 , and s^3 which we denote as \mathbb{S}^3 as shown in Fig. 8-1. We consider two particles with $|\uparrow\rangle$ eigenstate and one particles with $|\downarrow\rangle$ eigenstate in their spin DoF as we calculate entanglement with only spin DoF. The other DoF of each particle can take any arbitrary eigenvalues. Thus the general state can be written as

$$\begin{aligned}
|\Psi^{(3,2)}\rangle &= \sum_{\alpha^i \in \mathbb{S}^3, i \in \mathbb{N}_3} \eta^u \kappa_{a_1^1 a_2^1, a_1^2 a_2^2, a_1^3 a_2^3}^{\alpha^1, \alpha^2, \alpha^3} |\alpha^1 a_1^1 a_2^1, \alpha^2 a_1^2 a_2^2, \alpha^3 a_1^3 a_2^3\rangle \\
&= \sum_{a_2^i \in \mathbb{D}_2} \eta^{u_2} \kappa_{\uparrow a_2^1, \uparrow a_2^2, \downarrow a_2^3}^{\alpha^1, \alpha^2, \alpha^3} |\alpha^1 \uparrow a_2^1, \alpha^2 \uparrow a_2^2, \alpha^3 \downarrow a_2^3\rangle \\
&\quad + \sum_{a_2^i \in \mathbb{D}_2} \eta^{(1+u_2)} \kappa_{\uparrow a_2^1, \downarrow a_2^2, \uparrow a_2^3}^{\alpha^1, \alpha^2, \alpha^3} |\alpha^1 \uparrow a_2^1, \alpha^2 \downarrow a_2^2, \alpha^3 \uparrow a_2^3\rangle \\
&\quad + \sum_{a_2^i \in \mathbb{D}_2} \eta^{u_2} \kappa_{\downarrow a_2^1, \uparrow a_2^2, \uparrow a_2^3}^{\alpha^1, \alpha^2, \alpha^3} |\alpha^1 \downarrow a_2^1, \alpha^2 \uparrow a_2^2, \alpha^3 \uparrow a_2^3\rangle.
\end{aligned} \tag{8.11}$$

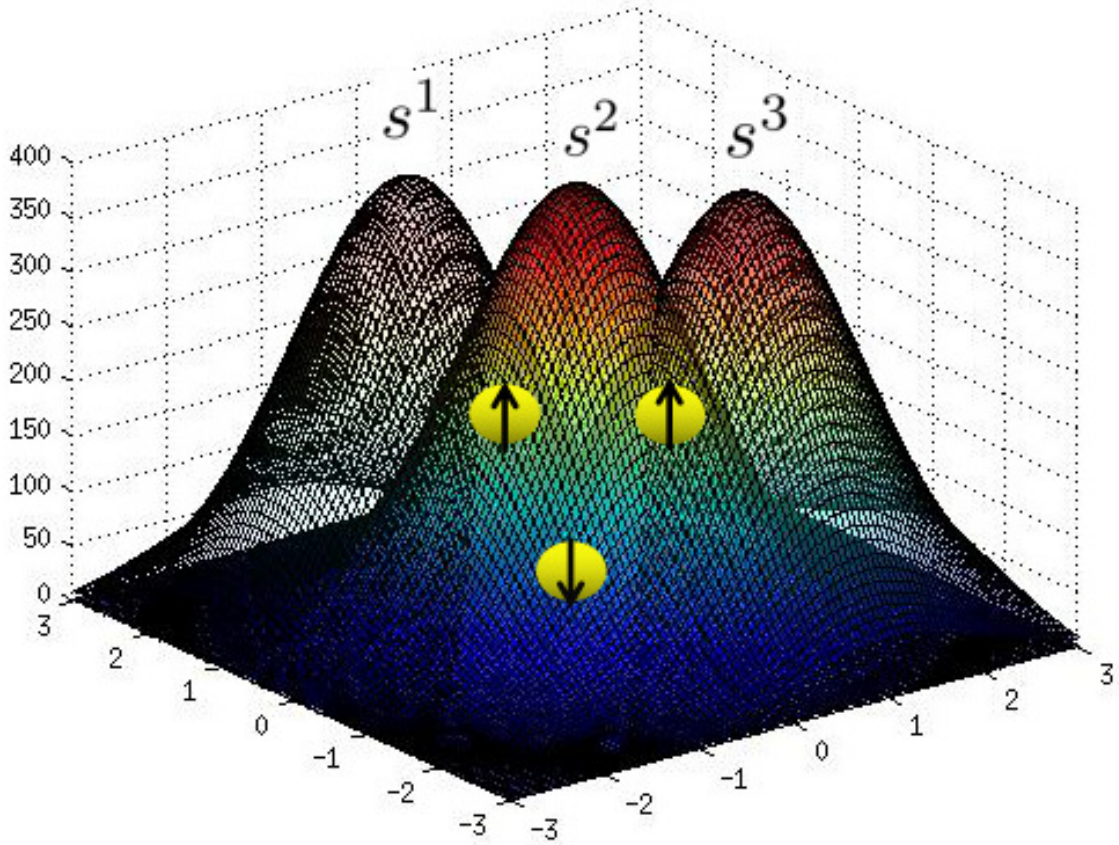


Figure 8-1: Overlapping of the wave-function of three indistinguishable particles in the localized regions s^1 , s^2 , and s^3 where two of them have $|\uparrow\rangle$ eigenstate and one having $|\downarrow\rangle$ eigenstate in spin degrees of freedom.

Here $a_1^i \in \{|\uparrow\rangle, |\downarrow\rangle\}$, $a_2^i \in \mathbb{D}_2$ for $i \in \{1, 2, 3\}$ such that $a_1^i \neq a_1^{i'}$ for all $i \neq i'$ and if $|\uparrow\rangle = -\frac{1}{2}, |\downarrow\rangle = +\frac{1}{2}$ then $\sum a_1^i = -\frac{1}{2}$. The value of $\eta = 0$ if $(\alpha^i = \alpha') \wedge (a_j^i = a_j^{i'})$ for all $i = i'$ where $j \in \mathbb{N}_2$.

The density matrix of Equation (8.11) can be written as

$$\rho^{(3,2)} = \sum_{\alpha^i, \beta^i \in \mathbb{S}^3 \& i \in \mathbb{N}_3} \eta^{(u+\bar{u})} \kappa_{a_1^1 a_2^1, a_1^2 a_2^2, a_1^3 a_2^3}^{\alpha^1, \alpha^2, \alpha^3} \kappa_{b_1^1 b_2^1, b_1^2 b_2^2, b_1^3 b_2^3}^{\beta^1, \beta^2, \beta^3*} |\alpha^1 a_1^1 a_2^1, \alpha^2 a_1^2 a_2^2, \alpha^3 a_1^3 a_2^3\rangle \langle \beta^1 b_1^1 b_2^1, \beta^2 b_1^2 b_2^2, \beta^3 b_1^3 b_2^3|. \quad (8.12)$$

Here $a_1^i, b_1^i \in \{|\uparrow\rangle, |\downarrow\rangle\}$, $a_2^i, b_2^i \in \mathbb{D}_2$ for $i \in \{1, 2, 3\}$ such that $a_1^i \neq a_1^{i'}$ and $b_1^i \neq b_1^{i'}$ for all $i \neq i'$. Also if we take $|\uparrow\rangle = -\frac{1}{2}, |\downarrow\rangle = +\frac{1}{2}$ then $\sum a_1^i = \sum b_1^i = -\frac{1}{2}$. The value of $\eta = 0$ if

$$\{(\alpha^i = \alpha') \vee (\beta^i = \beta')\} \wedge \{(a_j^i = a_j^{i'}) \vee (b_j^i = b_j^{i'})\}$$

for all $i = i'$ where $j \in \mathbb{N}_2$. Here the normalization condition is

$$\sum_{\alpha^i, \beta^i \in \mathbb{S}^3, a_1^i, b_1^i \in \{\uparrow, \downarrow\}, a_2^i, b_2^i \in \mathbb{D}_2} \kappa_{a_1^1 a_2^1 a_1^2 a_2^2 a_1^3 a_2^3}^{\alpha^1, \alpha^2, \alpha^3} \kappa_{b_1^1 b_2^1 b_1^2 b_2^2 b_1^3 b_2^3}^{\beta^1, \beta^2, \beta^3*} = 1, \quad (8.13)$$

where $\alpha^i = \beta^i$, $a_j^i = b_j^i$ for all $i \in \{1, 2, 3\}$ and $j \in \{1, 2\}$.

Next step, we have to apply the projector $\mathcal{P}_{s^1 s^2 s^3}$ so that in each of the location s^1 , s^2 , and s^3 have exactly one particle which is defined as

$$\mathcal{P}_{s^1 s^2 s^3} = \sum_{x_1^i \in \{\uparrow, \downarrow\}, x_2^i \in \mathbb{D}_2} |s^1 x_1^1 x_2^1, s^2 x_1^2 x_2^2, s^3 x_1^3 x_2^3\rangle \langle s^1 x_1^1 x_2^1, s^2 x_1^2 x_2^2, s^3 x_1^3 x_2^3|. \quad (8.14)$$

Thus after applying the projector, we get the density matrix as

$$\begin{aligned} \rho_{s^1 s^2 s^3}^{(3,2)} &= \frac{\mathcal{P}_{s^1 s^2 s^3} \rho^{(3,2)} \mathcal{P}_{s^1 s^2 s^3}}{\text{Tr}(\mathcal{P}_{s^1 s^2 s^3} \rho^{(3,2)})} \\ &= \sum_{a_2^i, b_2^i, x_2^i \in \mathbb{D}_2} \frac{\sum_{h,k \in \{1,2,3\}} \eta^{(k+u_2+\bar{u}_2-1)} z_h z_k^* \rho_{hk}^{(3,2)}}{\sum_{h \in \{1,2,3\}} z_h z_h^*}, \end{aligned} \quad (8.15)$$

where $a_2^i = b_2^i = x_2^i$. The values of

$$\begin{aligned} z_1 &= \kappa_{\uparrow a_2^1, \uparrow a_2^2, \downarrow a_2^3}^{s^1, s^2, s^3}, \\ z_2 &= \kappa_{\uparrow a_2^1, \downarrow a_2^2, \uparrow a_2^3}^{s^1, s^2, s^3}, \\ z_3 &= \kappa_{\downarrow a_2^1, \uparrow a_2^2, \uparrow a_2^3}^{s^1, s^2, s^3}, \end{aligned} \quad (8.16)$$

and the complex conjugates of z_j for $j \in \{1, 2, 3\}$ can be calculated accordingly.

Also $\rho_{hk}^{(3,2)} = |\psi\rangle_h^{(3,2)} \langle \psi|_k^{(3,2)}$ where

$$\begin{aligned} |\psi\rangle_1^{(3,2)} &= |s^1 \uparrow x_2^1, s^2 \uparrow x_2^2, s^3 \downarrow x_2^3\rangle, \\ |\psi\rangle_2^{(3,2)} &= |s^1 \uparrow x_2^1, s^2 \downarrow x_2^2, s^3 \uparrow x_2^3\rangle, \\ |\psi\rangle_3^{(3,2)} &= |s^1 \downarrow x_2^1, s^2 \uparrow x_2^2, s^3 \uparrow x_2^3\rangle, \end{aligned} \quad (8.17)$$

and the complex conjugates of $|\psi\rangle_j^{(3,2)}$ for $j \in \{1, 2, 3\}$ can be calculated accordingly.

Now we have to trace out the particle at the region s^3 . So, we get the reduced

density matrix as

$$\begin{aligned}
\rho_{s^1 s^2}^{(2,2)} &= \text{Tr}_{s^3} \left(\rho_{s^1 s^2 s^3}^{(3,2)} \right) \\
&= \sum_{m_1^3, m_2^3 \in \{\uparrow, \downarrow\}, m_3^3 \in \mathbb{D}_2} \langle s^3 m_1^3 m_2^3 | \rho_{s^1 s^2 s^3}^{(3,2)} | s^3 m_1^3 m_2^3 \rangle \\
&= \sum_{a_2^i, b_2^i, x_2^i \in \mathbb{D}_2} \frac{\sum_{h,k \in \{1,2,3\}} \eta^{(k+u_2+\bar{u}_2-1)} z_h z_k^* \rho_{hk}^{(2,2)}}{\sum_{h \in \{1,2,3\}} z_h z_h^*},
\end{aligned} \tag{8.18}$$

where $a_2^i = b_2^i = x_2^i$, and $m_2^3 = x_2^3$. The values of $\rho_{hk}^{(2,2)} = |\psi\rangle_h^{(2,2)} \langle \psi|_k^{(2,2)}$ where

$$\begin{aligned}
|\psi\rangle_1^{(2,2)} &= |s^1 \uparrow x_2^1, s^2 \uparrow x_2^2\rangle, \\
|\psi\rangle_2^{(2,2)} &= |s^1 \uparrow x_2^1, s^2 \downarrow x_2^2\rangle, \\
|\psi\rangle_3^{(2,2)} &= |s^1 \downarrow x_2^1, s^2 \uparrow x_2^2\rangle, \\
\rho_{12}^{(2,2)} &= \rho_{13}^{(2,2)} = \rho_{21}^{(2,2)} = \rho_{31}^{(2,2)} = 0,
\end{aligned} \tag{8.19}$$

and the complex conjugates of $|\psi\rangle_j^{(2,2)}$ for $j \in \{1, 2, 3\}$ can be calculated accordingly.

Finally Tracing out the second DoF of each particle we have

$$\begin{aligned}
\rho_{s^1, s^1}^{(2,1)} &= \sum_{m_2^1, m_2^2 \in \mathbb{D}_2} \langle s^1 m_2^1, s^2 m_2^2 | \rho_{s^1 s^2}^{(2,2)} | s^1 m_2^1, s^2 m_2^2 \rangle \\
&= \sum_{a_2^i, b_2^i, x_2^i \in \mathbb{D}_2} \frac{\sum_{h,k \in \{1,2,3\}} \eta^{(k+u_2+\bar{u}_2-1)} z_h z_k^* \rho_{hk}^{(2,1)}}{\sum_{h \in \{1,2,3\}} z_h z_h^*},
\end{aligned} \tag{8.20}$$

where $a_2^i = b_2^i = x_2^i = m_2^i$. The values of $\rho_{hk}^{(2,1)} = |\psi\rangle_h^{(2,1)} \langle \psi|_k^{(2,1)}$ where

$$\begin{aligned}
|\psi\rangle_1^{(2,1)} &= |s^1 \uparrow, s^2 \uparrow\rangle, \\
|\psi\rangle_2^{(2,1)} &= |s^1 \uparrow, s^2 \downarrow\rangle, \\
|\psi\rangle_3^{(2,1)} &= |s^1 \downarrow, s^2 \uparrow\rangle, \\
\rho_{12}^{(2,1)} &= \rho_{13}^{(2,1)} = \rho_{21}^{(2,1)} = \rho_{31}^{(2,1)} = 0,
\end{aligned} \tag{8.21}$$

and the complex conjugates of $|\psi\rangle_j^{(2,1)}$ for $j \in \{1, 2, 3\}$ can be calculated accordingly.

To calculate concurrence for $\rho_{s_1^1, s_1^2}^{(2,1)}$, we have to calculate the following

$$\tilde{\rho}_{s_1^1, s_1^2}^{(2,1)} = \sigma_y^{s_1^1} \otimes \sigma_y^{s_2^2} \rho_{s_1^1, s_1^2}^{(2,1)*} \sigma_y^{s_1^1} \otimes \sigma_y^{s_2^2}, \quad (8.22)$$

where $\sigma_y^{s_1^1} = |s^1\rangle\langle s^1| \otimes \sigma_y$, $\sigma_y^{s_2^2} = |s^2\rangle\langle s^2| \otimes \sigma_y$. Here σ_y is the Pauli matrix and the asterisk denotes complex conjugation. Finally, we have to calculate the eigenvalues of $\mathcal{R} = \rho_{s_1^1, s_1^2}^{(2,1)} \tilde{\rho}_{s_1^1, s_1^2}^{(2,1)}$.

So, the value of square of the concurrence $\mathcal{C}_{s_1^1|s_2^2}^2$ is

$$\mathcal{C}_{s_1^1|s_2^2}^2 = 2|z_2 z_3|^2 + z_2^2 z_3^{*2} + z_2^{*2} z_3^2 - 2|z_2 z_3^* z_2^* z_3 - z_2^2 z_3^2|^2. \quad (8.23)$$

Similarly, to calculate the squared concurrence $\mathcal{C}_{s_1^1, s_3^3}^2$, first step is to trace out the particle at the region s^2 from $\rho_{s_1^1, s_2^2, s_3^3}^{(3,2)}$ as shown in Eq. (8.15). So, we get the reduced density matrix as

$$\begin{aligned} \rho_{s_1^1, s_3^3}^{(2,2)} &= \text{Tr}_{s^2} \left(\rho_{s_1^1, s_2^2, s_3^3}^{(3,2)} \right) \\ &= \sum_{\substack{m_1^2 \in \{\uparrow, \downarrow\}, \\ m_2^2 \in \mathbb{D}_2}} \langle s^2 m_1^2 m_2^2 | \rho_{s_1^1, s_2^2, s_3^3}^{(3,2)} | s^2 m_1^2 m_2^2 \rangle \\ &= \sum_{a_2^i, b_2^j, x_2^j \in \mathbb{D}_2} \frac{\sum_{h, k \in \{1, 2, 3\}} \eta^{(k+u_2+\bar{u}_2-1)} z_h z_k^* \rho_{hk}^{(2,2)}}{\sum_{h \in \{1, 2, 3\}} z_h z_h^*}, \end{aligned} \quad (8.24)$$

where $a_2^i = b_2^i = x_2^i$, and $m_2^2 = x_2^2$. The values of $\rho_{hk}^{(2,2)} = |\psi\rangle_h^{(2,2)} \langle \psi|_k^{(2,2)}$ where

$$\begin{aligned} |\psi\rangle_1^{(2,2)} &= |s^1 \uparrow x_2^1, s^3 \uparrow x_2^3\rangle, \\ |\psi\rangle_2^{(2,2)} &= |s^1 \uparrow x_2^1, s^3 \downarrow x_2^3\rangle, \\ |\psi\rangle_3^{(2,2)} &= |s^1 \downarrow x_2^1, s^3 \uparrow x_2^3\rangle, \\ \rho_{12}^{(2,2)} &= \rho_{21}^{(2,2)} = \rho_{23}^{(2,2)} = \rho_{32}^{(2,2)} = 0, \end{aligned} \quad (8.25)$$

and the complex conjugates of $|\psi\rangle_j^{(2,2)}$ for $j \in \{1, 2, 3\}$ can be calculated accordingly.

Now following similar calculations as above we get square of the concurrence

between s^1 and s^3 is

$$\mathcal{C}_{s^1|s^3}^2 = 2|z_1 z_3|^2 + z_1^2 z_3^{*2} + z_1^{*2} z_3^2 - 2|z_1 z_3^* z_1^* z_3 - z_1^2 z_3^2|^2. \quad (8.26)$$

Thus the monogamy relation is

$$\mathcal{C}_{s^1|s^2}^2 + \mathcal{C}_{s^1|s^3}^2 = 4(1 - |z_3|^2)|z_3|^2 \leq 1. \quad (8.27)$$

If we further trace-out the particle at s^2 from Eq. (8.20), we get

$$\begin{aligned} \rho_{s^1}^{(1,1)} &= \sum_{m_1^2 \in \mathbb{D}_2} \langle s^2 m_1^2 | \rho_{s^1, s^2}^{(2,1)} | s^2 m_1^2 \rangle \\ &= (|z_1|^2 + |z_2|^2) |s^1 \uparrow\rangle \langle s^1 \uparrow| + |z_3|^3 |s^1 \downarrow\rangle \langle s^1 \downarrow|. \end{aligned} \quad (8.28)$$

Thus, as Eq. (8.11) is a pure state so, we have

$$\mathcal{C}_{s^1|s^2 s^3}^2 = 4 \det(\rho_{s^1}^{(1,1)}) = 4(1 - |z_3|^2)|z_3|^2 \leq 1. \quad (8.29)$$

So, we get

$$\mathcal{C}_{s^1|s^2}^2 + \mathcal{C}_{s^1|s^3}^2 = \mathcal{C}_{s^1|s^2 s^3}^2. \quad (8.30)$$

Case 3: Entanglement is calculated between two different DoFs. Here, if two particles are in the eigenstate $|\mathcal{D}\rangle_{j_k}$ of the j th DoF and one particle is in the eigenstate $|\mathcal{D}\rangle_{j'_l}$ of the j' th DoF where $j \neq j'$, then $\mathcal{C}_{s^1|s^2}^2 = 0$, $\mathcal{C}_{s^1|s^3}^2 = 0$, and $\mathcal{C}_{s^1|s^2 s^3}^2 = 0$. Similar result holds for p indistinguishable particles in \mathbb{S}^p locations with each particle having n DoFs where $(q+r)$ number of particles are in the eigenstate $|\mathcal{D}\rangle_{j_k}$ of the j th DoF and rest of $(p-q-r)$ number of particles are in the eigenstate $|\mathcal{D}\rangle_{j'_l}$ of the j' th DoF.

Case 4: Entanglement is calculated between two different DoFs. Here, if two particles are in the eigenstate $|\mathcal{D}\rangle_{j_k}$ and $|\mathcal{D}\rangle_{j_{k'}}$ of the j th DoF respectively and one particle is in the eigenstate $|\mathcal{D}\rangle_{j'_l}$ of the j' th DoF where $j \neq j'$ and $|\mathcal{D}\rangle_{j_{k'}} = |\mathcal{D}\rangle_{j_k}^\perp$, then $\mathcal{C}_{s^1|s^2}^2 \geq 0$, $\mathcal{C}_{s^1|s^3}^2 = 0$, and $\mathcal{C}_{s^1|s^2 s^3}^2 \geq 0$ as shown in the Section 8.2.2. Similar result holds for p indistinguishable particles in \mathbb{S}^p locations with each particle having n DoFs

where q and r number of particles are in the eigenstate $|\mathcal{D}\rangle_{j_k}$ and $|\mathcal{D}\rangle_{j_{k'}}$ respectively of the j th DoF and rest of $(p-q-r)$ number of particles are in the eigenstate $|\mathcal{D}\rangle_{j'_i}$ of the j' th DoF.

8.2.2 Monogamy of three indistinguishable particles where two particles are in $|\uparrow\rangle$ and $|\downarrow\rangle$ eigenstate respectively in spin DoF and one particle is in $|+l\rangle$ eigenstate in OAM DoF.

Consider two particles with spin DoF having $|\uparrow\rangle$ and $|\downarrow\rangle$ eigenstates respectively and one particle with orbital angular momentum DoF with $|+l\rangle$ eigenstate. The eigenvalues of spin DoF and OAM DoF are represented by $a_1^i \in \mathbb{D}_1 = \{|\uparrow\rangle, |\downarrow\rangle\}$ and $a_2^i \in \mathbb{D}_2 = \{|+l\rangle, |-l\rangle\}$ respectively where $i \in \{1, 2, 3\}$. The other non-contributing DoFs in entanglement of each particle can take any arbitrary eigenvalues. Thus the general state can be written as

$$\begin{aligned}
|\Psi^{(3,2)}\rangle = & \sum_{a_1^3 \in \mathbb{D}_1, a_2^1, a_2^2 \in \mathbb{D}_2} \eta^0 \kappa_{\uparrow a_2^1, \downarrow a_2^2, a_1^3 + l}^{\alpha^1, \alpha^2, \alpha^3} |\alpha^1 \uparrow a_2^1, \alpha^2 \downarrow a_2^2, \alpha^3 a_1^3 + l\rangle \\
& + \sum_{a_1^2 \in \mathbb{D}_1, a_2^1, a_2^3 \in \mathbb{D}_2} \eta^1 \kappa_{\uparrow a_2^1, a_1^2 + l, \downarrow a_2^3}^{\alpha^1, \alpha^2, \alpha^3} |\alpha^1 \uparrow a_2^1, \alpha^2 a_1^2 + l, \alpha^3 \downarrow a_2^3\rangle \\
& + \sum_{a_1^3 \in \mathbb{D}_1, a_2^1, a_2^2 \in \mathbb{D}_2} \eta^2 \kappa_{\downarrow a_2^1, \uparrow a_2^2, a_1^3 + l}^{\alpha^1, \alpha^2, \alpha^3} |\alpha^1 \downarrow a_2^1, \alpha^2 \uparrow a_2^2, \alpha^3 a_1^3 + l\rangle \\
& + \sum_{a_1^2 \in \mathbb{D}_1, a_2^3, a_2^1 \in \mathbb{D}_2} \eta^3 \kappa_{\downarrow a_2^1, a_1^2 + l, \uparrow a_2^3}^{\alpha^1, \alpha^2, \alpha^3} |\alpha^1 \downarrow a_2^1, \alpha^2 a_1^2 + l, \alpha^3 \uparrow a_2^3\rangle \\
& + \sum_{a_1^1 \in \mathbb{D}_1, a_2^1, a_2^3 \in \mathbb{D}_2} \eta^4 \kappa_{a_1^1 + l, \uparrow a_2^1, \downarrow a_2^3}^{\alpha^1, \alpha^2, \alpha^3} |\alpha^1 a_1^1 + l, \alpha^2 \uparrow a_2^1, \alpha^3 \downarrow a_2^3\rangle \\
& + \sum_{a_1^1 \in \mathbb{D}_1, a_2^1, a_2^2 \in \mathbb{D}_2} \eta^5 \kappa_{a_1^1 + l, \downarrow a_2^1, \uparrow a_2^2}^{\alpha^1, \alpha^2, \alpha^3} |\alpha^1 a_1^1 + l, \alpha^2 \downarrow a_2^1, \alpha^3 \uparrow a_2^2\rangle
\end{aligned} \tag{8.31}$$

where $\alpha^i \in \mathbb{S}^3$ for $i \in \mathbb{N}_3$. After projecting the state by the suitable projector so that in each location s^1 , s^2 , and s^3 have exactly one particle. Finally, we calculate entanglement with s^1 and s^2 in spin DoF and between s^1 and s^3 in spin DoF and OAM DoF

respectively. Following the above steps, we have

$$\begin{aligned}
\mathcal{C}_{s^1|s^2}^2 &= 4 \left(\kappa_{\uparrow a_2^1, \downarrow a_2^2, a_1^3+l}^{s^1, s^2, s^3} \right)^2 \left(\kappa_{\downarrow a_2^1, \uparrow a_2^2, a_1^3+l}^{s^1, s^2, s^3} \right)^2, \\
\mathcal{C}_{s^1|s^3}^2 &= 0, \\
\mathcal{C}_{s^1|s^2s^3}^2 &= 4 \left(\kappa_{\uparrow a_2^1, \downarrow a_2^2, a_1^3+l}^{s^1, s^2, s^3} \right)^2 \left(\kappa_{\downarrow a_2^1, \uparrow a_2^2, a_1^3+l}^{s^1, s^2, s^3} \right)^2.
\end{aligned} \tag{8.32}$$

So, we get

$$\mathcal{C}_{s^1|s^2}^2 + \mathcal{C}_{s^1|s^3}^2 = \mathcal{C}_{s^1|s^2s^3}^2. \tag{8.33}$$

Case 5: Entanglement is calculated between three different DoFs of three particles. If three particles are in the eigenstate $|\mathcal{D}\rangle_{j_k}$ of the j th DoF, $|\mathcal{D}\rangle_{j''_h}$ of the j'' th DoF, and $|\mathcal{D}\rangle_{j'_i}$ of the j' th DoF where $j \neq j' \neq j''$, then $\mathcal{C}_{s^1|s^2}^2 = 0$, $\mathcal{C}_{s^1|s^3}^2 = 0$, and $\mathcal{C}_{s^1|s^2s^3}^2 = 0$. Similar result holds for p indistinguishable particles in \mathbb{S}^p locations with each particle having n DoFs where q number of particles are in the the eigenstate $|\mathcal{D}\rangle_{j_k}$ of j th DoF, r number of particles are in the eigenstate $|\mathcal{D}\rangle_{j''_h}$ of j'' th DoF and rest of $(p - q - r)$ number of particles are in the eigenstate $|\mathcal{D}\rangle_{j'_i}$ of the j' th DoF.

Case 6: Entanglement is calculated in the same DoF of all particles. If two particles are in $|\mathcal{D}\rangle_{j_k}$ and one particle is in the superpositions of its eigenstate, i.e., $\kappa_{j_k} |\mathcal{D}\rangle_{j_k} + \kappa_{j_{k'}} e^{i\phi} |\mathcal{D}\rangle_{j_{k'}}$ where $\kappa_{j_k}^2 + \kappa_{j_{k'}}^2 = 1$, then $\mathcal{C}_{s^1|s^2}^2 \geq 0$, $\mathcal{C}_{s^1|s^3}^2 \geq 0$, and $\mathcal{C}_{s^1|s^2s^3}^2 \geq 0$. The calculations are similar as for case 2. Similar result holds for p indistinguishable particles in \mathbb{S}^p locations with each particle having n DoFs where $(q + r)$ particles are in $|\mathcal{D}\rangle_{j_k}$ and rest of $(p - q - r)$ particles are in the superpositions of its eigenstate, i.e., $\kappa_{j_k} |\mathcal{D}\rangle_{j_k} + \kappa_{j_{k'}} e^{i\phi} |\mathcal{D}\rangle_{j_{k'}}$.

Case 7: Entanglement is calculated in the same DoF of all particles. If two particles are in the eigenstate $|\mathcal{D}\rangle_{j_k}$ and $|\mathcal{D}\rangle_{j_{k'}}$ and one particle is in superpositions of its eigenstate, i.e., $\kappa_{j_k} |\mathcal{D}\rangle_{j_k} + \kappa_{j_{k'}} e^{i\phi} |\mathcal{D}\rangle_{j_{k'}}$ where $\kappa_{j_k}^2 + \kappa_{j_{k'}}^2 = 1$ of the j th DoF, then $\mathcal{C}_{s^1|s^2}^2 \geq 0$, $\mathcal{C}_{s^1|s^3}^2 \geq 0$, and $\mathcal{C}_{s^1|s^2s^3}^2 \geq 0$. The calculations are similar as for case 2. Similar result holds for p indistinguishable particles in \mathbb{S}^p locations with each particle having n DoFs where q number of particles are in $|\mathcal{D}\rangle_{j_k}$, r number of particles are in $|\mathcal{D}\rangle_{j_{k'}}$ and rest of $(p - q - r)$ number of particles are in superpositions of its eigenstate, i.e., $\kappa_{j_k} |\mathcal{D}\rangle_{j_k} + \kappa_{j_{k'}} e^{i\phi} |\mathcal{D}\rangle_{j_{k'}}$ where $\kappa_{j_k}^2 + \kappa_{j_{k'}}^2 = 1$.

Case 8: Entanglement is calculated in the same DoF of all particles. Each particles are in the superpositions of its eigenstate, i.e., $\kappa_{j_k} |\mathcal{D}\rangle_{j_k} + \kappa_{j_{k'}} e^{i\phi} |\mathcal{D}\rangle_{j_{k'}}$ where $\kappa_{j_k}^2 + \kappa_{j_{k'}}^2 = 1$. Now calculations show that $\mathcal{C}_{s^1|s^2}^2 = 0$, $\mathcal{C}_{s^1|s^3}^2 = 0$, and $\mathcal{C}_{s^1|s^2s^3}^2 = 0$. This case is similar as case 1 if we take a rotated basis to redefine the eigenstates as $\{|\tilde{\mathcal{D}}\rangle_{j_k}, |\tilde{\mathcal{D}}\rangle_{j_k}^\perp\}$ where $|\tilde{\mathcal{D}}\rangle_{j_k} = \kappa_{j_k} |\mathcal{D}\rangle_{j_k} + \kappa_{j_{k'}} e^{i\phi} |\mathcal{D}\rangle_{j_{k'}}$.

Case 9: Entanglement is calculated in the same DoF of all particles. Each particles are in different superpositions of its eigenstate, i.e., three particles are in the eigenstates $\kappa_{j_k} |\mathcal{D}\rangle_{j_k} + \kappa_{j_{k'}} e^{i\phi_1} |\mathcal{D}\rangle_{j_{k'}}$, $\kappa'_{j_k} |\mathcal{D}\rangle_{j_k} + \kappa'_{j_{k'}} e^{i\phi_2} |\mathcal{D}\rangle_{j_{k'}}$, and $\kappa''_{j_k} |\mathcal{D}\rangle_{j_k} + \kappa''_{j_{k'}} e^{i\phi_3} |\mathcal{D}\rangle_{j_{k'}}$ of the j th DoF where $\kappa_{j_k}^2 + \kappa_{j_{k'}}^2 = 1$, $\kappa'_{j_k}{}^2 + \kappa'_{j_{k'}}{}^2 = 1$, $\kappa''_{j_k}{}^2 + \kappa''_{j_{k'}}{}^2 = 1$, $\phi_1 \neq \phi_2 \neq \phi_3$, $\kappa_{j_k} \neq \kappa'_{j_k} \neq \kappa''_{j_k}$, and $\kappa_{j_{k'}} \neq \kappa'_{j_{k'}} \neq \kappa''_{j_{k'}}$. Now calculations show that $\mathcal{C}_{s^1|s^2}^2 \geq 0$, $\mathcal{C}_{s^1|s^3}^2 \geq 0$, and $\mathcal{C}_{s^1|s^2s^3}^2 \geq 0$. The calculations are similar as for case 8. Similar result holds for p indistinguishable particles in \mathbb{S}^p locations with each particle having n DoFs where q number particles are in $\kappa_{j_k} |\mathcal{D}\rangle_{j_k} + \kappa_{j_{k'}} e^{i\phi_1} |\mathcal{D}\rangle_{j_{k'}}$ eigenstate, r number particles are in $\kappa'_{j_k} |\mathcal{D}\rangle_{j_k} + \kappa'_{j_{k'}} e^{i\phi_2} |\mathcal{D}\rangle_{j_{k'}}$ eigenstate and $(p - q - r)$ number of particles are in $\kappa''_{j_k} |\mathcal{D}\rangle_{j_k} + \kappa''_{j_{k'}} e^{i\phi_3} |\mathcal{D}\rangle_{j_{k'}}$ eigenstate.

Case 10: Here entanglement is calculated among two different DoFs where two particles are in $|\mathcal{D}\rangle_{j_k}$ eigenstate of the j th DoF and one particle is in $\kappa_{j'_l} |\mathcal{D}\rangle_{j'_l} + \kappa_{j'_l'} e^{i\phi} |\mathcal{D}\rangle_{j'_l'}$ eigenstate in the j' th DoF. Here $j, j' \in \mathbb{N}_n$ and $\kappa_{j'_l}^2 + \kappa_{j'_l'}^2 = 1$. Now calculations show $\mathcal{C}_{s^1|s^2}^2 = 0$, $\mathcal{C}_{s^1|s^3}^2 = 0$, and $\mathcal{C}_{s^1|s^2s^3}^2 = 0$. This calculations is easier if we take a rotated basis as shown in case 8. Similar result holds for p indistinguishable particles in \mathbb{S}^p locations with each particle having n DoFs where $(q + r)$ number of particles are in $|\mathcal{D}\rangle_{j_k}$ eigenstate of the j th DoF and rest of $(p - q - r)$ number of particles are in $\kappa_{j'_l} |\mathcal{D}\rangle_{j'_l} + \kappa_{j'_l'} e^{i\phi} |\mathcal{D}\rangle_{j'_l'}$ eigenstate in the j' th DoF.

Case 11: Here entanglement is calculated among two different DoFs where two particles are in $|\mathcal{D}\rangle_{j_k}$ and $|\mathcal{D}\rangle_{j_{k'}}$ eigenstate of the j th DoF and one particle is in $\kappa_{j'_l} |\mathcal{D}\rangle_{j'_l} + \kappa_{j'_l'} e^{i\phi} |\mathcal{D}\rangle_{j'_l'}$ eigenstate in the j' th DoF. Here $j, j' \in \mathbb{N}_n$ and $\kappa_{j'_l}^2 + \kappa_{j'_l'}^2 = 1$. Now calculations show that $\mathcal{C}_{s^1|s^2}^2 \geq 0$, $\mathcal{C}_{s^1|s^3}^2 = 0$, and $\mathcal{C}_{s^1|s^2s^3}^2 \geq 0$. If we consider a rotated basis in j' DoF as $\{|\tilde{\mathcal{D}}\rangle_{j'_l}, |\tilde{\mathcal{D}}\rangle_{j'_l}^\perp\}$ where $|\tilde{\mathcal{D}}\rangle_{j'_l} = \kappa_{j'_l} |\mathcal{D}\rangle_{j'_l} + \kappa_{j'_l'} e^{i\phi} |\mathcal{D}\rangle_{j'_l'}$, then the calculations is similar as case 3. Similar result holds for p indistinguishable particles in \mathbb{S}^p locations with each particle having n DoFs where q and r number of particles

are in $|\mathcal{D}\rangle_{j_k}$ and $|\mathcal{D}\rangle_{j_{k'}}$ eigenstate respectively of the j th DoF and rest of $(p-q-r)$ number of particles are in $\kappa_{j'_l}|\mathcal{D}\rangle_{j'_l} + \kappa_{j'_l'}e^{i\phi}|\mathcal{D}\rangle_{j'_l'}$ eigenstate in j' th DoF.

Case 12: Here entanglement is calculated among two different DoFs two particles are in the $|\mathcal{D}\rangle_{j_k}$ eigenstate and $\kappa_{j_k}|\mathcal{D}\rangle_{j_k} + \kappa_{j_{k'}}e^{i\phi}|\mathcal{D}\rangle_{j_{k'}}$ eigenstate in the j th DoF, one particle is in the superposition, i.e., $\kappa_{j'_l}|\mathcal{D}_{j'_l}\rangle + \kappa_{j'_l'}e^{i\phi}|\mathcal{D}\rangle_{j'_l'}$ eigenstate in the j' th DoF. Now calculations show $\mathcal{C}_{s^1|s^2}^2 \geq 0$, $\mathcal{C}_{s^1|s^3}^2 = 0$, and $\mathcal{C}_{s^1|s^2s^3}^2 \geq 0$. Using appropriate rotated basis of the j th and j' th DoF, the calculations is similar as previous case. Similar result holds for p indistinguishable particles in \mathbb{S}^p locations with each particle having n DoFs where q number of particles are in $|\mathcal{D}\rangle_{j_k}$ eigenstate of the j th DoF, r number of particles are in the superposition, i.e., $\kappa_{j_k}|\mathcal{D}\rangle_{j_k} + \kappa_{j_{k'}}e^{i\phi}|\mathcal{D}\rangle_{j_{k'}}$ eigenstate in the j th DoF, and rest of $(p-q-r)$ number of particles are in the superposition, i.e., $\kappa_{j'_l}|\mathcal{D}_{j'_l}\rangle + \kappa_{j'_l'}e^{i\phi}|\mathcal{D}\rangle_{j'_l'}$ eigenstate in the j' th DoF.

Case 13: Entanglement is calculated between three different DoFs. Here, three particles are in the superpositions of its eigenstate, i.e., $\kappa_{j_k}|\mathcal{D}\rangle_{j_k} + \kappa_{j_{k'}}e^{i\phi}|\mathcal{D}\rangle_{j_{k'}}$ where $\kappa_{j_k}^2 + \kappa_{j_{k'}}^2 = 1$ of the j th DoF; $\kappa_{j''_h}|\mathcal{D}\rangle_{j''_h} + \kappa_{j''_h'}e^{i\phi''}|\mathcal{D}\rangle_{j''_h'}$ where $\kappa_{j''_h}^2 + \kappa_{j''_h'}^2 = 1$ of the j'' th DoF; and $\kappa_{j'_l}|\mathcal{D}\rangle_{j'_l} + \kappa_{j'_l'}e^{i\phi'}|\mathcal{D}\rangle_{j'_l'}$ where $\kappa_{j'_l}^2 + \kappa_{j'_l'}^2 = 1$ of the j' th DoF where $j \neq j' \neq j''$. Using appropriate rotated basis of the j th, j' th, and j'' th DoF, the calculations is similar as shown in case 5. Now calculations show $\mathcal{C}_{s^1|s^2}^2 = 0$, $\mathcal{C}_{s^1|s^3}^2 = 0$, and $\mathcal{C}_{s^1|s^2s^3}^2 = 0$. Similar result holds for p indistinguishable particles in \mathbb{S}^p locations with each particle having n DoFs where q number of particles are in superpositions of its eigenstate, i.e., $\kappa_{j_k}|\mathcal{D}\rangle_{j_k} + \kappa_{j_{k'}}e^{i\phi}|\mathcal{D}\rangle_{j_{k'}}$ of the j th DoF, Here, r number of particles are in superpositions of its eigenstate, i.e., $\kappa_{j''_h}|\mathcal{D}\rangle_{j''_h} + \kappa_{j''_h'}e^{i\phi''}|\mathcal{D}\rangle_{j''_h'}$ of j'' th DoF and rest of $(p-q-r)$ number of particles are in superpositions of its eigenstate, i.e., $\kappa_{j'_l}|\mathcal{D}\rangle_{j'_l} + \kappa_{j'_l'}e^{i\phi'}|\mathcal{D}\rangle_{j'_l'}$ of j' th DoF.

One may think that there might be more cases. Upon careful inspection, it can be concluded that all those cases is equivalent with any of the above mentioned cases.

From all the above cases we can see that the monogamy holds for pure states with an equality relation. On the other hand, for mixed states, we use the convexity of the concurrence function to prove the monogamy relation. Since any mixed state can be expressed as an ensemble of the pure states, we can apply the concurrence function

on those ensembles, i.e., the convex combinations for pure states and minimize it to get the required inequality for any arbitrary mixed states as shown in next section.

8.2.3 Monogamy of indistinguishable particles for mixed states

In this section, we generalize the relation for monogamy of entanglement of indistinguishable particles for mixed states. We have proved in Corollary 1.1 the the main text that for all pure states $\rho_{\alpha_i\beta_j\gamma_k}$

$$\mathcal{C}_{\alpha_i|\beta_j}^2(\rho_{\alpha_i\beta_j}) + \mathcal{C}_{\alpha_i|\gamma_k}^2(\rho_{\alpha_i\gamma_k}) = \mathcal{C}_{\alpha_i|\beta_j\gamma_k}^2(\rho_{\alpha_i\beta_j\gamma_k}). \quad (8.34)$$

But this relation is not valid for mixed states as the right hand side is not defined for mixed states. Since all mixed states are convex combination some pure states, we can write $\rho_{\alpha_i\beta_j\gamma_k}$ as a convex combination of pure states, as

$$\rho_{\alpha_i\beta_j\gamma_k} = \sum_m \text{Pr}_m |\psi_m\rangle_{\alpha_i\beta_j\gamma_k} \langle\psi_m|_{\alpha_i\beta_j\gamma_k}, \quad (8.35)$$

where Pr_m denotes the probability of $|\psi_m\rangle_{\alpha_i\beta_j\gamma_k}$. For each m , we can write from Eq. (8.34) as

$$\begin{aligned} & \mathcal{C}_{\alpha_i|\beta_j}^2(|\psi_m\rangle_{\alpha_i\beta_j} \langle\psi_m|_{\alpha_i\beta_j}) + \mathcal{C}_{\alpha_i|\gamma_k}^2(|\psi_m\rangle_{\alpha_i\gamma_k} \langle\psi_m|_{\alpha_i\gamma_k}) \\ &= \mathcal{C}_{\alpha_i|\beta_j\gamma_k}^2(|\psi_m\rangle_{\alpha_i\beta_j\gamma_k} \langle\psi_m|_{\alpha_i\beta_j\gamma_k}). \end{aligned} \quad (8.36)$$

Multiplying both sides with Pr_m , we get

$$\begin{aligned} & \text{Pr}_m \mathcal{C}_{\alpha_i|\beta_j}^2(|\psi_m\rangle_{\alpha_i\beta_j} \langle\psi_m|_{\alpha_i\beta_j}) + \text{Pr}_m \mathcal{C}_{\alpha_i|\gamma_k}^2(|\psi_m\rangle_{\alpha_i\gamma_k} \langle\psi_m|_{\alpha_i\gamma_k}) \\ &= \text{Pr}_m \mathcal{C}_{\alpha_i|\beta_j\gamma_k}^2(|\psi_m\rangle_{\alpha_i\beta_j\gamma_k} \langle\psi_m|_{\alpha_i\beta_j\gamma_k}). \end{aligned} \quad (8.37)$$

Summing up for all the pure constituents,

$$\begin{aligned} & \sum_m \text{Pr}_m \mathcal{C}_{\alpha_i|\beta_j}^2(|\psi_m\rangle_{\alpha_i\beta_j} \langle\psi_m|_{\alpha_i\beta_j}) + \sum_m \text{Pr}_m \mathcal{C}_{\alpha_i|\gamma_k}^2(|\psi_m\rangle_{\alpha_i\gamma_k} \langle\psi_m|_{\alpha_i\gamma_k}) \\ &= \sum_m \text{Pr}_m \mathcal{C}_{\alpha_i|\beta_j\gamma_k}^2(|\psi_m\rangle_{\alpha_i\beta_j\gamma_k} \langle\psi_m|_{\alpha_i\beta_j\gamma_k}). \end{aligned} \quad (8.38)$$

Now consider the decomposition, say $\left\{ \left(\Pr_m^*, |\psi_m\rangle_{\alpha_i \beta_j \gamma_k}^* \right) \right\}$, that minimizes the right hand side of Eq. (8.38) and denote it by

$$\left(\mathcal{C}_{\alpha_i | \beta_j \gamma_k}^2 \right)^{\min} := \min_{\left\{ \left(\Pr_m, |\psi_m\rangle_{\alpha_i \beta_j \gamma_k} \right) \right\}} \sum_m \Pr_m \mathcal{C}_{\alpha_i | \beta_j \gamma_k}^2 \left(|\psi_m\rangle_{\alpha_i \beta_j \gamma_k} \langle \psi_m |_{\alpha_i \beta_j \gamma_k} \right). \quad (8.39)$$

Now expressing $\rho_{\alpha_i \beta_j \gamma_k}$ by the above minimizing decomposition as in Eq. (8.39), we have

$$\begin{aligned} & \mathcal{C}_{\alpha_i | \beta_j}^2 \left(\rho_{\alpha_i \beta_j} \right) + \mathcal{C}_{\alpha_i | \gamma_k}^2 \left(\rho_{\alpha_i \gamma_k} \right) \\ = & \mathcal{C}_{\alpha_i | \beta_j}^2 \left(\sum_m \Pr_m^* |\psi_m\rangle_{\alpha_i \beta_j}^* \langle \psi_m |_{\alpha_i \beta_j}^* \right) + \mathcal{C}_{\alpha_i | \gamma_k}^2 \left(\sum_m \Pr_m^* |\psi_m\rangle_{\alpha_i \gamma_k}^* \langle \psi_m |_{\alpha_i \gamma_k}^* \right) \\ \leq & \sum_m \Pr_m^* \mathcal{C}_{\alpha_i | \beta_j}^2 \left(|\psi_m\rangle_{\alpha_i \beta_j}^* \langle \psi_m |_{\alpha_i \beta_j}^* \right) + \sum_m \Pr_m^* \mathcal{C}_{\alpha_i | \gamma_k}^2 \left(|\psi_m\rangle_{\alpha_i \gamma_k}^* \langle \psi_m |_{\alpha_i \gamma_k}^* \right) \\ & \hspace{15em} \text{(by the convexity of } \mathcal{C}^2 \text{ [209])} \quad (8.40) \\ = & \sum_m \Pr_m^* \left\{ \mathcal{C}_{\alpha_i | \beta_j}^2 \left(|\psi_m\rangle_{\alpha_i \beta_j}^* \langle \psi_m |_{\alpha_i \beta_j}^* \right) + \mathcal{C}_{\alpha_i | \gamma_k}^2 \left(|\psi_m\rangle_{\alpha_i \gamma_k}^* \langle \psi_m |_{\alpha_i \gamma_k}^* \right) \right\} \\ = & \sum_m \Pr_m^* \mathcal{C}_{\alpha_i | \beta_j \gamma_k}^2 \left(|\psi_m\rangle_{\alpha_i \beta_j \gamma_k}^* \langle \psi_m |_{\alpha_i \beta_j \gamma_k}^* \right) \quad \text{(from Eq. (8.36))} \\ = & \left(\mathcal{C}_{\alpha_i | \beta_j \gamma_k}^2 \right)^{\min} \quad \text{(from Eq. (8.39)).} \end{aligned}$$

Thus we have for mixed states

$$\mathcal{C}_{\alpha_i | \beta_j}^2 \left(\rho_{\alpha_i \beta_j} \right) + \mathcal{C}_{\alpha_i | \gamma_k}^2 \left(\rho_{\alpha_i \gamma_k} \right) \leq \mathcal{C}_{\alpha_i | \beta_j \gamma_k}^2 \left(\rho_{\alpha_i \beta_j \gamma_k} \right). \quad (8.41)$$

8.3 Physical significance of monogamy of entanglement for indistinguishable particles having multiple DoFs

Existence of indistinguishable particles is a special feature of quantum mechanics. There has been substantial interest in the community to use indistinguishable particles as a resource [280] for many quantum information processing tasks such as teleportation [247, 163], entanglement swapping [176] etc., that are commonly imple-

mented using distinguishable particles. Recently a class of results have been published which explicitly demonstrate that certain properties and applications are exclusive to indistinguishable (or distinguishable) particles. We call such results as the separation results between these two domains. Das *et al.* [244] showed that unit fidelity quantum teleportation can only be performed using distinguishable particles, and on the other hand, hyper-hybrid entangled state can only be produced using indistinguishable particles. Further, if a quantum protocol can be performed using both distinguishable and indistinguishable particles, one of them may give some advantages over the other. For example entanglement swapping can be performed using minimum two indistinguishable particles [244], whereas atleast three particles are required for the distinguishable case [53, 54]. Another separation result between these two domains is given by Paul *et al.* [258]. They show that using two indistinguishable particles each having multiple degrees of freedom, it is possible to violate monogamy of entanglement maximally, which is not feasible for distinguishable particles [262].

In continuation of these separation results, this chapter contributes one property of indistinguishable particles that are different from distinguishable particles. The inequality of monogamy of entanglement using squared concurrence for three or more distinguishable particles as shown in [66] becomes equality for pure indistinguishable states, whereas the inequality may hold only for mixed indistinguishable states. The physical significance of this result is that for all pure states, if MoE is calculated for three or more indistinguishable particle, then the residual entanglement in the whole state is zero, i.e., entanglement is distributed among all its bipartitions. Note that, this equality is different from the one proposed in [281]. This result is extremely helpful to calculate the entanglement in the scenarios where particles are indistinguishable like quantum dots [168, 170], ultracold atomic gases [215], Bose-Einstein condensates [213, 214], quantum meteorology [282, 283], etc.

Chapter 9

Applications of entangled distinguishable and indistinguishable particles

In this section, we discuss some applications of distinguishable and indistinguishable particles. First we show an application using extra degrees of freedom as an ancilla qubit to reduce the resource in some cryptographic protocols based on our work in [264]. Next, we show how using indistinguishability can create an attack in some cryptographic protocols based on our work in [259]. Finally, we show an entanglement swapping protocol using only two indistinguishable particles and without using Bell state measurement based on our work in [244].

This chapter is based on the works in [244, 264, 259].

9.1 Reducing the resource requirement in cryptographic protocols

Security and efficiency are two major criteria of a cryptographic protocols. If two cryptographic systems with different resource requirements provide the same level of security, the one with less resources becomes the natural choice. Here, we present a

generic scheme to reduce the number of particles used in device-independent [284] (DI) quantum private query [226, 227] (QPQ) without affecting the security that can be used for both distinguishable and indistinguishable particles.

In quantum cryptography, DI tests [284] are required to establish secure key between two parties when the devices are not trustworthy. In QPQ, a user queries a database about some specific entry and gets back only the corresponding data without revealing the query to the server. To achieve this, a secure key must be established between the database owner and the user such that the database owner knows the full key but the user knows a fraction of that key. In DI-QPQ [227] using Clauser-Horne-Shimony-Holt test [29], the maximum success probability is $\cos^2 \frac{\pi}{8} \approx 85\%$ using two qubits. With an ancilla particle, this success probability can be increased asymptotically to unity using quantum pseudo-telepathy game [178, 179].

The cost of adding an ancilla particle can be bypassed by using an additional DoF and creating multi-DoF entanglement. In doing so, the success probability remains the same but the generalized SF changes.

In Section 2.10.3, it is shown that the success probability of a quantum private query protocol as described in 2.10.1 can be increased asymptotically to unity using an ancilla particle X as an extra qubit. Now instead of choosing the ancilla as another particle, if another DoF of A is used as the ancilla, then we can reduce the number of particles used in the quantum pseudo-telepathy test. Then the state in Eq. (2.46) can be written as

$$|\psi\rangle_{BA_1A_2} = \frac{1}{\sqrt{2}} \left(\cos \frac{\theta}{2} |000\rangle_{BA_1A_2} + \sin \frac{\theta}{2} |010\rangle_{BA_1A_2} + \cos \frac{\theta}{2} |111\rangle_{BA_1A_2} - \sin \frac{\theta}{2} |100\rangle_{BA_1A_2} \right). \quad (9.1)$$

Assuming each particle have two DoFs, i.e., $n=2$, the generalized singlet fraction for the state in Eq. (2.46) is

$$F_g^{(2)} = \max \left\{ \max_i \left\{ \max_{\psi_{a_i b_j}} \left\{ \sum_{j=1}^2 \langle \psi_{a_i b_j} | \rho_{a_i b_j} | \psi_{a_i b_j} \rangle \right\} \right\}, \max_j \left\{ \max_{\psi_{a_i b_j}} \left\{ \sum_{i=1}^2 \langle \psi_{a_i b_j} | \rho_{a_i b_j} | \psi_{a_i b_j} \rangle \right\} \right\} \right\} \\ = \frac{1}{2} + \cos^2 \frac{\theta}{2} \quad (9.2)$$

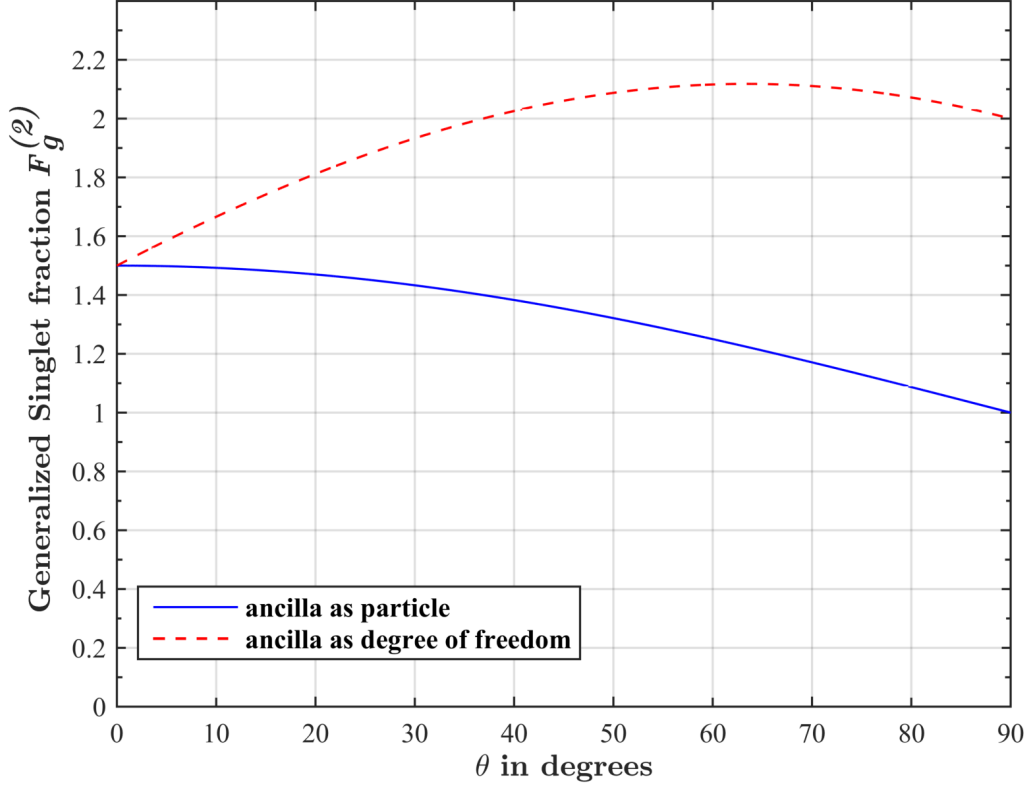


Figure 9-1: The variation of generalized SF $F_g^{(n)}$ for the quantum pseudo-telepathy test using ancilla as particle and using ancilla as degrees of freedom with varying θ in degrees.

where $\rho_{a_i b_j} := \text{Tr}_{a_i b_j}(\rho_{AB}^{(2)})$ and $\rho_{AB}^{(2)} = \text{Tr}_X(|\psi\rangle_{BAX}\langle\psi|_{BAX})$.

Similarly if we calculate the generalized singlet fraction for the state in Eq. (9.1), we get $\frac{1}{2} + \cos^2 \frac{\theta}{2} + 2 \cos \frac{\theta}{2} \sin \frac{\theta}{2}$. The values of generalized singlet fraction for the states in Eq. (2.46) and Eq. (9.1) are shown in Fig. 9-1

Thus in many ancilla assisted quantum processing protocols like quantum process tomography [285], entanglement stabilization [286], quantum secret sharing [287], quantum error correction [288], quantum measurement [289], weak value amplification [290], quantum channel discrimination [291], coherent-state superposition generation [292], etc., where the resource can be reduced by using additional DoF as ancilla instead of a particle.

9.2 Attacks on the security of cryptographic protocols.

There are scenarios where particles are indistinguishable like quantum dots [168, 170], ultracold atomic gases [215], Bose-Einstein condensates [213, 214], our method will be extremely helpful to calculate the entanglement and monogamy in those situations. Indistinguishability can be created manually by particle exchange [216, 217], using which we present a generic one-step indistinguishability module as a plug-in to many protocols. This may have an effect in modifying their output.

Suppose A is sending a pair of particles to B and C whose joint state is $|\psi\rangle_{BC}$. After B and C perform some local operations U_B and U_C respectively, the joint state becomes $|\phi\rangle_{BC}$ as shown in Fig. 9-2 (a).

If the particles sent by A become indistinguishable so that the particle intended solely for B now goes to B and C with probability α and $(1 - \alpha)$ respectively. Similarly, the particle intended solely for C now goes to C and B with probability β and $(1 - \beta)$ respectively. So the output becomes $|\phi'\rangle_{BC}$ as shown in Fig. 9-2 (b). If $U_B = U_C$ and the state $|\psi\rangle_{BC}$ is symmetric with respect to B and C , then $|\phi'\rangle_{BC} = |\phi\rangle_{BC}$. However, if $U_B \neq U_C$, or the state $|\psi\rangle_{BC}$ is asymmetric with respect to B and C , or both, then due to indistinguishability the output can be changed, i.e., $|\phi'\rangle_{BC} \neq |\phi\rangle_{BC}$.

For example, the output of Hardy's test as shown in Section 2.2.2 which is used in quantum byzantine agreement [40], random number generation [38], quantum key distribution [293] etc., can be different due to indistinguishability as follows. Assume Alice and Bob share an entangled state as [230]

$$|\psi\rangle_{AB} = \frac{\cos\theta}{\sqrt{2}}(|00\rangle + |10\rangle) + \frac{\sin\theta}{\sqrt{2}}(|01\rangle + e^{i2\phi}|11\rangle), \quad (9.3)$$

where $0 < \theta, \phi < 90^\circ$. The Hardy's probability for this state for the measurements stated in [230] is

$$q = \left| \frac{1}{2} \cos\theta \cos\chi \left(1 - e^{-2i\phi}\right) \right|^2 \quad (9.4)$$

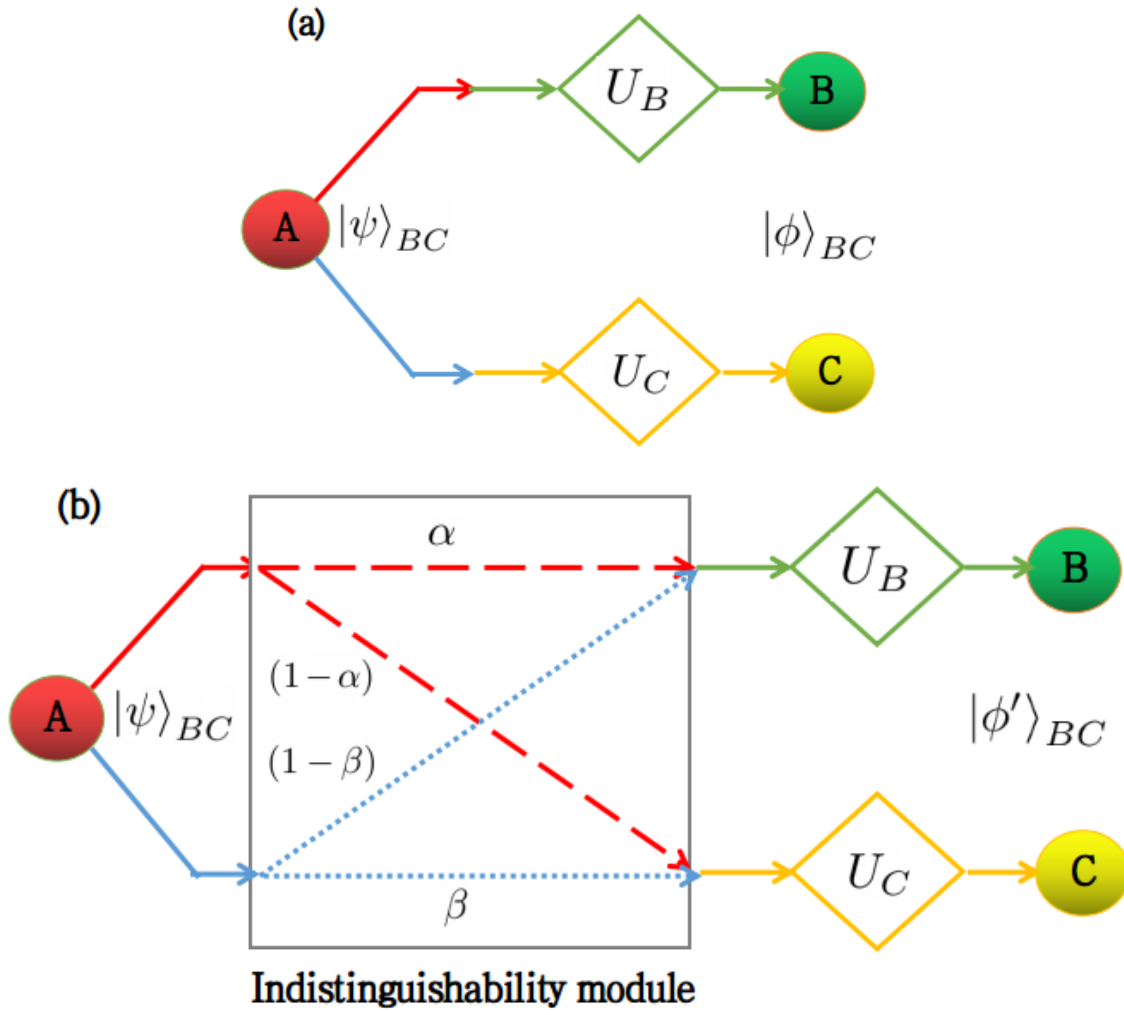
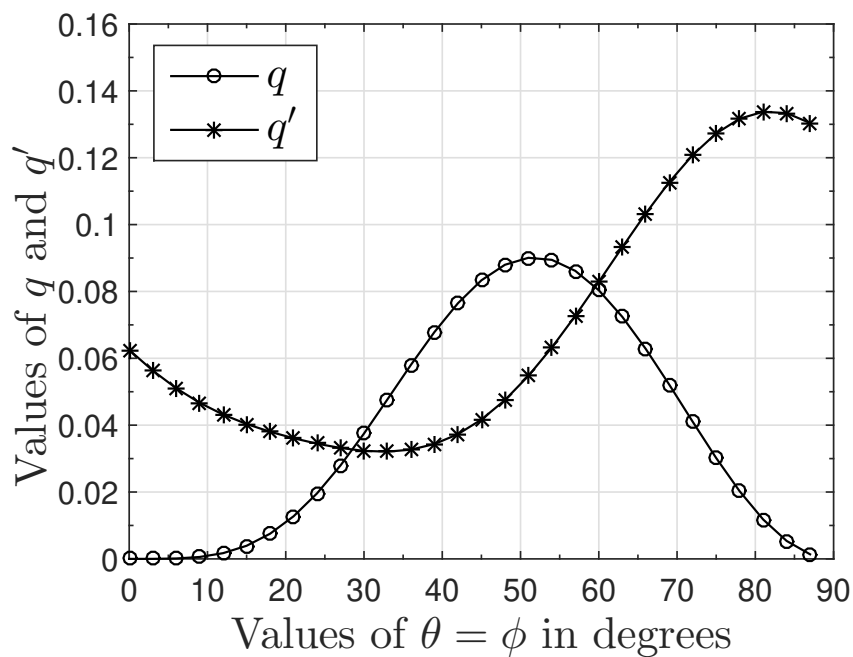


Figure 9-2: A general protocol with A as the sender and B and C are the receivers. $|\psi\rangle_{BC}$ is the initial state at A that has to be shared between B and C . Here U_B and U_C are the unitary operations performed by B and C on their respective particles. (a) The final state after the unitary operations performed by B and C is $|\phi\rangle_{BC}$. (b) If an indistinguishability module is present on the path from A to B and C , then the final state is $|\phi'\rangle_{BC}$.

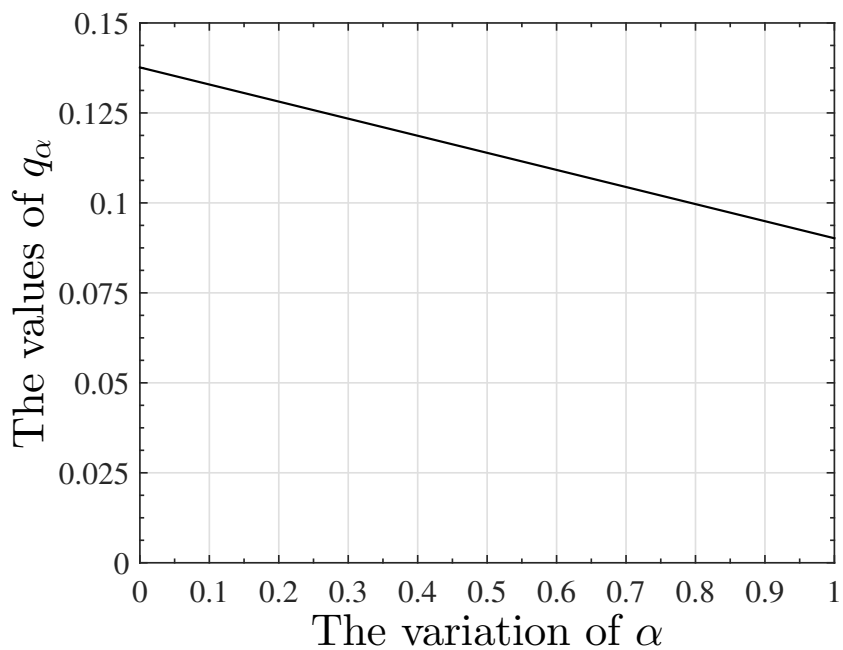
where

$$\cot \chi = \tan \theta \cos \phi \quad (9.5)$$

The maximum value of Hardy's probability, i.e., $q_{\max} \approx 0.09017$ occurs when $\theta = \phi = 51.827^\circ$. If the particle intended for Alice goes to Bob and vice-versa, the modified



(a)



(b)

Figure 9-3: Effects of indistinguishability on Hardy's probability with $\theta = \phi$ in degrees. (a) The variation of Hardy's probability q and modified Hardy's probability due to indistinguishability q' where $\alpha = \beta = \frac{1}{2}$. (b) The variation of modified Hardy's probability q_α with α where $\alpha = \beta$ and $\theta = \phi = 51.827^\circ$.

probability becomes

$$q' = \left| \frac{1}{2} \cos \chi \left(\cos \theta - \sin \theta e^{2i\phi} \right) - \sin \chi e^{-i\phi} (\cos \theta - \sin \theta) \right|^2. \quad (9.6)$$

If $\alpha = \beta$ (as in Fig. 9-2), then the final Hardy's probability due to indistinguishability is

$$q_\alpha = \alpha^2 q + (1 - \alpha)^2 q' \quad (9.7)$$

In Fig. 9-3 (a), we compare the values q and q' . The horizontal axis represents the value of θ where $0 \leq \theta (= \phi) \leq 90^\circ$. We see that the Hardy's probability q' increases significantly in the presence of the indistinguishability module. In Fig. 9-3 (b), we plot the variation of q_{\max} for $\theta = \phi = 51.827^\circ$ with the value of α vs. q_α which shows that the values of q_α decreases with increasing α . Similar result holds if Hardy's paradox is performed between more than two parties.

9.3 Entanglement Swapping using only two indistinguishable particles

The seminal work [44] on Entanglement Swapping (ES) required four distinguishable particles as a resource along with Bell state measurement (BSM) and local operations and classical communications (LOCC) as tools. Better versions with only three distinguishable particles were proposed in two subsequent works, one [53] with BSM and another [54] without BSM. Recently, Castellini *et al.* [176] have shown that ES for the indistinguishable case is also possible with four particles (with BSM for bosons and without BSM for fermions). This has been experimentally realized in [223]. Thus, in terms of resource requirement, the existing best distinguishable versions outperform the indistinguishable one. We turn around this view, by proposing an ES protocol without BSM using only two indistinguishable particles.

Here we present an ES protocol using two indistinguishable particles, say, A and B , without BSM by suitably modifying the circuit of Li *et al.* [1] as described in

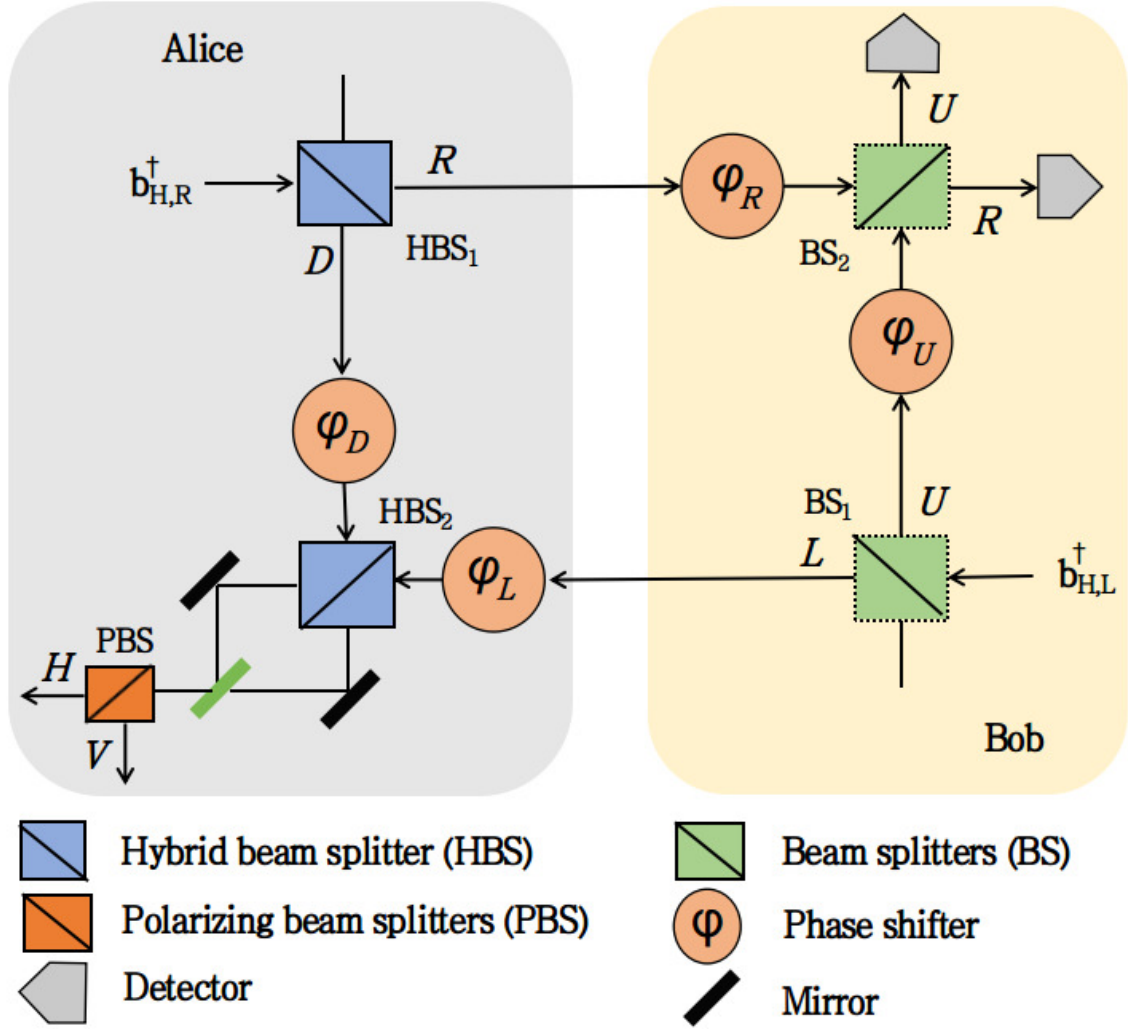


Figure 9-4: Entanglement swapping with only two indistinguishable particles without Bell state measurements.

Section 2.7.2. The basic idea is to use any method that destroys the identity of the individual particles, like particle exchange [216, 217] or measurement induced entanglement [294]. Such methods added with suitable unitary operations transfer the intraparticle hybrid entanglement in A (or B) to inter-particle hybrid-entanglement between A and B .

Next, we present an optical realization using particle exchange method. Suppose Alice and Bob have two horizontally polarized photons A and B , entering into the two modes R and L of a HBS [1] and a BS, respectively. In second quantization notation, the initial joint state is given by $|\Psi_i\rangle = b_{H,R}^\dagger b_{H,L}^\dagger |0\rangle$, where $|H\rangle$ and $|V\rangle$ denote hori-

zontal and vertical polarization, respectively, and $b_{H,R}$ and $b_{H,L}$ are the corresponding bosonic creation operators satisfying the canonical commutation relations:

$$[b_{i,\mathbf{p}_i}, b_{j,\mathbf{p}_j}] = 0, [b_{i,\mathbf{p}_i}, b_{j,\mathbf{p}_j}^\dagger] = \delta(\mathbf{p}_i - \mathbf{p}_j)\delta_{ij}. \quad (9.8)$$

After passing through HBS₁, Alice's photon is converted into intraparticle hybrid-entangled state $\frac{1}{\sqrt{2}}(b_{H,R}^\dagger + ib_{V,D}^\dagger)$. The particle exchange operation is performed between Alice and Bob, such that the photons coming from D (U) and L (R) mode go into Alice's (Bob's) side. Next, Alice applies path dependent (or polarization dependent) phase shifts φ_D and φ_L on the photons coming from her and Bob's parts, respectively, which go into HBS₂. Similarly, Bob applies path-dependent phase shifts φ_U and φ_R on the photons coming from his and Alice's parts, respectively, which go into BS₂ as shown in Fig. 9-4. The final state is given by

$$\begin{aligned} |\Psi_f\rangle &= \frac{1}{4} \left[e^{i\varphi_R} (b_{H,R}^\dagger + ib_{H,U}^\dagger) + ie^{i\varphi_D} (b_{V,D}^\dagger + ib_{H,L}^\dagger) \right] \\ &\otimes \left[e^{i\varphi_L} (b_{H,L}^\dagger + ib_{V,D}^\dagger) + ie^{i\varphi_U} (b_{H,U}^\dagger + ib_{H,R}^\dagger) \right] |0\rangle. \end{aligned} \quad (9.9)$$

If Alice measures in the polarization DOF and Bob measures in the path DOF, from Eq. (9.9) the probabilities that both of them detect one particle are given by

	B : R	B : U	
A : H	$\frac{1}{4}\cos^2\varphi$	$\frac{1}{4}\sin^2\varphi$,
A : V	$\frac{1}{4}\sin^2\varphi$	$\frac{1}{4}\cos^2\varphi$	

(9.10)

where $\varphi = (\varphi_D - \varphi_L - \varphi_R + \varphi_U)/2$. With suitable values of the phase shifts, one can get the Bell violation in the CHSH [29] test up to Tsirelson's bound [246]. It can be easily verified that after particle exchange, the particle received at Alice's side (or Bob's side) has no hybrid entanglement, because it is transferred between them.

Note that the difference between the circuit of Li *et al.* [1, Fig. 2] and Fig. 9-4 is that both the HBSs in Bob's side in the former circuit are replaced by BSs in the latter. Thus, the intra particle hybrid entanglement of one particle is transferred into

the inter-particle hybrid-entanglement of two particles.

Chapter 10

Conclusion

In this chapter, we discuss the summary, open problems, and future work of each of the previous contributory chapters.

As quantum non-locality is the subset and the strongest form of quantum entanglement, we have performed an experimental verification of Hardy's paradox of non-locality for the first time in superconducting circuits in Chapter 3. Our initial motivation was to check it for two qubits in the *ibmqx4* five-qubit chip, by choosing any two from the five qubits. When $\Sigma_4 < q \leq q_{max}$, the estimated lower bound \hat{q}_{lb} on Hardy's probability is found to be greater than zero, supporting non-locality. But when $q \leq \Sigma_4$, we get $\hat{q}_{lb} \leq 0$, because then the errors become of the same order as q . Interestingly, though $\bar{\epsilon}_5^{max}$ decreases with q , experimental results show that $\bar{\epsilon}_5^{max}$ does not occur at $q = q_{max}$, rather we get a shift of $\bar{\epsilon}_5^{max}$ to the right for the (Q_3, Q_4) pair of qubits. We also show that the shift direction is not constant, whether it is to the right or left depends on the pair of qubits. Moreover, we have shown that the above type of shift can occur during the practical implementation of any Hardy's paradox based quantum protocols like quantum Byzantine agreement and we have also discussed possible remedies. Based on the results of our experiments, we have proposed two performance measures of any quantum computer for two qubits. First, the minimum value of q above which non-locality is established. Second, the amount of shift needed to get the experimental maximum value of $\bar{\epsilon}_5^{max}$ of Hardy's probability. Further, we have performed experiments to show how decreasing the number of gates in the cir-

circuits decreases the errors in the circuit for all possible pairs of qubits. We have also studied the change of errors in IBM quantum computer over time and concluded that errors are decreasing over time. From the theoretical analysis of the Hardy's experimental set-up, we have found that this test fails for all non-maximally entangled states, where the value of $\phi=90$ and $\theta \neq \{0, 45, 90\}$ degrees. The possibility of a new test for Hardy's paradox for two qubits, so that it does not fail for any non-maximally entangled states is an open problem. Also, the verification of Hardy's test for more than two qubits will be also an interesting work. Further, the comparison between different quantum computers using Hardy's test will be a good research work. We, plan to execute this survey in near future.

Next, in Chapter 4 we settle several important open questions that arise due to the recent work on hyper-hybrid entanglement for two indistinguishable bosons by Li *et al.* [1]. In particular, we have shown that such entanglement can also exist for two indistinguishable fermions. Further, we have argued that, if in their circuit the particles are made distinguishable, such type of entanglement vanishes. We have also proved the following two no-go results (A) no hyper-hybrid entangled state for distinguishable particles and (B) no unit fidelity quantum teleportation for indistinguishable particles, as in either case the no-signaling principle is violated. Our results establish that there exists some quantum correlation or application unique to indistinguishable particles only and yet some unique to distinguishable particles only, giving a separation between the two domains. The present results can motivate researchers to find more quantum correlations and applications that are either unique to distinguishable or indistinguishable particles or applicable to both. For the latter case, a comparative analysis of the resource requirements and the efficiency or fidelity can also be a potential future work. We plan to find new quantum applications unique for either distinguishable or indistinguishable particles.

Hereafter, we focus to the most important tool to analysis entangled systems, i.e., the partial trace-out operation in Chapter 5. The normal trace-out rule for distinguishable particles was not useful for indistinguishable particles. So, Lo Franco *et al.* [161, 163] have proposed a trace-out rule that is applicable only when each particles

has a single degree of freedom. Thus, we have proposed a trace-out rule applicable for both distinguishable and indistinguishable particles where each particle have single or multiple degree of freedom. How the new trace-out rule can be applicable to different quantum applications using multiple DoFs is an open area of research. Also, some more tools for indistinguishable particles need to be develop in future to complete the theory of indistinguishability. In future, we will try to develop new applications of this trace-out rule.

In Chapter 6, we found that the relation between teleportation fidelity and singlet fraction is only applicable to distinguishable particles having single degree of freedom. So we established generalized expressions for teleportation fidelity and singlet fraction and derive their relations, applicable for both distinguishable and indistinguishable particles with single or multiple degrees of freedom. We further derive an upper bound for the generalized singlet fraction for distinguishable particles and indistinguishable particles. Our new relation finds application in characterizing different types of composite states in terms of their distinguishability, separability, presence of maximally entangled structure and the number of degrees of freedom. Also we have proposed an optical circuit to illustrate the non-triviality of our relation. In future, how this relation will be applicable to different quantum information processing protocols will be an interesting research work. Also, one can find new relations for distinguishable particles having single DoF and try to generalized it for both distinguishable and indistinguishable particles having single or multiple DoFs will also be potential future works. We will try to find new applications of the generalized teleportation fidelity and generalized singlet fraction for cryptographic applications.

Monogamy of entanglement, in essence, is a no-go theorem that is a restriction on the shareability of entanglement. We have established the following counter-intuitive result in Chapter 7: monogamy of entanglement can be violated maximally for indistinguishable particles by any bipartite entanglement measure that is known to be monogamous for distinguishable particles. Our result lifts this restriction for indistinguishable particles. It also opens up a new area where researchers can investigate whether the applications of monogamy of entanglement using distinguishable particles

are also applicable using indistinguishable ones and their advantages and disadvantages. Also, what happens to the monogamy relation for indistinguishable particles for more than two-qubits is also an open problem. We try to solve the monogamy relation for more than three qubits for indistinguishable particles having single or multiple DoFs.

Recently, a class of results have been published which explicitly demonstrate that certain properties and applications are exclusive to indistinguishable (or distinguishable) particles. In continuation of these separation results, the Chapter 8 contributes one property of indistinguishable particles that are different from distinguishable particles. The inequality of monogamy of entanglement using squared concurrence for three or more distinguishable particles as shown in [66] becomes equality for pure indistinguishable states, whereas the inequality may hold only for mixed indistinguishable states. Note that, this equality is different from the one proposed in [281]. This result is extremely helpful to calculate the entanglement in the scenarios where particles are indistinguishable like quantum dots [168, 170], ultracold atomic gases [215], Bose-Einstein condensates [213, 214], quantum meteorology [282, 283], etc.

Finally, we propose two new applications useful for quantum cryptography and one for application useful for quantum networks by entangled distinguishable and indistinguishable particles using the above properties, tools, theorems, relations, and results in Chapter 9. If two cryptographic systems with different resource requirements provide the same level of security, the one with less resources becomes the natural choice. First, we present a generic scheme to reduce the number of particles used in device-independent quantum private query without affecting the security that can be used for both distinguishable and indistinguishable particles. In doing so, the success probability remains the same but the generalized singlet fraction changes. Thus in many ancilla assisted quantum processing protocols like quantum process tomography [285], entanglement stabilization [286], quantum secret sharing [287], quantum error correction [288], quantum measurement [289], weak value amplification [290], quantum channel discrimination [291], coherent-state superposition generation [292], etc., where the resource can be reduced by using additional DoF as ancilla instead of a

particle. Further, we show that entangled indistinguishable particles may alter certain important parameters in cryptographic protocols. In particular, we demonstrate how indistinguishability can change Hardy's probability which is used in quantum byzantine agreement [40], random number generation [38], quantum key distribution [293] etc. Similar attacks can be performed on other quantum cryptographic protocols such as quantum private query [226, 227], quantum secure direct communication [295, 296], quantum secret sharing [297, 298], quantum state splitting [299, 300] etc. that use asymmetric entangled states. How these attacks can be neutralized and where our monogamy result can be utilized can be interesting research works. Finally we show a novel entanglement swapping protocol without Bell state measurement using only two indistinguishable particles. Thus, these applications will be very useful in the security and reducing the resource requirements of many quantum protocols.

Bibliography

- [1] Yanna Li, Manuel Gessner, Weidong Li, and Augusto Smerzi. Hyper- and hybrid nonlocality. *Phys. Rev. Lett.*, 120:050404, Feb 2018.
- [2] Max Planck. Ueber das gesetz der energieverteilung im normalspectrum. *Annalen der Physik*, 309(3):553–563, 1901.
- [3] Max Planck. Original papers in quantum physics. 1, 1972.
- [4] Albert Einstein. "U on a heuristic point of view concerning the generation and transformation of light. *annals of physics*, 4, 1905.
- [5] Walther Gerlach and Otto Stern. Der experimentelle nachweis der richtungsquantelung im magnetfeld. *Zeitschrift für Physik*, 9(1):349–352, 1922.
- [6] Ludwig Zehnder. Ein neuer interferenzrefraktor. 1891.
- [7] Ludwig Mach. Ueber einen interferenzrefraktor. *Zeitschrift für Instrumentenkunde*, 12(3):89, 1892.
- [8] E. Schrödinger. An undulatory theory of the mechanics of atoms and molecules. *Phys. Rev.*, 28:1049–1070, Dec 1926.
- [9] Angelo Bassi, Kinjalk Lochan, Seema Satin, Tejinder P. Singh, and Hendrik Ulbricht. Models of wave-function collapse, underlying theories, and experimental tests. *Rev. Mod. Phys.*, 85:471–527, Apr 2013.
- [10] M Jarmmer. The philosophy of quantum mechanics. the interpretations of quantum mechanics in historical perspective. 1974.
- [11] Jan Faye. Copenhagen interpretation of quantum mechanics. 2002.
- [12] Bryce Seligman DeWitt and Neill Graham. *The many-worlds interpretation of quantum mechanics*, volume 63. Princeton University Press, 2015.
- [13] Christopher Gordon Timpson. Quantum bayesianism: A study. *Studies in History and Philosophy of Science Part B: Studies in History and Philosophy of Modern Physics*, 39(3):579–609, 2008.
- [14] Robert B Griffiths. Consistent histories and the interpretation of quantum mechanics. *Journal of Statistical Physics*, 36(1):219–272, 1984.

- [15] David Bohm. A suggested interpretation of the quantum theory in terms of "hidden" variables. i. *Phys. Rev.*, 85:166–179, Jan 1952.
- [16] Detlef Dürr, Sheldon Goldstein, and Nino Zanghi. Bohmian mechanics as the foundation of quantum mechanics. In *Bohmian mechanics and quantum theory: an appraisal*, pages 21–44. Springer, 1996.
- [17] John G. Cramer. The transactional interpretation of quantum mechanics. *Rev. Mod. Phys.*, 58:647–687, Jul 1986.
- [18] John G Cramer. An overview of the transactional interpretation of quantum mechanics. *International Journal of Theoretical Physics*, 27(2):227–236, 1988.
- [19] John G Cramer. Transactional interpretation of quantum mechanics. In *Compendium of Quantum Physics*, pages 795–798. Springer, 2009.
- [20] Michael A. Nielsen and Isaac L. Chuang. *Quantum computation and quantum information*. Cambridge University Press, 2019.
- [21] John Von Neumann. *Mathematical foundations of quantum mechanics*. Princeton university press, 2018.
- [22] Claude Elwood Shannon. A mathematical theory of communication. *ACM SIGMOBILE mobile computing and communications review*, 5(1):3–55, 2001.
- [23] Benjamin Schumacher. Quantum coding. *Phys. Rev. A*, 51:2738–2747, Apr 1995.
- [24] Richard Jozsa and Benjamin Schumacher. A new proof of the quantum noiseless coding theorem. *Journal of Modern Optics*, 41(12):2343–2349, 1994.
- [25] Alexander Semenovich Holevo. Bounds for the quantity of information transmitted by a quantum communication channel. *Problemy Peredachi Informatsii*, 9(3):3–11, 1973.
- [26] Paul Adrien Maurice Dirac. A new notation for quantum mechanics. In *Mathematical Proceedings of the Cambridge Philosophical Society*, volume 35, pages 416–418. Cambridge University Press, 1939.
- [27] Albert. Einstein, Boris. Podolsky, and Nathan Rosen. Can quantum-mechanical description of physical reality be considered complete? *Phys. Rev.*, 47:777–780, May 1935.
- [28] John S. Bell. On the einstein podolsky rosen paradox. *Physics Physique Fizika*, 1:195–200, Nov 1964.
- [29] John F. Clauser, Michael A. Horne, Abner Shimony, and Richard A. Holt. Proposed experiment to test local hidden-variable theories. *Phys. Rev. Lett.*, 23:880–884, Oct 1969.

- [30] Nathaniel David Mermin. Extreme quantum entanglement in a superposition of macroscopically distinct states. *Phys. Rev. Lett.*, 65:1838–1840, Oct 1990.
- [31] Daniel M. Greenberger, Michael A. Horne, Abner Shimony, and Anton Zeilinger. Bell’s theorem without inequalities. *American Journal of Physics*, 58(12):1131–1143, 1990.
- [32] Jian-Wei Pan, Dik Bouwmeester, Matthew Daniell, Harald Weinfurter, and Anton Zeilinger. Experimental test of quantum nonlocality in three-photon greenberger-horne-zeilinger entanglement. *Nature*, 403(6769):515–519, 2000.
- [33] Nicolas Brunner, Daniel Cavalcanti, Stefano Pironio, Valerio Scarani, and Stephanie Wehner. Bell nonlocality. *Rev. Mod. Phys.*, 86:419–478, Apr 2014.
- [34] Lucien Hardy. Quantum mechanics, local realistic theories, and lorentz-invariant realistic theories. *Phys. Rev. Lett.*, 68:2981–2984, May 1992.
- [35] Lucien Hardy. Nonlocality for two particles without inequalities for almost all entangled states. *Phys. Rev. Lett.*, 71:1665–1668, Sep 1993.
- [36] Nathaniel David Mermin. The best version of bell’s theorem. *Annals of the New York Academy of Sciences*, 755(1):616–623, 1995.
- [37] José L. Cereceda. Hardy’s nonlocality for generalized n-particle ghz states. *Physics Letters A*, 327(5):433 – 437, 2004.
- [38] Hong-Wei Li, Marcin Pawłowski, Ramij Rahaman, Guang-Can Guo, and Zheng-Fu Han. Device- and semi-device-independent random numbers based on non-inequality paradox. *Phys. Rev. A*, 92:022327, Aug 2015.
- [39] Stefano Pironio, Antonio Acín, Nicolas Brunner, Nicolas Gisin, Serge Massar, and Valerio Scarani. Device-independent quantum key distribution secure against collective attacks. *New Journal of Physics*, 11(4):045021, apr 2009.
- [40] Ramij Rahaman, Marcin Wieśniak, and Marek Żukowski. Quantum byzantine agreement via hardy correlations and entanglement swapping. *Phys. Rev. A*, 92:042302, Oct 2015.
- [41] Nicolas Brunner, Daniel Cavalcanti, Stefano Pironio, Valerio Scarani, and Stephanie Wehner. Bell nonlocality. *Rev. Mod. Phys.*, 86:419–478, Apr 2014.
- [42] Charles H. Bennett and Stephen J. Wiesner. Communication via one- and two-particle operators on einstein-podolsky-rosen states. *Phys. Rev. Lett.*, 69:2881–2884, Nov 1992.
- [43] Charles H. Bennett, Gilles Brassard, Claude Crépeau, Richard Jozsa, Asher Peres, and William K. Wootters. Teleporting an unknown quantum state via dual classical and einstein-podolsky-rosen channels. *Phys. Rev. Lett.*, 70:1895–1899, Mar 1993.

- [44] M. Żukowski, A. Zeilinger, M. A. Horne, and A. K. Ekert. “event-ready-detectors” bell experiment via entanglement swapping. *Phys. Rev. Lett.*, 71:4287–4290, Dec 1993.
- [45] C. H. Bennett and G. Brassard. Quantum cryptography: Public key distribution and coin tossing. In *Proceedings of IEEE International Conference on Computers, Systems and Signal Processing*, 175:8, 1984.
- [46] Dominic Mayers and Andrew Yao. Quantum cryptography with imperfect apparatus. In *Proceedings 39th Annual Symposium on Foundations of Computer Science (Cat. No. 98CB36280)*, pages 503–509. IEEE, 1998.
- [47] Roope Uola, Ana C. S. Costa, H. Chau Nguyen, and Otfried Gühne. Quantum steering. *Rev. Mod. Phys.*, 92:015001, Mar 2020.
- [48] Marco Piani and John Watrous. Necessary and sufficient quantum information characterization of einstein-podolsky-rosen steering. *Phys. Rev. Lett.*, 114:060404, Feb 2015.
- [49] Harold Ollivier and Wojciech H. Zurek. Quantum discord: A measure of the quantumness of correlations. *Phys. Rev. Lett.*, 88:017901, Dec 2001.
- [50] Alexander Streltsov, Gerardo Adesso, and Martin B. Plenio. Colloquium: Quantum coherence as a resource. *Rev. Mod. Phys.*, 89:041003, Oct 2017.
- [51] Dik Bouwmeester, Jian-Wei Pan, Klaus Mattle, Manfred Eibl, Harald Weinfurter, and Anton Zeilinger. Experimental quantum teleportation. *Nature*, 390(6660):575–579, December 1997.
- [52] Michał Horodecki, Paweł Horodecki, and Ryszard Horodecki. General teleportation channel, singlet fraction, and quasidistillation. *Phys. Rev. A*, 60:1888–1898, Sep 1999.
- [53] Satyabrata Adhikari, A. S. Majumdar, D. Home, A. K. Pan, Dipankar Home, Guruprasad Kar, and Archan S. Majumda. Swapping path-spin intraparticle entanglement onto spin-spin mixed interparticle entanglement involving amplitude damping channel. AIP, 2011.
- [54] Asmita Kumari, Abhishek Ghosh, Mohit Lal Bera, and A. K. Pan. Swapping intraphoton entanglement to interphoton entanglement using linear optical devices. *Phys. Rev. A*, 99:032118, Mar 2019.
- [55] Martin B. Plenio and Shashank Virmani. An introduction to entanglement measures. *Quantum Info. Comput.*, 7(1):1–51, January 2007.
- [56] Otfried Gühne and Géza Tóth. Entanglement detection. *Physics Reports*, 474(1-6):1–75, April 2009.

- [57] Charles H. Bennett, Herbert J. Bernstein, Sandu Popescu, and Benjamin Schumacher. Concentrating partial entanglement by local operations. *Phys. Rev. A*, 53:2046–2052, Apr 1996.
- [58] Karol Życzkowski, Paweł Horodecki, Anna Sanpera, and Maciej Lewenstein. Volume of the set of separable states. *Phys. Rev. A*, 58:883–892, Aug 1998.
- [59] G. Vidal and R. F. Werner. Computable measure of entanglement. *Phys. Rev. A*, 65:032314, Feb 2002.
- [60] Jeong San Kim. Tsallis entropy and entanglement constraints in multiqubit systems. *Phys. Rev. A*, 81:062328, Jun 2010.
- [61] Yu Luo, Tian Tian, Lian-He Shao, and Yongming Li. General monogamy of tsallis q -entropy entanglement in multiqubit systems. *Phys. Rev. A*, 93:062340, Jun 2016.
- [62] Jeong San Kim and Barry C Sanders. Monogamy of multi-qubit entanglement using rényi entropy. *Journal of Physics A: Mathematical and Theoretical*, 43(44):445305, October 2010.
- [63] Wei Song, Yan-Kui Bai, Mou Yang, Ming Yang, and Zhuo-Liang Cao. General monogamy relation of multiqubit systems in terms of squared rényi- α entanglement. *Phys. Rev. A*, 93:022306, Feb 2016.
- [64] Jeong San Kim and Barry C Sanders. Unified entropy, entanglement measures and monogamy of multi-party entanglement. *Journal of Physics A: Mathematical and Theoretical*, 44(29):295303, June 2011.
- [65] Awais Khan, Junaid ur Rehman, Kehao Wang, and Hyundong Shin. Unified monogamy relations of multipartite entanglement. *Scientific Reports*, 9(1), November 2019.
- [66] Valerie Coffman, Joydip Kundu, and William K. Wootters. Distributed entanglement. *Phys. Rev. A*, 61:052306, Apr 2000.
- [67] M. Pawłowski. Security proof for cryptographic protocols based only on the monogamy of bell’s inequality violations. *Phys. Rev. A*, 82:032313, Sep 2010.
- [68] Marco Tomamichel, Serge Fehr, Jędrzej Kaniewski, and Stephanie Wehner. A monogamy-of-entanglement game with applications to device-independent quantum cryptography. *New Journal of Physics*, 15(10):103002, October 2013.
- [69] Nathaniel Johnston, Rajat Mittal, Vincent Russo, and John Watrous. Extended non-local games and monogamy-of-entanglement games. *Proceedings of the Royal Society A: Mathematical, Physical and Engineering Sciences*, 472(2189):20160003, May 2016.

- [70] W. Dür, G. Vidal, and J. I. Cirac. Three qubits can be entangled in two inequivalent ways. *Phys. Rev. A*, 62:062314, Nov 2000.
- [71] Joonwoo Bae and Antonio Acín. Asymptotic quantum cloning is state estimation. *Phys. Rev. Lett.*, 97:030402, Jul 2006.
- [72] Giulio Chiribella and Giacomo Mauro D’Ariano. Quantum information becomes classical when distributed to many users. *Phys. Rev. Lett.*, 97:250503, Dec 2006.
- [73] Xiao song Ma, Borivoje Dakic, William Naylor, Anton Zeilinger, and Philip Walther. Quantum simulation of the wavefunction to probe frustrated heisenberg spin systems. *Nature Physics*, 7(5):399–405, February 2011.
- [74] Artur García-Sáez and José I. Latorre. Renormalization group contraction of tensor networks in three dimensions. *Phys. Rev. B*, 87:085130, Feb 2013.
- [75] Fernando G. S. L. Brandão, Marco Piani, and Paweł Horodecki. Generic emergence of classical features in quantum darwinism. *Nature Communications*, 6(1), August 2015.
- [76] K. Rama Koteswara Rao, Hemant Katiyar, T. S. Mahesh, Aditi Sen (De), Ujjwal Sen, and Anil Kumar. Multipartite quantum correlations reveal frustration in a quantum ising spin system. *Phys. Rev. A*, 88:022312, Aug 2013.
- [77] Vittorio Giovannetti, Seth Lloyd, and Lorenzo Maccone. Quantum metrology. *Phys. Rev. Lett.*, 96:010401, Jan 2006.
- [78] W. K. Wootters and W. H. Zurek. A single quantum cannot be cloned. *Nature*, 299(5886):802–803, October 1982.
- [79] Valerio Scarani, Sofyan Iblisdir, Nicolas Gisin, and Antonio Acín. Quantum cloning. *Rev. Mod. Phys.*, 77:1225–1256, Nov 2005.
- [80] Heng Fan, Yi-Nan Wang, Li Jing, Jie-Dong Yue, Han-Duo Shi, Yong-Liang Zhang, and Liang-Zhu Mu. Quantum cloning machines and the applications. *Physics Reports*, 544(3):241–322, November 2014.
- [81] W. Heisenberg. ber den anschaulichen inhalt der quantentheoretischen kinematik und mechanik. *Zeitschrift f r Physik*, 43(3-4):172–198, March 1927.
- [82] Emanuel Knill and Raymond Laflamme. Theory of quantum error-correcting codes. *Phys. Rev. A*, 55:900–911, Feb 1997.
- [83] R. P. Feynman. *Statistical Mechanics*. Benjamin, Reading, MA, 1972.
- [84] J. J. Sakurai. *Modern Quantum Mechanics*. Addison-Wesley, Reading, MA, 1994.

- [85] Giuseppe Compagno, Alessia Castellini, and Rosario Lo Franco. Dealing with indistinguishable particles and their entanglement. *Philosophical Transactions of the Royal Society A: Mathematical, Physical and Engineering Sciences*, 376(2123):20170317, May 2018.
- [86] Farzam Nosrati, Alessia Castellini, Giuseppe Compagno, and Rosario Lo Franco. Robust entanglement preparation against noise by controlling spatial indistinguishability. *npj Quantum Information*, 6(1), May 2020.
- [87] Gordon E Moore et al. Cramming more components onto integrated circuits, 1965.
- [88] Alan Mathison Turing et al. On computable numbers, with an application to the entscheidungsproblem. *J. of Math.*, 58(345-363):5, 1936.
- [89] Richard P Feynman. Simulating physics with computers. In *Feynman and computation*, pages 133–153. CRC Press, 2018.
- [90] David P DiVincenzo. The physical implementation of quantum computation. *Fortschritte der Physik: Progress of Physics*, 48(9-11):771–783, 2000.
- [91] David G Cory, Amr F Fahmy, and Timothy F Havel. Ensemble quantum computing by nmr spectroscopy. *Proceedings of the National Academy of Sciences*, 94(5):1634–1639, 1997.
- [92] Ivan Oliveira, Roberto Sarthour Jr, Tito Bonagamba, Eduardo Azevedo, and Jair CC Freitas. *NMR quantum information processing*. Elsevier, 2011.
- [93] Dawei Lu, Aharon Brodutch, Jihyun Park, Hemant Katiyar, Tomas Jochym-O’Connor, and Raymond Laflamme. Nmr quantum information processing. In *Electron Spin Resonance (ESR) Based Quantum Computing*, pages 193–226. Springer, 2016.
- [94] Hartmut Häffner, Christian F Roos, and Rainer Blatt. Quantum computing with trapped ions. *Physics reports*, 469(4):155–203, 2008.
- [95] Jan Benhelm, Gerhard Kirchmair, Christian F Roos, and Rainer Blatt. Towards fault-tolerant quantum computing with trapped ions. *Nature Physics*, 4(6):463–466, 2008.
- [96] Philip Krantz, Morten Kjaergaard, Fei Yan, Terry P Orlando, Simon Gustavsson, and William D Oliver. A quantum engineer’s guide to superconducting qubits. *Applied Physics Reviews*, 6(2):021318, 2019.
- [97] Morten Kjaergaard, Mollie E Schwartz, Jochen Braumüller, Philip Krantz, Joel I-J Wang, Simon Gustavsson, and William D Oliver. Superconducting qubits: Current state of play. *Annual Review of Condensed Matter Physics*, 11:369–395, 2020.

- [98] Jeremy L O’Brien. Optical quantum computing. *Science*, 318(5856):1567–1570, 2007.
- [99] Pieter Kok, William J Munro, Kae Nemoto, Timothy C Ralph, Jonathan P Dowling, and Gerard J Milburn. Linear optical quantum computing with photonic qubits. *Reviews of modern physics*, 79(1):135, 2007.
- [100] Emanuel Knill, Raymond Laflamme, and Gerald J Milburn. A scheme for efficient quantum computation with linear optics. *nature*, 409(6816):46–52, 2001.
- [101] Daniel Loss and David P DiVincenzo. Quantum computation with quantum dots. *Physical Review A*, 57(1):120, 1998.
- [102] Christoph Kloeffel and Daniel Loss. Prospects for spin-based quantum computing in quantum dots. *Annu. Rev. Condens. Matter Phys.*, 4(1):51–81, 2013.
- [103] Craig S Lent and P Douglas Tougaw. A device architecture for computing with quantum dots. *Proceedings of the IEEE*, 85(4):541–557, 1997.
- [104] Radu Ionicioiu, Gehan Amaratunga, and Florin Udrea. Quantum computation with ballistic electrons. *International Journal of Modern Physics B*, 15(02):125–133, 2001.
- [105] Nicklas Ohlsson, R Krishna Mohan, and Stefan Kröll. Quantum computer hardware based on rare-earth-ion-doped inorganic crystals. *Optics communications*, 201(1-3):71–77, 2002.
- [106] <https://www.research.ibm.com/ibmq/>. Ibm quantum experience.
- [107] Simon J. Devitt. Performing quantum computing experiments in the cloud. *Phys. Rev. A*, 94:032329, Sep 2016.
- [108] Mario Berta, Stephanie Wehner, and Mark M Wilde. Entropic uncertainty and measurement reversibility. *New Journal of Physics*, 18(7):073004, jul 2016.
- [109] Emilie Huffman and Ari Mizel. Violation of noninvasive macrorealism by a superconducting qubit: Implementation of a leggett-garg test that addresses the clumsiness loophole. *Phys. Rev. A*, 95:032131, Mar 2017.
- [110] Martin Hebenstreit, Daniel Alsina, José I. Latorre, and Barbara Kraus. Compressed quantum computation using a remote five-qubit quantum computer. *Phys. Rev. A*, 95:052339, May 2017.
- [111] Maika Takita, Andrew W. Cross, A. D. Córcoles, Jerry M. Chow, and Jay M. Gambetta. Experimental demonstration of fault-tolerant state preparation with superconducting qubits. *Phys. Rev. Lett.*, 119:180501, Oct 2017.
- [112] Robin Harper and Steven T. Flammia. Fault-tolerant logical gates in the ibm quantum experience. *Phys. Rev. Lett.*, 122:080504, Feb 2019.

- [113] Bikash K. Behera, Anindita Banerjee, and Prasanta K. Panigrahi. Experimental realization of quantum cheque using a five-qubit quantum computer. *Quantum Information Processing*, 16(12), November 2017.
- [114] İskender Yalçınkaya and Zafer Gedik. Optimization and experimental realization of the quantum permutation algorithm. *Phys. Rev. A*, 96:062339, Dec 2017.
- [115] Sayan Gangopadhyay, Manabputra, Bikash K. Behera, and Prasanta K. Panigrahi. Generalization and demonstration of an entanglement-based deutsch-jozsa-like algorithm using a 5-qubit quantum computer. *Quantum Information Processing*, 17(7), May 2018.
- [116] Mirko Amico, Zain H. Saleem, and Muir Kumph. Experimental study of shor’s factoring algorithm using the ibm q experience. *Phys. Rev. A*, 100:012305, Jul 2019.
- [117] Yonghae Lee, Jaewoo Joo, and Soojoon Lee. Hybrid quantum linear equation algorithm and its experimental test on ibm quantum experience. *Scientific Reports*, 9(1):4778, 2019.
- [118] <https://quantumai.google/>. Google quantum computing.
- [119] https://www.intel.in/content/www/in/en/research/quantum_computing.html. Intel quantum computing.
- [120] <https://www.xanadu.ai/>. Xanadu quantum computing.
- [121] <https://www.rigetti.com/>. Rigetti quantum computing.
- [122] <https://www.dwavesys.com/>. D-wave quantum computing.
- [123] <https://ionq.com/>. Ionq quantum computing.
- [124] https://azure.microsoft.com/en-us/solutions/quantum_computing/. Microsoft quantum computing.
- [125] <https://www.toshiba.co.jp/qkd/en/index.htm>. Tosiba quantum computing.
- [126] <https://damo.alibaba.com/labs/quantum>. Alibaba quantum computing.
- [127] <https://aws.amazon.com/braket/>. Amazon quantum computing.
- [128] <https://1qbit.com/>. 1qbit quantum computing.
- [129] Zhi Zhao, Tao Yang, Yu-Ao Chen, An-Ning Zhang, Marek Żukowski, and Jian-Wei Pan. Experimental violation of local realism by four-photon greenberger-horne-zeilinger entanglement. *Phys. Rev. Lett.*, 91:180401, Oct 2003.

- [130] Ben P. Lanyon, Michael Zwerger, Petar Jurcevic, C. Hempel, Wolfgang Dür, Hans J. Briegel, Rainer Blatt, and C. F. Roos. Experimental violation of multipartite bell inequalities with trapped ions. *Phys. Rev. Lett.*, 112:100403, Mar 2014.
- [131] Daniel Alsina and José Ignacio Latorre. Experimental test of mermin inequalities on a five-qubit quantum computer. *Phys. Rev. A*, 94:012314, Jul 2016.
- [132] Giovanni Di Giuseppe, Francesco De Martini, and D. Boschi. Experimental test of the violation of local realism in quantum mechanics without bell inequalities. *Phys. Rev. A*, 56:176–181, Jul 1997.
- [133] William T. M. Irvine, Juan F. Hodelin, Christoph Simon, and Dirk Bouwmeester. Realization of hardy’s thought experiment with photons. *Phys. Rev. Lett.*, 95:030401, Jul 2005.
- [134] Jeff S. Lundeen and Aephraim M. Steinberg. Experimental joint weak measurement on a photon pair as a probe of hardy’s paradox. *Phys. Rev. Lett.*, 102:020404, Jan 2009.
- [135] Kazuhiro Yokota, Takashi Yamamoto, Masato Koashi, and Nobuyuki Imoto. Direct observation of hardy's paradox by joint weak measurement with an entangled photon pair. *New Journal of Physics*, 11(3):033011, mar 2009.
- [136] Giuseppe Vallone, Ilaria Gianani, Enrique B. Inostroza, Carlos Saavedra, Gustavo Lima, Adán Cabello, and Paolo Mataloni. Testing hardy’s nonlocality proof with genuine energy-time entanglement. *Phys. Rev. A*, 83:042105, Apr 2011.
- [137] Lixiang Chen and Jacqueline Romero. Hardy’s nonlocality proof using twisted photons. *Opt. Express*, 20(19):21687–21692, Sep 2012.
- [138] Ebrahim Karimi, Filippo Cardano, Maria Maffei, Corrado de Lisio, Lorenzo Marrucci, Robert W. Boyd, and Enrico Santamato. Hardy’s paradox tested in the spin-orbit hilbert space of single photons. *Phys. Rev. A*, 89:032122, Mar 2014.
- [139] Xiong Zhang, Yifan Sun, Xinbing Song, and Xiangdong Zhang. Realization of hardy’s thought experiment using classical light. *Journal of Optics*, 18(9):095604, aug 2016.
- [140] Dai-He Fan, Mao-Chun Dai, Wei-Jie Guo, and Lian-Fu Wei. Experimentally testing hardy’s theorem on nonlocality with entangled mixed states. *Chinese Physics B*, 26(4):040302, apr 2017.
- [141] Lixiang Chen, Wuhong Zhang, Ziwen Wu, Jikang Wang, Robert Fickler, and Ebrahim Karimi. Experimental ladder proof of hardy’s nonlocality for high-dimensional quantum systems. *Phys. Rev. A*, 96:022115, Aug 2017.

- [142] E. Schrödinger. Discussion of probability relations between separated systems. *Mathematical Proceedings of the Cambridge Philosophical Society*, 31(4):555–563, October 1935.
- [143] Y. S. Li, B. Zeng, X. S. Liu, and G. L. Long. Entanglement in a two-identical-particle system. *Phys. Rev. A*, 64:054302, Oct 2001.
- [144] R. Paškauskas and L. You. Quantum correlations in two-boson wave functions. *Phys. Rev. A*, 64:042310, Sep 2001.
- [145] John Schliemann, J. Ignacio Cirac, Marek Kuś, Maciej Lewenstein, and Daniel Loss. Quantum correlations in two-fermion systems. *Phys. Rev. A*, 64:022303, Jul 2001.
- [146] Paolo Zanardi. Quantum entanglement in fermionic lattices. *Phys. Rev. A*, 65:042101, Mar 2002.
- [147] GianCarlo Ghirardi, Luca Marinatto, and Tullio Weber. *Journal of Statistical Physics*, 108(1/2):49–122, 2002.
- [148] H. M. Wiseman and John A. Vaccaro. Entanglement of indistinguishable particles shared between two parties. *Phys. Rev. Lett.*, 91:097902, Aug 2003.
- [149] GianCarlo Ghirardi and Luca Marinatto. General criterion for the entanglement of two indistinguishable particles. *Phys. Rev. A*, 70:012109, Jul 2004.
- [150] Vlatko Vedral. Entanglement in the second quantization formalism. *Open Physics*, 1(2), January 2003.
- [151] Howard Barnum, Emanuel Knill, Gerardo Ortiz, Rolando Somma, and Lorenza Viola. A subsystem-independent generalization of entanglement. *Phys. Rev. Lett.*, 92:107902, Mar 2004.
- [152] Howard Barnum, Emanuel Knill, Gerardo Ortiz, Rolando Somma, and Lorenza Viola. A subsystem-independent generalization of entanglement. *Phys. Rev. Lett.*, 92:107902, Mar 2004.
- [153] Paolo Zanardi, Daniel A. Lidar, and Seth Lloyd. Quantum tensor product structures are observable induced. *Phys. Rev. Lett.*, 92:060402, Feb 2004.
- [154] Yasser Omar. Indistinguishable particles in quantum mechanics: an introduction. *Contemporary Physics*, 46(6):437–448, 2005.
- [155] Quantum correlations in systems of indistinguishable particles. *Annals of Physics*, 299(1):88–127, 2002.
- [156] Janusz Grabowski, Marek Kuś, and Giuseppe Marmo. Entanglement for multipartite systems of indistinguishable particles. *Journal of Physics A: Mathematical and Theoretical*, 44(17):175302, mar 2011.

- [157] Toshihiko Sasaki, Tsubasa Ichikawa, and Izumi Tsutsui. Entanglement of indistinguishable particles. *Phys. Rev. A*, 83:012113, Jan 2011.
- [158] M.C. Tichy, F. de Melo, M. Kuś, F. Mintert, and A. Buchleitner. Entanglement of identical particles and the detection process. *Fortschritte der Physik*, 61(2-3):225–237, 2013.
- [159] N. Killoran, M. Cramer, and M. B. Plenio. Extracting entanglement from identical particles. *Phys. Rev. Lett.*, 112:150501, Apr 2014.
- [160] F. Benatti, R. Floreanini, F. Franchini, and U. Marzolino. Remarks on entanglement and identical particles. *Open Systems & Information Dynamics*, 24(03):1740004, 2017.
- [161] Rosario Lo Franco and Giuseppe Compagno. Quantum entanglement of identical particles by standard information-theoretic notions. *Scientific Reports*, 6(1), February 2016.
- [162] Daniel Braun, Gerardo Adesso, Fabio Benatti, Roberto Floreanini, Ugo Marzolino, Morgan W. Mitchell, and Stefano Pirandola. Quantum-enhanced measurements without entanglement. *Rev. Mod. Phys.*, 90:035006, Sep 2018.
- [163] Rosario Lo Franco and Giuseppe Compagno. Indistinguishability of elementary systems as a resource for quantum information processing. *Phys. Rev. Lett.*, 120:240403, Jun 2018.
- [164] Malte C Tichy, Florian Mintert, and Andreas Buchleitner. Essential entanglement for atomic and molecular physics. *Journal of Physics B: Atomic, Molecular and Optical Physics*, 44(19):192001, September 2011.
- [165] Immanuel Bloch, Jean Dalibard, and Wilhelm Zwerger. Many-body physics with ultracold gases. *Rev. Mod. Phys.*, 80:885–964, Jul 2008.
- [166] David Hayes, Paul S. Julienne, and Ivan H. Deutsch. Quantum logic via the exchange blockade in ultracold collisions. *Phys. Rev. Lett.*, 98:070501, Feb 2007.
- [167] Marco Anderlini, Patricia J Lee, Benjamin L Brown, Jennifer Sebby-Strabley, William D Phillips, and James V Porto. Controlled exchange interaction between pairs of neutral atoms in an optical lattice. *Nature*, 448(7152):452–456, 2007.
- [168] J. R. Petta, A. C. Johnson, J. M. Taylor, E. A. Laird, A. Yacoby, M. D. Lukin, C. M. Marcus, M. P. Hanson, and A. C. Gossard. Coherent manipulation of coupled electron spins in semiconductor quantum dots. *Science*, 309(5744):2180–2184, 2005.
- [169] Anders Lundskog, Chih-Wei Hsu, K Fredrik Karlsson, Supaluck Amloy, Daniel Nilsson, Urban Forsberg, Per Olof Holtz, and Erik Janzén. Direct generation

- of linearly polarized photon emission with designated orientations from site-controlled ingan quantum dots. *Light: Science & Applications*, 3(1):e139–e139, 2014.
- [170] Z. B. Tan, D. Cox, T. Nieminen, P. Lähteenmäki, D. Golubev, G. B. Lesovik, and P. J. Hakonen. Cooper pair splitting by means of graphene quantum dots. *Phys. Rev. Lett.*, 114:096602, Mar 2015.
- [171] Menno Veldhorst, CH Yang, JCC Hwang, W Huang, JP Dehollain, JT Muhonen, S Simmons, A Laucht, FE Hudson, Kohei M Itoh, et al. A two-qubit logic gate in silicon. *Nature*, 526(7573):410–414, 2015.
- [172] Richard Jozsa. Fidelity for mixed quantum states. *Journal of Modern Optics*, 41(12):2315–2323, 1994.
- [173] Barbara M Terhal. Is entanglement monogamous? *IBM Journal of Research and Development*, 48(1):71–78, 2004.
- [174] N. Lütkenhaus, J. Calsamiglia, and K.-A. Suominen. Bell measurements for teleportation. *Phys. Rev. A*, 59:3295–3300, May 1999.
- [175] Charles H. Bennett, Gilles Brassard, Sandu Popescu, Benjamin Schumacher, John A. Smolin, and William K. Wootters. Purification of noisy entanglement and faithful teleportation via noisy channels. *Phys. Rev. Lett.*, 76:722–725, Jan 1996.
- [176] Alessia Castellini, Bruno Bellomo, Giuseppe Compagno, and Rosario Lo Franco. Activating remote entanglement in a quantum network by local counting of identical particles. *Phys. Rev. A*, 99:062322, Jun 2019.
- [177] William Feller. *An Introduction to Probability Theory and Its Applications*, volume 1. Wiley, January 1968.
- [178] Gilles Brassard, Anne Broadbent, and Alain Tapp. Multi-party pseudo-telepathy. In *Lecture Notes in Computer Science*, pages 1–11. Springer Berlin Heidelberg, 2003.
- [179] Jyotirmoy Basak and Subhamoy Maitra. Clauser–horne–shimony–holt versus three-party pseudo-telepathy: on the optimal number of samples in device-independent quantum private query. *Quantum Inf. Process.*, 17(4):77, feb 2018.
- [180] Rafael Rabelo, Law Yun Zhi, and Valerio Scarani. Device-independent bounds for hardy’s experiment. *Phys. Rev. Lett.*, 109:180401, Oct 2012.
- [181] Sheldon Goldstein. Nonlocality without inequalities for almost all entangled states for two particles. *Phys. Rev. Lett.*, 72:1951–1951, Mar 1994.
- [182] John F. Clauser, Michael A. Horne, Abner Shimony, and Richard A. Holt. Proposed experiment to test local hidden-variable theories. *Phys. Rev. Lett.*, 23:880–884, Oct 1969.

- [183] Daniel Braun and Mahn-Soo Choi. Hardy’s test versus the Clauser-Horne-Shimony-Holt test of quantum nonlocality: Fundamental and practical aspects. *Phys. Rev. A*, 78:032114, Sep 2008.
- [184] Alessandro Fedrizzi, Marcelo P. Almeida, Matthew A. Broome, Andrew G. White, and Marco Barbieri. Hardy’s paradox and violation of a state-independent Bell inequality in time. *Phys. Rev. Lett.*, 106:200402, May 2011.
- [185] Yi-Han Luo, Hong-Yi Su, He-Liang Huang, Xi-Lin Wang, Tao Yang, Li Li, Nai-Le Liu, Jing-Ling Chen, Chao-Yang Lu, and Jian-Wei Pan. Experimental test of generalized Hardy’s paradox. *Science Bulletin*, 63(24):1611 – 1615, 2018.
- [186] Mu Yang, Hui-Xian Meng, Jie Zhou, Zhen-Peng Xu, Ya Xiao, Kai Sun, Jing-Ling Chen, Jin-Shi Xu, Chuan-Feng Li, and Guang-Can Guo. Stronger Hardy-type paradox based on the Bell inequality and its experimental test. *Phys. Rev. A*, 99:032103, Mar 2019.
- [187] Wei Hu. Empirical analysis of a quantum classifier implemented on IBM’s 5q quantum computer. *Journal of Quantum Information Science*, 08(01):1–11, 2018.
- [188] F. Benatti, R. Floreanini, and U. Marzolino. Sub-shot-noise quantum metrology with entangled identical particles. *Annals of Physics*, 325(4):924–935, 2010.
- [189] F. Benatti, R. Floreanini, and U. Marzolino. Bipartite entanglement in systems of identical particles: The partial transposition criterion. *Annals of Physics*, 327(5):1304–1319, 2012.
- [190] F. Benatti, R. Floreanini, and K. Titimbo. Entanglement of identical particles. *Open Systems & Information Dynamics*, 21(01n02):1440003, 2014.
- [191] Paul G. Kwiat. Hyper-entangled states. *Journal of Modern Optics*, 44(11-12):2173–2184, 1997.
- [192] Yu-Bo Sheng, Fu-Guo Deng, and Gui Lu Long. Complete hyperentangled-bell-state analysis for quantum communication. *Phys. Rev. A*, 82:032318, Sep 2010.
- [193] Bao-Cang Ren, Fang-Fang Du, and Fu-Guo Deng. Hyperentanglement concentration for two-photon four-qubit systems with linear optics. *Phys. Rev. A*, 88:012302, Jul 2013.
- [194] Bao-Cang Ren and Fu-Guo Deng. Hyperentanglement purification and concentration assisted by diamond NV centers inside photonic crystal cavities. *Laser Physics Letters*, 10(11):115201, October 2013.
- [195] Quantum hyperentanglement and its applications in quantum information processing. *Science Bulletin*, 62(1):46–68, 2017.

- [196] Marek Żukowski and Anton Zeilinger. Test of the bell inequality based on phase and linear momentum as well as spin. *Physics Letters A*, 155(2-3):69–72, May 1991.
- [197] Xiao-song Ma, Angie Qarry, Johannes Kofler, Thomas Jennewein, and Anton Zeilinger. Experimental violation of a bell inequality with two different degrees of freedom of entangled particle pairs. *Phys. Rev. A*, 79:042101, Apr 2009.
- [198] P. van Loock, T. D. Ladd, K. Sanaka, F. Yamaguchi, Kae Nemoto, W. J. Munro, and Y. Yamamoto. Hybrid quantum repeater using bright coherent light. *Phys. Rev. Lett.*, 96:240501, Jun 2006.
- [199] Xiao-Song Ma, Johannes Kofler, Angie Qarry, Nuray Tetik, Thomas Scheidl, Rupert Ursin, Sven Ramelow, Thomas Herbst, Lothar Ratschbacher, Alessandro Fedrizzi, Thomas Jennewein, and Anton Zeilinger. Quantum erasure with causally disconnected choice. *Proceedings of the National Academy of Sciences*, 110(4):1221–1226, January 2013.
- [200] Ying Sun, Qiao-Yan Wen, and Zheng Yuan. High-efficient quantum key distribution based on hybrid entanglement. *Optics Communications*, 284(1):527–530, January 2011.
- [201] Zeng-Bing Chen, Guang Hou, and Yong-De Zhang. Quantum nonlocality and applications in quantum-information processing of hybrid entangled states. *Phys. Rev. A*, 65:032317, Feb 2002.
- [202] Leonardo Neves, Gustavo Lima, Aldo Delgado, and Carlos Saavedra. Hybrid photonic entanglement: Realization, characterization, and applications. *Phys. Rev. A*, 80:042322, Oct 2009.
- [203] Ulrik L. Andersen, Jonas S. Neergaard-Nielsen, Peter van Loock, and Akira Furusawa. Hybrid discrete- and continuous-variable quantum information. *Nature Physics*, 11(9):713–719, September 2015.
- [204] Scott Hill and William K. Wootters. Entanglement of a pair of quantum bits. *Phys. Rev. Lett.*, 78:5022–5025, Jun 1997.
- [205] M. B. Plenio. Logarithmic negativity: A full entanglement monotone that is not convex. *Phys. Rev. Lett.*, 95:090503, Aug 2005.
- [206] Igor Devetak and Andreas Winter. Distillation of secret key and entanglement from quantum states. *Proceedings of the Royal Society A: Mathematical, Physical and Engineering Sciences*, 461(2053):207–235, January 2005.
- [207] Matthias Christandl and Andreas Winter. “squashed entanglement”: An additive entanglement measure. *Journal of Mathematical Physics*, 45(3):829–840, March 2004.

- [208] Fernando G. S. L. Brandão, Matthias Christandl, and Jon Yard. Faithful squashed entanglement. *Communications in Mathematical Physics*, 306(3):805–830, August 2011.
- [209] William K. Wootters. Entanglement of formation of an arbitrary state of two qubits. *Phys. Rev. Lett.*, 80:2245–2248, Mar 1998.
- [210] Tobias J. Osborne and Frank Verstraete. General monogamy inequality for bipartite qubit entanglement. *Phys. Rev. Lett.*, 96:220503, Jun 2006.
- [211] Yong-Cheng Ou. Violation of monogamy inequality for higher-dimensional objects. *Phys. Rev. A*, 75:034305, Mar 2007.
- [212] Stefano Pirandola, Jens Eisert, Christian Weedbrook, Akira Furusawa, and Samuel L Braunstein. Advances in quantum teleportation. *Nature photonics*, 9(10):641–652, 2015.
- [213] Oliver Morsch and Markus Oberthaler. Dynamics of bose-einstein condensates in optical lattices. *Rev. Mod. Phys.*, 78:179–215, Feb 2006.
- [214] J. Estève, C. Gross, A. Weller, S. Giovanazzi, and M. K. Oberthaler. Squeezing and entanglement in a bose–einstein condensate. *Nature*, 455(7217):1216–1219, October 2008.
- [215] D. Leibfried, R. Blatt, C. Monroe, and D. Wineland. Quantum dynamics of single trapped ions. *Rev. Mod. Phys.*, 75:281–324, Mar 2003.
- [216] Bernard Yurke and David Stoler. Bell’s-inequality experiments using independent-particle sources. *Phys. Rev. A*, 46:2229–2234, Sep 1992.
- [217] Bernard Yurke and David Stoler. Einstein-podolsky-rosen effects from independent particle sources. *Phys. Rev. Lett.*, 68:1251–1254, Mar 1992.
- [218] Konrad Tschernig, Chris Müller, Malte Smoor, Tim Kroh, Janik Wolters, Oliver Benson, Kurt Busch, and Armando Perez-Leija. Direct observation of the particle exchange phase of photons. *Nature Photonics*, 15(9):671–675, June 2021.
- [219] Rosario Lo Franco. Directly proving the bosonic nature of photons. *Nature Photonics*, 15(9):638–639, August 2021.
- [220] Ze-Yan Hao Zheng-Hao Liu Kai Sun Jin-Shi Xu Chuan-Feng Li Guang-Can Guo Roberto Morandotti Giuseppe Compagno Rosario Lo Franco Yan Wang, Matteo Piccolini. Direct measurement of particle statistical phase. *arXiv:2202.00575*, 2022.
- [221] Kai Sun, Yan Wang, Zheng-Hao Liu, Xiao-Ye Xu, Jin-Shi Xu, Chuan-Feng Li, Guang-Can Guo, Alessia Castellini, Farzam Nosrati, Giuseppe Compagno, and Rosario Lo Franco. Experimental quantum entanglement and teleportation by tuning remote spatial indistinguishability of independent photons. *Optics Letters*, 45(23):6410, nov 2020.

- [222] Mariana R. Barros, Seungbeom Chin, Tanumoy Pramanik, Hyang-Tag Lim, Young-Wook Cho, Joonsuk Huh, and Yong-Su Kim. Entangling bosons through particle indistinguishability and spatial overlap. *Optics Express*, 28(25):38083, December 2020.
- [223] Zheng-Hao Liu-Kai Sun Jin-Shi Xu-Chuan-Feng Li-Guang-Can Guo-Alessia Castellini Bruno Bellomo Giuseppe Compagno Rosario Lo Franco Yan Wang, Ze-Yan Hao. Experimental remote entanglement distribution in a photonic quantum network through multinode indistinguishability. *arXiv:2107.03999*, 2021.
- [224] W. Pauli. Über den zusammenhang des abschlusses der elektronengruppen im atom mit der komplexstruktur der spektren. *Zeitschrift für Physik*, 31(1):765–783, February 1925.
- [225] Sandu Popescu. Bell’s inequalities versus teleportation: What is nonlocality? *Phys. Rev. Lett.*, 72:797–799, Feb 1994.
- [226] Vittorio Giovannetti, Seth Lloyd, and Lorenzo Maccone. Quantum private queries. *Phys. Rev. Lett.*, 100:230502, Jun 2008.
- [227] Arpita Maitra, Goutam Paul, and Sarbani Roy. Device-independent quantum private query. *Phys. Rev. A*, 95:042344, Apr 2017.
- [228] Charles Ci Wen Lim, Christopher Portmann, Marco Tomamichel, Renato Renner, and Nicolas Gisin. Device-independent quantum key distribution with local bell test. *Phys. Rev. X*, 3:031006, Jul 2013.
- [229] Charles H. Bennett. Quantum cryptography using any two nonorthogonal states. *Phys. Rev. Lett.*, 68:3121–3124, May 1992.
- [230] Soumya Das and Goutam Paul. A new error-modeling of hardy’s paradox for superconducting qubits and its experimental verification. *ACM Transactions on Quantum Computing*, 1(1):1–24, 2020.
- [231] GianCarlo Ghirardi and Luca Marinatto. Hardy’s proof of nonlocality in the presence of noise. *Phys. Rev. A*, 74:062107, Dec 2006.
- [232] Claude E. Shannon. A mathematical theory of communication. *Bell System Technical Journal*, 27(3):379–423, 1948.
- [233] John Preskill. Quantum Computing in the NISQ era and beyond. *Quantum*, 2:79, August 2018.
- [234] Jay M. Gambetta, Jerry M. Chow, and Matthias Steffen. Building logical qubits in a superconducting quantum computing system. *npj Quantum Information*, 3(1), January 2017.

- [235] Patrick Krantz, Morten Kjaergaard, Feng Yan, Terry P. Orlando, Simon Gustavsson, and William D. Oliver. A quantum engineer's guide to superconducting qubits. *Applied Physics Reviews*, 6(2):021318, June 2019.
- [236] H HAFFNER, C ROOS, and R BLATT. Quantum computing with trapped ions. *Physics Reports*, 469(4):155–203, December 2008.
- [237] Philipp Treutlein, Tilo Steinmetz, Yves Colombe, Benjamin Lev, Peter Hommelhoff, Jakob Reichel, Markus Greiner, Olaf Mandel, Arthur Widera, Tim Rom, Immanuel Bloch, and Theodor W. Hänsch. Quantum information processing in optical lattices and magnetic microtraps. *Fortschritte der Physik*, 54(8-10):702–718, August 2006.
- [238] Daniel Loss and David P. DiVincenzo. Quantum computation with quantum dots. *Physical Review A*, 57(1):120–126, January 1998.
- [239] Stefanie J. Beale, Joel J. Wallman, Mauricio Gutiérrez, Kenneth R. Brown, and Raymond Laflamme. Quantum error correction decoheres noise. *Physical Review Letters*, 121(19), November 2018.
- [240] Joel Wallman, Chris Granade, Robin Harper, and Steven T Flammia. Estimating the coherence of noise. *New Journal of Physics*, 17(11):113020, November 2015.
- [241] Andrew W. Cross, Lev S. Bishop, Sarah Sheldon, Paul D. Nation, and Jay M. Gambetta. Validating quantum computers using randomized model circuits. *Physical Review A*, 100(3), September 2019.
- [242] Alexander J. McCaskey, Zachary P. Parks, Jacek Jakowski, Shirley V. Moore, Titus D. Morris, Travis S. Humble, and Raphael C. Pooser. Quantum chemistry as a benchmark for near-term quantum computers. *npj Quantum Information*, 5(1), November 2019.
- [243] Salonik Resch and Ulya R. Karpuzcu. Benchmarking quantum computers and the impact of quantum noise, 2019.
- [244] Soumya Das, Goutam Paul, and Anindya Banerji. Hyper-hybrid entanglement, indistinguishability, and two-particle entanglement swapping. *Phys. Rev. A*, 102:052401, Nov 2020.
- [245] Kai Sun, Zheng-Hao Liu, Yan Wang, Ze-Yan Hao, Xiao-Ye Xu, Jin-Shi Xu, Chuan-Feng Li, Guang-Can Guo, Alessia Castellini, Ludovico Lami, Andreas Winter, Gerardo Adesso, Giuseppe Compagno, and Rosario Lo Franco. Activation of indistinguishability-based quantum coherence for enhanced metrological applications with particle statistics imprint. *Proceedings of the National Academy of Sciences*, 119(21), May 2022.
- [246] B. S. Cirel'son. Quantum generalizations of bell's inequality. *Letters in Mathematical Physics*, 4(2):93–100, March 1980.

- [247] Ugo Marzolino and Andreas Buchleitner. Quantum teleportation with identical particles. *Phys. Rev. A*, 91:032316, Mar 2015.
- [248] G. C. Wick, A. S. Wightman, and E. P. Wigner. The intrinsic parity of elementary particles. *Phys. Rev.*, 88:101–105, Oct 1952.
- [249] Stephen D. Bartlett, Terry Rudolph, and Robert W. Spekkens. Reference frames, superselection rules, and quantum information. *Rev. Mod. Phys.*, 79:555–609, Apr 2007.
- [250] Yakir Aharonov and Leonard Susskind. Charge superselection rule. *Phys. Rev.*, 155:1428–1431, Mar 1967.
- [251] T Paterek, P Kurzyński, D K L Oi, and D Kaszlikowski. Reference frames for bell inequality violation in the presence of superselection rules. *New Journal of Physics*, 13(4):043027, apr 2011.
- [252] Michał Horodecki, Paweł Horodecki, and Ryszard Horodecki. General teleportation channel, singlet fraction, and quasidistillation. *Phys. Rev. A*, 60:1888–1898, Sep 1999.
- [253] S. Bose and D. Home. Duality in entanglement enabling a test of quantum indistinguishability unaffected by interactions. *Phys. Rev. Lett.*, 110:140404, Apr 2013.
- [254] Marcin Karczewski and Paweł Kurzyński. How to observe duality in entanglement of two distinguishable particles. *Phys. Rev. A*, 94:032124, Sep 2016.
- [255] T. Baumgratz, M. Cramer, and M. B. Plenio. Quantifying coherence. *Phys. Rev. Lett.*, 113:140401, Sep 2014.
- [256] Jan Sperling, Armando Perez-Leija, Kurt Busch, and Ian A. Walmsley. Quantum coherences of indistinguishable particles. *Phys. Rev. A*, 96:032334, Sep 2017.
- [257] Matteo Fadel, Tilman Zibold, Boris Décamps, and Philipp Treutlein. Spatial entanglement patterns and einstein-podolsky-rosen steering in bose-einstein condensates. *Science*, 360(6387):409–413, April 2018.
- [258] Goutam Paul, Soumya Das, and Anindya Banerji. Maximum violation of monogamy of entanglement for indistinguishable particles by measures that are monogamous for distinguishable particles. *Phys. Rev. A*, 104:L010402, Jul 2021.
- [259] Soumya Das, Goutam Paul, and Ritabrata Sengupta. Monogamy and cryptographic applications of entangled indistinguishable particles. *Submitted to Phys. Rev. Lett.*, 2021.

- [260] Ebrahim Karimi, Jonathan Leach, Sergei Slussarenko, Bruno Piccirillo, Lorenzo Marrucci, Lixiang Chen, Weilong She, Sonja Franke-Arnold, Miles J. Padgett, and Enrico Santamato. Spin-orbit hybrid entanglement of photons and quantum contextuality. *Phys. Rev. A*, 82:022115, Aug 2010.
- [261] D. Bhatti, J. von Zanthier, and G. S. Agarwal. Entanglement of polarization and orbital angular momentum. *Phys. Rev. A*, 91:062303, Jun 2015.
- [262] S. Camalet. Monogamy inequality for any local quantum resource and entanglement. *Phys. Rev. Lett.*, 119:110503, Sep 2017.
- [263] S. Camalet. Internal entanglement and external correlations of any form limit each other. *Phys. Rev. Lett.*, 121:060504, Aug 2018.
- [264] Soumya Das, Goutam Paul, and Anindya Banerji. Generalized relation between teleportation fidelity and singlet fraction for (in)-distinguishable particles and its cryptographic applications. *Submitted to Phy. Rev. A*, 2021.
- [265] Alastair Kay, Dagomir Kaszlikowski, and Ravishankar Ramanathan. Optimal cloning and singlet monogamy. *Phys. Rev. Lett.*, 103:050501, Jul 2009.
- [266] Chithrabhanu Perumangatt, Aadhi Abdul Rahim, Gangi Reddy Salla, Shashi Prabhakar, Goutam Kumar Samanta, Goutam Paul, and Ravindra Pratap Singh. Three-particle hyper-entanglement: teleportation and quantum key distribution. *Quantum Information Processing*, 14(10):3813–3826, 2015.
- [267] Yuji Hasegawa, Rudolf Loidl, Gerald Badurek, Matthias Baron, and Helmut Rauch. Violation of a bell-like inequality in single-neutron interferometry. *Nature*, 425(6953):45–48, September 2003.
- [268] Cécilia Lancien, Sara Di Martino, Marcus Huber, Marco Piani, Gerardo Adesso, and Andreas Winter. Should entanglement measures be monogamous or faithful? *Physical review letters*, 117(6):060501, 2016.
- [269] Jeong San Kim, Anirban Das, and Barry C Sanders. Entanglement monogamy of multipartite higher-dimensional quantum systems using convex-roof extended negativity. *Physical Review A*, 79(1):012329, 2009.
- [270] Alexander Streltsov, Gerardo Adesso, Marco Piani, and Dagmar Bruß. Are general quantum correlations monogamous? *Physical review letters*, 109(5):050503, 2012.
- [271] HC Braga, CC Rulli, Thiago R de Oliveira, and MS Sarandy. Monogamy of quantum discord by multipartite correlations. *Physical Review A*, 86(6):062106, 2012.
- [272] R Prabhu, Arun Kumar Pati, Aditi Sen, Ujjwal Sen, et al. Conditions for monogamy of quantum correlations: Greenberger-horne-zeilinger versus w states. *Physical Review A*, 85(4):040102, 2012.

- [273] Yan-Kui Bai, Na Zhang, Ming-Yong Ye, and ZD Wang. Exploring multipartite quantum correlations with the square of quantum discord. *Physical Review A*, 88(1):012123, 2013.
- [274] Si-Yuan Liu, Yu-Ran Zhang, Li-Ming Zhao, Wen-Li Yang, and Heng Fan. General monogamy property of global quantum discord and the application. *Annals of Physics*, 348:256–269, 2014.
- [275] Chandrashekar Radhakrishnan, Manikandan Parthasarathy, Segar Jambulingam, and Tim Byrnes. Distribution of quantum coherence in multipartite systems. *Physical review letters*, 116(15):150504, 2016.
- [276] Marcos LW Basso and Jonas Maziero. Monogamy and trade-off relations for correlated quantum coherence. *Physica Scripta*, 95(9):095105, 2020.
- [277] Margaret D Reid. Monogamy inequalities for the einstein-podolsky-rosen paradox and quantum steering. *Physical Review A*, 88(6):062108, 2013.
- [278] Antony Milne, Sania Jevtic, David Jennings, Howard Wiseman, and Terry Rudolph. Quantum steering ellipsoids, extremal physical states and monogamy. *New Journal of Physics*, 16(8):083017, 2014.
- [279] Shuming Cheng, Antony Milne, Michael JW Hall, and Howard M Wiseman. Volume monogamy of quantum steering ellipsoids for multiqubit systems. *Physical Review A*, 94(4):042105, 2016.
- [280] Benjamin Morris, Benjamin Yadin, Matteo Fadel, Tilman Zibold, Philipp Treutlein, and Gerardo Adesso. Entanglement between identical particles is a useful and consistent resource. *Phys. Rev. X*, 10:041012, Oct 2020.
- [281] Gilad Gour and Guo Yu. Monogamy of entanglement without inequalities. *Quantum*, 2:81, August 2018.
- [282] Vittorio Giovannetti, Seth Lloyd, and Lorenzo Maccone. Quantum metrology. *Phys. Rev. Lett.*, 96:010401, Jan 2006.
- [283] F Benatti, R Floreanini, and U Marzolino. Entanglement and squeezing with identical particles: ultracold atom quantum metrology. *J. Phys. B*, 44(9):091001, apr 2011.
- [284] Antonio Acín, Nicolas Brunner, Nicolas Gisin, Serge Massar, Stefano Pironio, and Valerio Scarani. Device-independent security of quantum cryptography against collective attacks. *Phys. Rev. Lett.*, 98:230501, Jun 2007.
- [285] J. B. Altepeter, D. Branning, E. Jeffrey, T. C. Wei, P. G. Kwiat, R. T. Thew, J. L. O’Brien, M. A. Nielsen, and A. G. White. Ancilla-assisted quantum process tomography. *Phys. Rev. Lett.*, 90:193601, May 2003.

- [286] Christian Kraglund Andersen, Ants Remm, Stefania Lazar, Sebastian Krinner, Johannes Heinsoo, Jean-Claude Besse, Mihai Gabureac, Andreas Wallraff, and Christopher Eichler. Entanglement stabilization using ancilla-based parity detection and real-time feedback in superconducting circuits. *npj Quant. Inf.*, 5(1):69, aug 2019.
- [287] Arpita Maitra, Sourya Joyee De, Goutam Paul, and Asim K. Pal. Proposal for quantum rational secret sharing. *Phys. Rev. A*, 92:022305, Aug 2015.
- [288] Ben Criger, Osama Moussa, and Raymond Laflamme. Quantum error correction with mixed ancilla qubits. *Phys. Rev. A*, 85:044302, Apr 2012.
- [289] G. Brida, L. Ciavarella, I. P. Degiovanni, M. Genovese, A. Migdall, M. G. Mingolla, M. G. A. Paris, F. Piacentini, and S. V. Polyakov. Ancilla-assisted calibration of a measuring apparatus. *Phys. Rev. Lett.*, 108:253601, Jun 2012.
- [290] Shengshi Pang, Justin Dressel, and Todd A. Brun. Entanglement-assisted weak value amplification. *Phys. Rev. Lett.*, 113:030401, Jul 2014.
- [291] Joonwoo Bae, Dariusz Chruściński, and Marco Piani. More entanglement implies higher performance in channel discrimination tasks. *Phys. Rev. Lett.*, 122:140404, Apr 2019.
- [292] Hiroki Takahashi, Kentaro Wakui, Shigenari Suzuki, Masahiro Takeoka, Kazuhiro Hayasaka, Akira Furusawa, and Masahide Sasaki. Generation of large-amplitude coherent-state superposition via ancilla-assisted photon subtraction. *Phys. Rev. Lett.*, 101:233605, Dec 2008.
- [293] Ramij Rahaman, Matthew G. Parker, Piotr Mironowicz, and Marcin Pawłowski. Device-independent quantum key distribution based on measurement inputs. *Phys. Rev. A*, 92:062304, Dec 2015.
- [294] C. W. Chou, H. de Riedmatten, D. Felinto, S. V. Polyakov, S. J. van Enk, and H. J. Kimble. Measurement-induced entanglement for excitation stored in remote atomic ensembles. *Nature*, 438(7069):828–832, December 2005.
- [295] G. L. Long and X. S. Liu. Theoretically efficient high-capacity quantum-key-distribution scheme. *Phys. Rev. A*, 65:032302, Feb 2002.
- [296] Wei Zhang, Dong-Sheng Ding, Yu-Bo Sheng, Lan Zhou, Bao-Sen Shi, and Guang-Can Guo. Quantum secure direct communication with quantum memory. *Phys. Rev. Lett.*, 118:220501, May 2017.
- [297] Mark Hillery, Vladimír Bužek, and André Berthiaume. Quantum secret sharing. *Phys. Rev. A*, 59:1829–1834, Mar 1999.
- [298] Richard Cleve, Daniel Gottesman, and Hoi-Kwong Lo. How to share a quantum secret. *Phys. Rev. Lett.*, 83:648–651, Jul 1999.

- [299] Chiara Vitelli, Nicolò Spagnolo, Lorenzo Aparo, Fabio Sciarrino, Enrico Santamato, and Lorenzo Marrucci. Joining the quantum state of two photons into one. *Nat. Photonics*, 7(7):521–526, May 2013.
- [300] Elsa Passaro, Chiara Vitelli, Nicolò Spagnolo, Fabio Sciarrino, Enrico Santamato, and Lorenzo Marrucci. Joining and splitting the quantum states of photons. *Phys. Rev. A*, 88:062321, Dec 2013.